

## NFPA 204

Standard for

Smoke and Heat Venting

2002 Edition

Copyright © 2002, National Fire Protection Association, All Rights Reserved

This edition of NFPA 204, *Standard for Smoke and Heat Venting*, was prepared by the Technical Committee on Smoke Management Systems and acted on by NFPA at its November Association Technical Meeting held November 10–14, 2001, in Dallas, TX. It was issued by the Standards Council on January 11, 2002, with an effective date of January 31, 2002, and supersedes all previous editions.

This edition of NFPA 204 was approved as an American National Standard on January 31, 2002.

### **Origin and Development of NFPA 204**

This project was initiated in 1956 when the NFPA Board of Directors referred the subject to the Committee on Building Construction. A tentative guide was submitted to NFPA in 1958. Revised and tentatively adopted in 1959 and again in 1960, the guide was officially adopted in 1961. In 1968 a revised edition was adopted that included a new section, Inspection and Maintenance.

In 1975, a reconfirmation action failed as concerns over use of the guide in conjunction with automatic sprinklered buildings surfaced. Because of this controversy, work on a revision to the guide continued at a slow pace.

The Technical Committee and Subcommittee members agreed that the state of the art had progressed sufficiently to develop improved technology-based criteria for design of venting; therefore, the 1982 edition of the document represented a major advance in engineered smoke and heating venting, although reservations over vent and sprinkler applications still existed.

At the time the guide was formulated, the current venting theory was considered unwieldy for this format; consequently, the more adaptable theory as described herein was adopted.

## Annex G Informational References

### G.1 Referenced Publications.

The following documents or portions thereof are referenced within this standard for informational purposes only and are thus not part of the requirements of this document unless also listed in Chapter 2. There are additional lists of references at the ends of Annexes B, C, and D.

**G.1.1 NFPA Publications.** National Fire Protection Association, 1 Batterymarch Park, P.O. Box 9101, Quincy, MA 02269-9101.

NFPA 13, *Standard for the Installation of Sprinkler Systems*, 1999 edition.

NFPA 68, *Guide for Venting of Deflagrations*, 2002 edition.

NFPA 72<sup>®</sup>, *National Fire Alarm Code*<sup>®</sup>, 1999 edition.

NFPA 90A, *Standard for the Installation of Air-Conditioning and Ventilating Systems*, 1999 edition.

NFPA 92B, *Guide for Smoke Management Systems in Malls, Atria, and Large Areas*, 2000 edition.

NFPA 96, *Standard for Ventilation Control and Fire Protection of Commercial Cooking Operations*, 2001 edition.

NFPA 287, *Standard Test Methods for Measurement of Flammability of Materials in Cleanrooms Using a Fire Propagation Apparatus (FPA)*, 2001 edition.

### G.1.2 Other Publications.

**G.1.2.1 ASTM Publications.** American Society for Testing and Materials, 100 Barr Harbor Drive, West Conshohocken, PA 19428-2959.

ASTM D 635, *Test Method for Rate of Burning and/or Extent and Time of Burning of Self-Supporting Plastics in a Horizontal Position*, 1991.

ASTM E 1321, *Standard Test Method for Determining Material Ignition and Flame Spread Properties*, 1993.

ASTM E 1354, *Standard Test Method for Heat and Visible Smoke Release Rates for Materials and Products Using an Oxygen Consumption Calorimeter*, 1994.

ASTM E 2058, *Standard Test Methods for Measurement of Synthetic Polymer Material Flammability Using a Fire Propagation Apparatus (FPA)*, 2001.

**G.1.2.2 Computer Programs.** DETACT-QS, DETACT-T2, and LAVENT (Link-Activated VENTS) are all available from the National Institute of Standards and Technology (NIST), and can be downloaded via the World Wide Web at URL <http://www.bfrl.nist.gov>. When downloading LAVENT, it is also necessary to download the file GRAPH which is needed to display the graphics produced by LAVENT.

## G.2 Informational References.

The following documents or portions thereof are listed here as informational resources only. They are not a part of the requirements of this document.

Alpert, R. L., and Ward, E. J., "Evaluation of Unsprinklered Fire Hazards," *Fire Safety Journal* 7 (1984), 127–143.

Babrauskas, V., "Burning Rates," Section 3, Chapter 1 of *SFPE Handbook of Fire Protection Engineering*, second edition, 1995, pp. 3–2 to 3–4.

Carslaw, H. S., and Jaeger, J. C., *Conduction of Heat Solids*, Oxford, 1959.

Delichatsios, M.A., "The Flow of Fire Gases Under a Beamed Ceiling," *Combustion and Flame* 43:1–10, 1981.

DiNunno, P. J., et al., eds., Table B-7 of *SFPE Handbook of Fire Protection Engineering*, second edition, 1995, pp. A-35 to A-36.

Drysdale, D., *An Introduction to Dynamics*, Wiley, 1985.

Evans, D. D., and Stroup, D. W., "Methods to Calculate the Response Time of Heat and Smoke Detectors Installed Below Large Unobstructed Ceilings," *Fire Technology* 22 (No. 1): February 1985, 54.

Gustafsson, N. E., "Smoke Ventilation and Sprinklers — A Sprinkler Specialist's View," Seminar at the Fire Research Station, Borehamwood, UK, May 11, 1992.

Heskestad, G. "Venting Practices," in *Fire Protection Handbook*, seventh edition, ed. by A. E. Cote, National Fire Protection Association, Quincy, Massachusetts, 1991, pp. 6-104 to 6-116.

Heskestad, G., "Fire Plumes," Section 2, Chapter 2 of *SFPE Handbook of Fire Protection Engineering*, second edition 1995, pp. 2-9 to 2-19.

Heskestad, G., "Model Studies of Automatic Smoke and Heat Vent Performance in Sprinklered Fires," Technical Report FMRC Serial No. 21933RC74-T-29, Factory Mutual Research Corp., Norwood, MA, September 1974.

Heskestad, G., and Delichatsios, M.A., "Environments of Fire Detectors — Phase I: Effect of Fire Size, Ceiling Height and Material," Volume II — "Analysis," Technical Report, FMRC 22427, Factory Mutual Research Corporation, Norwood, MA, July 1977.

Heskestad, G., and Delichatsios, M.A., "Environments of Fire Detectors — Phase II: Effect of Ceiling Configuration," Volume I — "Measurements," Technical Report, FMRC 22534, Factory Mutual Research Corporation, Norwood, MA, June 1978.

Hinkley, P. L., "Smoke and Heat Venting," Section 2, Chapter 3 of *SFPE Handbook of Fire Protection Engineering*, second edition, 1995, pp. 3-160 to 3-173.

Hinkley, P. L., Hansell, G. O., Marshall, N. R. and Harrison, R., "Sprinklers and Vents Interaction: Experiments at Ghent," Colt International, U.K. Fire Research Station, Borehamwood, England, *Fire Surveyor*, Vol. 21, No. 5, October 18–23, 1992.

Koslowski, C.C., and Motevalli, V., "Behavior of a 2-Dimensional Ceiling Jet Flow: A

Beamed Ceiling Configuration,” *Fire Safety Science — Proceedings of the Fourth International Symposium*, 469–480, 1994.

McGrattan, Kevin B., Hamins, Anthony, and Stroup, David, “International Fire Sprinkler-Smoke & Heat Vent –Draft Curtain Fire Test Project, Large Scale Experiments and Model Development,” Technical Report, National Fire Protection Research Foundation, September 1998.

Miller, E. E., a Position Paper to NFPA 204 Subcommittee, “Fire Venting of Sprinklered Properties,” 1980.

Nelson, H. E., and Forssell, E. W., “Use of Small-Scale Test Data in Hazard Analysis,” *Fire Safety Science — Proceedings of the Fourth International Symposium*, International Association for Fire Safety Science, 1994, pp. 971–982.

Notarianni, K. E., “Predicting the Response of Sprinklers and Detectors in Large Spaces,” extended abstracts from the SFPE Seminar “Large Fires: Causes and Consequences,” November 16–18, 1992, Dallas, Society for Fire Protection Engineers, Boston.

Rouse, H., Yih, C.S., and Humphreys, H. W., “Gravitational Convection from a Boundary Source,” *Tellus* 4, 201-210, 1952.

Tien, C. L., Lee, K. Y., and Stretton, A. J., “Radiation Heat Transfer,” Section 1, Chapter 4 of *SFPE Handbook of Fire Protection Engineering*, second edition 1995, pp. 1-65 to 1-79.

Troup, J. M. A., *Large Scale Fire Tests of Rack Stored Group A Plastics in Retail Operation Scenarios Protected by Extra Large Orifice (ELO) Sprinklers*, FMRC Serial No. J.I. 0X1R0.RR for Group A Plastics Committee, Factory Mutual Research Corp., Norwood, MA, November 1994.

Walton, W. D., and Notarianni, K. E., “A Comparison of Ceiling Jet Temperatures Measured in an Aircraft Hangar Tests Fire With Temperatures Predicted by the DETACT-QS and LAVENT Computer Models,” NISTIR 4947, National Institute of Standards and Technology, Gaithersburg MD, 1993.

Waterman, T. E., et al., *Fire Venting of Sprinklered Buildings*, IITRI Project J08385 for Venting Research Committee, IIT Research Institute, Chicago, IL 60616, July 1982.

Yokoi, S., “Study on the Prevention of Fire Spread Caused by Hot Upward Current,” Report No. 34, Building Research Institute, Ministry of Construction, Japanese Government, November 1960.

Yu, H. Z., and Stavrianidis, P., “The Transient Ceiling Flows of Growing Rack Storage Fires,” *Fire Safety Science — Proceedings of the Third International Symposium*, Elsevier Applied Science, London, 1991, pp. 281–290.

### **G.3 References for Extracts.**

The following documents are listed here to provide reference information, including title and edition, for extracts given throughout this standard as indicated by a reference in brackets [ ] following a section or paragraph. These documents are not a part of the requirements of this document unless also listed in Chapter 2 for other reasons.

**G.3.1 NFPA Publications.** National Fire Protection Association, 1 Batterymarch Park, P.O. Box 9101, Quincy, MA 02269-9101.

NFPA 33, *Standard for Spray Application Using Flammable or Combustible Materials*, 2000 editions.

*NFPA 72*®, *National Fire Alarm Code*®, 1999 edition.

NFPA 92B, *Guide For Smoke Management Systems in Malls, Atria, and Large Areas*, 2000 edition.

NFPA 220, *Standard on Types of Building Construction*, 1999 edition.

NFPA 318, *Standard for the Protection of Cleanrooms*, 2000 edition.

Appreciation must be extended to Dr. Gunnar Heskestad at the Factory Mutual Research Corporation for his major contribution to the theory applied in this standard, which is detailed in Annex B.

The 1985 edition again revised Chapter 6 on the subject of venting in sprinklered buildings. Test data from work done at the Illinois Institute of Technology Research, which had been submitted to the Committee as part of a public proposal, did not permit consensus to be developed on whether sprinkler control was impaired or enhanced by the presence of automatic roof vents of typical spacing and area. The revised wording of Chapter 6 encouraged the designer to use the available tools and data referenced in the document while the use of automatic venting in sprinklered buildings was under review.

The 1991 edition made minor changes to Chapter 6 to acknowledge that a design basis existed for using sprinklers and automatic heat venting together but that such had not received wide recognition.

The 1998 edition represented a complete revision of the guide. The rewrite deleted the previous tables that listed vent areas and incorporated engineering equations and referenced computer models, such as LAVENT and DETACT, to provide the designer with the necessary tools to develop vent designs based on performance objectives. This rewrite was based extensively on state-of-the-art technology published in the references. In many cases, the authors of these references participated in the task group's rewrite efforts.

The 2002 edition of NFPA 204 was converted from a guide to a standard, thus implementing mandatory requirements and updated language. The document was also updated to meet NFPA *Manual of Style* requirements.

### **Technical Committee on Smoke Management Systems**

**James A. Milke** *Chair*  
University of Maryland, MD [SE]

**Daniel L. Arnold** The RJA Group, Inc., GA [SE]

**Donald W. Belles** Koffel Associates, Inc., TN [M]  
Rep. American Architectural Manufacturers Association

**Jack B. Buckley**, Houston, TX [SE]

**Lydia A. Butterworth**, Smithsonian Institute, DC [U]

**Paul J. Carrafa**, Building Inspection Underwriters, Inc., NJ [E]

**Paul David Compton**, Colt International, Limited, England [M]

**Michael Earl Dillon**, Dillon Consulting Engineers, Inc., CA [SE]

**Douglas H. Evans**, Clark County Building Department, NV [E]

**Gunnar Heskestad**, FM Global, MA [I]

**Winfield T. Irwin**, Irwin Services, PA [M]  
Rep. North American Insulation Manufacturers Association

**John E. Kampmeyer**, Triad Fire Protection Engineering Corporation, PA [SE]  
Rep. National Society of Professional Engineers

**John H. Klote**, Fire and Smoke Consulting, VA [SE]

**Gary D. Lougheed**, National Research Council of Canada, Canada [RT]

**Francis J. McCabe**, Prefco Products, PA [M]

**Gregory R. Miller**, Code Consultants Inc., MO [SE]

**Harold E. Nelson**, Hughes Associates Inc., VA [SE]

**Dale Rammien**, Home Ventilating Institute, IL [M]  
Rep. Air Movement & Control Association Inc/International FireStop Council

**Todd E. Schumann**, Industrial Risk Insurers, IL [I]

**J. Brooks Semple**, Smoke/Fire Risk Management Inc., VA [SE]

**Lawrence J. Shudak**, Underwriters Laboratories Inc., IL [RT]

**Paul Simony**, Tristar Skylights, CA [M]

**James S. Slater**, System Sensor, IL [M]  
Rep. National Electrical Manufacturers Association

**Paul G. Turnbull**, Siemens Building Technologies, Inc., IL [M]

**Robert Van Becelaere**, Ruskin Manufacturing Division, MO [M]  
Rep. American Society of Mechanical Engineers

**Stacy R. Welch**, Marriott International, Inc., DC [U]

#### **Alternates**

**Craig Beyler**, Hughes Associates, Inc. MD [SE]  
(Alt. to H. E. Nelson)

**Richard J. Davis**, FM Global, MA [I]  
(Alt. to G. Heskestad)

**Henry F. Harrington**, Simplex Time Recorder Company, MA [M]  
(Alt. to J. S. Slater)

**Daniel J. Kaiser**, Underwriters Laboratories Inc., IL [RT]  
(Alt. to L. J. Shudak)

**Geraldine Massey**, Dillon Consulting Engineers, Inc., CA [SE]  
(Alt. to M. E. Dillon)

**James E. Richardson**, Colt International, Limited, England [M]  
(Alt. to P. D. Compton)

**Randolph W. Tucker**, The RJA Group, Inc., TX [SE]  
(Alt. to D. L. Arnold)

**Peter J. Gore Willse**, Industrial Risk Insurers, CT [I]  
(Alt. to T. E. Schumann)

**Michael L. Wolf**, Greenheck, WI [M]  
(Alt. to D. Rammien)

**Steven D. Wolin**, Code Consultants Inc., MO [SE]  
(Alt. to G. R. Miller)

### **Nonvoting**

**Bent A. Borresen**, Techno Consultants, Norway  
(Alt. to C. N. Madsen)

**E. G. Butcher**, Fire Check Consultants, England  
(Alt. to A. C. Parnell)

**Christian Norgaard Madsen**, Techno Consultants, Norway

**Alan Charles Parnell**, Fire Check Consultants, England

**Steven E. Younis**, NFPA Staff Liaison

**Committee Scope:** This Committee shall have primary responsibility for documents on the design, installation, testing, operation, and maintenance of systems for the control, removal, or venting of heat or smoke from fires in buildings.

*This list represents the membership at the time the Committee was balloted on the final text of this edition. Since that time, changes in the membership may have occurred. A key to classifications is found at the back of the document.*

NOTE: Membership on a committee shall not in and of itself constitute an endorsement of the Association or any document developed by the committee on which the member serves.

**NFPA 204**  
**Standard for**  
**Smoke and Heat Venting**  
**2002 Edition**

NOTICE: An asterisk (\*) following the number or letter designating a paragraph indicates that explanatory material on the paragraph can be found in Annex A.

A reference in brackets [ ] following a section or paragraph indicates material that has been extracted from another NFPA document. As an aid to the user, Annex G lists the complete title and edition of the source documents for both mandatory and nonmandatory extracts. Editorial changes to extracted material consist of revising references to an appropriate division in this document or the inclusion of the document number with the division number when the reference is to the original document. Requests for interpretations or revisions of extracted text shall be sent to the appropriate technical committee.

Information on referenced publications can be found in Chapter 2 and Annex G.

## **Chapter 1 Administration**

### **1.1 Scope.**

**1.1.1\*** This standard shall apply to the design of venting systems for the emergency venting of products of combustion from fires in buildings. The provisions of Chapters 4 through 10 shall apply to the design of venting systems for the emergency venting of products of combustion from fires in nonsprinklered, single-story buildings using both hand calculations and computer-based solution methods as provided in Chapter 9. Chapter 11 shall apply to venting in sprinklered buildings.

**1.1.2\*** This standard shall not specify under which conditions venting is to be provided or required.

**1.1.3** Where a conflict exists between a general requirement and a specific requirement, the specific requirement shall be applicable.

### **1.2 Purpose. (Reserved)**

### **1.3 Application.**

**1.3.1\*** This standard shall not apply to ventilation within a building designed for regulation of environmental air for personnel comfort, to regulation of commercial cooking operations, to regulation of odor or humidity in toilet and bathing facilities, or to regulation of cooling of production equipment or to venting for explosion pressure relief.

**1.3.2** This standard shall apply to building construction of all types.

**1.3.3** This standard shall apply to venting fires in building spaces with ceiling heights that permit the design fire plume and smoke layer to develop.

**1.3.4\*** This standard shall apply to situations in which the hot smoke layer does not enhance the burning rate of the fuel array. Vent designs developed with this standard shall

not be valid for those time intervals where smoke layer temperatures exceed 600°C.

**1.3.5\*** This standard shall not be valid for fires having heat release rates greater than  $Q_{feasible}$  as determined in accordance with the following equation:

$$(1.1) \quad Q_{feasible} = 12,000(z_s)^{5/2}$$

where:

$Q_{feasible}$  = feasible fire heat release rate (kW)

$z_s$  = height of the smoke layer boundary above the fire base (m)

**1.3.6\*** The engineering equations or computer-based models incorporated into this standard shall be used to calculate the time duration that the smoke layer boundary is maintained at or above the design elevation in a curtained area, relative to the design interval time.

#### **1.4 Retroactivity.**

**1.4.1** The provisions of this standard shall not be required to be applied retroactively.

**1.4.2** Where a system is being altered, extended, or renovated, the requirements of this standard shall apply only to the work being undertaken.

#### **1.5 Equivalency.**

Nothing in this standard is intended to prevent the use of systems, methods, or devices of equivalent or superior quality, strength, fire resistance, effectiveness, durability, and safety over those prescribed by this standard. Technical documentation shall be submitted to the authority having jurisdiction to demonstrate equivalency. The system, method, or device shall be approved for the intended purpose by the authority having jurisdiction.

#### **1.6 Units and Formulas.**

The following symbols define the variables in the equations used throughout the body of this standard:

$A$	=	area (of burnin g surfac e)
$A_i$	=	inlet area for fresh air, below design level of smoke

$A_v$	=	layer bound ary total vent area of all vents in a curtain ed area
$\alpha$	=	therma l diffusi vity,
$\alpha_g$	=	$k/P_c$ fire growth coeffic ient
$\beta$	=	exhaus t locatio n factor (dimen sionles s)
$c_p$	=	specifi c heat
$C_{d,v}$	=	vent discha rge coeffic ient
$C_{d,i}$	=	inlet discha rge coeffic ient
$d$	=	smoke layer depth
$d_c$	=	depth of draft curtain
$D$	=	base diamet er of the fire
$g$	=	acceler ation of gravity
$H$	=	ceiling

		height above base of fire
$h_c$	=	heat of combu stion
$h_g$	=	heat of gasific ation
$K$	=	fractio n of adiaba tic temper ature rise
$k$	=	therma l condu ctivity
$k_e \beta$	=	consta nt used in Equati on E.3
$k P_c$	=	therma l inertia thickn ess
$l$	=	mean flame height above the base of the fire
$L$	=	flame height above the base of the fire
$L_f$	=	flame length, measu red from leadin g edge of burnin g region
$L_v$	=	length of vent openin g in the longer directi

$\dot{m}^*$	=	on mass burnin g rate
$\dot{m}''$	=	mass burnin g rate per unit area
$\dot{m}_{\infty}''$	=	mass burnin g rate per unit area for an infini te diamet er pool
$\dot{m}_v$	=	mass flow rate throug h vent
$\dot{m}_p$	=	mass flow rate in the plume
$\dot{m}_{pL}$	=	mass flow rate in the plume at mean flame height ( $L$ )
$\dot{q}_i''$	=	incide nt heat flux per unit area
$Q$	=	total heat release rate
$Q''$	=	total heat release rate per

$Q_c$	=	unit floor area convec tive heat release rate = $\chi_c Q$
$Q_{feasible}$	=	feasibl e fire heat release rate (kW)
$r$	=	radius from fire axis
RTI	=	respon se time index $\tau_u^{1/2}$
$\tau$	=	time consta nt of heat- respon sive eleme nt for convec tive heatin g
$\rho$	=	densit y
$\rho_o$	=	ambie nt air densit y
$t$	=	time
$t_d$	=	time to detect or activat ion
$t_g$	=	growth time of fire
$t_{ig}$	=	time to ignitio n
$t_r$	=	design interva

$t_{sa}$	=	l time time to sprinkl er activat ion
$t_{vo}$	=	time to vent openin g
$\Delta T$	=	gas temper ature rise (from ambie nt) at detect or site
$\Delta T_a$	=	adiaba tic temper ature rise
$\Delta T_e$	=	temper ature rise (from ambie nt) of heat- respon sive eleme nt
$T$	=	smoke layer temper ature (K)
$T_o$	=	ambie nt air temper ature
$T_{ig}$	=	ignitio n temper ature
$T_s$	=	surfac e temper ature
$u$	=	gas velocit y at detect

$W_{min}$  = or site lateral fire spread by radiation  
 $W_s$  = largest horizontal dimension of fire  
 $W_v$  = width of vent opening in the shorter direction  
 $V$  = flame spread velocity  
 $\chi_c$  = convective fraction of total heat release rate (fraction carried as heat in plume above flames)  
 ) where  $\chi_c$  is a convective-heat fraction between 0.6 and 0.7  
 $\chi_r$  = radiant fraction

		fraction of total heat release rate
$y$	=	elevation of smoke layer boundary
$y_{ceil}$	=	elevation of ceiling
$y_{curt}$	=	elevation of bottom of draft curtain
$y_{fire}$	=	elevation of the base of the fire above the floor
$z_s$	=	height of the smoke layer boundary above base of fire
$z_{si}$	=	height of the smoke layer interface above the base of the fire
$z_o$	=	height of virtual origin above base of fire (below

base of  
fire, if  
negati  
ve)

## Chapter 2 Referenced Publications

### 2.1\* General.

The documents or portions thereof listed in this chapter are referenced within this standard and shall be considered part of the requirements of this document.

### 2.2 NFPA Publications.

National Fire Protection Association, 1 Batterymarch Park, P.O. Box 9101, Quincy, MA 02269-9101.

*NFPA 72*®, *National Fire Alarm Code*®, 1999 edition.

NFPA 92B, *Guide for Smoke Management Systems in Malls, Atria, and Large Areas*, 2000 edition.

NFPA 220, *Standard on Types of Building Construction*, 1999 edition.

NFPA 255, *Standard Method of Test of Surface Burning Characteristics of Building Materials*, 2000 edition.

NFPA 259, *Standard Test Method for Potential Heat of Building Materials*, 1998 edition.

### 2.3 Other Publications.

#### 2.3.1 ASTM Publication.

American Society for Testing and Materials, 100 Barr Harbor Drive, West Conshohocken, PA 19428-2959.

ASTM E 136, *Standard Test Method for Behavior of Materials in a Vertical Tube Furnace at 750°C*, 1996.

#### 2.3.2 FMRC Publication.

Factory Mutual Research Corporation, 1151 Boston-Providence Tpk., P.O. Box 9102, Norwood, MA 02061.

FM 4430, *Heat and Smoke Vents*, 1980.

#### 2.3.3 ICBO Publication.

International Conference of Building Officials, 5360 Workman Mill Road, Whittier, CA 90601.

UBC Standard 15-7, *Automatic Smoke and Heat Vents*, 1997.

#### 2.3.4 NIST Publications.

National Institute of Standards and Technology, 100 Bureau Dr., Gaithersburg, MD 20899-3460.

Link Actuated Vents (LAVENT), software.

DETECT-QS software.

DETECT-T2 software.

### **2.3.5 UL Publication.**

Underwriters Laboratories Inc., 333 Pfingsten Road, Northbrook, IL 60062.

UL 793, *Standard for Automatically Operated Roof Vents for Smoke and Heat*, 1997.

## **Chapter 3 Definitions**

### **3.1 General.**

The definitions contained in this chapter shall apply to the terms used in this standard. Where terms are not included, common usage of the term shall apply.

### **3.2 Official NFPA Definitions.**

**3.2.1\* Approved.** Acceptable to the authority having jurisdiction.

**3.2.2\* Authority Having Jurisdiction (AHJ).** The organization, office, or individual responsible for approving equipment, materials, an installation, or a procedure.

**3.2.3 Labeled.** Equipment or materials to which has been attached a label, symbol, or other identifying mark of an organization that is acceptable to the authority having jurisdiction and concerned with product evaluation, that maintains periodic inspection of production of labeled equipment or materials, and by whose labeling the manufacturer indicates compliance with appropriate standards or performance in a specified manner.

**3.2.4\* Listed.** Equipment, materials, or services included in a list published by an organization that is acceptable to the authority having jurisdiction and concerned with evaluation of products or services, that maintains periodic inspection of production of listed equipment or materials or periodic evaluation of services, and whose listing states that either the equipment, material, or service meets appropriate designated standards or has been tested and found suitable for a specified purpose.

**3.2.5 Shall.** Indicates a mandatory requirement.

**3.2.6 Should.** Indicates a recommendation or that which is advised but not required.

### **3.3 General Definitions.**

**3.3.1 Ceiling Jet.** A flow of hot smoke under the ceiling, extending radially from the point of fire plume impingement on the ceiling.

**3.3.2 Clear (Air) Layer.** The zone within a building containing air that has not been contaminated by the smoke produced from a fire in the building, and that is located

between the floor and the smoke layer boundary.

**3.3.3\* Clear Layer Interface.** The boundary between a smoke layer and smoke-free air.

**3.3.4 Continuously Growing Fires.** Fires that, if unchecked, will continue to grow over the design interval time.

**3.3.5 Curtained Area.** An area of a building that has its perimeter delineated by draft curtains, full height partitions, exterior walls, or any combinations thereof.

**3.3.6 Design Depth of the Smoke Layer.** The difference between the height of the ceiling and the minimum height of the smoke layer boundary above the finished floor level that meets design objectives.

**3.3.7 Design Fire.** The time-rate heat release history selected as the input for the calculations prescribed herein.

**3.3.8 Design Interval Time.** The duration of time for which a design objective is to be met, measured from the time of detector activation.

**3.3.9 Draft Curtain.** A solid material, beam, girder, or similar material or construction that is attached to the underside of the ceiling and that protrudes a limited distance downward and creates a reservoir for collecting smoke.

**3.3.10\* Effective Ignition.** The time at which a *t*-squared design fire starts.

**3.3.11 Fuel Array.** A collection and arrangement of materials that can support combustion.

**3.3.12 Heat Detector.** A fire detector that detects either abnormally high temperature or rate of temperature rise, or both. [ 72:1.4]

**3.3.13 Limited Combustible.** As applied to a material of construction, any material that does not meet the definition of noncombustible, as stated elsewhere in this section, and that, in the form in which it is used, has a potential heat value not exceeding 3,500 Btu/lb (8141 kJ/kg) when tested in accordance with NFPA 259, *Standard Test Method for Potential Heat of Building Materials*, and also meets one of the following subparagraphs (a) or (b). (a) Materials having a structural base of noncombustible material, with a surfacing not exceeding a thickness of  $\frac{1}{8}$  in. (3.2 mm) that has a flame spread rating not greater than 50, when tested in accordance with NFPA 255, *Standard Method of Test of Surface Burning Characteristics of Building Materials*. (b) Materials, in the form and thickness used and not described by (a) above, having neither a flame spread rating greater than 25 nor evidence of continued progressive combustion and having such composition that surfaces that would be exposed by cutting through the material in any plane have neither a flame spread rating greater than 25 nor evidence of continued progressive combustion, when tested in accordance with NFPA 255, *Standard Method of Test of Surface Burning Characteristics of Building Materials*. (NFPA 220, *Standard on Types of Building Construction*, Chapter 2.) [ 33:1.6]

**3.3.14 Limited-Growth Fires.** Fires that are not expected to grow beyond a predictable maximum heat release rate.

**3.3.15 Mechanical Smoke Exhaust System.** A dedicated or shared-duty fan system designed and suitable for the removal of heat and smoke.

**3.3.16 Noncombustible Material.** A material that, in the form in which it is used and under the conditions anticipated, will not ignite, burn, support combustion, or release flammable vapors, when subjected to fire or heat. Materials that are reported as passing ASTM E 136, *Standard Test Method for Behavior of Materials in a Vertical Tube Furnace at 750°C*, shall be considered noncombustible materials. [ 220:2.1]

### **3.3.17 Plastics.**

**3.3.17.1\* Class CC1 Plastics.** Materials that have a burning extent of 25 mm or less when tested at a nominal thickness of 0.152 mm (0.060 in.) or in the thickness intended for use.

**3.3.17.2\* Class CC2 Plastics.** Materials that have a burning rate of 1.06 mm/s or less when tested at a nominal thickness of 0.152 mm (0.060 in.), or in the thickness intended for use.

**3.3.18 Plugholing.** Exhaust of air from the clear layer below the smoke layer.

**3.3.19 Smoke.** The airborne solid and liquid particulates and gases evolved when a material undergoes pyrolysis or combustion, together with the quantity of air that is entrained or otherwise mixed into the mass. [ 318:1.4]

**3.3.20\* Smoke Layer.** The accumulated thickness of smoke below a physical or thermal barrier. [ 92B:1.4]

**3.3.21\* Smoke Layer Boundary.** An effective boundary centered in a transition zone between the dense portion of the smoke layer and the first indication of smoke.

**3.3.22 Vent.** A device or construction which, when activated, is an opening directly to the exterior at or near the roof level of a building that relies on the buoyant forces created by a fire to exhaust smoke and heat.

**3.3.23 Vent System.** A system used for the removal of smoke from a fire that utilizes manually or automatically operated heat and smoke vents at roof level and that exhausts smoke from a reservoir bounded by exterior walls, interior walls, or draft curtains to achieve the design rate of smoke mass flow through the vents, and that includes provision for makeup air.

## **Chapter 4 Fundamentals**

### **4.1\* Design Objectives.**

The design objectives to be achieved over the design interval time by a vent system design during a design fire or design fires shall include the following:

- (1) The minimum allowable smoke layer boundary height
- (2) The maximum allowable smoke layer temperature

### **4.2\* Design Basis.**

A design for a given building and its combustible contents and their distribution shall comprise selecting a design basis (limited-growth versus continuous-growth fire) and establishing the following parameters:

- (1) Layout of curtained areas
- (2) A draft curtain depth
- (3) Type detector and specific characteristics
- (4) Detector spacing
- (5) A design interval time,  $t_r$ , following detection for maintaining a clear layer (for continuous-growth fires)
- (6) Total vent area per curtained area
- (7) Distribution of individual vents
- (8) An air inlet area

### **4.3 Determination of Contents Hazard.**

**4.3.1** The determination of contents hazard shall take into account the fuel loading and the rate of heat release anticipated from the combustible materials or flammable liquids contained within the building.

**4.3.2** The heat release rate of the design fire shall be quantified in accordance with Chapter 8.

### **4.4 Venting.**

**4.4.1 Design Objectives.** In order to satisfy design objectives, a vent system shall be designed to slow, stop, or reverse the descent of a smoke layer produced by fire in a building, by exhausting smoke to the exterior.

#### **4.4.2\* Vent System Designs and Smoke Production.**

**4.4.2.1** Vent systems shall be designed in accordance with this standard by calculating the vent area required to achieve a mass rate of flow through the vents that equals the mass rate of smoke production.

**4.4.2.2** Vent system designs shall limit the descent of the smoke layer to the design elevation of the smoke layer boundary.

**4.4.2.3** Alternative vent system designs shall be permitted to be developed in accordance with this standard by calculating the vent area required to achieve a mass rate of flow through the vents that is less than the mass rate of smoke production, such that the descent of the smoke layer is slowed to meet the design objectives.

**4.4.3\* Vent Mass Flow.** Vent system designs shall be computed on the basis that the mass flow rate through a vent is determined primarily by buoyancy pressure.

### **4.5 Smoke Production.**

**4.5.1\* Base of the Fire.** For the purposes of the equations in this standard, the base of the fire shall be at the bottom of the burning zone.

**4.5.2\* Fire Size.** Burning and entrainment rates of possible fire scenarios shall be

considered before establishing the conditions of the design fire.

#### **4.5.3\* Entrainment.**

**4.5.3.1** The entrainment formulas specified in this standard shall be applied only to a single fire origin.

**4.5.3.2** Smoke entrainment relationships shall be valid for axisymmetric plumes.

**4.5.3.3** For line-like fires where a long, narrow plume is created by a fuel or storage array, the smoke production calculated in accordance with this standard shall be valid only if the height of the smoke layer boundary above the base of the fire ( $z_s$ ) is greater than  $5 W_s$ , where  $W_s$  is the largest horizontal dimension of the fire.

**4.5.3.4\*** If  $z_s$  is smaller than  $5 W_s$ , the smoke production rates calculated in accordance with this standard shall be increased by the factor  $[5 W/(z_s)]^{2/3}$ .

**4.5.4\* Virtual Origin.** Predicted plume mass flow above the top of the flame shall take into account the virtual origin,  $z_o$ , of the fire as determined in 9.2.3.2.

#### **4.6 Vent Flows.**

##### **4.6.1\* Buoyancy and Vent Flow.**

**4.6.1.1** Flow through a vent shall be calculated on the basis of buoyancy pressure difference, assuming that no pressure is contributed by the expansion of gases.

**4.6.1.2** Wind effects shall not be taken into account.

##### **4.6.2\* Inlet Air.**

**4.6.2.1** Predicted vent flows shall take into account the area of inlet air openings.

**4.6.2.2** Inlet air shall be introduced below the smoke layer boundary.

**4.6.2.3** Wall and ceiling leakage above the smoke layer boundary in the curtained area shall not be included in vent flow calculations. (*See Chapter 6 for information on air inlets.*)

## **Chapter 5 Vents**

### **5.1 Listed Vents.**

Normally, closed vents shall be listed and labeled in accordance with UL 793, *Standard for Automatically Operated Roof Vents for Smoke and Heat*; UBC Standard 15-7, *Automatic Smoke and Heat Vents*; Factory Mutual Research Standard 4430, *Heat and Smoke Vents*; or other approved, nationally recognized standards.

### **5.2 Vent Design Constraints.**

**5.2.1\*** The means of vent actuation shall be selected with regard to the full range of expected ambient conditions.

**5.2.2\*** Vents shall consist of a single unit (vent), in which the entire unit (vent) opens fully with the activation of a single detector, or multiple units (vents) in rows or arrays (ganged vents) in which the units (vents) open simultaneously with the activation of a single heat detector, a fusible link, a smoke detector, a sprinkler waterflow switch, or other means of detection to satisfy the venting requirements for a specific hazard.

**5.2.3\*** Where the hazard is localized, vents shall open directly above such hazard.

**5.2.4** Vents, and their supporting structure and means of actuation, shall be designed so that they can be inspected visually after installation.

### **5.3 Methods of Operation.**

**5.3.1\*** Normally, closed vents shall be designed to open automatically in a fire to meet design objectives or to comply with performance objectives or requirements.

**5.3.2\*** Vents, other than thermoplastic drop-out vents, shall be designed to fail in the open position such that failure of a vent-operating component results in an open vent.

**5.3.3** Vents shall be opened using gravity or other approved opening force.

**5.3.4** The opening mechanism shall not be prevented from opening the vent by snow, roof debris, or internal projections.

**5.3.5\*** All vents shall be designed to open by manual means. Means of opening shall be either internal or external, as approved by the authority having jurisdiction.

**5.3.6** Vents designed for remote operation shall utilize approved fusible links and shall also be capable of actuation by an electric power source, heat-responsive device, or other approved means.

**5.3.7** Vents designed to activate by smoke detection, sprinkler waterflow, or other activation methods external to the vent shall be approved in accordance with Section 5.1.

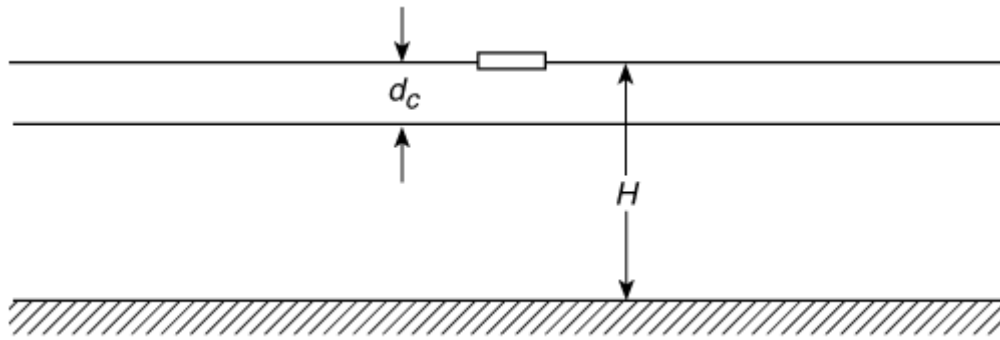
### **5.4 Dimensions and Spacing of Vents.**

**5.4.1** The dimensions and spacing of vents shall meet the requirements of 5.4.1.1 and 5.4.1.2 to avoid plugholing.

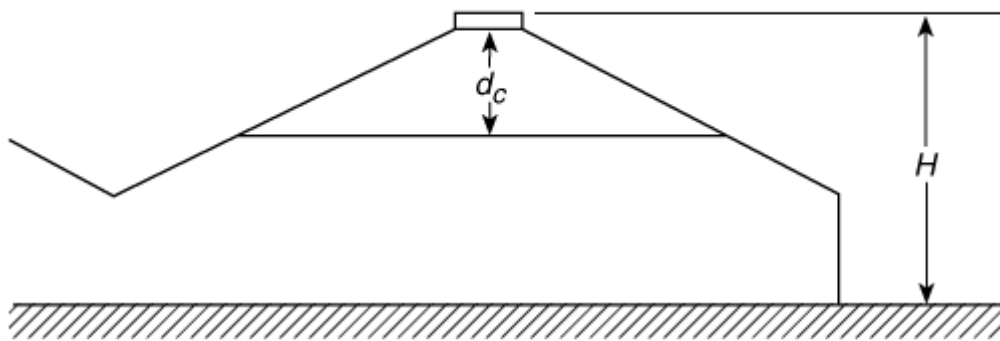
**5.4.1.1** The area of a unit vent shall not exceed  $2d^2$ , where  $d$  is the design depth of the smoke layer.

**5.4.1.2\*** For vents with  $L_v/W_v > 2$ , the width,  $W_v$ , shall not exceed the design depth of the smoke layer,  $d$ .

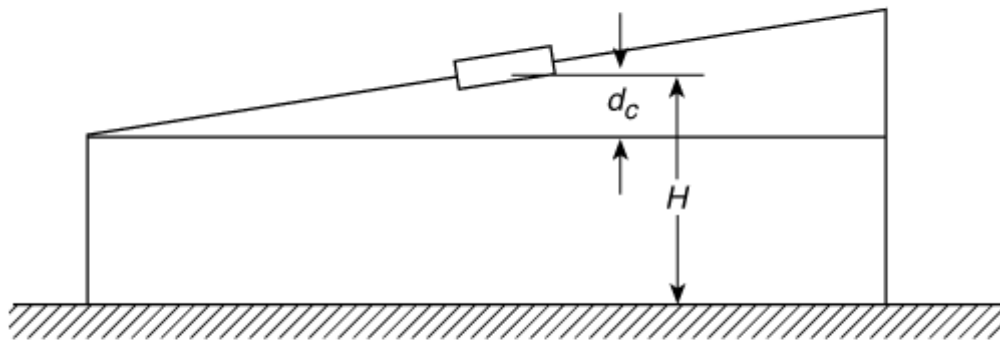
**5.4.2** In plan view, the center-to-center spacing of vents within a curtained area shall not exceed  $2.8H$ , where  $H$  is the ceiling height as shown in Figure 5.4.2, parts (a) through (d).



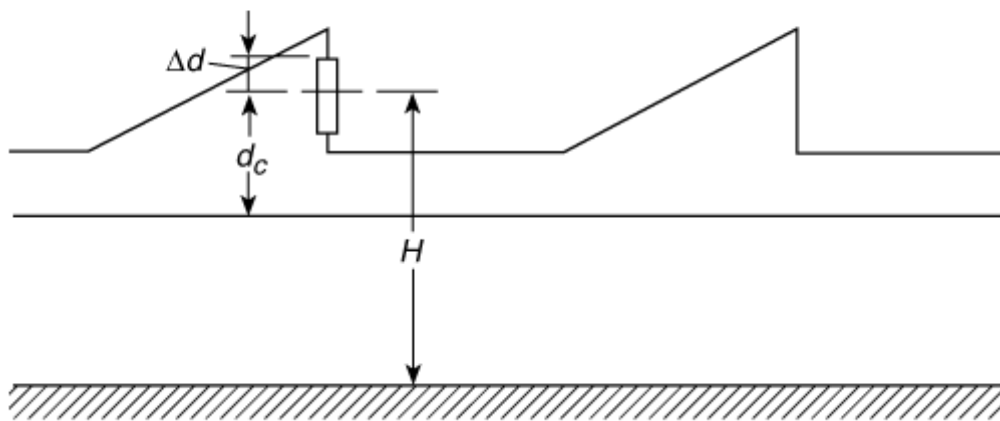
(a) Flat roof



(b) Gabled roof



(c) Sloped roof



(d) Sawtooth roof

**FIGURE 5.4.2 Measurement of Ceiling Height ( $H$ ) and Curtain Board Depth ( $d_c$ ).**

**5.4.3** The spacing of vents, in plan view, shall be such that the horizontal distance from any point on a wall or draft curtain to the center of the nearest vent, within a curtained area, does not exceed  $1.4 H$ .

**5.4.4** The total vent area per curtained area shall be sized to meet the design objectives and the performance objectives relative to the design fire, determined in accordance with Chapter 8.

**5.5 Mechanical Smoke Exhaust Systems.**

Mechanical smoke exhaust systems shall be designed in accordance with Chapter 10.

## Chapter 6 Air Inlets

**6.1\* General.**

Air inlets shall be provided for supplying makeup air for vent systems.

**6.2 Construction.**

Air inlets consisting of louvers, doors, dampers, windows, shutters, or other approved openings shall be designed and constructed to provide passage of outdoor air into the building.

**6.3 Location.**

Air inlets shall be installed in external walls of the building below the height of the design level of the smoke layer boundary and shall be clearly identified or marked as air inlets.

**6.4 Installation.**

**6.4.1** Materials of construction and methods of installation for air inlets shall resist expected extremes of temperature, wind, building movement, rain, hail, snow, ice, sunlight, corrosive environment, internal and external dust, dirt, and debris.

**6.4.2** The means of air inlet actuation shall be selected with regard to the full range of expected ambient conditions.

**6.4.3** To satisfy the vent system requirements, air inlets shall consist of one of the following:

- (1) A single unit (air inlet) in which the entire unit (air inlet) opens fully with the activation of a single detector
- (2) Multiple units (air inlets) in rows or arrays (ganged air inlets) in which the units (air inlets) open simultaneously with the activation of a single heat detector, a fusible link, a smoke detector, a sprinkler waterflow switch, or other means of detection to satisfy the vent system requirements

**6.4.4** Air inlets and their supporting structures and means of actuation shall be designed

such that they can be inspected visually after installation.

### **6.5 Methods of Operation.**

**6.5.1** Air inlets shall be either constantly open or automatically placed in the open position after a fire is detected.

**6.5.2** Air inlets shall be designed to open in a fire to meet design objectives or to comply with performance objectives or requirements.

**6.5.3** Air inlets shall be designed to fail in the open position such that failure of an air inlet–operating component results in an open air inlet.

**6.5.4** Air inlets shall be opened using an approved means as the opening force.

**6.5.5** Air inlet opening mechanisms shall not be prevented from opening the air inlet by snow, debris, or internal projections.

**6.5.6** Operating mechanisms for air inlets shall be jam-proof, corrosion-resistant, dust resistant, and resistant to pressure differences arising from applicable positive or negative loading resulting from environmental conditions, process operations, overhead doors, or traffic vibrations.

**6.5.7** Air inlets designed for remote operation shall be activated by approved devices and shall be capable of actuation by an electrical power source, heat-responsive device, or other approved means.

### **6.6 Dimensions and Spacing of Air Inlets.**

**6.6.1** The total inlet area per curtained area shall be sized to meet the design objectives and the performance objectives or requirements specified relative to the design fire, determined in accordance with Chapter 8.

**6.6.2** One inlet area shall be permitted to serve more than one curtained area.

## **Chapter 7 Draft Curtains**

### **7.1\* General.**

In large, open areas, draft curtains shall be provided for prompt activation of vents and to increase vent effectiveness by containing the smoke in the curtained area and increasing the depth of the smoke layer.

### **7.2\* Construction.**

**7.2.1** Draft curtains shall be constructed of noncombustible or limited-combustible materials in buildings of Type I or Type II construction as defined by NFPA 220, *Standard on Types of Building Construction*, and shall be designed and constructed to resist the passage of smoke.

**7.2.2** Draft curtains shall remain in place and shall confine smoke when exposed to the maximum predicted temperature for the design interval time, assuming a design fire in

close proximity to the draft curtain.

### 7.3 Location and Depth.

**7.3.1\*** Draft curtains shall extend vertically downward from the ceiling the minimum distance required so that the value of  $d_c$ , as shown in Figure 5.4.2, is a minimum of 20 percent of the ceiling height,  $H$ , measured as follows:

- (1) For flat roofs and sawtooth roofs with flat ceiling areas, from the ceiling to the floor
- (2) For sloped roofs, from the center of the vent to the floor

**7.3.2** Where there are differing vent heights,  $H$ , each vent shall be calculated individually.

### 7.4 Spacing.

**7.4.1\*** Neither the length nor the width of a curtained area shall exceed 8 times the ceiling height.

**7.4.2\*** Where draft curtains extend to a depth of less than 30 percent of the ceiling height, the distance between draft curtains shall be not less than one ceiling height.

## Chapter 8 The Design Fire

### 8.1\* General.

**8.1.1** The design fire shall be selected from among a number of challenging candidate fires, consistent with the building and its intended use, considering all of the following factors that tend to increase the challenge:

- (1) A low-level flame base (usually floor level)
- (2) Increasing fire growth rate
- (3) Increasing ultimate heat release rate in the design interval time

**8.1.2** The candidate fire that produces a vent system design meeting the design objectives for all candidate fires shall be selected as the design fire.

### 8.2 Steady (Limited-Growth) Fires.

**8.2.1** For steady fires, or fires that do not develop beyond a maximum size, the required vent area per curtained area shall be calculated based on the maximum calculated heat release rate ( $Q$  and  $Q_c$ ), the associated distance from the fire base to the design elevation of the smoke layer boundary ( $z_s$ ), and the predicted fire diameter ( $D$ ).

**8.2.2\*** Steady fires shall be permitted to include special-hazard fires and fires in occupancies with concentrations of combustibles separated by aisles of sufficient width to prevent the spread of fire by radiation beyond the initial fuel package or initial storage array.

**8.2.3** The minimum aisle width required to prevent lateral fire spread by radiation,  $W_{min}$ , shall be calculated for radiant heat flux from a fire based on an ignition flux of 20 kW/m<sup>2</sup> in accordance with the following equation:

$$(8.1) \quad W_{min} = 0.042Q_{max}^{1/2}$$

where:

$W_{min}$  = minimum aisle width required to prevent lateral fire spread by radiation (m)

$Q_{max}$  = maximum anticipated heat release rate (kW)

**8.2.4** The fire diameter,  $D$ , shall be the diameter of a circle having the same area as the floor area of the fuel concentration.

**8.2.5** The heat release rate shall be the heat release rate per unit area times the floor area of the fuel concentration, using the maximum storage height above the fire base and associated heat release rate.

**8.2.6\*** The heat release rate per unit area shall be determined from Table 8.2.6. To establish estimates for other than specified heights, the heat release rate per unit area has been shown to be directly proportional to the storage height.

**Table 8.2.6**  
**Unit Heat**  
**Release**  
**Rate for**  
**Commodities**

Commodity	Heat Release Rate (kW per m <sup>2</sup> of floor area)*
Wood pallets, stacked 0.46 m high (6%–12% moisture)	1,420

Wood 4,000  
pallets,  
stacked  
1.52  
m high  
(6%–  
12%  
moisture)

Wood 6,800  
pallets,  
stacked  
3.05  
m high  
(6%–  
12%  
moisture)

Wood 10,200  
pallets,  
stacked  
4.88  
m high  
(6%–  
12%  
moisture)

Mail 400  
bags,  
filled,  
stored  
1.52 m  
high

Carton 1,700  
s,  
compartmented,  
stacked  
4.5  
m high

PE 8,500  
letter  
trays,  
filled,  
stacked  
1.5  
m high  
on cart

PE 2,000  
trash  
barrels  
in  
carton  
s,  
stacke  
d 4.5  
m high  
FRP 1,400  
showe  
r stalls  
in  
carton  
s,  
stacke  
d 4.6  
m high  
PE 6,200  
bottles  
packed  
in  
compa  
rtment  
ed  
carton  
s,  
stacke  
d 4.5  
m high  
PE 2,000  
bottles  
in  
carton  
s,  
stacke  
d 4.5  
m high  
PU 1,900  
insulat  
ion  
board,  
rigid  
foam,  
stacke  
d 4.6  
m high

PS jars 14,200  
packed  
in  
compa  
rtment  
ed  
carton  
s,  
stacke  
d 4.5  
m high  
PS 5,400  
tubs  
nested  
in  
carton  
s,  
stacke  
d 4.2  
m high  
PS toy 2,000  
parts  
in  
carton  
s,  
stacke  
d 4.5  
m high  
PS 3,300  
insulat  
ion  
board,  
rigid  
foam,  
stacke  
d 4.2  
m high  
PVC 3,400  
bottles  
packed  
in  
compa  
rtment  
ed  
carton  
s,  
stacke  
d 4.5  
m high

PP 4,400  
tubs  
packed  
in  
compa  
rtment  
ed  
carton  
s,  
stacke  
d  
4.5 m  
high  
PP and 6,200  
PE  
film in  
rolls,  
stacke  
d  
4.1 m  
high  
Methy 740  
l  
alcoho  
l  
Gasoli 2,500  
ne  
Kerose 1,700  
ne  
Fuel 1,700  
oil, no.  
2

---

Note:  
PE =  
polyethy  
lene; PP  
=  
polypro  
pylene;  
PS =  
polystyr  
ene; PU  
=  
polyuret  
hane;  
PVC =  
polyviny  
l  
chloride;  
FRP =  
fiberglas  
s-  
reinforc  
ed  
polyeste  
r  
\* Heat  
release  
rate per  
unit  
floor  
area of  
fully  
involved  
combust  
ibles,  
based on  
negligibl  
e  
radiative  
feedbac  
k from  
the  
surround  
ings and  
100  
percent  
combust  
ion  
efficienc  
y.

### **8.3 Growing (Continuous-Growth) Fires.**

**8.3.1\*** A *t*-squared fire growth shall be assumed as shown in Figure 8.3.1 and in accordance with the following equation:

$$(8.2) \quad Q = \alpha_g t^2$$

where:

$Q$  = heat release rate of fire (kW)

$t$  = time from effective ignition following an incubation period (s)

$t_g$  = time at which the fire exceeds an intermediate size of 1000 kW (s)

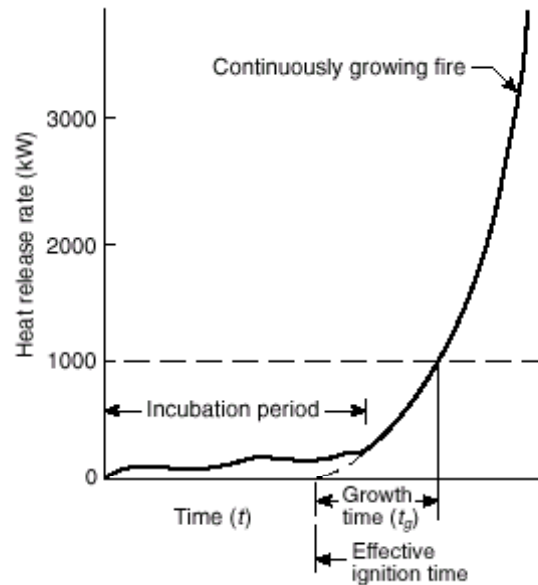


**FIGURE 8.3.1 Conceptual Illustration of Continuous-Growth Fire.**

**8.3.2\*** A  $t$ -squared fire growth shall be permitted to be expressed in terms of a fire growth coefficient,  $\alpha_g$ , in lieu of growth time,  $t_g$ , as follows:

$$(8.3) \quad Q = \alpha_g t^2$$

where:

$Q$  = heat release rate of fire (kW)

$t$  = time (s)

$\alpha_g$  = fire growth coefficient (kW/s<sup>2</sup>)

**8.3.3** The instantaneous heat release rate per unit height of the storage array shall be considered to be constant, regardless of the storage height. Accordingly, for different storage heights, the growth time,  $t_g$ , shall be calculated as being inversely proportional to the square root of the storage height, and the fire growth coefficient,  $\alpha_g$ , shall be calculated as being directly proportional to the storage height. (See Annex F.1.)

**8.3.4** For fuel configurations that have not been tested, the procedures in Chapter 8 shall be applied.

**8.3.5\*** The vent system shall maintain the smoke boundary layer above the design

elevation from the time of effective ignition until the end of the design interval time,  $t_r$ , where  $t_r$  is measured from the time of detection,  $t_d$ .

**8.3.6** The heat release rate at the end of the design interval time shall be calculated in accordance with the following equation:

$$(8.4) \quad Q = 1000 \left( \frac{t_r + t_d}{t_g} \right)^2$$

where:

$Q$  = heat release rate (kW)

$t_r$  = time at end of design interval (s)

$t_d$  = time of detection (s)

$t_g$  = time at which fire exceeds 1000 kW (s)

**8.3.7** The end of the design interval time,  $t_r$ , shall be selected to correspond to the design objectives as determined for the specific project design.

**8.3.8** The instantaneous diameter of the fire needed for the calculation of  $L$  and  $z_o$  shall be calculated from the instantaneous heat release rate,  $Q$ , and data on the heat release rate per unit floor area,  $Q''$ , where  $Q''$  is proportional to storage height in accordance with the following equation:

$$(8.5) \quad D = \left( \frac{4Q}{\pi Q''} \right)^{1/2}$$

where:

$D$  = instantaneous fire diameter (m)

$Q$  = instantaneous heat release rate (kW)

$Q''$  = heat release rate per unit floor area (kW/m<sup>2</sup>)

## Chapter 9 Sizing Vents

### 9.1\* General.

**9.1.1\*** The design vent area in a curtained area shall equal the vent area required to meet the design objectives for the most challenging fire predicted for the combustibles within the curtained area.

**9.1.2** Vent areas shall be determined using hand calculations in accordance with Section 9.2 or by use of a computer-based model in accordance with Section 9.3.

**9.1.3** The design fire used in the evaluation of a proposed vent design in accordance with Section 9.1 shall be determined in accordance with Chapter 8.

9.1.4\* Vent systems shall be designed specifically for the hazard of each curtained area in a building.

## 9.2 Hand Calculations.

9.2.1 Vent System Designs. Vent systems, other than those complying with Section 9.3, shall be sized and actuated to meet design objectives in accordance with Section 9.2.

### 9.2.2 Design Concepts.

9.2.2.1\* Equilibrium shall be assumed as illustrated in Figure 9.2.2.1, where symbols are as defined in Section 1.6.

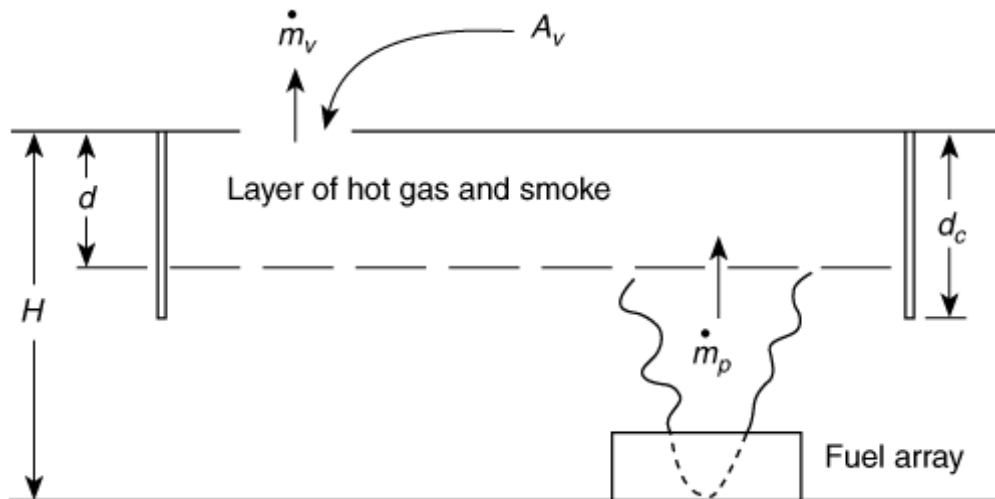


FIGURE 9.2.2.1 Schematic of Venting System.

9.2.2.2 The smoke layer boundary shall be at or above the bottom of the draft curtains.

9.2.2.3 At equilibrium, the mass flow rate into the smoke layer shall be equal to the mass flow rate out of the vent or vents ( $\dot{m}_p = \dot{m}_v$ ).

### 9.2.3 Mass Flow Rate in Plume.

9.2.3.1\* The mean flame height shall be calculated in accordance with the following equation:

$$(9.1) \quad L = -1.02D + 0.235 Q^{2/5}$$

where:

$L$  = mean flame height above the base of the fire (m)

$D$  = base diameter of fire (m)

$Q$  = total heat release rate (kW)

9.2.3.2 The virtual origin,  $z_o$ , is the effective point source of the fire plume and shall be calculated in accordance with the following equation:

$$(9.2) \quad z_o = 0.083Q^{2/5} - 1.02D$$

where:

$Q$  = total heat release rate (kW)

$D$  = base diameter of fire (m)

**9.2.3.3** Smoke entrainment relationships shall be applicable to axisymmetric plumes.

**9.2.3.4** For line-like fires where a long, narrow plume is created by a fuel or storage array, the smoke production calculated in accordance with this standard shall be applicable only if the height of the smoke layer boundary above the base of the fire ( $z_s$ ) is greater than or equal to 4 times the largest horizontal dimension of the fire,  $W_s$ .

**9.2.3.5** If  $z_s$  is smaller than  $4 W_s$ , the smoke production rates calculated in accordance with this standard shall be increased by the factor  $[4 W_s/(z_s)]^{2/3}$ .

**9.2.3.6** When the mean flame height,  $L$ , is below the smoke layer boundary ( $L < z_s$ ), the mass flow rate in the fire plume shall be calculated in accordance with the following equation:

$$(9.3) \quad \dot{m}_p = \left[ 0.071 Q_c^{1/3} (z_s - z_o)^{5/3} \right] \left[ 1 + 0.027 Q_c^{2/3} (z_s - z_o)^{-5/3} \right]$$

where:

$\dot{m}_p$  = mass flow rate in the plume (kg/s)

$Q_c$  = convective heat release rate =  $0.7 Q$  (kW)

$z_s$  = height of the smoke layer boundary above the base of the fire (m)

$z_o$  = height of virtual origin above the base of the fire (if below the base of the fire,  $z_o$  is negative) (m)

**9.2.3.7** When the mean flame height ( $L$ ) is equal to or above the smoke layer boundary ( $L \geq z_s$ ), the mass flow rate shall be calculated in accordance with the following equation:

$$(9.4) \quad \dot{m}_p = (0.0056Q_c) \frac{z_s}{L}$$

where:

$\dot{m}_p$  = mass flow rate in the plume (kg/s)

$Q_c$  = convective heat release rate =  $0.7 Q$  (kW)

$z_s$  = height above the base of the fire (m)

$L$  = mean flame height (m)

**9.2.3.8** The base of the fire shall be the lowest point of the fuel array.

## 9.2.4 Mass Flow Rate Through Vents.

**9.2.4.1\*** The mass flow through the vent shall be calculated in accordance with the following equation:

$$\dot{m}_v = \frac{C_{d,v} A_v}{\sqrt{1 + \frac{C_{d,v}^2 A_v^2}{C_{d,i}^2 A_i^2} \left( \frac{T_o}{T} \right)}} \sqrt{(2\rho_o^2 g d)} \sqrt{\frac{T_o (T - T_o)}{T^2}}$$

(9.5)

where:

- $\dot{m}_v$  = mass flow through vent (kg/s)
- $C_{d,v}$  = vent discharge coefficient
- $C_{d,i}$  = inlet discharge coefficient
- $A_v$  = vent area (m<sup>2</sup>)
- $A_i$  = inlet area (m<sup>2</sup>)
- $T_o$  = ambient temperature (K)
- $T$  = smoke layer temperature (K)
- $\rho_o$  = ambient density (kg/m<sup>3</sup>)
- $g$  = acceleration due to gravity (9.81 m/s<sup>2</sup>)
- $d$  = smoke layer depth (m)

**9.2.4.2\*** The discharge coefficients for the vents and inlets used shall be those provided by the vent or inlet manufacturer. If no data are available, the discharge coefficient shall be taken to be 0.6 for vents unless an analysis or data acceptable to the authority having jurisdiction are provided by the designer to validate the use of an alternative value.

**9.2.4.3** The smoke layer temperature,  $T$ , used in 9.2.4.1 shall be determined from the following equation:

$$T = T_o + \frac{KQ_c}{c_p \dot{m}_p}$$

(9.6)

where:

- $T_o$  = ambient temperature (K)
- $T$  = smoke layer temperature (K)
- $K$  = fraction of convected energy contained in the smoke layer gases (*see 9.2.4.4*)
- $Q_c$  = convective heat release rate (kW)
- $c_p$  = specific heat of the smoke layer gases (kJ/kg-K)
- $\dot{m}_p$  = plume mass flow rate (kg/s) (*see 9.2.3*)

**9.2.4.4** The value of  $K$  used in Equation 9.6 shall be 0.5, unless an analysis acceptable to the authority having jurisdiction is provided by the designer to validate the use of an alternative value.

## 9.2.5 Required Vent Area and Inlet Area.

**9.2.5.1 Vent Area.** The required vent area shall be the minimum total area of all vents within a curtained area required to be open to prevent the smoke from descending below the design level of the smoke layer boundary when used in conjunction with the required inlet area.

**9.2.5.2 Inlet Area.** The required inlet area shall be the minimum total area of all inlets required to be open to prevent the smoke from descending below the design level of the smoke layer boundary when used in conjunction with the required vent area(s).

**9.2.5.3 Area Calculation.** The required vent area and inlet areas shall be calculated by equating the plume mass flow rate determined in 9.2.3 and the vent mass flow rates determined in 9.2.4.

### 9.2.5.4 Detection and Activation.

**9.2.5.4.1\*** Detection, for the purpose of automatically actuating vents, shall be by one of the following methods:

- (1) By either by heat or smoke at the vent location
- (2) By activation of fire protection systems
- (3) By heat or smoke detectors installed on a regular matrix within the curtained area in accordance with *NFPA 72*<sup>®</sup>, *National Fire Alarm Code*<sup>®</sup>
- (4) By other approved means shown to meet design objectives

**9.2.5.4.2** For calculating both the detection time,  $t_d$ , of the first detector to operate and the detection time,  $t_{vo}$ , of the detector controlling the actuation of the last vent to operate in a curtained area prior to the end of the design interval time, the location of the design fire shall be assumed to be the farthest distance possible from both the first and last detectors to operate the vents within the curtained area.

**9.2.5.4.2.1\*** Detection times for heat detectors or fusible links shall be determined in accordance with *NFPA 72*, *National Fire Alarm Code*.

**9.2.5.4.3** Detection times for smoke detectors shall be determined as the time to reach a certain temperature rise,  $\Delta T$ , at activation. In the case of continuous-growth,  $t$ -squared fires, gas temperatures shall be determined in accordance with the following equation, where  $\Delta T$  is assumed to be 0 when the numerator of the first bracket is zero or negative:

$$(9.7) \quad \Delta T = \frac{3575}{t_g^{4/5} H^{3/5}} \left[ \frac{t / (c_g^{2/5} H^{4/5}) - 0.442(1 + r/H)}{1 + 1.65r/H} \right]^{4/3}$$

where:

$H$  = ceiling height above the base of the fire (m)

$r$  = radius from fire axis (m)

$T$  = temperature (°C)

$t_g$  = fire growth time (s)

**9.2.5.4.3.1\*** The temperature rise for activation shall be based on dedicated tests, or the equivalent, for the combustibles associated with the occupancy and the detector model to be installed.

**9.2.5.4.3.2** Where the data described in 9.2.5.4.3.1 are not available, a minimum temperature rise of 20°C shall be used.

#### **9.2.5.4.4 Detection Computer Programs.**

**9.2.5.4.4.1\*** As an alternate to the calculations specified in 9.2.5.4.2, DETACT-T2 shall be permitted to be used to calculate detection times in continuous growth and  $t$ -squared fires.

**9.2.5.4.4.2\*** As an alternative to the calculations specified in 9.2.5.4.2, DETACT-QS, shall be permitted to be used to calculate detection times in fires of any fire growth history.

**9.2.5.4.4.3** Other computer programs determined to calculate detection times reliably shall be permitted to be used when approved by the authority having jurisdiction.

### **9.3 Models.**

**9.3.1** Vents, other than vent systems designed in accordance with Section 9.2, shall be sized and actuated to meet design objectives in accordance with Section 9.3.

**9.3.2** The computer model LAVENT or other approved mathematical models shall be used to assess the effects of the design fire and to establish that a proposed vent system design meets design objectives. (*See Annex F.2.*)

**9.3.3** When models other than LAVENT are used, evidence shall be submitted to demonstrate efficacy of the model to evaluate the time-varying events of a fire and to calculate the effect of vent designs reliably in terms of the design objectives.

**9.3.4** The design fire used in the evaluation of a proposed vent system design in accordance with Section 9.3 shall be determined in accordance with Chapter 8.

## **Chapter 10 Mechanical Smoke Exhaust Systems**

### **10.1 General.**

**10.1.1\*** Mechanical smoke exhaust systems shall be permitted in lieu of the vent systems described in Chapter 9.

**10.1.2** Mechanical smoke exhaust systems and vent systems shall not serve the same curtained area.

**10.1.3** Mechanical smoke exhaust systems shall be designed in accordance with Section 10.2 through Section 10.4.

### **10.2 Exhaust Rates.**

Exhaust rates per curtained area shall be not less than the mass plume flow rates,  $\dot{m}_p$ , as determined in accordance with 9.2.3.

### 10.3 Fire Exposure.

**10.3.1** Mechanical smoke exhaust systems shall be capable of functioning under the expected fire exposure.

**10.3.2** The temperature of the smoke layer shall be determined in accordance with 9.2.4.3 and 9.2.4.4.

### 10.4\* Plugholing.

To avoid plugholing, the maximum mass flow rate extracted using a single exhaust inlet shall not exceed  $\dot{m}_{max}$ , determined in accordance with the following equation:

$$(10.1) \quad \dot{m}_{max} = 3.13\beta d^{5/2} [(T_s - T_o)/T_s]^{1/2} [T_o/T_s]^{1/2}$$

where:

$\dot{m}_{max}$  = maximum mass rate of exhaust without plugholing (kg/s)

$T_s$  = temperature of the smoke layer (K)

$T_o$  = ambient air temperature (K)

$d$  = depth of smoke layer below exhaust inlet (m)

$\beta$  = exhaust location factor (dimensionless)

### 10.5 Intake Air.

Intake air shall be provided to make up air required to be exhausted by the mechanical smoke exhaust systems. (See Chapter 6 for additional information on the location of air inlets.)

## Chapter 11 Venting in Sprinklered Buildings

### 11.1 Design.

Where provided, the design of venting for sprinklered buildings shall be based on a performance analysis acceptable to the authority having jurisdiction, demonstrating that the established objectives are met. (See Annex F.3.)

## Chapter 12 Inspection and Maintenance

### 12.1\* General.

Smoke and heat venting systems and mechanical smoke exhaust systems shall be inspected and maintained in accordance with Chapter 12.

## **12.2\* Requirements.**

**12.2.1 Mechanically Opened Vents.** Mechanically opened vents shall be provided with manual release devices that allow direct activation to facilitate inspection, maintenance, and replacement of actuation components.

**12.2.2 Thermoplastic Drop-Out Vents.** Thermoplastic drop-out vents do not allow nondestructive operation; however, inspection of installed units shall be conducted to ensure that the units are installed in accordance with the manufacturer's instructions and that all components are in place, undamaged, and free of soiling, debris, and extraneous items that might interfere with the operation and function of the unit.

**12.2.3 Inspection and Maintenance.** The inspection and maintenance of multiple-function vents shall ensure that other functions do not impair the intended fire protection operation.

## **12.3 Inspection, Maintenance, and Acceptance Testing.**

### **12.3.1 Inspection Schedules.**

**12.3.1.1** A written inspection schedule and procedures for inspection and maintenance shall be developed.

**12.3.1.2** Inspection programs shall provide written notations of the date and time of inspections and of discrepancies found.

**12.3.1.3** All deficiencies shall be corrected immediately.

**12.3.1.4\*** Vents shall be inspected and maintained in an operating condition in accordance with Chapter 12.

### **12.3.2 Mechanically Opened Vents.**

**12.3.2.1** An acceptance performance test and inspection of all mechanically opened vents shall be conducted immediately following installation to establish that all operating mechanisms function properly and that installation is in accordance with this standard and the manufacturer's specifications.

**12.3.2.2\*** Mechanically opened vents shall be inspected and subjected to an operational test annually, following the manufacturer's recommendations.

**12.3.2.3\*** All pertinent characteristics of performance shall be recorded.

**12.3.2.4** Special mechanisms, such as gas cylinders, thermal sensors, or detectors, shall be checked annually or as specified by the manufacturer.

### **12.3.3 Thermoplastic Drop-Out Vents.**

**12.3.3.1\*** An acceptance inspection of all thermoplastic drop-out vents shall be conducted immediately after installation and shall include verification of compliance with the manufacturer's drawings and recommendations by visual examination.

**12.3.3.2\*** Thermoplastic drop-out vents shall be inspected annually in accordance with 12.4.2 and the manufacturer's recommendations.

**12.3.3.3** Changes in appearance, damage to any components, fastening security, weather

tightness, and the adjacent roof and flashing condition shall be noted at the time of inspection, and any deficiency shall be corrected.

**12.3.3.4** Any soiling, debris, or encumbrances that could impair the operation of the vent shall be promptly removed without causing damage to the vent.

**12.3.4 Inlet Air Sources.** Where required for the operation of vent systems, intake air sources shall be inspected at the same frequency as vents.

## **12.4 Conduct and Observation of Operational Tests.**

### **12.4.1 Mechanically Opened Vents and Air Inlets.**

**12.4.1.1** Mechanically opened vents and air inlets shall be operated during tests by simulating actual fire conditions.

**12.4.1.2** The restraining cable at the heat-responsive device (or other releasing device) shall be disconnected, releasing the restraint and allowing the trigger or latching mechanism to operate.

**12.4.1.3\*** When the heat-responsive device restraining cable for mechanically opened vents or air inlets is under tension, observation shall be made of its whip and travel path to determine any possibility that the vent, building construction feature, or service piping could obstruct complete release. Any interference shall be corrected by removal of the obstruction, enclosure of cable in a suitable conduit, or other appropriate arrangement.

**12.4.1.4** Following any modification, the unit shall be retested for evaluation of adequacy of corrective measures.

**12.4.1.5** Latches shall release smoothly and the vent or air inlet shall open immediately and move through its design travel to the fully opened position without any assistance and without any problems such as undue delay indicative of a sticking weather seal, corroded or unaligned bearings, or distortion binding.

**12.4.1.6** Manual releases shall be tested to verify that the vents and air inlets operate as designed.

**12.4.1.7** All operating levers, latches, hinges, and weather-sealed surfaces shall be examined to determine conditions, such as deterioration and accumulation of foreign material. An operational test shall be conducted after corrections are completed, when conditions are found to warrant corrective action.

**12.4.1.8** Following painting of the interior or exterior of vents and air inlets or the addition of sealants or caulking, the units shall be opened and inspected to check for paint, sealants, or caulking that causes the parting surfaces to adhere to each other.

**12.4.1.9** Heat-responsive devices coated with paint or other substances that could affect their response shall be replaced with devices having an equivalent temperature and load rating.

### **12.4.2 Thermoplastic Drop-Out Vents.**

**12.4.2.1** All weather-sealed surfaces on thermoplastic drop-out vents shall be examined to

determine any adverse conditions, such as any indication of deterioration and accumulation of foreign material. Any adverse condition that interferes with normal vent operation, such as caulking or sealant bonding the drop-out vent to the frame, shall be corrected.

**12.4.2.2** Following painting of the interior or exterior of the frame or flashing of the vents, the units shall be inspected for paint adhering surfaces together; any paint that interferes with normal operation shall be removed or the vent shall be replaced with a new, listed and labeled unit having comparable operating characteristics.

**12.4.2.3** Manual releases shall be tested annually.

### **12.4.3 Inspection, Maintenance, and Testing of Mechanical Smoke-Exhaust Systems.**

#### **12.4.3.1 Component Testing.**

**12.4.3.1.1** The operational testing of each individual system component of the mechanical smoke-exhaust system shall be performed as each component is completed during construction.

**12.4.3.1.2** It shall be documented in writing that each individual system component's installation is complete and that the component has been tested and found to be functional.

#### **12.4.3.2 Acceptance Testing.**

**12.4.3.2.1** Acceptance tests shall be conducted to demonstrate that the mechanical smoke-exhaust system installation complies with and meets the design objectives and is functioning as designed.

**12.4.3.2.2** Documentation from component system testing shall be available for review during final acceptance testing.

**12.4.3.2.3** If standby power has been provided for the operation of the mechanical smoke-exhaust system, the acceptance testing shall be conducted while on both normal and standby power.

**12.4.3.2.4** Acceptance testing shall be performed on the mechanical smoke-exhaust system as follows by completing the following steps:

- (1) Activate the mechanical smoke-exhaust system.
- (2) Verify and record the operation of all fans, dampers, doors, and related equipment.
- (3) Measure fan exhaust capacities, air velocities through inlet doors and grilles, or at supply grilles if there is a mechanical makeup air system.

**12.4.3.2.5** Operational tests shall be performed on the applicable part of the smoke-exhaust system wherever there are system changes and modifications.

**12.4.3.2.6** Upon completion of acceptance testing, a copy of all operational testing documentation shall be provided to the owner and shall be maintained and made available for review by the authority having jurisdiction.

#### **12.4.3.3 Periodic Testing.**

**12.4.3.3.1** Mechanical smoke-exhaust systems shall be tested semiannually by persons

who are knowledgeable in the operation, testing, and maintenance of the systems.

**12.4.3.3.2** The results of the tests shall be documented and made available for inspection.

**12.4.3.3.3** Tests shall be conducted under standby power where applicable.

#### **12.4.3.4 Exhaust System Maintenance.**

**12.4.3.4.1** During the life of the building, maintenance shall be performed to ensure that mechanical smoke-exhaust systems will perform their intended function under fire conditions.

**12.4.3.4.2** Maintenance of the systems shall include the testing of all equipment, including initiating devices, fans, dampers, and controls.

**12.4.3.4.3** Equipment shall be maintained in accordance with the manufacturer's recommendations.

#### **12.4.3.5 Inspection Schedule.**

**12.4.3.5.1** A written inspection schedule and procedures for inspection and maintenance for mechanical smoke-exhaust systems shall be developed.

**12.4.3.5.2** Inspection programs shall provide written notations of date and time of inspections and for discrepancies found.

**12.4.3.5.3** All system components shall be inspected semiannually in conjunction with operational tests.

**12.4.3.5.4** Any deficiencies noted in the system components or smoke-exhaust system performance shall be corrected immediately.

#### **12.5 Air Inlets.**

**12.5.1** Air inlets necessary for operation of smoke and heat vents or mechanical smoke-exhaust systems shall be maintained clear and free of obstructions.

**12.5.2** Operating air inlet louvers, doors, dampers, and shutters shall be examined and operated to assure movement to fully open positions.

**12.5.3** Operating equipment shall be maintained and lubricated as necessary.

#### **12.6 Ice and Snow Removal.**

Ice and snow shall be removed from vents promptly, following any accumulation.

## **Chapter 13 Design Documentation**

### **13.1\* Documentation Required.**

All of the following documents shall be generated by the designer during the design process:

- (1) Design brief

- (2) Conceptual design report
- (3) Detailed design report
- (4) Operations and maintenance manual

**13.1.1 Design Brief.** The design brief shall contain a statement of the goals and objectives of the vent system and shall provide the design assumptions to be used in the conceptual design.

**13.1.1.1** The design brief shall include, as a minimum, all of the following:

- (1) System performance goals and design objectives (*see Section 4.1 and 4.4.1*)
- (2) Performance criteria (including design tenability criteria, where applicable)
- (3) Building characteristics (height, area, layout, use, ambient conditions, other fire protection systems)
- (4) Design basis fire(s) (*see 4.5.2 and Chapter 8*)
- (5) Design fire location(s)
- (6) Identified design constraints
- (7) Proposed design approach

**13.1.1.2** The design brief shall be developed in the first stage of the design process to assure that all stakeholders understand and agree to the goals, objectives, design fire, and design approach, so that the conceptual design can be developed on an agreed-upon basis. Stakeholders shall include, as a minimum, the building owner and the authority having jurisdiction.

**13.1.2 Conceptual Design Report.** The conceptual design report shall provide the details of the conceptual design, based upon the design brief, and shall document the design calculations.

**13.1.2.1** The conceptual design shall include, as a minimum, all of the following design elements and the technical basis for the design elements:

- (1) Areas of curtained spaces
- (2) Design depth of the smoke layer and draft curtain depth
- (3) Detection method, detector characteristics, and spacing
- (4) Design interval time (if applicable)
- (5) Vent size and number per curtained area, method of vent operation, and vent spacing
- (6) Inlet vent area(s), location(s), and operation method

**13.1.2.2** The conceptual design report shall include all design calculations performed to establish the design elements, all design assumptions, and all building use limitations that arise out of the system design.

### **13.1.3 Detailed Design Report.**

**13.1.3.1** The detailed design report shall provide documentation of the vent system as it is to be installed.

**13.1.3.2** The detailed design report shall include, as a minimum, all of the following:

- (1) Vent and draft curtain specifications
- (2) Inlet and vent operation system specifications
- (3) Detection system specifications
- (4) Detailed inlet, vent, and draft curtain siting information
- (5) Detection and vent operation logic
- (6) Systems commissioning procedures

**13.1.4 Operations and Maintenance Manual.** The operations and maintenance manual shall provide to the building owner the requirements to ensure the intended operation of the vent system over the life of the building.

**13.1.4.1** The procedures used in the initial commissioning of the vent system shall be described in the manual, as well as the measured performance of the system at the time of commissioning.

**13.1.4.2** The manual shall describe the testing and inspection requirements for the system and system components and the required frequency of testing. *(See Chapter 12 for testing frequency.)*

**13.1.4.3** The manual shall describe the critical design assumptions used in the design and shall provide limitations on the building and its use that arise out of the design assumptions and limitations.

**13.1.4.4** Copies of the operations and maintenance manual shall be provided to the owner and to the authority having jurisdiction.

**13.1.4.5** The building owner shall be responsible for all system testing and shall maintain records of all periodic testing and maintenance using the operations and maintenance manual.

**13.1.4.6** The building owner shall be responsible for providing a copy of the operations and maintenance manual, including testing results, to all tenants of the space protected by the vent system.

**13.1.4.7** The building owner and tenants shall be responsible for limiting the use of the space in a manner consistent with the limitations provided in the operations and maintenance manual.

## **Annex A Explanatory Material**

*Annex A is not a part of the requirements of this NFPA document but is included for informational purposes only. This annex contains explanatory material, numbered to*

*correspond with the applicable text paragraphs.*

**A.1.1.1** This standard incorporates engineering equations (hand calculations) and references models to provide a designer with the tools to develop vent system designs. The designs are based on selected design objectives, stated in 4.4.1, related to specific building and occupancy conditions. Engineering equations are included for calculating vent flows, smoke layer depths, and smoke layer temperatures, based on a prescribed burning rate. Examples using the hand calculations and the LAVENT (Link-Activated VENTs) computer model are presented in Annex D.

Previous editions of this document have included tables listing vent areas based on preselected design objectives. These tables were based on the hot upper layer at 20 percent of the ceiling height. Different layer depths were accommodated by using a multiplication factor. Draft curtain and vent spacing rules were set. Minimum clear visibility times were related to fire growth rate, ceiling height, compartment size, curtain depth, and detector activation times, using engineering equations.

The following list provides a general description of the significant phenomena that occur during a fire when a fire-venting strategy is implemented:

- (1) Due to buoyancy, hot gases rise vertically from the combustion zone and flow horizontally below the roof until blocked by a vertical barrier (a wall or draft curtain), thus forming a layer of hot gases below the roof.
- (2) The volume and temperature of gases to be vented are a function of the fire's rate of heat release and the amount of air entrained into the buoyant plume produced.
- (3) As the depth of the layer of hot gases increases, the layer temperature continues to rise and the vents open.
- (4) The operation of vents within a curtained area enables some of the upper layer of hot gases to escape and thus slows the thickening rate of the layer of hot gases. With sufficient venting area, the thickening rate of the layer can be arrested and even reversed. The rate of discharge through a vent of a given area is primarily determined by the depth of the layer of hot gases and the layer temperature. Adequate quantities of replacement inlet air from air inlets located below the hot upper layer are needed if the products of combustion-laden upper gases are to be exhausted according to design. See Figure A.1.1.1(a) for an illustration of the behavior of fire under a vented and curtained roof, and Figure A.1.1.1(b) for an example of a roof with vents.

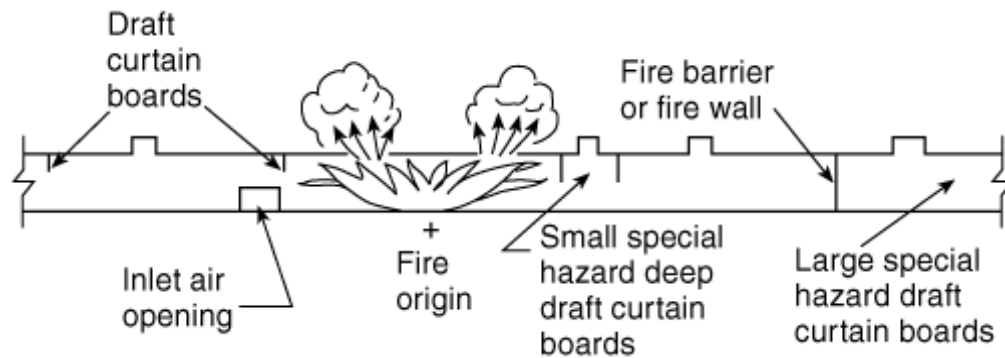


**FIGURE A.1.1.1(a) Behavior of Combustion Products Under Vented and Curtained Roof.**



**FIGURE A.1.1.1(b) View of Roof Vents on Building.**

The majority of the information provided in this standard applies to nonsprinklered buildings. A limited amount of guidance is provided in Chapter 11 for sprinklered buildings.

The provisions of this standard can be applied to the top story of multiple-story buildings. Many features of these provisions would be difficult or impracticable to incorporate into the lower stories of such buildings.

**A.1.1.2** The decision whether to provide venting in a building depends on design objectives set by a building owner or occupant or on local building code and fire code requirements.

**A.1.3.1** See NFPA 90A, *Standard for the Installation of Air-Conditioning and Ventilating Systems*, for ventilation to regulate environmental air for personnel comfort. See NFPA 96, *Standard for Ventilation Control and Fire Protection of Commercial Cooking Operations*, for regulation of commercial cooking operations. See NFPA 68, *Guide for Venting of Deflagrations*, for venting for explosion pressure relief.

**A.1.3.4** The distance from the fire base to the smoke layer boundary,  $z_s$ , is a dominant

variable and should be considered carefully. Additionally, some design situations can result in smoke layer temperatures, as expressed in Equation 9.6 (with  $K = 0.5$ ), that exceed  $600^{\circ}\text{C}$ . In such cases, the radiation from the smoke layer can be sufficient to ignite all of the combustibles under the curtained area at this temperature, and perhaps in the adjacent area, which is unacceptable.

**A.1.3.5** The feasibility of roof venting should be questioned when the heat release rate approaches values associated with ventilation control of the burning process (i.e., where the fire becomes controlled by the inlet air replacing the vented hot gas and smoke). Ventilation-controlled fires might be unable to support a clear layer.

To maintain a clear layer, venting at heat release rates greater than  $Q_{feasible}$  necessitates vent areas larger than those indicated by the calculation scheme provided in this standard.

**A.1.3.6** Large, undivided floor areas present extremely difficult fire-fighting problems because the fire department might need to enter these areas in order to combat fires in central portions of the building. If the fire department is unable to enter because of the accumulation of heat and smoke, fire-fighting efforts might be reduced to an application of hose streams to perimeter areas while fire continues in the interior. Windowless buildings also present similar fire-fighting problems. One fire protection tool that can be a valuable asset for fire-fighting operations in such buildings is smoke and heat venting.

An appropriate design time facilitates such activities as locating the fire, appraising the fire severity and its extent, evacuating the building, and making an informed decision on the deployment of personnel and equipment to be used for fire fighting.

**A.2.1** Some of these documents might also be referenced in this standard for specific informational purposes and are therefore also listed in Annex G.

**A.3.2.1 Approved.** The National Fire Protection Association does not approve, inspect, or certify any installations, procedures, equipment, or materials; nor does it approve or evaluate testing laboratories. In determining the acceptability of installations, procedures, equipment, or materials, the authority having jurisdiction may base acceptance on compliance with NFPA or other appropriate standards. In the absence of such standards, said authority may require evidence of proper installation, procedure, or use. The authority having jurisdiction may also refer to the listings or labeling practices of an organization that is concerned with product evaluations and is thus in a position to determine compliance with appropriate standards for the current production of listed items.

**A.3.2.2 Authority Having Jurisdiction (AHJ).** The phrase “authority having jurisdiction,” or its acronym AHJ, is used in NFPA documents in a broad manner, since jurisdictions and approval agencies vary, as do their responsibilities. Where public safety is primary, the authority having jurisdiction may be a federal, state, local, or other regional department or individual such as a fire chief; fire marshal; chief of a fire prevention bureau, labor department, or health department; building official; electrical inspector; or others having statutory authority. For insurance purposes, an insurance inspection department, rating bureau, or other insurance company representative may be the authority having jurisdiction. In many circumstances, the property owner or his or her designated agent assumes the role of the authority having jurisdiction; at government installations, the commanding officer or departmental official may be the authority having jurisdiction.

**A.3.2.4 Listed.** The means for identifying listed equipment may vary for each organization concerned with product evaluation; some organizations do not recognize equipment as listed unless it is also labeled. The authority having jurisdiction should utilize the system employed by the listing organization to identify a listed product.

**A.3.3.3 Clear Layer Interface.** See Figure A.3.3.3 for a description of the clear layer interface, smoke layer, and smoke layer boundary.

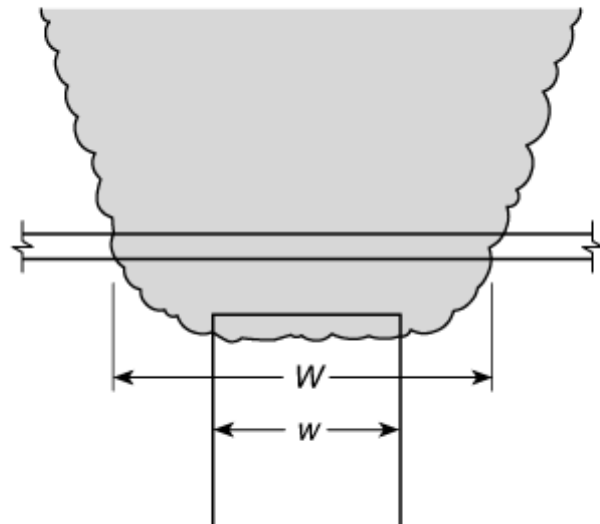
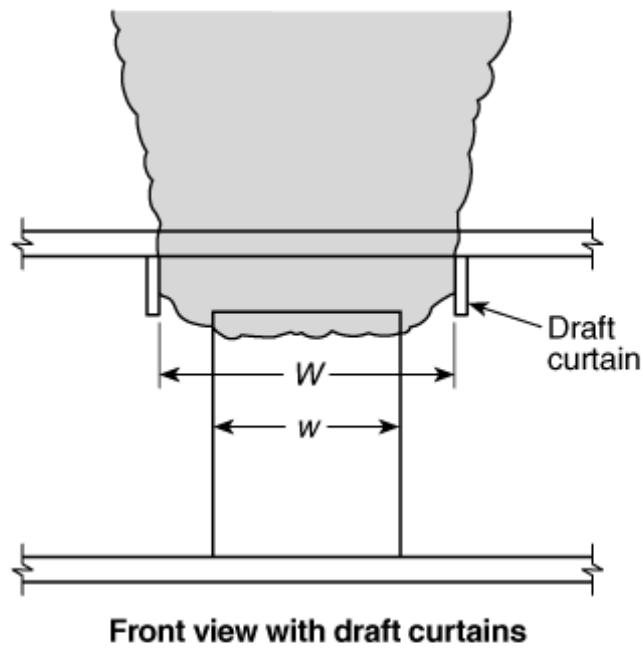
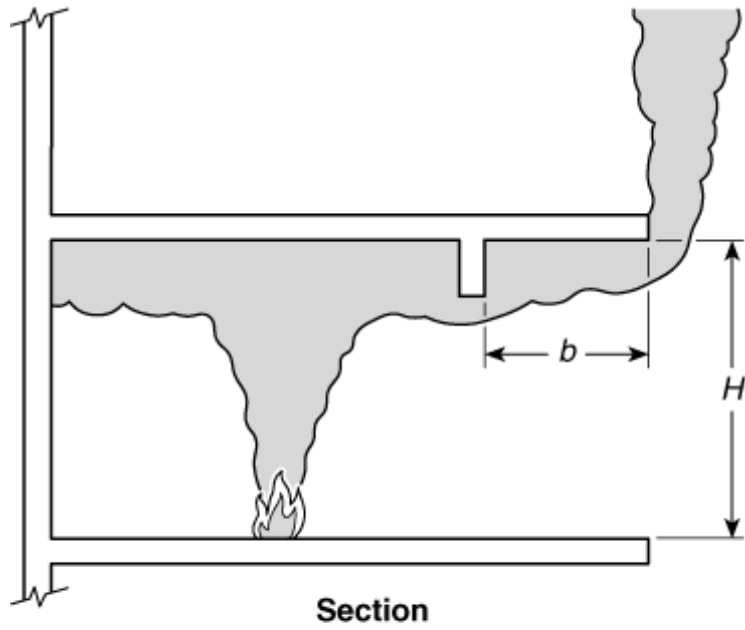


### **FIGURE A.3.3.3 Smoke Layer.**

**A.3.3.10 Effective Ignition.** See Figure 8.3.1 for a conceptual illustration of continuous fire growth and effective ignition time.

**A.3.3.17.1 Class CC1 Plastics.** Burning extent can be determined in accordance with ASTM D 635, *Test Method for Rate of Burning and/or Extent and Time of Burning of Self-Supporting Plastics in a Horizontal Position*.

**A.3.3.17.2 Class CC2 Plastics.** Burning rate can be determined in accordance with ASTM D 635, *Test Method for Rate of Burning and/or Extent and Time of Burning of Self-Supporting Plastics in a Horizontal Position*.

**A.3.3.20 Smoke Layer.** See Figure A.3.3.3 for a description of the clear layer interface, smoke layer, and smoke layer boundary.

**A.3.3.21 Smoke Layer Boundary.** See Figure A.3.3.3 for a description of the clear layer interface, smoke layer, and smoke layer boundary.

**A.4.1** Design objectives for a vent system can include one or more of the following goals:

- (1) To provide occupants with a safe path of travel to a safe area
- (2) To facilitate manual fire fighting
- (3) To reduce the damage to buildings and contents due to smoke and hot gases

**A.4.2** Tests and studies provide a basis for the division of occupancies into classes, depending on the fuel available for contribution to fire. Wide variation is found in the quantities of combustible materials in the many kinds of buildings and areas of buildings.

**A.4.4.2** The heat release rate of a fire, the fire diameter, and the height of the clear layer above the base of the fire are major factors affecting the production of smoke.

**A.4.4.3** Mass flow through a vent is governed mainly by the vent area and the depth of the smoke layer and its temperature. Venting becomes more effective with smoke temperature differentials between ambient temperature and an upper layer of approximately 110°C or higher. Where temperature differences of less than 110°C are expected, vent flows might be reduced significantly; therefore, consideration should be given to using powered exhaust. NFPA 92B, *Guide for Smoke Management Systems in Malls, Atria, and Large Areas*, should be consulted for guidance for power venting at these lower temperatures.

The vent designs in this standard allow the fire to reach a size such that the flame plume enters the smoke layer. Flame height may be estimated using Equation 9.1.

**A.4.5.1** The rate of smoke production depends on the rate of air entrainment into a column of hot gases produced by and located above a fire. Entrainment is affected by the fire diameter and rate of heat release, and it is strongly affected by the distance between the base of the fire and the point at which the smoke plume enters the smoke layer.

**A.4.5.2** Because smoke production is related to the size of a fire, it follows that, all factors being equal, larger fires produce more smoke. Entrainment, however, is strongly affected by the distance between the base of a fire and the bottom of the hot layer. The base of the fire (where combustion and entrainment begin) should be selected on the basis of the worst

case. It is possible for a smaller fire having a base near the floor to produce more smoke than a larger fire with a base at a higher elevation. Air entrainment is assumed to be limited to the clear height between the base of the fire and the bottom of the hot layer. The buoyant plume associated with a fire produces a flow into the hot upper layer. As the plume impinges on the ceiling, the plume turns and forms a ceiling jet. The ceiling jet flows radially outward along the ceiling.

**A.4.5.3** Where the possibility of multiple fires and, therefore, multiple plumes exists, smoke production rates increase beyond the rate predicted for a single plume for a fire of equivalent output. Multiple fires are beyond the scope of this standard.

**A.4.5.3.4** The factor  $[5 W_s / z_s]^{2/3}$  is an estimate, below a height of  $5 W_s$ , of the mass flow rate in a line plume [Rouse et al. 1952] in ratio to the mass flow rate in an axisymmetric plume from a point source (approximately  $0.071 Q_c^{1/3} z^{5/3}$  from Equation 9.3). There is evidence that plumes from rectangular/line sources become similar to those of axisymmetric sources beginning at a height of approximately  $5 W_s$  [Yokoi 1960]. For lower heights, it has been assumed that mass flows are approximately the same as in plumes from line sources.

**A.4.5.4** Plume mass flow above the flame level is based on the concept that, except for absolute scales, the shapes of velocity and temperature profiles at the mean flame height are invariable. This concept leads to an expression for mass flow above the flames that involves the so-called *virtual origin*, a point source from which the plume above the flames appears to originate. The virtual origin might be above or below the base of the fire.

**A.4.6.1** It is assumed that openings exist to the outside and therefore no pressure results from the expansion of gases. Also, wind effects are not taken into account because wind might assist or interfere with vent flows, depending on specific circumstances. It is also assumed that the fire environment in a building space is divided into two zones — a hot upper layer and a relatively cool, clear (comparatively free of smoke) lower region. When a fire grows to a size approaching ventilation-limited burning, the building might no longer maintain a clear lower region, and this standard would no longer be applicable. Finally, caution must be exercised when using this standard for conditions under which the upper-gas-layer temperature approaches 600°C, because flashover might occur within the area. When a fire develops to flashover or ventilation-limited burning, the relationships provided in this standard are not applicable.

Buoyancy pressure is related to the depth of the hot layer, the absolute temperature of the hot layer, the temperature rise above ambient of the hot layer, and the density of the ambient air. The mass rate of flow of hot gases through a vent is a function of vent area, layer depth, and hot layer temperature. The temperature of the hot layer above ambient affects mass flow through a vent. Maximum flow occurs at temperature differences of approximately 300°C above ambient. Flows at other temperature differentials are diminished, as shown in Figure A.4.6.1.

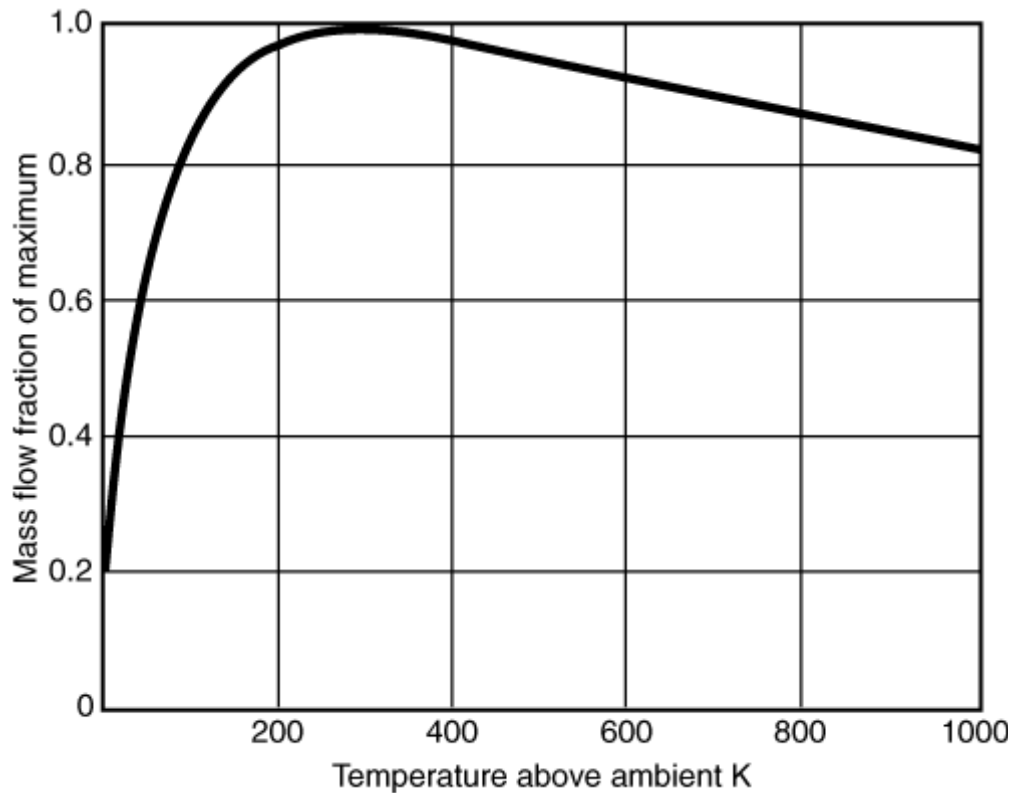


**FIGURE A.4.6.1 Effect of Temperature on Mass Flow Through a Vent.**

**A.4.6.2** To function as intended, a building venting system needs sufficiently large fresh air inlet openings at low levels. It is essential that a dependable means for admitting or supplying inlet air be provided promptly after the first vent opens.

**A.5.2.1** Compatibility between the vent-mounting elements (e.g., holding power, electrochemical interaction, wind lift, building movement) and the building structure to which they are attached needs to be ensured.

**A.5.2.2** To avoid inadvertent operation, it is important that the actuating means be selected with regard to the full range of expected ambient conditions.

**A.5.2.3** Dip tanks or discrete solvent storage areas are examples of localized hazards where the vents are to be located directly above such hazard.

**A.5.3.1** An automatic mechanism for opening the roof vents is stipulated for effective release of heat, smoke, and gaseous by-products. The means of automatic vent actuation must take the anticipated fire into consideration, and an appropriate means of opening vents should be used. If design objectives cannot be met using heat-actuated devices, smoke detectors with appropriate linkages to open vents or other devices that respond more quickly should be considered for use.

**A.5.3.2** Latching mechanisms should be jam-proof, corrosion-resistant, dust-resistant, and resistant to pressure differences arising from applicable positive or negative loading resulting from environmental conditions, process operations, overhead doors, or traffic vibrations.

**A.5.3.5** The location of the manual device must be coordinated with tactics of the reporting

fire department.

**A.5.4.1.2** See Figure 5.4.2 for the measurement of ceiling height and curtain board depth.

**A.6.1** The simplest method of introducing makeup air into the space is through direct openings to the outside, such as doors and louvers, which can be opened upon system activation. Such openings can be coordinated with the architectural design and can be located as required below the design smoke layer. For locations having mechanical smoke exhaust systems where such openings are impractical, a powered supply system could be considered. This could possibly be an adaptation of the building's HVAC system if capacities, outlet grille locations, and velocities are suitable. For such systems, means should be provided to prevent supply systems from operating until exhaust flow has been established, to avoid pressurization of the fire area. For those locations where climates are such that the damage to the space or contents could be extensive during testing or frequent inadvertent operation of the system, consideration should be given to heating the makeup air. See NFPA 92B, *Guide for Smoke Management Systems in Malls, Atria, and Large Areas*, for additional information on mechanical systems.

**A.7.1** A draft curtain is intended to be relatively smoke tight. The function of a draft curtain is to intercept the ceiling jet and the entrained smoke produced by a fire in the building. The curtain should prevent the smoke from spreading along the underside of the roof deck to areas of the building located beyond the draft curtain and should create a hot smoke layer that develops buoyancy forces sufficient to exhaust the smoke through the vent openings in the roof. A full-height partition or wall, including an exterior wall, can serve as a draft curtain.

**A.7.2** Materials suitable for use as draft curtains include steel sheeting, cementitious panels, and gypsum board.

**A.7.3.1** If  $d_c$  exceeds 20 percent of  $H$ ,  $H - d_c$  should be not less than 3 m. For Figure 5.4.2(d), this concept is valid where  $\Delta d / d_c$  is much less than 1.

Consideration should be given to minimizing of the expected smoke layer depth with respect to the occupancy. Such arrangement can allow the smoke layer to be maintained above the top of equipment or storage, thus maximizing visibility and reducing nonthermal damage to contents. For buildings of limited height, it can also allow the designer to utilize the primary structural frame to act as a draft curtain (if solid webbed) or support one (if open webbed), thus reducing costs.

Also, in a transient situation, prior to achieving equilibrium mass flow, if the smoke layer extends below the top of equipment or storage, that volume displaced by equipment or storage should be subtracted from available space for the smoke layer to accumulate, or the smoke layer depth will extend below that estimated.

**A.7.4.1** To ensure that vents remote from the fire within the curtained compartment are effective, the distance between draft curtains or between walls must be limited.

**A.7.4.2** From reanalysis of this issue based on Delichatsios [1981], Heskestad and Delichatsios [1978], and Koslowski and Motevalli [1994].

**A.8.1** Chapter 8 presents techniques for predicting the heat release rate of various fuel

arrays likely to be present in buildings where smoke and heat venting is a potential fire safety provision. It primarily addresses the estimation of fuel concentrations found in storage and manufacturing locations. NFPA 92B, *Guide for Smoke Management Systems in Malls, Atria, and Large Areas*, addresses the types of fuel arrays more common to the types of building situations covered by that document. The methods provided in Chapter 8 for predicting the rate of heat release are based on “free burning” conditions, in which no ceiling or smoke layer effects are involved.

**A.8.2.2** The minimum aisle width to prevent lateral spread by radiation,  $W_{min}$  in Equation 8.1, is based on Alpert and Ward [1984]. The values produced by Equation 8.1 can be produced from the following equation if  $X_r$  is assumed to be 0.5:

$$(A.8.1) \quad \dot{q}_i'' = \frac{X_r}{4\pi r^2}$$

**A.8.2.6** The heat release rate is taken as the heat release rate per unit area times the floor area of the fuel concentration. The maximum foreseeable storage height (above the fire base) and associated heat release rate should be considered.

The heat release rate per unit area might be available from listings for a given storage height, such as Table 8.2.6. To establish estimates for other than specified heights, it can be assumed that the heat release rate per unit area is proportional to the storage height, based on tests [Yu and Stavrianidis 1991] and the data in Table 8.2.6 for wood pallets. For fuel configurations that have not been tested, other procedures should be used. See Annex E for estimating heat release rates of other fuel arrays.

There is a distinct possibility that a combustible storage array could collapse before the end of the design interval of the venting system. The design interval might end, for example, when manual fire fighting is expected to begin. The fire diameter increases, contributing to increased smoke production (via a lower flame height and virtual origin). However, the heat release rate and fire growth rate after collapse are likely to be smaller than with no collapse. Consequently, it is reasonable to assume that the net effect of collapse is not significant for the calculation procedure.

**A.8.3.1** The growth time,  $t_g$ , is a measure of the fire growth rate: The smaller the growth time, the faster the fire grows.

**A.8.3.2** By comparing Equations 8.2 and 8.3, the following relation exists:

$$(A.8.2) \quad \alpha_g = \frac{1000}{t_g^2}$$

**A.8.3.5** Design objectives and the design interval time,  $t_r$ , should take into consideration all of the following critical events:

- (1) Arrival and deployment of the emergency response team
- (2) Arrival and deployment of fire fighters from the public fire department

- (3) Completion of evacuation
- (4) Other critical events

**A.9.1** The procedures in Chapter 9 are based on the automatic activation of vents by a heat-responsive device with an established response time index (RTI) and known activation temperature. These assumptions do not preclude other means of vent activation, as long as the activation time of the alternative means is known or can be calculated using the procedures contained herein or can be established as acceptable by a specific listing, specific test data, or engineering analysis. Activation by heat detectors, smoke detectors, thermoplastic drop-out vent panels, or other approved means is acceptable as long as the design objectives are met.

The equations and procedures for hand calculations in Section 9.2 and the models in Section 9.3 address the venting of limited-growth fires and continuously growing fires.

**A.9.1.1** The vent area in a curtained area should not be required to exceed the vent area calculated for the largest limited-growth fire predicted for the combustibles beneath any curtained area. Using sufficiently small concentrations of combustibles and aisles of sufficient width to prevent spread according to Equation 8.1, it might be possible to satisfy venting requirements by using vent areas smaller than those required for a vent design and a continuous-growth fire.

**A.9.1.4** Many large facilities have buildings or areas subject to differing fire hazards.

**A.9.2.2.1** In Figure 9.2.2.1,  $z_s$  is the height of the smoke layer boundary above the base of the fire;  $H$  is the distance between the base of the fire and the ceiling;  $d_c$  is the depth of the draft curtains and  $d$  is the depth of the smoke layer;  $\dot{m}_p$  is the mass flow rate of hot gas from the fire plume into the smoke layer;  $\dot{m}_v$  is the mass flow rate of hot gas out of the vent (or vents) in the curtained area; and  $A_v$  is the vent area in the curtained area (total vent area in the curtained area if more than one vent is provided).

The vent area calculated for equilibrium conditions corresponds to the area needed for a long-term steady fire or to the area needed at the end of a design interval for a slow-growing fire. For shorter-term steady fires and for faster-growing fires, the calculated equilibrium vent area will prevent the smoke layer boundary from descending completely to the bottom of the draft curtains. Therefore, equilibrium calculations represent a safety factor in the design.

**A.9.2.3.1** The mass flow rate in the plume depends on whether locations above or below the mean flame height are considered (i.e., whether the flames are below the smoke layer boundary or reach into the smoke layer).

**A.9.2.4.1** The mass flow rate through the vent is the product of gas density, velocity, and cross-sectional area of the flow in the vent. The velocity follows from equating the buoyancy head across the vent to the dynamic head in the vent, with consideration of the pressure drop across the air inlets. The factor  $[(T_o \Delta T) / T^2]^{1/2}$  is quite insensitive to temperature as long as the smoke layer temperature rise,  $\Delta T$ , is not small. For example,

assuming  $T_o = 294$  K, the factor varies through 0.47, 0.50, and 0.47 as the smoke layer temperature rise varies through 150 K, 320 K, and 570 K. At a temperature rise of 60 K, the factor is 0.38, and at a temperature rise of 20 K, it is 0.24, or about one-half its maximum value. Consequently, roof venting by natural ventilation becomes increasingly less effective as the smoke layer temperature decreases. For low smoke layer temperatures, powered ventilation as covered in NFPA 92B, *Guide for Smoke Management Systems in Malls, Atria, and Large Areas*, should be considered.

Where high upper-layer temperatures of 400 K above ambient are anticipated, 80 percent of the predicted vent flow is expected to be achieved with an inlet area/vent area ratio of one, whereas it is expected that 90 percent of the vent flow will result from a ratio of two. Where relatively low upper-layer temperatures, such as 200 K above ambient, are expected, a ratio of inlet air/vent area of one would result in about 70 percent of the predicted vent flow, whereas a ratio of two would be expected to produce about 90 percent of the predicted vent flow.

**A.9.2.4.2** The aerodynamic vent area is always smaller than the geometric vent area,  $A_v$ . A discharge coefficient of 0.6 should be reasonable for most vents and for doors and windows that open at least 45 degrees. However, the discharge coefficient can be different for other types of openings. For example, an opening with a louver can have a coefficient ranging between 0.1 and 0.4.

**A.9.2.5.4.1** For continuous-growth fires, the earlier the fire is detected and vents actuated, the smaller the fire size at the end of the design interval and the smaller the required vent area. In the case of limited-growth fires, the earlier the fire is detected and the vents actuated, the less likely to occur are an initial underspill of smoke at the draft curtains and smoke layer descent to low heights.

If a design objective is to confine smoke to the curtained area of origin, the time the last required vent opens,  $t_{vo}$ , should not exceed the time the smoke layer boundary drops below draft curtains, which can be determined in accordance with Equation A.9.1 for steady fires and Equation A.9.2 for unsteady fires.

$$(A.9.1) \quad \frac{z_{si}}{H} = 0.67 - 0.28 \ln \left[ \frac{(Q^{1/3} / H^{4/3})}{(A / H^2)} \right]$$

where:

$A_c$  = curtained area being filled with smoke (m<sup>2</sup>)

$t$  = time (s)

$$(A.9.2) \quad \frac{z_{si}}{H} = 0.23 \left[ \frac{t}{t_g^{2/5} (H^{4/5}) (A / H^2)^{3/5}} \right]^{-1.45}$$

**A.9.2.5.4.2.1** The response data in NFPA 72, *National Fire Alarm Code*, assume extensive, flat, horizontal ceilings.

This assumption might appear optimistic for installations involving beamed ceilings. However, any delay in operation due to beams is at least partially offset by the opposite effects of the following:

- (1) Heat banking up under the ceiling because of draft curtains or walls
- (2) The nearest vent or detector usually being closer to the fire than the assumed, greatest possible distance

Fusible links are commonly used as actuators for mechanically opened heat and smoke vents. Where the RTI and fusing temperature of a fusible link are known, and assuming that the link is submerged in the ceiling jet, the relationships described in *NFPA 72, National Fire Alarm Code*, for heat-actuated alarm devices can be used to estimate the opening of a mechanical vent.

**A.9.2.5.4.3.1** This requirement does not have a parallel in *NFPA 72, National Fire Alarm Code*. Temperature rise for activation of smoke detectors depends on the specific detector as well as the material undergoing combustion. Limited data on temperature rise at detection have previously been recorded in the range of 2°C–42°C, depending on the detector/material combination [Heskestad and Delichatsios 1977].

**A.9.2.5.4.4.1** A computer program known as DETACT-T2 (DETECTOR ACTUATION-time squared) [Evans and Stroup 1985] is available for calculating the detection times of heat detectors or fusible links in continuous growth, *t*-squared fires. DETACT-T2 assumes the detector is located in a large compartment with an unconfined ceiling, where there is no accumulation of hot gases at the ceiling. Thus, heating of the detector is only from the flow of hot gases along the ceiling. Input data consist of ceiling height, time constant or RTI of the detector, operating temperature, distance of the detector from plume centerline, and fire growth rate. The model calculates detection times for smoke detectors (*see 9.2.5.4.3*), based on the predecessor equations. The predecessor equations assume complete combustion of the test fuel used in the experiments used to develop the equations based on the actual heat of combustion:

$$(A.9.3) \quad \frac{u}{(\Delta T_g / T_o)gH^{1/2}} = 0.59 \left( \frac{r}{H} \right)^{-0.63}$$

where:

$T_o$  = ambient air temperature

$\Delta T_g$  = gas temperature rise from ambient at detector/sprinkler site

$g$  = acceleration of gravity

$H$  = ceiling height (above combustibles)

$r$  = radius from fire axis

However, DETACT-T2 can still be used, provided that the projected fire growth coefficient,  $\alpha_g$ , is multiplied by the factor 1.67. In addition, when DETACT-T2 is used, the outputs of heat release rate at detector response from the program calculations must be divided by 1.67 in order to establish heat release rates at detector response.

**A.9.2.5.4.4.2** Another program, DETACT-QS (DETECTOR ACTUATION — quasi-steady) [Evans and Stroup 1985], is available for calculating detection times of heat detectors, fusible links, and smoke detectors in fires of arbitrary fire growth. DETACT-QS assumes that the detector is located in a large compartment with an unconfined ceiling, where there is no accumulation of hot gases at the ceiling. Thus, heating of the detector is only from the flow of hot gases along the ceiling. Input data consist of ceiling height, time constant or RTI of the detector, operating temperature, distance of the detector from the plume centerline, and fire growth rate. The model calculates detection times for smoke detectors (*see* 9.2.5.4.3) based on the predecessor equations. Quasi-steady temperatures and velocities are assumed (i.e., instantaneously, gas temperatures and velocities under the ceiling are assumed to be related to the heat release rate as in a steady fire). Compared to DETACT-T2, DETACT-QS provides a means of addressing fires that cannot be approximated as *t*-squared fires. However, for *t*-squared fires, DETACT-QS is less accurate than DETACT-T2 (if the projected fire growth coefficient is increased as described in 9.2.5.4.4.1 and A.9.2.5.4.4.1), especially for fast-growing fires.

**A.10.1.1** Where temperature differences of less than 110°C are expected, vent flows might be reduced significantly; therefore, consideration should be given to using powered exhaust. NFPA 92B, *Guide for Smoke Management Systems in Malls, Atria, and Large Areas*, should be consulted for guidance for power venting at these lower temperatures.

**A.10.4** When the smoke layer depth below an exhaust inlet is relatively shallow, a high exhaust rate can lead to entrainment of cold air from the clear layer. This phenomenon is called plugholing. The number of exhaust inlets must be chosen so that the maximum flow rates for exhaust without plugholing are not exceeded. Accordingly, more than one exhaust inlet may be needed.

Based on limited information, suggested values of  $\beta$  in Equation 10.1 are 2.0 for a ceiling exhaust inlet near a wall, 2.0 for a wall exhaust inlet near the ceiling, and 2.8 for a ceiling exhaust inlet far from any walls. In addition to Equation 10.1, it is suggested that  $d/D_i$  be greater than 2, where  $D_i$  is the diameter of the inlet. For rectangular exhaust inlets, use  $D_i = 2ab_i/(a_i + b_i)$ , where  $a$  and  $b$  are the length and width of the exhaust inlet.

**A.12.1** Regular inspection and maintenance is essential for emergency equipment and systems that are not subjected to their intended use for many years.

**A.12.2** Various types of approved automatic thermal smoke and heat vents are available commercially. These vents fall into two general categories:

- (1) Mechanically opened vents, which include spring-lift, pneumatic-lift, or electric motor-driven vents
- (2) Thermoplastic drop-out vents, which include polyvinyl chloride (PVC) or acrylic drop-out panels

Thermoplastic drop-out vents do not allow nondestructive operation.

**A.12.3.1.4** Vents designed for multiple functions (e.g., the entrance of day-lighting, roof access, comfort ventilation) need maintenance of the fire protection function that might be impaired by the other uses. These impairments can include loss of spring tension, racking

or wear of moving parts, adverse exterior cooling effects on the fire protection release mechanism, adverse changes in performance sequence such as premature heat actuation leading to opening of the vent, or reduced sensitivity to heat.

**A.12.3.2.2** Inspection schedules should include provisions for testing all units at 12-month intervals or on a schedule based on a percentage of the total units to be tested every month or every two months. Such procedures improve reliability. A change in occupancy, or in neighboring occupancies, and in materials being used could introduce a significant change in the nature or severity of corrosive atmosphere exposure, debris accumulation, or physical encumbrance and could necessitate a change in the inspection schedule.

**A.12.3.2.3** Recording and logging of all pertinent characteristics of performance allows results to be compared with those of previous inspections or acceptance tests and thus provides a basis for determining the need for maintenance or for modifying the frequency of the inspection schedule to fit the experience.

**A.12.3.3.1** The same general considerations for inspection that apply to mechanically opened vents also pertain to thermoplastic drop-out vents. The thermoplastic panels of these vents are designed to soften and drop out from the vent opening in response to the heat of a fire. This makes an operational test after installation impracticable. Recognized fire protection testing laboratories have developed standards and procedures for evaluating thermoplastic drop-out vents, including factory and field inspection schedules. It is suggested that laboratory recommendations be followed for the field inspection of such units.

**A.12.3.3.2** Thermoplastic drop-out vents utilize various types of plastics such as PVC and acrylic. Without the presence of ultraviolet stabilizers, exposure to ultraviolet rays can cause degradation and failure of the thermoplastic component (dome). Indication of ultraviolet degradation includes yellowing, browning, or blackening of the dome, as well as cracking or a brittle texture of the dome. This condition can cause failure of the thermoplastic to respond to the design activation temperature. Corrective action requires replacing the thermoplastic dome with a dome having an equivalent thermal response.

**A.12.4.1.3** The whipping action of the cable on release presents a possibility of injury to anyone in the area. For this reason, the person conducting the test should ensure that all personnel are well clear of the area where whipping of the cable might occur.

**A.13.1** Design documentation is critical to the proper installation, operation, and maintenance of the smoke and heat vent systems. It forms the basis for evaluating the system's adequacy to perform as intended if the building or its use is modified.

## **Annex B The Theoretical Basis of LAVENT**

*This annex is not a part of the requirements of this NFPA document but is included for informational purposes only.*

### **B.1 Overview.**

This annex develops the physical basis and an associated mathematical model for estimating the fire-generated environment and the response of sprinkler links in well-

ventilated compartment fires with curtain boards and ceiling vents actuated by heat-responsive elements such as fusible links or thermoplastic drop-out panels. Complete equations and assumptions are presented. Phenomena taken into account include the following:

- (1) Flow dynamics of the upward-driven, buoyant fire plume
- (2) Growth of the elevated-temperature smoke layer in the curtained compartment
- (3) Flow of smoke from the layer to the outside through open ceiling vents
- (4) Flow of smoke below curtain partitions to building spaces adjacent to the curtained space of fire origin
- (5) Continuation of the fire plume in the upper layer
- (6) Heat transfer to the ceiling surface and the thermal response of the ceiling as a function of radial distance from the point of plume–ceiling impingement
- (7) Velocity and temperature distribution of plume-driven near-ceiling flows and the response of near-ceiling–deployed fusible links as functions of distance below the ceiling
- (8) Distance from plume–ceiling impingement

The theory presented here is the basis of the LAVENT computer program that is supported by a user guide, which is presented in Annex C, and that can be used to study parametrically a wide range of relevant fire scenarios [1, 2, 3].

## **B.2 Introduction.**

The space under consideration is a space of a plan area,  $A$ , defined by ceiling-mounted curtain boards with a fire of time-dependent energy release rate,  $\dot{Q}(t)$ , and with open ceiling vents of total time-dependent area,  $A_V(t)$ . The curtained area can be considered as one of several such spaces in a large building compartment. Also, by specifying that the curtains be deep enough, they can be thought of as simulating the walls of a single, uncurtained compartment. This annex presents the physical basis and associated mathematical model for estimating the fire-generated environment and the response of sprinkler links in curtained compartment fires with ceiling vents actuated by heat-responsive elements such as fusible links or thermoplastic drop-out panels.

The overall building compartment is assumed to have near-floor wall vents that are large enough to maintain the inside environment, below any near-ceiling smoke layers that could form, at assumed initial outside-ambient conditions. Figure F.2(a) depicts the generic fire scenario for the space under consideration. The assumption of large near-floor wall vents necessitates that the modeling be restricted to conditions where  $y$ , the elevation of the smoke layer interface, is above the floor elevation (i.e.,  $y > 0$ ). The assumption also has important implications with regard to the cross-ceiling vent pressure differential. This is the pressure differential that drives elevated-temperature upper-layer smoke through the ceiling vents to the outside. Therefore, below the smoke layer (i.e., from the floor of the facility to the elevation of the smoke layer interface), the inside-to-outside hydrostatic pressure

differential exists at all elevations in the reduced-density smoke layer itself (higher pressure inside the curtained area, lower pressure in the outside environment), the maximum differential occurring at the ceiling and across the open ceiling vents.

### B.3 The Basic Equations.

A two-layer, zone-type compartment fire model is used to describe the phenomena under investigation. As is typical in such models, the upper smoke layer of total mass,  $m_U$ , is assumed to be uniform in density,  $\rho_U$ , and absolute temperature,  $T_U$ .

The following time-dependent equations describe conservation of energy, mass, and the perfect gas law in the upper smoke layer.

Conservation of energy,

$$(B.1) \quad \frac{d[(y_{ceil} - y)\rho_U T_U A C_V]}{dt} = \dot{q}_U + \left( \rho_U A \frac{dy}{dt} \right)$$

Conservation of mass,

$$(B.2) \quad \frac{dm_U}{dt} = \dot{m}_U$$

$$(B.3) \quad m_U = (y_{ceil} - y)\rho_U A$$

Perfect gas law,

$$(B.4) \quad \frac{\rho_U}{R} \propto \frac{\rho}{R} = constant = \rho_U T_U = \rho_{amb} T_{amb}$$

That is,

$$(B.5) \quad T_U = \frac{T_{amb} \rho_{amb}}{\rho_U}$$

In the preceding equations,  $y_{ceil}$  is the elevation of the ceiling above the floor,  $R = C_p - C_V$  is the gas constant,  $C_p$  and  $C_V$  are the specific heats at a constant pressure and volume, respectively, and  $p$  is a constant characteristic pressure (e.g.,  $p_{atm}$ ) at the floor elevation.

In Equation B.1,  $\dot{q}_U$  is the net rate of enthalpy flow plus heat transfer to the upper layer and is made up of flow components as follows:  $\dot{q}_{curt}$ , from below the curtain;  $\dot{q}_{plume}$ , from the plume;  $\dot{q}_{vent}$ , from the ceiling vent; and the component  $\dot{q}_{HT}$ , the total heat transfer rate.

$$(B.6) \quad \dot{q}_U = \dot{q}_{curt} + \dot{q}_{plume} + \dot{q}_{vent} + \dot{q}_{HT}$$

In Equation B.2,  $\dot{m}_U$  is the net rate of mass flow to the upper layer with flow components;  $\dot{m}_{curt}$ , from below the curtain;  $\dot{m}_{plume}$ , from the plume; and  $\dot{m}_{vent}$ , from the ceiling vent.

$$(B.7) \quad \dot{m}_U = \dot{m}_{curt} + \dot{m}_{plume} + \dot{m}_{vent}$$

Using Equation B.3 in Equation B.1 leads to

$$(B.8) \quad \frac{dy}{dt} = \frac{\dot{q}_U}{AC_p \rho_{amb} T_{amb}}$$

if

$$y = y_{ceil} \text{ and } \dot{q}_U \geq 0$$

or

$$0 < y < y_{ceil} \text{ and } \dot{q}_U \text{ is arbitrary}$$

Because both of these conditions are satisfied, Equation B.8 is always applicable.

The basic problem of mathematically simulating the growth and properties of the upper layer for the generic Figure F.2(a) scenario necessitates the solution of the system of Equation B.2 and Equation B.8 for  $\dot{m}_U$  and  $y$ . When  $\dot{m}_U > 0$ ,  $\rho_U$  can be computed from Equation B.3 according to

$$(B.9) \quad \rho_U = \frac{(y_{ceil} - y)A}{\dot{m}_U}; \text{ if } \dot{m}_U > 0$$

and  $T_U$  can be determined from Equation B.5.

## B.4 Mass Flow and Enthalpy Flow Plus Heat Transfer.

**B.4.1 Flow to the Upper Layer from the Vents.** Conservation of momentum across all open ceiling vents as expressed by Bernoulli's equation leads to the following:

$$(B.10) \quad V = C \left( \frac{2\Delta\rho_{ceil}}{\rho_U} \right)^{1/2}$$

$$(B.11) \quad \dot{m}_{vent} = -\rho_U A_V V = -A_V C (2\rho_U \Delta\rho_{ceil})^{1/2}$$

where:

$V$  = the average velocity through all open vents

$C$  = the vent flow coefficient (0.68) [4]

$\Delta \rho_{ceil}$  = the cross-vent pressure difference

From hydrostatics,

$$\begin{aligned} \Delta \rho_{ceil} &= \rho_U (y = y_{ceil}) - \rho_{amb} (y = y_{ceil}) \\ &= (\rho_{amb} - \rho_U) g (y_{ceil} - y) \end{aligned} \quad (\text{B.12})$$

where:

$g$  = the acceleration of gravity.

Substituting Equation B.12 into Equation B.11 leads to the desired  $\dot{m}_{vent}$  result as follows:

$$\dot{m}_{vent} = -A_V C \left[ 2 \rho_U (\rho_{amb} - \rho_U) g (y_{ceil} - y) \right]^{1/2} \quad (\text{B.13})$$

which is equivalent to the equations used to estimate ceiling vent flow rates, Equation 6.8 and references [5] and [6]. Using Equation B.13, the desired  $\dot{q}_{vent}$  result is as follows:

$$\dot{q}_{vent} = \dot{m}_{vent} C_P T_U \quad (\text{B.14})$$

**B.4.2 Flow to the Layer from the Plume and Radiation from the Fire.** It is assumed that the mass generation rate of the fire is small compared to  $\dot{m}_{ent}$ , the rate of mass of air entrained into the plume between the fire elevation,  $y_{fire}$ , and the layer interface, or compared to other mass flow rate components of  $\dot{m}_U$ . It is also assumed that all of the  $\dot{m}_{ent}$  penetrates the layer interface and enters the upper layer. Therefore,

$$\dot{m}_{plume} = \dot{m}_{ent} \quad (\text{B.15})$$

$$\dot{q}_{plume} = \dot{m}_{ent} C_P T_{amb} + (1 - \lambda_r) \dot{Q} \quad (\text{B.16})$$

The first term on the right side of Equation B.16 is the enthalpy associated with  $\dot{m}_{ent}$ , and  $\lambda_r$ , in the second term in Equation B.16, is the effective fraction of  $\dot{Q}$  assumed to be radiated isotropically from the fire's combustion zone.

It is assumed that the smoke layer is relatively transparent and that it does not participate in any significant radiation heat transfer exchanges. In particular, all of the  $\lambda_r \dot{Q}$  radiation is assumed to be incident on the bounding surfaces of the compartment. Therefore, the last term of Equation B.16 is the net amount of enthalpy added to the upper layer from the

combustion zone and its buoyancy-driven plume. Flaming fires exhibit values for  $\lambda_r$  of  $0 < \lambda_r < 0.6$  (e.g., smallest values for small methane fires and highest values for large polystyrene fires). However, for a hazardous fire involving a wide range of common groupings of combustibles, it is reasonable to approximate flame radiation by choosing  $\lambda_r \approx 0.35$  [7].

A specific plume entrainment model is necessary to complete Equations B.14 and B.15 for  $\dot{m}_{plume}$  and  $\dot{q}_{plume}$ . The following estimate for  $\dot{m}_{ent}$  [8 and 9] is adopted as follows:

$$\dot{m}_{ent} = \begin{cases} 0; & \text{if } y - y_{fire} \leq 0; \\ 0.0054 \left[ (1 - \lambda_r) \dot{Q} \right] \frac{y - y_{fire}}{L_{flame}}; & \text{if } 0 < \frac{y - y_{fire}}{L_{flame}} < 1 \\ 0.071 \left[ (1 - \lambda_r) \dot{Q} \right]^{1/3} \\ \times \left\{ (y - y_{fire} - L_{flame}) + 0.166 \left[ (1 - \lambda_r) \dot{Q} \right]^{2/5} \right\}^{5/3} & \text{(B.17)} \\ \times \left[ 1 + \left[ (1 - \lambda_r) \dot{Q} \right]^{2/3} \right] \\ \times \left\{ (y - y_{fire} - L_{flame}) + 0.166 \left[ (1 - \lambda_r) \dot{Q} \right]^{2/5} \right\}^{-5/3}; \\ \text{if } \frac{y - y_{fire}}{L_{flame}} \geq 1 \end{cases}$$

where  $\dot{m}_{ent}$  is in kg/s,  $\dot{Q}$  is in kW, and  $y$ ,  $y_{fire}$ , and  $L_{flame}$  are in m and where

$$\frac{L_{flame}}{D_{fire}} = \begin{cases} 0; & \text{if } \frac{0.249 \left[ (1 - \lambda_r) \dot{Q} \right]^{2/5}}{D_{fire}} - 1.02 < 0 \\ \frac{0.249 \left[ (1 - \lambda_r) \dot{Q} \right]^{2/5}}{D_{fire}} - 1.02; \\ \text{if } \frac{0.249 \left[ (1 - \lambda_r) \dot{Q} \right]^{2/5}}{D_{fire}} - 1.02 \geq 0 \end{cases} \quad \text{(B.18)}$$

where  $\dot{Q}$  is in kW,  $D_{fire}$  is in m, and

$$(B.19) \quad \epsilon = \left( \frac{0.0054}{0.071} \right) - (0.166)^{5/3} = 0.02591682... \approx 0.026$$

In Equations B.17 through B.19,

$L_{flame}$  is the fire's flame length.

$D_{fire}$  is the effective diameter of the fire source ( $\pi D_{fire}^2/4 = \text{area of the fire source}$ ).

$\epsilon$  is chosen so that, analytically, the value of  $\dot{m}_{ent}$  is exactly continuous at the elevation  $y = y_{fire} + L_{flame}$ .

**B.4.3 Flow to the Layer from Below the Curtains.** If the upper layer interface,  $y$ , drops below the elevation of the bottom of the curtains,  $y_{curt}$ , mass and enthalpy flows occur from the upper layer of the curtained area where the fire is located to adjacent curtained areas of the overall building compartment. The mass flow rate is the result of hydrostatic cross-curtain pressure differentials. Provided adjacent curtained areas are not yet filled with smoke, this pressure difference increases linearly from zero at the layer interface to  $\Delta p_{curt}$  at  $y = y_{curt}$ .

From hydrostatics,

$$(B.20) \quad \begin{aligned} \Delta p_{curt} &= \rho_U (y = y_{curt}) - \rho_{amb} (y = y_{curt}) \\ &= (\rho_{amb} - \rho_U) g (y_{curt} - y) \end{aligned}$$

Using Equation B.20 together with well-known vent flow relations (e.g., Equation 32 of reference [4]),  $\dot{m}_{curt}$  and  $\dot{q}_{curt}$  can be estimated from the following:

$$(B.21) \quad \dot{m}_{curt} = \begin{cases} 0; & \text{if } y \geq y_{curt} \\ -\frac{L_{curt}}{3} \left[ 8(y_{curt} - y)^3 \rho_U (\rho_{amb} - \rho_U) g \right]^{1/2}; & \text{if } y \leq y_{curt} \end{cases}$$

$$(B.22) \quad \dot{q}_{curt} = \dot{m}_{curt} C_P T_U$$

where  $L_{curt}$  is that length of the perimeter of the curtained areas of the fire origin that is connected to other curtained areas of the overall building compartment. For example, if the curtained area is in one corner of the building compartment, then the length of its two sides coincident with the walls of the compartment are not included in  $L_{curt}$ . Because the generic vent flow configuration under consideration in this case is long and deep, a flow coefficient for the vent flow incorporated into Equation B.21 is taken to be 1.

**B.4.4 Heat Transfer to the Upper Layer.** As discussed in B.4.3, where the fire is below the layer interface, the buoyant fire plume rises toward the ceiling, and all of its mass and

enthalpy flow,  $\dot{m}_{plume}$  and  $\dot{q}_{plume}$ , are assumed to be deposited into the upper layer. Having penetrated the interface, the plume continues to rise toward the ceiling of the curtained compartment. As it impinges on the ceiling surface, the plume flow turns and forms a relatively high-temperature, high-velocity, turbulent ceiling jet that flows radially outward along the ceiling and transfers heat to the relatively cool ceiling surface. The ceiling jet is cooled by convection, and the ceiling material is heated by conduction. The convective heat transfer rate is a strong function of the radial distance from the point of plume–ceiling impingement and reduces rapidly with increasing radius. It is dependent also on the characteristics of the plume immediately upstream of ceiling impingement.

The ceiling jet is blocked eventually by the curtains, wall surfaces, or both. It then turns downward and forms vertical surface flows. In the case of wall surfaces and very deep curtains, the descent of these flows is stopped eventually by upward buoyant forces, and they finally mix with the upper layer. In this case, it is assumed that the plume–ceiling impingement point is relatively far from the closest curtain or wall surface (e.g., greater than a few fire-to-ceiling lengths). Under such circumstances, the ceiling jet–wall flow interactions are relatively weak, and compared to the net rate of heat transfer from the ceiling and near the plume–ceiling impingement point, the heat transfer to the upper layer from all vertical surfaces is relatively small.

Define  $\lambda_{conv}$  as the fraction of  $\dot{Q}$  that is transferred by convection from the upper-layer gas ceiling jet to the ceiling and to the vertical wall and curtain surfaces as follows:

$$(B.23) \quad \dot{q}_{HT} = -\lambda_{conv}\dot{Q}$$

Once the values of  $\lambda_{conv}\dot{Q}$  and  $\dot{q}_{HT}$  are determined from a time-dependent solution to the coupled, ceiling jet–ceiling material, convection-conduction problem, the task of determining an estimate for each component of  $\dot{q}_U$  and  $\dot{m}_U$  in Equations B.6 and B.7, respectively, is complete.

**B.4.4.1 Properties of the Plume in the Upper Layer When  $y_{fire} < y$ .** Those instances of the fire elevation being below the interface (i.e., when  $y_{fire} < y$ ) are considered here.

As the plume flow moves to the center of the upper layer, the forces of buoyancy that act to drive the plume toward the ceiling (i.e., as a result of relatively high-temperature, low-density plume gases being submerged in a relatively cool, high-density ambient environment) are reduced immediately because of the temperature increase of the upper-layer environment over that of the lower ambient. As a result, the continued ascent of the plume gases is less vigorous (i.e., ascent is at reduced velocity) and of higher temperature than it would be in the absence of the layer. Indeed, some of the penetrating plume flow will be at a lower temperature than  $T_U$ . The upper-layer buoyant forces on this latter portion of the flow actually retard and can possibly stop its subsequent rise to the ceiling.

A simple point-source plume model [10] is used to simulate the plume flow, first immediately below or upstream of the interface and then throughout the depth of the upper layer itself.

A plume above a point source of buoyancy [10], where the source is below the interface, will be considered to be equivalent to the plume of a fire (in the sense of having identical mass and enthalpy flow rates at the interface) if the point-source strength is  $(1 - \lambda_r) \dot{Q}^*$  and the elevation of the equivalent source,  $y_{eq}$ , satisfies the following:

$$(B.24) \quad \dot{m}_{plume} = 0.21 \rho_{amb} g^{1/2} (y - y_{eq})^{5/2} \dot{Q}_{eq}^{*1/3}$$

In Equation B.24,  $\dot{Q}_{eq}^*$ , a dimensionless measure of the strength of the fire plume at the interface, is defined as follows:

$$(B.25) \quad \dot{Q}_{eq}^* = \frac{(1 - \lambda_r) \dot{Q}}{\rho_{amb} C_P T_{amb} g^{1/2} (y - y_{eq})^{5/2}}$$

It should be noted that at an arbitrary moment of time on the simulation of a fire scenario,  $\dot{m}_{plume}$  in Equation B.24, is a known value that is determined previously from Equations B.15 and B.17.

Using Equations B.24 and B.25 to solve for  $y_{eq}$  and  $\dot{Q}_{eq}^*$ ,

$$(B.26) \quad y_{eq} = y - \left[ \frac{(1 - \lambda_r) \dot{Q}}{\dot{Q}_{eq}^* \rho_{amb} C_P T_{amb} g^{1/2}} \right]^{2/5}$$

$$(B.27) \quad \dot{Q}_{eq}^* = \left[ \frac{0.21(1 - \lambda_r) \dot{Q}}{C_P T_{amb} \dot{m}_{plume}} \right]^{3/2}$$

As the plume crosses the interface, the fraction,  $\dot{m}^*$ , of  $\dot{m}_{plume}$ , that is still buoyant relative to the upper-layer environment and presumably continues to rise to the ceiling, entraining upper-layer gases along the way, is predicted [11] to be as follows:

$$(B.28) \quad \dot{m}^* = \begin{cases} 0; & \text{if } -1 < \sigma \leq 0 \\ \frac{1.04599\sigma + 0.360391\sigma^2}{1.0 + 1.37748\sigma + 0.360391\sigma^2}; & \text{if } \sigma > 0 \end{cases}$$

where the dimensionless parameter,  $\sigma$ , is defined as follows:

$$(B.29) \quad \sigma = \frac{1 - \alpha + C_T \dot{Q}_{eq}^{*2/3}}{\alpha - 1}$$

$$\alpha = \frac{T_U}{T_{amb}}$$

(B.30)

where  $C_T = 9.115$  and where  $\dot{Q}_{eq}^*$  is the value computed in Equation B.27.

The parameters necessary to describe plume flow continuation in the upper layer (i.e., between  $y$  and  $y_{ceiling}$ ) are further identified (see [11]) according to a point-source plume (see [10]). It has been determined that this plume can be modeled as being driven by a nonradiating buoyant source of strength,  $\dot{Q}'$ , located a distance

$$H = y_{ceiling} - y'_{source} > y_{ceiling} - y_{fire}$$

(B.31)

below the ceiling in a downward-extended upper-layer environment of temperature,  $T_U$ , and density,  $\rho_U$ . The relevant parameters predicted [11] are as follows:

$$\dot{Q}' = \frac{(1 - \lambda_r) \dot{Q} \sigma \dot{m}^*}{1 + \sigma}$$

(B.32)

$$y'_{source} = y - (y - y_{eq}) \alpha^{3/5} \dot{m}^{*2/5} \left( \frac{1 + \sigma}{\sigma} \right)^{1/5}$$

(B.33)

The fire and the equivalent source in the lower layer and the continuation source in the upper layer are depicted in Figure B.4.4.1, parts (a) through (c). Those times during a fire simulation when Equation B.29 predicts  $\sigma > 1$  are related to states of the fire environment in which the temperature distribution above  $T_{amb}$  of the plume flow, at the elevation of interface penetration, is predicted to be mostly much larger than  $T_U - T_{amb}$ . Under such circumstances, the penetrating plume flow is still very strongly buoyant as it enters the upper layer. The plume continues to rise to the ceiling and to drive ceiling jet convective heat transfer at rates that differ only slightly (due to the elevated temperature upper-layer environment) from the heat transfer rates that could occur in the absence of an upper layer.

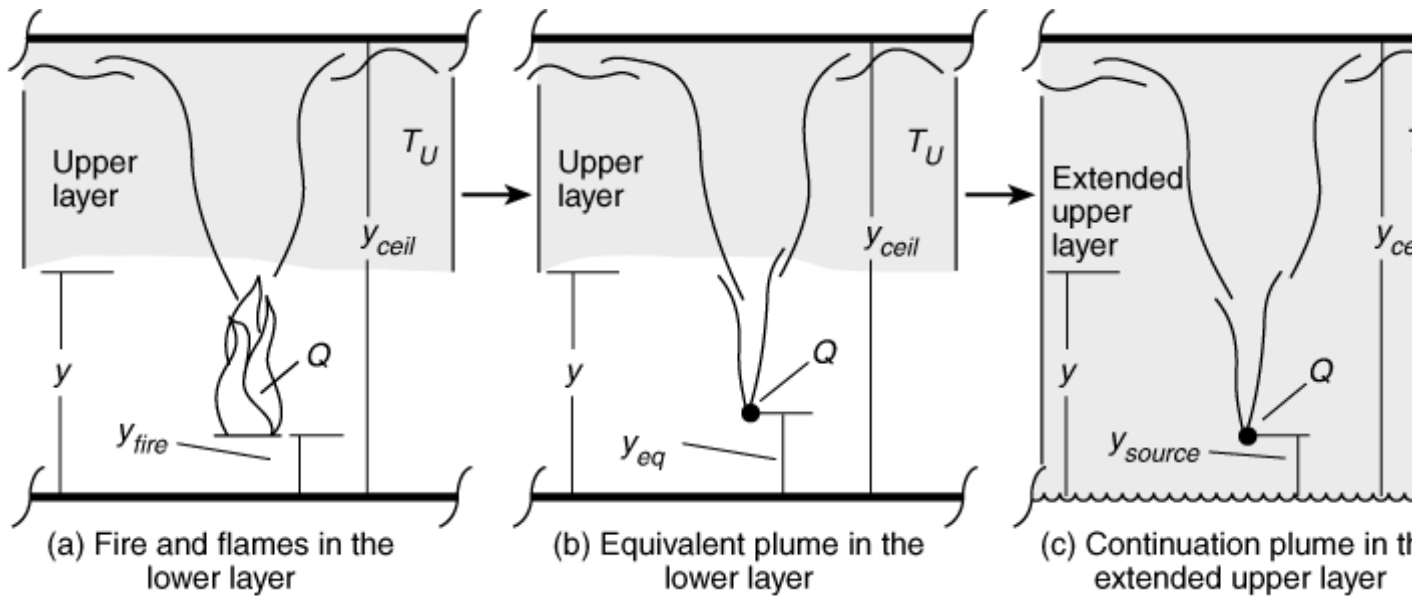


**FIGURE B.4.4.1 Fire and Equivalent Source.**

Conditions where Equation B.29 predicts  $\sigma < 0$  are related to times during a fire scenario when the temperature of the plume at the elevation of interface penetration is predicted to be uniformly less than  $T_U$ . Under such circumstances, the penetration plume flow is not positively (i.e., upward) buoyant at any point as it enters the upper layer. Therefore, while all of this flow is assumed to enter and mix with the upper layer, it is predicted that none of it rises to the ceiling in a coherent plume (i.e.,  $\dot{Q}' = 0$ ). For this reason, where  $\sigma < 0$ , the existence of any significant ceiling jet flow is precluded, along with significant convective heat transfer to the ceiling surface or to near-ceiling-deployed fusible links.

The preceding analysis assumes that  $y_{fire} < y$ . However, at the onset of the fire scenario,  $y_{fire} < y = y_{ceil}$  and  $\alpha$ ,  $\sigma$ , and  $\dot{m}^*$  of Equation B.28 through Equation B.31, which depend on the indeterminate initial value of  $T_U$ , are themselves undefined. The situation at  $t = 0$  is properly taken into account if  $\dot{Q} = (1 - \lambda_r)\dot{Q}$  and  $y_{source} = y_{eq}$  at  $t = 0$ .

**B.4.4.2 General Properties of the Plume in the Upper Layer.** When the fire is below the interface, the results of Equations B.32 and B.33 allow the fire-driven plume dynamics in the upper layer to be described according to the point-source plume model [10]. If the fire is at or above the interface (i.e.,  $y_{fire} \geq y$ ), then  $\dot{m}_{plume} = 0$ ,  $\dot{q}_{plume} = (1 - \lambda_r)\dot{Q}$ , and the point-source model is used once again to simulate the upper-layer plume flow. All cases can be treated using the following modified versions of original Equations B.32 and B.33:

$$(B.34) \quad \dot{Q}' = \begin{cases} \frac{(1 - \lambda_r)\dot{Q}\sigma\dot{m}^*}{(1 + \sigma)}; & \text{if } y_{fire} < y < y_{ceil} \\ (1 - \lambda_r)\dot{Q}; & \text{if } y_{fire} \geq y \text{ or if } y = y_{ceil} \end{cases}$$

$$y'_{source} = \begin{cases} y_{fire}, & \text{if } y \leq y_{fire} < y_{ceil} \\ y - (y - y_{eq}) \alpha^{3/5} \dot{m}^{*2/5} \left( \frac{1 + \sigma}{\sigma} \right)^{1/5}; & \text{if } y_{fire} < y < y_{ceil} \\ y_{eq}; & \text{if } y = y_{ceil} \end{cases}$$

(B.35)

where  $y_{eq}$ ,  $\dot{m}^*$ ,  $\sigma$ , and  $\alpha$  are calculated from Equations B.26 through B.30.

**B.4.5 Computing  $q_{HT}$  and the Thermal Response of the Ceiling.** Where the fire is below the interface and the interface is below the ceiling, the method used for calculating the heat transfer from the plume-driven ceiling jet to the ceiling and the thermal response of the ceiling is from reference [12]. This method was developed to treat generic, confined-ceiling, room fire scenarios. As outlined in this method [12], the confined ceiling problem is solved by applying the unconfined ceiling heat transfer solution [13, 14, 15] to the problem of an upper-layer source in an extended upper-layer environment equivalent to Equations B.34 and B.35. When the fire is about the interface, the unconfined ceiling methodology applies directly.

To use these methods [12 through 15], an arbitrary moment of time during the course of the fire development is considered. It is assumed that the temperature distribution of the ceiling material,  $T$ , has been computed up to this moment and is known as a function of distance,  $Z$ , measured upward from the bottom surface of the ceiling, and radial distance,  $r$ , measured from the constant point of plume-ceiling impingement. The equivalent, extended upper-layer, unconfined ceiling flow and heat transfer problem is depicted in Figure

B.4.4.1(c). It involves the equivalent  $\dot{Q}'$  heat source from Equation B.34 located a distance,  $H$ , below the ceiling surface in an extended ambient environment of density,  $\rho_U$ , and absolute temperature,  $T_U$ , where  $H$  is determined from Equations B.31 and B.33.

The objective is to estimate the instantaneous convective heat transfer flux from the upper-layer gas to the lower-ceiling surface,  $\dot{q}_{conv,L}''(r,t)$ , and the net heat transfer fluxes to the upper and lower ceiling surface of the ceiling,  $\dot{q}_u''(r,t)$  and  $\dot{q}_L''(r,t)$ , respectively. With this information, the time-dependent solution for the in-depth thermal response of the ceiling material can be advanced to subsequent times. Also,  $\dot{q}_{conv,L}''$  can be integrated over the lower-ceiling surface to obtain the desired instantaneous value for  $\dot{q}_{HT}$ .

In view of the assumptions of the relatively large distance of the fire from walls or curtains and on the relatively small contribution of heat transfer to these vertical surfaces, it is reasonable to carry out a somewhat simplified calculation for  $q_{HT}$ . Therefore,  $q_{HT}$  is approximated by the integral of  $\dot{q}_{conv,L}''$  over an effective circular ceiling area,  $A_{eff}$ , with a

diameter,  $D_{eff}$ , centered at the point of impingement:

$$\begin{aligned}
 \dot{q}_{HT} &= \lambda_{conv} \dot{Q}(t) \\
 &= - \int_A \dot{q}_{conv,L}''(r,t) dA \\
 &\approx -2\pi \int_0^{D_{eff}/2} \dot{q}_{conv,L}''(r,t) r dr
 \end{aligned}
 \tag{B.36}$$

The value  $A_{eff} = \pi D_{eff}^2 / 4$  is taken to be the actual area of the curtained space,  $A$ , plus the portion of the vertical curtain and wall surfaces estimated to be covered by ceiling jet-driven wall flows. An estimate for this extended, effective ceiling surface area is obtained [16], where it is concluded with some generality that ceiling jet-driven wall flows penetrate for a distance of approximately  $0.8H$  from the ceiling in a downward direction. Therefore,

$$\begin{aligned}
 A_{eff} &= \frac{\pi D_{eff}^2}{4} \\
 &= A + 0.8H(P - L_{curt}) + L_{curt} \min[0.8H, (y_{ceil} - y_{curt})]
 \end{aligned}
 \tag{B.37}$$

where  $P$  = the total length of the perimeter of the curtained area.

**B.4.5.1 Net Heat Transfer Flux to the Ceiling's Lower Surface.** The net heat transfer flux to the ceiling's lower surface,  $\dot{q}_L''$ , is made by means of up to three components — incident radiation,  $\dot{q}_{rad-fire}''$ ; convection,  $\dot{q}_{conv,L}''$ ; and reradiation,  $\dot{q}_{rerad,L}''$  — as follows:

$$\dot{q}_L'' = \dot{q}_{rad-fire}'' + \dot{q}_{conv,L}'' + \dot{q}_{rerad,L}''
 \tag{B.38}$$

As discussed in B.4.4, the radiant energy from the fire,  $\lambda_r \dot{Q}^*$ , is assumed to be radiated isotropically from the fire with negligible radiation absorption and emission from the compartment gases.

$$\dot{q}_{rad-fire}'' = \left[ \frac{\lambda_r \dot{Q}}{4\pi (y_{ceil} - y_{fire})^2} \right] \left[ 1 + \left( \frac{r}{y_{ceil} - y_{fire}} \right)^2 \right]^{-3/2}
 \tag{B.39}$$

The convective heat transfer flux from the upper-layer gas to the ceiling's lower surface can be calculated [13, 14] as follows:

$$\dot{q}_{conv,L}'' = h_L (T_{AD} - T_{S,L})
 \tag{B.40}$$

where:

$T_{S,L}$  = the absolute temperature of the ceiling's lower surface

$T_{AD}$  = the temperature that is measured adjacent to an adiabatic lower-ceiling surface

$h_L$  = a heat transfer coefficient

Equations B.41 and B.42 determine  $h_L$  and  $T_{AD}$  as follows:

$$(B.41) \quad \frac{h_L}{\tilde{h}} = \begin{cases} 8.82Re_H^{-1/2}Pr^{-2/3} \left[ 1 - (5.0 - 0.284Re_H^{0.2}) \left( \frac{r}{H} \right) \right]; \\ \text{if } 0 \leq \frac{r}{H} < 0.2 \\ 0.283Re_H^{-0.3}Pr^{-2/3} \left( \frac{r}{H} \right)^{-1/2} \left( \frac{\frac{r}{H} - 0.0771}{\frac{r}{H} + 0.279} \right); \\ \text{if } 0.2 \leq \frac{r}{H} \end{cases}$$

$$(B.42) \quad \frac{T_{AD} - T_U}{T_U \dot{Q}_H^{*2/3}} = \begin{cases} 10.22 - \frac{14.9r}{H}; & \text{if } 0 \leq \frac{r}{H} < 0.2 \\ 8.39f \left( \frac{r}{H} \right); & \text{if } 0.2 \leq \frac{r}{H} \end{cases}$$

where:

$$(B.43) \quad f \left( \frac{r}{H} \right) = \frac{1 - 1.10 \left( \frac{r}{H} \right)^{0.8} + 0.808 \left( \frac{r}{H} \right)^{1.6}}{1 - 1.10 \left( \frac{r}{H} \right)^{0.8} + 2.20 \left( \frac{r}{H} \right)^{1.6} + 0.690 \left( \frac{r}{H} \right)^{2.4}}$$

$$(B.44) \quad \begin{aligned} \tilde{h} &= \rho_U C_p g^{1/2} H^{1/2} \dot{Q}_H^{*1/3} \\ Re_H &= \frac{g^{1/2} H^{3/2} \dot{Q}_H^{*1/3}}{v_U} \\ \dot{Q}_H^* &= \frac{\dot{Q}'}{\rho_U C_p T_U (gH)^{1/2} H^2} \end{aligned}$$

In Equation B.41,  $Pr$  is the Prandtl number (taken to be 0.7), and in Equation B.44,  $v_u$  is

the kinematic viscosity of the upper-layer gas, which is assumed to have the properties of air. Also,  $\dot{Q}_H^*$ , a dimensionless number, is a measure of the strength of the plume, and  $Re_H$  is a characteristic Reynolds number of the plume at the elevation of the ceiling.

The following estimate for  $v_u$  [17] is used when computing  $Re_H$  from Equation B.44:

$$(B.45) \quad v_U = \frac{0.04128 (10^{-7}) T_U^{5/2}}{T_U + 110.4}$$

where  $v_u$  is in m<sup>2</sup>/s and  $T_U$  is in K.

Equations B.40 through B.45 use a value for  $T_U$ . At  $t = 0$ , where it is undefined,  $T_U$  should be set equal to  $T_{amb}$ . This yields the correct limiting result for the convective heat transfer to the ceiling, specifically, convective heat transfer to the initially ambient temperature ceiling from an unconfined ceiling jet in an ambient environment.

As the fire simulation proceeds, the ceiling's lower surface temperature,  $T_{S,L}$ , initially at  $T_{amb}$ , begins to increase. At all times, the lower-ceiling surface is assumed to radiate diffusely to the initially ambient temperature floor surface and to exposed surfaces of the building contents. In response to this radiation and to the direct radiation from the fire's combustion zone, the temperatures of these surfaces also increase with time. However, for times of interest here, it is assumed that their effective temperature increases are relatively small compared to the characteristic increases of  $T_{S,L}$ . Accordingly at a given radial position of the ceiling's lower surface, the net radiation exchange between the ceiling and floor-contents surfaces can be approximated by the following:

$$(B.46) \quad \dot{q}_{\text{rerad},L}'' = \frac{\sigma (T_{amb}^4 - T_{S,L}^4)}{\frac{1}{\epsilon_L} + \frac{1}{\epsilon_{\text{floor}}} - 1}$$

where  $\sigma$  is the Stefan–Boltzmann constant and  $\epsilon_L$  and  $\epsilon_{\text{floor}}$  are the effective emittance-absorptance of the ceiling's lower surface and the floor and contents surfaces (assumed to be gray), respectively, both of which are taken to be 1.

**B.4.5.2 Net Heat Transfer Flux to Ceiling's Upper Surface.** It is assumed that the ceiling's upper surface is exposed to a relatively constant-temperature far-field environment at  $T_{amb}$ . Therefore, the net heat transfer flux to this surface,  $\dot{q}_U$ , is made up of two components, convection,  $\dot{q}_{\text{conv},U}''$ , and reradiation,  $\dot{q}_{\text{rerad},U}''$  as follows:

$$(B.47) \quad \dot{q}_U'' = \dot{q}_{\text{conv},U}'' + \dot{q}_{\text{rerad},U}''$$

These can be estimated from the following:

$$(B.48) \quad \dot{q}_{conv,U}'' = h_U (T_{amb} - T_{S,U})$$

$$(B.49) \quad \dot{q}_{rad,U}'' = \frac{\sigma (T_{amb}^4 - T_{S,U}^4)}{\frac{1}{\epsilon_U} + \frac{1}{\epsilon_{far}} - 1}$$

where  $T_{S,U}$  is the absolute temperature of the upper surface of the ceiling,  $h_U$  is a heat transfer coefficient, and  $\epsilon_{far}$  and  $\epsilon_U$  are the effective emittance-absorptance of the far-field and ceiling's upper surface (assumed to be gray), respectively, both of which are taken to be 1.

The value for  $h_U$  to be used [18] is as follows:

$$(B.50) \quad h_U = 1.65 (T_{amb} - T_{S,U})^{1/3}$$

where  $h_U$  is in  $W/m^2$ , and  $T_{amb}$  and  $T_{S,U}$  are in K.

**B.4.5.3 Solving for the Thermal Response of the Ceiling for  $q_{HT}^*$ .** The temperature of the ceiling material is assumed to be governed by the Fourier heat conduction equation. By way of the lower-ceiling-surface boundary condition, the boundary value problem is coupled to, and is to be solved together with, the system of Equations B.2 and B.8.

Initially, the ceiling is taken to be of uniform temperature,  $T_{amb}$ . The upper- and lower-ceiling surfaces are then exposed to the radial- and time-dependent rates of heat transfer,  $\dot{q}_U''$  and  $\dot{q}_L''$ , determined from Equations B.47 and B.38, respectively. For times of interest

here, radial gradients of  $\dot{q}_U''$  and  $\dot{q}_L''$  are assumed to be small enough so that conduction in the ceiling is quasi-one-dimensional in space [i.e.,  $T = T(Z, t; r)$ ]. Therefore, the two-dimensional thermal response for the ceiling can be obtained from the solution to a set of one-dimensional conduction problems for

$$T_n(Z, t) = T(Z, t; r = r_n); \quad n = 1 \text{ to } N_{rad}$$

where  $N_{rad}$  is the number of discrete radial positions necessary to obtain a sufficiently smooth representation of the overall ceiling temperature distribution. The  $r_n$  radial positions are depicted in Figure B.4.5.3.

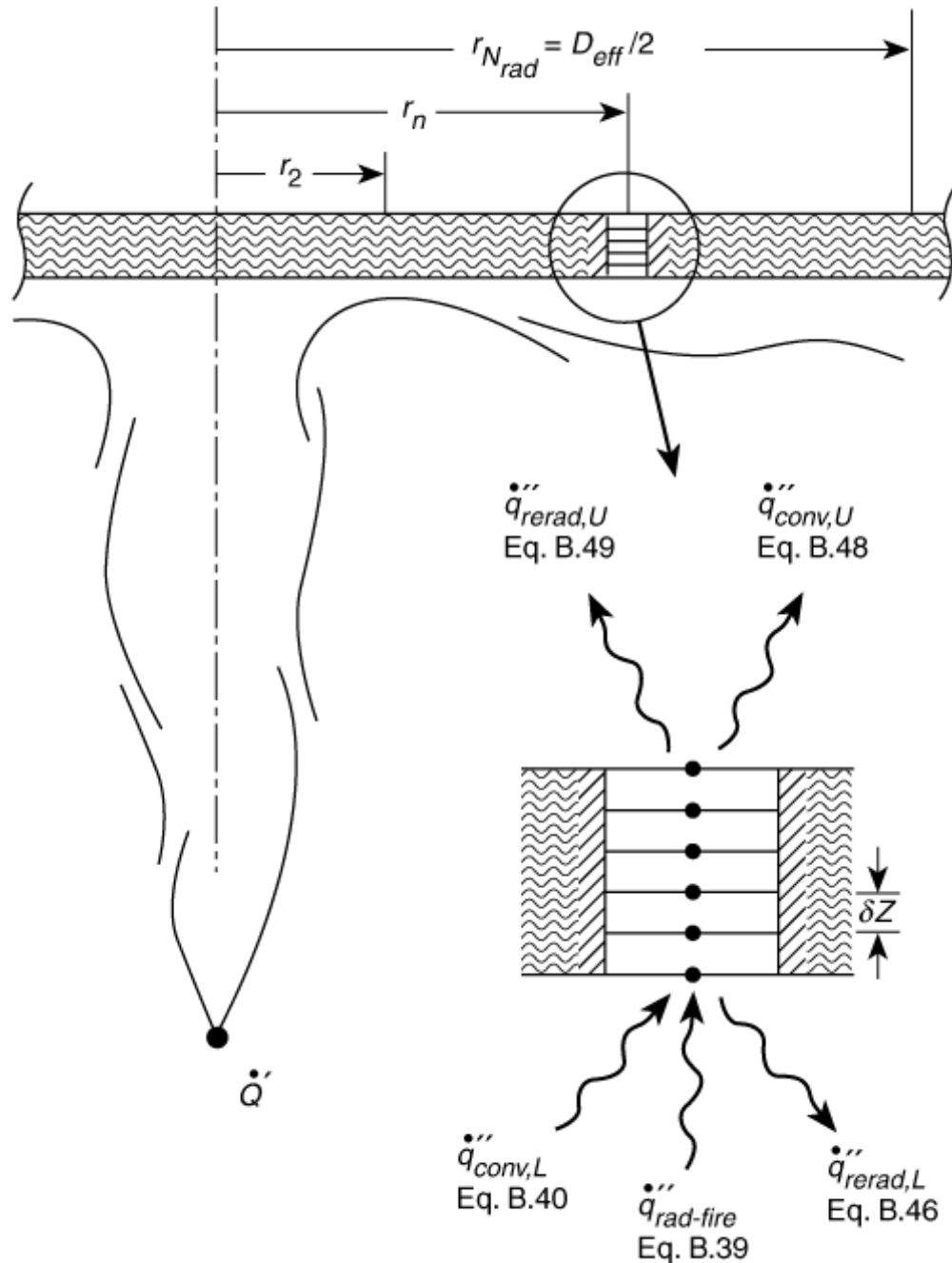


**FIGURE B.4.5.3 Illustration of the Geometry for the Boundary Value Problems of the Temperature Distributions,  $T_n$ , Through the Ceiling at Radial Positions  $r_n$ .**

Characteristic changes in ceiling temperature will occur over changes in  $r/H$  of the order of 1 (see [15]). Therefore, it is reasonable to expect accurate results for the Equation B.36

integral  $\dot{q}_{conv,L}''$  of by interpolating between values of  $\dot{q}_{conv,L}''$  calculated at radial positions separated by  $r/H$  intervals of 0.1 to 0.2.

Using the preceding ideas, the following procedure for finding the thermal response of the ceiling and solving for  $\dot{q}_{HT}''$  is implemented:

- (1) Because  $y_{ceil} - y_{fire}$  is a measure of  $H$  in the current problem and  $D_{eff}/2$  is a measure of the maximum value of  $r$ ,  $N_{rad}$  is chosen as several multiples of the following:

$$\frac{D_{eff}/2}{y_{ceil} - y_{fire}}$$

In this case,  $N_{rad}$  is chosen as the first integer equal to or greater than

$$\frac{5(D_{eff}/2)}{y_{ceil} - y_{fire}} + 2$$

- (2) One temperature calculation point is placed at  $r = 0$  and the remaining  $N_{rad}$  calculation points are distributed with uniform separation at and between  $r = 0.2(y_{ceil} - y_{fire})$  and  $r = D_{eff}/2$ , the latter value being the upper limit of the integral of Equation B.36; that is,

$$\begin{aligned} r_1 &= 0 \\ r_2 &= 0.2(y_{ceil} - y_{fire}) \\ r_{N_{rad}} &= \frac{D_{eff}}{2} \\ r_n &= r_{n-1} + \Delta r \quad \text{if } 2 < n < N_{rad} \end{aligned}$$

where  $\Delta r = (r_{N_{rad}} - r_2) / (N_{rad} - 3)$

- (3) The boundary value problems are solved for the  $N_{rad}$  temperature distributions,  $T_n$ . At arbitrary radius,  $r_n$ , these are indicated in the inset portion of Figure B.4.5.3.
- (4) For any moment of time during the calculation, the lower surface values of the  $T_n$  are used to compute the corresponding discrete values of  $\dot{q}_{conv,L,n}''(t) = \dot{q}_{conv,L}''(r = r_n, t)$  from Equation B.40.
- (5) The  $\dot{q}_{conv,L}''$  distribution in  $r$  is approximated by interpolating linearly between the  $\dot{q}_{conv,L,n}''$ . The integration indicated in Equation B.36 is carried out.

The procedure for solving for the  $T_n$  is the same as that used in reference [15]. It requires the thickness, thermal conductivity, and thermal diffusivity of the ceiling material. The

solution to the one-dimensional heat conduction equation involves an explicit finite difference scheme that uses an algorithm taken from references [19, 20]. For a given set of calculations,  $N \leq 20$  equal-spaced nodes are positioned at the surfaces and through the thickness of the ceiling at every radius position,  $r_n$ . The spacing,  $\delta Z$  (see Figure B.4.5.3), of these is selected to be large enough (based on a maximum time step) to ensure stability of the calculation.

## B.5 Actuation of Vents and Sprinklers.

It is an objective of this standard to simulate conditions in building spaces where ceiling vents and sprinkler links can be actuated by the responses of near-ceiling-deployed fusible links. The concept is that, during the course of a compartment fire, a deployed link is engulfed by the near-ceiling convective flow of the elevated-temperature products of combustion and entrained air of the fire-generated plume. As the fire continues, convective heating of the link leads to an increase in its temperature. If and when its fuse temperature is reached, any devices being operated by the link are actuated.

The near-ceiling flow engulfing the link is the plume-driven ceiling jet referred to previously, which transfers heat to the lower-ceiling surface and is cooled as it traverses under the ceiling from the point of plume-ceiling impingement. In the case of relatively smooth ceiling configurations, assumed to be representative of the facilities studied in this standard, the ceiling jet flows outward radially from the point of impingement, and its gas velocity and temperature distributions,  $V_{CJ}$  and  $T_{CJ}$ , respectively, are a function of radius from the impingement point,  $r$ , distance below the ceiling,  $z$ , and time,  $t$ .

Vents actuated by alternate means, such as thermoplastic drop-out panels with equivalent performance characteristics, can also be modeled using LAVENT. Refer to A.9.1.

**B.5.1 Predicting the Thermal Response of the Fusible Links.** The thermal response of deployed fusible links is calculated up to their fuse temperature,  $T_F$ , by the convective heating flow model of [21]. It is assumed that the specific link is positioned at a specified radius from the impingement point,  $r = r_L$ , and distance below the lower-ceiling surface,  $z = z_L$ .  $T_L$  is defined as the link's assumed, nearly uniform temperature. Instantaneous changes in  $T_L$  are determined by the following:

$$(B.51) \quad \frac{dT_L}{dt} = \frac{(T_{CJ,L} - T_L)V_{CJ,L}^{1/2}}{RTI}$$

where  $T_{CJ,L}$  and  $V_{CJ,L}$  are the values of  $V_{CJ}$  and  $T_{CJ}$ , respectively, evaluated near the link position, and where  $RTI$  (response time index), a property of the link and relative flow orientation, can be measured in the “plunge test” [21, 22]. The  $RTI$  for ordinary sprinkler links ranges from low values of  $22 \text{ (m} \cdot \text{s)}^{1/2}$  for quick-operating residential sprinklers, to  $375 \text{ (m} \cdot \text{s)}^{1/2}$  for slower standard sprinklers [23]. The utility of Equation B.51, which has been shown in [24] to be valid typically through the link-fusing processes, is discussed further in [23], where it was used to predict link response in a parametric study involving

two-layer compartment fire scenarios. Also, in the latter work, the link response prediction methodology was shown to demonstrate favorable comparisons between predicted and measured link responses in a full-scale, one-room, open-doorway compartment fire experiment.

Computing  $T_L$  from Equation B.51 for a different link location necessitates estimates of  $V_{CJ,L}$  and  $T_{CJ,L}$  for arbitrary link positions,  $r_L$  and  $z_L$ .

**B.5.2 The Velocity Distributions of the Ceiling Jet.** Outside of the plume–ceiling impingement stagnation zone, defined approximately by  $r/H \leq 0.2$ , and at a given  $r$ ,  $V_{CJ}$  rises rapidly from zero at the ceiling's lower surface,  $z = 0$ , to a maximum,  $V_{max}$ , at a distance  $z = 0.23\delta$ ,  $\delta(r)$  being the distance below the ceiling where  $V/V_{max} = 1/2$  [16]. In this region outside the stagnation zone,  $V_{CJ}$  can be estimated [16] as follows:

$$\text{if } \frac{r}{H} \geq 0.2;$$

(B.52)

$$\frac{V_{CJ}}{V_{max}} = \begin{cases} \left(\frac{8}{7}\right) \left(\frac{z}{0.23\delta}\right)^{1/7} \left[1 - \frac{z/(0.23\delta)}{8}\right]; & \text{if } 0 \leq \frac{z}{0.23\delta} \leq 1 \\ \cosh^{-2} \left\{ \left(\frac{0.23}{0.77}\right) \operatorname{arccosh}(2^{1/2}) \times \left[\frac{z}{0.23\delta} - 1\right] \right\}; & \text{if } 1 \leq \frac{z}{0.23\delta} \end{cases}$$

$$\frac{V_{max}}{V} = 0.85 \left(\frac{r}{H}\right)^{-1.1}$$

$$\frac{\delta}{H} = 0.10 \left(\frac{r}{H}\right)^{0.9}$$

(B.53) 
$$V = g^{1/2} H^{1/2} \dot{Q}_H^{*1/3}$$

where  $\dot{Q}_H^*$  is defined in Equation B.44.  $V_{CJ}/V_{max}$  per Equation B.52 is plotted in Figure B.5.2.

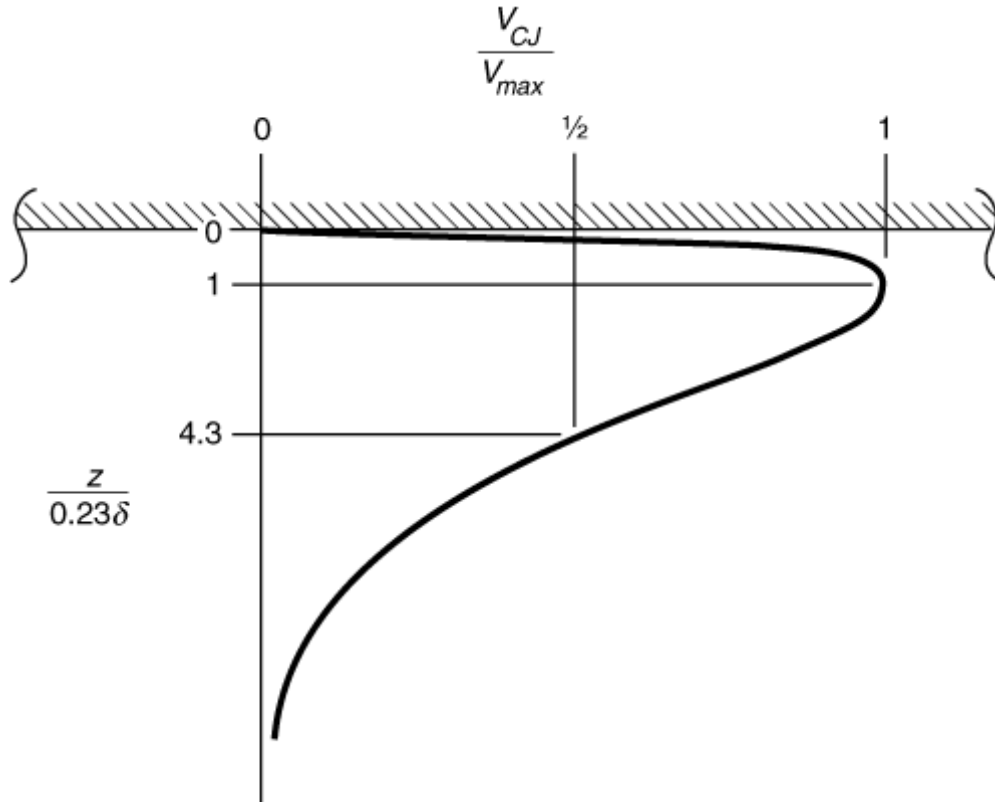


**FIGURE B.5.2** A Plot of Dimensionless Ceiling Jet Velocity Distribution,  $V_{CJ}/V_{max}$ , as a Function of  $z/0.23\delta$  per Equation B.52.

In the vicinity of near-ceiling-deployed links located inside the stagnation zone, the fire-driven flow is changing directions from an upward-directed plume flow to an outward-directed ceiling jet-type flow. There the flow velocity local to the link, the velocity that drives the link's connective heat transfer, involves generally a significant vertical as well as radial component of velocity. Nevertheless, at such link locations, it is reasonable to continue to approximate the link response using Equation B.51 with  $V_{CJ}$  estimated using Equations B.52 and B.53 and with  $r/H$  set equal to 0.2; that is,

$$(B.54) \quad V_{CJ} = V_{CJ} \left( \frac{r}{H} = 0.2 \right); \quad \text{if } 0 \leq \frac{r}{H} < 0.2$$

**B.5.3 The Temperature Distribution of the Ceiling Jet.** Outside of the plume-ceiling impingement stagnation zone (i.e., where  $r/H \geq 0.2$ ) and at a given value of  $r$ ,  $T_{CJ}$  rises very rapidly from the temperature of the ceiling's lower surface,  $T_{S,L}$ , at  $z = 0$ , to a maximum,  $T_{max}$ , somewhat below the ceiling surface. It is assumed that this maximum value of  $T_{CJ}$  occurs at the identical distance below the ceiling as does the maximum of  $V_{CJ}$  (i.e., at  $z = 0.23\delta$ ). Below this elevation,  $T_{CJ}$  drops with increasing distance from the ceiling until it reaches the upper-layer temperature,  $T_U$ . In this latter, outer region of the ceiling jet, the shape of the normalized  $T_{CJ}$  distribution,  $(T_{CJ} - T_U)/(T_{max} - T_U)$ , has the same characteristics as that of  $V_{CJ}/V_{max}$ . Also, because the boundary flow is

turbulent, it is reasonable to estimate the characteristic thicknesses of the outer region of both the velocity and temperature distributions as being identical, both dictated by the distribution of the turbulent eddies there.

For these reasons, the dimensionless velocity and temperature distribution are approximated as being identical in the outer region of the ceiling jet flow,  $0.23\delta \leq z$ . In the inner region of the flow, between  $z = 0$  and  $0.23\delta$ , the normalized temperature distribution is approximated by a quadratic function of  $z/(0.23\delta)$ , with  $T_{CJ} = T_{S,L}$  at  $z = 0$  and  $T_{CJ} = T_{max}$ ,  $dT_{CJ}/dz = 0$  at  $z = 0.23\delta$ . Therefore, where  $r/H \geq 0.2$ ,

$$\Theta \equiv \frac{T_{CJ} - T_U}{T_{max} - T_U} = \begin{cases} \Theta_s + 2 \left[ (1 - \Theta_s) \left( \frac{z}{0.23\delta} \right) \right] - \left[ (1 - \Theta_s) \left( \frac{z}{0.23\delta} \right) \right]^2; & \text{if } 0 \leq \frac{z}{0.23\delta} \leq 1 \\ \frac{V_{CJ}}{V_{max}}; & \text{if } 1 \leq \frac{z}{0.23\delta} \end{cases}$$

(B.55)

$$\Theta_s \equiv \Theta(T_{CJ} = T_{S,L}) = \frac{T_{S,L} - T_U}{T_{max} - T_U}$$

(B.56)

It should be noted that  $\Theta_s$  is negative when the ceiling surface temperature is less than the upper-layer temperature (e.g., relatively early in a fire, when the original ambient-temperature ceiling surface has not yet reached the average temperature of the growing upper layer). Also,  $\Theta_s$  is greater than 1 when the ceiling surface temperature is greater than  $T_{max}$ . This is possible, for example, during times of reduced fire size when the fire's near-ceiling plume temperature is reduced significantly, perhaps temporarily, from previous values, but the ceiling surface, heated previously to relatively high temperatures, has not cooled substantially. Plots of  $\Theta$  per Equation B.55 are shown in Figure B.5.3 for cases where  $\Theta_s$  is  $< 0$ , between 0 and 1, and  $> 0$ .

$$\Delta T_{CJ} = T_{CJ} - T_U$$

= ceiling jet temperature – upper layer temperature

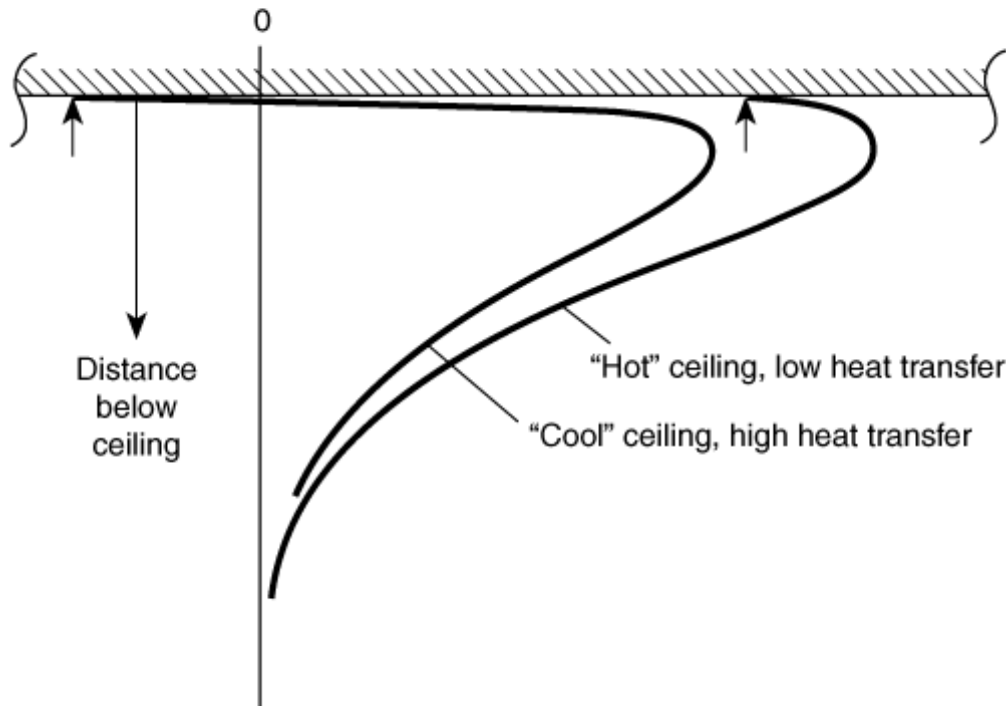


**FIGURE B.5.3** Plots of Dimensionless Ceiling Jet Temperature Distribution,  $\Theta$ , as a Function of  $z/0.23\delta$  per Equation B.55 for cases where  $\Theta_s$  is  $< 0$ , between  $0$  and  $1$ , and  $> 0$ .

In a manner similar to the treatment of  $V_{CJ}/V_{max}$ , for the purpose of calculating  $T_L$ , from Equation B.51,  $\Theta_s$  is approximated inside the stagnation zone by the description of Equations B.55 and B.56, with  $r/H$  set equal to  $0.2$  as follows:

$$(B.57) \quad \Theta_s = \Theta_s \left( \frac{r}{H} = 0.2 \right); \quad \text{if } 0 \leq \frac{r}{H} \leq 0.2$$

With the radial distribution for  $T_{S,L}$  and  $T_U$  already calculated up to a specific time, only  $T_{max}$  is needed to complete the derived estimate from Equations B.55 through B.57 for the ceiling jet temperature distribution. This estimate is obtained by invoking conservation of energy. Therefore, at an arbitrary  $r$  outside the stagnation zone, the total rate of radial outflow of enthalpy (relative to the upper-layer temperature) of the ceiling jet is equal to the uniform rate of enthalpy flow in the upper-layer portion of the plume,  $\dot{Q}'$ , less the integral (from the plume–ceiling impingement prior to  $r$ ) of the flux of convective heat transfer from the ceiling jet to the ceiling surface as follows:

$$2\pi \int_0^{\infty} \rho_U C_P (T_{CJ} - T_U) V_{CJ} r dz = \dot{Q}' - 2\pi \int_0^r \dot{q}_{conv,L}''(r,t) r dr$$

$$\equiv (1 - \lambda'_{conv}) \dot{Q}'; \quad \text{if } 0.2 \leq \frac{r}{H}$$

(B.58)

$\lambda'_{conv}$  is the fraction of  $\dot{Q}'$  transferred by convection to the ceiling from the point of ceiling impingement to  $r$  as follows:

$$\lambda'_{conv}(r) = \frac{2\pi \int_0^r \dot{q}_{conv,L}''(r,t) r dr}{\dot{Q}'}$$

(B.59)

In Equations B.58 and B.59,  $\dot{Q}'$  has been calculated previously in Equation B.34. Also, the integral on the right-hand sides of Equations B.58 and B.59 can be calculated by

approximating  $\dot{q}_{conv,L}''(r,t)$ , as shown in Equation B.59, as a linear function of  $r$  between previously calculated values of  $\dot{q}_{conv,L}(r = r_n, t)$ .

The integral on the left-hand side of Equation B.58 is calculated using  $V_{CJ}$  of Equations B.52 and B.53 and  $T_{CJ}$  of Equations B.55 and B.56. From this, the desired distribution for  $T_{max}$  is determined as follows:

(B.60)

$$(T_{max} - T_U) = 2.6 (1 - \lambda'_{conv}) \left( \frac{r}{H} \right)^{-0.8} \dot{Q}_H^{*2/3} T_U - 0.090 (T_{S,L} - T_U);$$

$$\text{if } 0.2 \leq \frac{r}{H}$$

The result of Equation B.60, together with Equations B.55 and B.56, represents the desired estimate for  $T_{CJ}$ . This and the estimate derived from Equations B.52 through B.54 for  $T_{CJ}$  are used to calculate  $T_L$  from Equation B.51.

**B.5.4 Dependence of Open Vent Area on Fusible-Link-Actuated Vents.** As discussed, the influence of ceiling vent action on the fire-generated equipment is dependent on the active area of the open ceiling vents,  $A_V$ . A variety of basic vent opening design strategies is possible, and a major application of the current model equations is to evaluate these strategies within the context of the developing fire environment. For example, one of the simplest strategies [9] assumes that all vents deployed in the specified curtained area are opened by whatever means at the onset of the fire. In general,  $A_V$  will be time-dependent.

To the extent that a strategy of vent opening is dependent directly on the fusing of any one or several deployed fusible links, the location of these links and their characteristics (i.e., likely spacings from plume–ceiling impingement, distance below the ceiling, and the  $RTI$ ) and the functional relationship between link fusing and  $A_V$  need to be specified. These matters can be examined in the context of different solutions to the overall problem by exercising parametrically the LAVENT computer program [2], which implements all the model equations provided in this annex.

**B.5.5 Concluding Remarks — A Summary of Guidelines, Assumptions, and Limitations.** The theory presented here is the basis of LAVENT, a user-friendly computer program [2] that is supported by a user guide [3] and that can be used to study parametrically a wide range of relevant fire scenarios.

The assumptions made in the development of the set of model equations limit fire scenarios or aspects of fire scenarios that can be simulated and studied with confidence. A summary of guidelines and assumptions that characterize what are perhaps the most critical of these limitations follows. These are the result of explicit or implicit assumptions necessary for valid application of the variety of submodels introduced throughout this work.

$L$  and  $W$  are the length and width, respectively, of the plan area of the curtained space. Simulated configurations should be limited to those with aspect ratios,  $L/W$ , that are not much different from 1 (e.g.,  $0.5 \leq L/W < 2$ ). Also, in such configurations, the fire should not be too close to or too far from the walls [e.g., the fire should be no closer to a wall than  $(y_{ceil} - y_{fire})/2$  and no farther than  $3(y_{ceil} - y_{fire})$ ].

The curtain boards should be deep enough to satisfy  $(y_{ceil} - y_{curt}) \geq 0.2(y_{ceil} - y_{fire})$ , unless the equations and the standard are used to simulate an unconfined ceiling scenario where  $(y_{ceil} - y_{curt}) = 0$ .

The ceiling of the curtained space should be relatively smooth, with protuberances having depths significantly less than  $0.1(y_{ceil} - y_{fire})$ . Except at the locations of the curtain boards, below-ceiling–mounted barriers to flow, such as solid beams, should be avoided. Ceiling surface protuberances near to and upstream of fusible links (i.e., between the links and the fire) should be significantly smaller than link-to-ceiling distances.

$W_V$  is the width, that is, the smaller dimension of a single ceiling vent (or vent cluster). If vents are open, the prediction of smoke layer thickness,  $y_{ceil} - y$ , is reliable only after the time that  $(y_{ceil} - y)/W_V$  is greater than 1. (For smaller layer depths, “plugholing” flow through the vents could occur, leading to possible significant inaccuracies in vent flow estimates.) Note that this places an additional limitation on the minimum depth of the curtain boards [i.e.,  $(y_{ceil} - y_{curt})/W_V$  should exceed 1].

At all times during a simulated fire scenario, the overall building space should be vented to the outside (e.g., through open doorways).

In this regard, compared to the open ceiling vents in the curtained compartment, the area of the outside vents must be large enough such that the pressure drop across the outside vents

is small compared to the pressure drop across ceiling vents. For example, under near-steady-state conditions, when the rate of mass flow into the outside vents is approximately equal to the rate of mass outflow from the ceiling vents, the outside vent area must satisfy  $(A_{Vout}/A_V)^2(T_U/T_{amb})^2 \gg 1$ , or, more conservatively and independent of  $T_U$ ,  $(A_{Vout}/A_V)^2 \gg 1$ . The latter criterion will always be reasonably satisfied if  $A_{Vout}/A_V > 2$ .

Under flashover-level conditions — say, when  $T_U/T_{amb} = 3$  — the former criterion will be satisfied if  $(3 A_{Vout}/A_V)^2 \gg 1$  — say, if  $A_{Vout} = A_V$ , or even if  $A_{Vout}$  is somewhat smaller than  $A_V$ .

The simulation assumes a relatively quiescent outside environment (i.e., without any wind) and a relatively quiescent inside environment (i.e., remote from vent flows, under-curtain flows, ceiling jets, and the fire plume). In real fire scenarios, such an assumption should be valid where the characteristic velocities of actual flows in these quiescent environments are much less than the velocity of the fire plume near its ceiling impingement point (i.e., where the characteristic velocities are much less than  $V_{max}$  of Equation B.53). It should be noted that, for a given fire strength,  $Q$ , this latter assumption places a restriction on the maximum size of  $(y_{ceil} - y_{fire})$ , which is a measure of  $H$ , since  $V_{max}$  is approximately proportional to  $(y_{ceil} - y_{fire})^{-1/3}$ .

In configurations where smoke flows below curtain partitions to adjacent curtained spaces, the simulation is valid only up to the time that it takes for any one of the adjacent spaces to fill with smoke to the level of the bottom of the curtain. While it is beyond the scope of this guide to provide any general guidelines for this limiting time, the following rule can be useful where all curtained spaces of a building are similar and where the fire is not growing too rapidly: The time to fill an adjacent space is of the order of the time to fill the original space.

The reliability of the simulation begins to degrade subsequent to the time that the top of the flame penetrates the layer elevation, and especially if Equation B.20 predicts a flame height that reaches the ceiling.

It is assumed that the smoke is relatively transparent and that the rate of radiation absorbed by or emitted from the smoke layer is small compared to the rate of radiation transfer from the fire's combustion zone. The assumption is typically true, and a simulation is valid at least up to those times that the physical features of the ceiling can be discerned visually from the floor elevation.

It should be emphasized that the preceding limitations are intended only as guidelines. Therefore, even when the characteristics of a particular fire scenario satisfy these limitations, the results should be regarded with caution until solutions to the overall model equations have been validated by a substantial body of experimental data. Also, where a fire scenario does not satisfy the preceding limitations but is close to doing so, it is possible that the model equations can still provide useful quantitative descriptions of the simulated phenomena.

## B.6 References for Annex B.

- (1) L.Y. Cooper, "Estimating the Environment and the Response of Sprinkler Links in

- Compartment Fires with Draft Curtains and Fusible Link-Actuated Ceiling Vents,” *Fire Safety Journal* 16:37–163, 1990.
- (2) LAVENT software, available from National Institute of Standards and Technology, Gaithersburg, MD.
  - (3) W.D. Davis, and L.Y. Cooper, “Estimating the Environment and the Response of Sprinkler Links in Compartment Fires with Draft Curtains and Fusible Link-Actuated Ceiling Vents—Part II: User Guide for the Computer Code LAVENT,” NISTIR 89-4122, National Institute of Standards and Technology, Gaithersburg, MD, August 1989.
  - (4) H.W. Emmons, “The Flow of Gases Through Vents,” Harvard University Home Fire Project Technical Report No. 75, Cambridge, MA, 1987.
  - (5) P.H. Thomas, et al., “Investigations into the Flow of Hot Gases in Roof Venting,” Fire Research Technical Paper No. 7, HMSO, London, 1963.
  - (6) G. Heskestad, “Smoke Movement and Venting,” *Fire Safety Journal* 11:77–83, 1986, and Appendix A, *Guide for Smoke and Heat Venting*, NFPA 204M, National Fire Protection Association, Quincy, MA, 1982.
  - (7) L.Y. Cooper, “A Mathematical Model for Estimating Available Safe Egress Time in Fires,” *Fire and Materials* 6 (3/4):135–144, 1982.
  - (8) G. Heskestad, “Engineering Relations for Fire Plumes,” *Fire Safety Journal* 7:25–32, 1984.
  - (9) P.L. Hinkley, “Rates of ‘Production’ of Hot Gases in Roof Venting Experiments,” *Fire Safety Journal* 10:57–64, 1986.
  - (10) E.E. Zukoski, T. Kubota, and B. Cetegen, *Fire Safety Journal* 3:107, 1981.
  - (11) L.Y. Cooper, “A Buoyant Source in the Lower of Two, Homogeneous, Stably Stratified Layers,” 20th International Symposium on Combustion, Combustion Institute, Michigan Univ., Ann Arbor, MI, pp. 1567–1573, 1984.
  - (12) L.Y. Cooper, “Convective Heat Transfer to Ceilings Above Enclosure Fires,” 19th Symposium (International) on Combustion, Combustion Institute, Haifa, Israel, pp. 933–939, 1982.
  - (13) L.Y. Cooper, “Heat Transfer from a Buoyant Plume to an Unconfined Ceiling,” *Journal of Heat Transfer* 104:446–451, August 1982.
  - (14) L.Y. Cooper, and A. Woodhouse, “The Buoyant Plume-Driven Adiabatic Ceiling Temperature Revisited,” *Journal of Heat Transfer* 108:822–826, November 1986.
  - (15) L.Y. Cooper, and D.W. Stroup, “Thermal Response of Unconfined Ceilings Above Growing Fires and the Importance of Convective Heat Transfer,” *Journal of Heat Transfer* 109:172–178, February 1987.
  - (16) L.Y. Cooper, “Ceiling Jet-Driven Wall Flows in Compartment Fires,” *Combustion Science and Technology* 62:285–296, 1988.

- (17) J. Hilsenrath, "Tables of Thermal Properties of Gases," Circular 564, National Bureau of Standards, Gaithersburg, MD, November 1955.
- (18) W.W. Yousef, J.D. Tarasuk, and W.J. McKeen, "Free Convection Heat Transfer from Upward-Facing, Isothermal, Horizontal Surfaces," *Journal of Heat Transfer* 104:493–499, August 1982.
- (19) H.W. Emmons, "The Prediction of Fire in Buildings," 17th Symposium (International) in Combustion, Combustion Institute, Leeds, England, pp. 1101–1111, 1979.
- (20) H.E. Mitler, and H.W. Emmons, "Documentation for the Fifth Harvard Computer Fire Code," Harvard University, Home Fire Project Technical Report 45, Cambridge, MA, 1981.
- (21) G. Heskestad, and H.F. Smith, "Investigation of a New Sprinkler Sensitivity Approval Test: The Plunge Test," Technical Report Serial No. 22485, RC 76-T-50, Factory Mutual Research Corporation, Norwood, MA, 1976.
- (22) G. Heskestad, "The Sprinkler Response Time Index (RTI)," Paper RC-81-Tp-3 presented at the Technical Conference on Residential Sprinkler Systems, Factory Mutual Research Corporation, Norwood, MA, April 28–29, 1981.
- (23) D.D. Evans, "Calculating Sprinkler Actuation Times in Compartments," *Fire Safety Journal* 9:147–155, 1985.
- (24) D.D. Evans, "Characterizing the Thermal Response of Fusible Link Sprinklers," NBSIR 81-2329, National Bureau of Standards, Gaithersburg, MD, 1981.
- (25) L.Y. Cooper, and D.W. Stroup, "Test Results and Predictions for the Response of Near-Ceiling Sprinkler Links in Full-Scale Compartment Fires." In *Fire Safety Science—Proceedings of the Second International Symposium*, Tokyo, June 13–17, 1988, pp. 623–632, T. Wakumatsu et al. eds., International Association of Fire Safety Science, Hemisphere Publishing Co., New York, 1989.

## B.7 Nomenclature for Annex B.

$A$  = plan area of single curtain space

$A_{eff}$  = effective area for heat transfer to the extended lower-ceiling surface,  $\pi D_{eff}^2 / 4$

$A_V$  = total area of open ceiling vents in curtained space

$A_{Vout}$  = total area of open vents to outside exclusive of  $A_V$

$C$  = vent flow coefficient (0.68)

$C_P$  = specific heat at constant pressure

$C_T$  = 9.115, dimensionless constant in plume model

$C_V$  = specific heat at constant volume

$D_{eff}$  = effective diameter of  $A_{eff}$

$D_{fire}$  = effective diameter of fire source ( $\pi D_{fire}^2 / 4$  = area of fire source)

$g$  = acceleration of gravity

$H$  = distance below ceiling of equivalent source

$\tilde{h}$  = characteristic heat transfer coefficient

$h_L, h_U$  = lower-, upper-ceiling surface heat transfer coefficient

$L$  = characteristic length of the plan area of curtained space

$L_{curt}$  = length of the perimeter of  $A$  connected to other curtained areas of the building

$L_{flame}$  = flame length

$\dot{m}_{curt}$  = mass flow rate from below curtain to upper layer

$\dot{m}_{ent}$  = rate of plume mass entrainment between the fire and the layer interface

$\dot{m}_{plume}$  = mass flow rate of plume at interface

$m_U$  = total mass of the upper layer

$\dot{m}_U$  = net mass flow rate to upper layer

$\dot{m}_{vent}$  = mass flow rate through ceiling vents to upper layer

$N$  = number of equal-spaced nodes through the ceiling

$N_{rad}$  = number of values of  $r_n$

$P$  = length of perimeter of single curtained area

$Pr$  = Prandtl number, taken to be 0.7

$p$  = pressure

$p_U, p_{amb}$  = pressure in upper-layer, outside ambient

$\dot{Q}$  = energy release rate of fire

$\dot{Q}'$  = strength of continuation source in extended upper layer

$\dot{Q}_H^*$  = dimensionless strength of plume at ceiling

$\dot{Q}_{eq}^*$  = dimensionless strength of plume at interface

$\dot{q}_{conv,L}'' , \dot{q}_{conv,U}''$  = convective heat transfer flux to lower-, upper-ceiling surface

$\dot{q}_{conv,L,n}'' = \dot{q}_{conv,L}''(r = r_n, t)$

$\dot{q}_{curt}$  = enthalpy flow rate from below curtain to upper layer

$\dot{q}_{HT}$  = heat transfer rate to upper layer

$\dot{q}_{plume}$  = enthalpy flow rate of plume at interface

$\dot{q}_{rad-fire}$  = radiation flux incident on lower surface of ceiling

$\dot{q}_{rerad,L}'' , \dot{q}_{rerad,U}''$  = reradiation flux to lower, upper surface of ceiling

$\dot{q}_U$  = net enthalpy flow rate plus heat transfer rate to upper layer

$\dot{q}_L'' , \dot{q}_U''$  = net heat transfer fluxes to upper-, lower-ceiling surface

$\dot{q}_{vent}$  = enthalpy flow rate through ceiling vent to upper layer

$R$  = gas constant,  $C_P - C_V$

$Re_H$  = Reynolds number of plume at ceiling elevation

$RTI$  = response time index

$r$  = radial distance from plume-ceiling impingement

$r_L$  =  $r$  at link

$r_n$  = discrete values of  $r$

$T$  = absolute temperature of ceiling material

$T_{AD}$  = adiabatic lower-ceiling surface temperature

$T_{CJ}$  = temperature distribution of ceiling jet gas

$T_{CJ,L} = T_{CJ}$  at link

$T_{max}(t) = T_{S,L}(r = 0, t) = T(Z = 0, t, r = 0)$

$T_{S,L}, T_{S,U}$  = absolute temperature of lower-, upper-ceiling surface

$$T_{S,L,n}(t) = T_{S,L}(r = r_n, t) = T_n(Z = 0, t, r = r_n)$$

$T_U, T_{amb}$  = absolute temperature of upper-layer, outside ambient

$$T_n = T(Z, t, r = r_n)$$

$t$  = time

$V$  = average flow velocity through all open vents

$V$  = characteristic value of  $V_{CJ}$

$V_{CJ}$  = velocity distribution of ceiling jet gas

$V_{CJ,L}$  =  $V_{CJ}$  at link

$V_{max}$  = maximum value of  $V_{CJ}$  at a given  $r$

$W$  = characteristic width of plan area of curtained space

$W_V$  = width of a single ceiling vent (or vent cluster)

$y, y_{ceil}, y_{curt}, y_{eq}, y_{fire}$  = elevation of smoke layer interface, ceiling, bottom of curtain, equivalent source fire above floor

$y'_{source}$  = elevation of plume continuation point source in extended upper layer above floor

$Z$  = distance into the ceiling, measured from bottom surface

$z, z_L$  = distance below lower-ceiling surface,  $z$ , at link

$$\alpha = T_U/T_{amb}$$

$\tau$  = ratio of specific heat,  $C_p/C_V$

$\Delta p_{ceil}$  = cross-vent pressure difference

$\Delta p_{curt}$  = cross-curtain pressure difference

$\delta$  = value of  $z$  where  $V_{CJ} = V_{max}/2$

$\delta Z$  = distance between nodes through the ceiling thickness

$\epsilon$  = constant, Equations B.17 and B.19

$\epsilon_L, \epsilon_U, \epsilon_{floor}, \epsilon_{far}$  = emittance-absorptance of lower, upper, floor, and far-field gray surfaces, all taken to be 1

$\Theta$  = normalized, dimensionless ceiling jet temperature distribution,  $(T_{CJ} - T_U)/(T_{max} - T_U)$

$\Theta_S = \Theta$  at lower-ceiling surface,  $(T_{S,L} - T_U)/(T_{max} - T_U)$

$\lambda_r$  = fraction of  $\dot{Q}$  radiated from combustion zone

$\lambda_{conv}$  = fraction of  $\dot{Q}$  transferred by convection from upper layer

$\lambda'_{conv}$  = fraction of  $\dot{Q}'$  transferred to the ceiling in a circle of radius,  $r$ , and centered at  $r = 0$ , Equation B.56.

$\nu_U$  = kinematic viscosity of upper-layer gas

$\rho_U, \rho_{amb}$  = density of upper-layer, outside ambient

$\sigma$  = dimensionless variable, Equation B.28

## Annex C User Guide for the LAVENT Computer Code

*This annex is not a part of the requirements of this NFPA document but is included for informational purposes only.*

### C.1 Overview.

This annex is a user guide for the LAVENT computer code (Link-Actuated VENTs), Version 1.1, and an associated graphics code called GRAPH. As discussed in Section 9.3 and Annex B, LAVENT has been developed to simulate the environment and the response of sprinkler links in compartment fires with curtain boards and fusible-link-actuated ceiling vents. Vents actuated by alternative means such as thermoplastic drop-out panels with equivalent performance characteristics can also be modeled using LAVENT. Refer to A.1.1.1.

A fire scenario simulated by LAVENT is defined by the following input parameters:

- (1) Area and height of the curtained space
- (2) Separation distance from the floor to the bottom of the curtain
- (3) Length of the curtain (A portion of the perimeter of the curtained space can include floor-to-ceiling walls.)
- (4) Thickness and properties of the ceiling material (density, thermal conductivity, and heat capacity)
- (5) Constants that define a specified time-dependent energy release rate of the fire
- (6) Fire elevation
- (7) Area or characteristic energy release rate per unit area of the fire

- (8) Total area of ceiling vents whose openings are actuated by a single fusible link (Multiple vent area/link system combinations may be permitted in any particular simulation.)
- (9) Identifying numbers of fusible links used to actuate single sprinkler heads or groups of sprinkler heads (Multiple sprinkler links are permitted in any particular simulation.)

The characteristics of the simulated fusible links are defined by the following input parameters:

- (1) Radial distance of the link from the fire–ceiling impingement point
- (2) Ceiling–link separation distance
- (3) Link fuse temperature
- (4) The response time index (RTI) of the link

For any particular run of LAVENT, the code outputs a summary of the input information and simulation results of the calculation, in tabular form, at uniform simulation time intervals requested by the user. The output results include the following:

- (1) Temperature of the upper smoke layer
- (2) Height of the smoke layer interface
- (3) Total mass in the layer
- (4) Fire energy release rate
- (5) Radial distributions of the lower-ceiling surface temperature
- (6) Radial distribution of heat transfer rates to the lower- and upper-ceiling surfaces
- (7) The temperature for each link and the local velocity and temperature of the ceiling jet

This annex explains LAVENT using a series of exercises in which the reader reviews and modifies a default input data file that describes vent and sprinkler actuation during fire growth in an array of wood pallets located in a warehouse-type occupancy. Results of the default simulation are discussed.

LAVENT is written in Fortran 77. The executable code operates on IBM PC-compatible computers and needs a minimum of 300 kilobytes of memory.

## **C.2 Introduction — The Phenomena Simulated by LAVENT.**

Figure C.2 depicts the generic fire scenario simulated by LAVENT. This scenario involves a fire in a building space with ceiling-mounted curtain boards and near-ceiling, fusible-link-actuated ceiling vents and sprinklers. The curtained area can be considered as one of several such spaces in a single large building compartment. By specifying that the curtains be deep enough, they can be thought of as simulating the walls of a single uncurtained compartment that is well-ventilated near the floor.

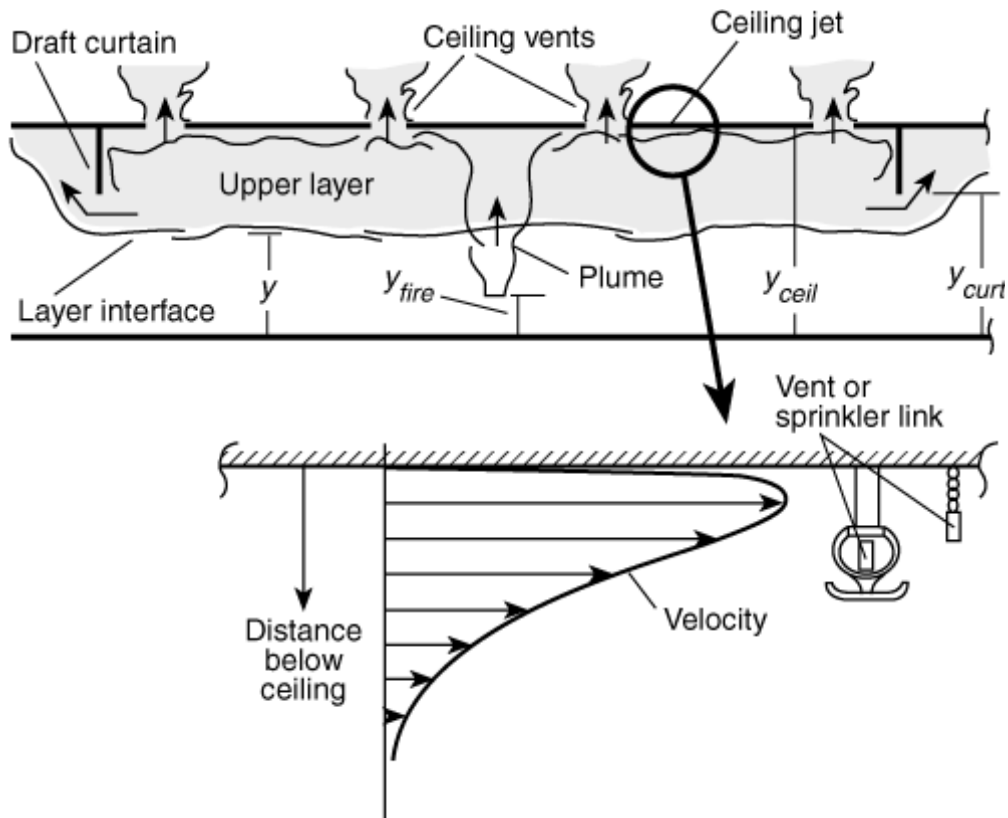


**FIGURE C.2 Fire in a Building Space with Curtain Boards, Ceiling Vents, and Fusible Links.**

The fire generates a mixture of gaseous and solid-soot combustion products. Because of high temperature, buoyancy forces drive the products upward toward the ceiling, forming a plume of upward-moving hot gases and particulates. Cool gases are laterally entrained and mixed with the plume flow, reducing its temperature as it continues its ascent to the ceiling.

When the hot plume flow impinges on the ceiling, it spreads under it, forming a relatively thin, high-temperature ceiling jet. Near-ceiling-deployed fusible links engulfed by the ceiling jet are depicted in Figure C.2. There is reciprocal convective cooling and heating of the ceiling jet and of the cooler lower-ceiling surface, respectively. The lower-ceiling surface is also heated due to radiative transfer from the combustion zone and cooled due to reradiation to the floor of the compartment. The compartment floor is assumed to be at ambient temperature. The upper-ceiling surface is cooled as a result of convection and radiation to a far-field, ambient temperature environment.

When the ceiling jet reaches a bounding vertical curtain board or wall surface, its flow is redistributed across the entire curtained area and begins to form a relatively quiescent smoke layer (now somewhat reduced in temperature) that submerges the continuing ceiling jet flow activity. The upper smoke layer grows in thickness. Away from bounding surfaces, the time-dependent layer temperature is assumed to be relatively uniform throughout its thickness. It should be noted that the thickness and temperature of the smoke layer affect the upper-plume characteristics, the ceiling jet characteristics, and the heat-transfer exchanges to the ceiling.

If the height of the bottom of the smoke layer drops to the bottom of the curtain board and

continues downward, the smoke begins to flow below the curtain into the adjacent curtained spaces. The growth of the upper layer is retarded.

Fusible links that are designed to actuate the opening of ceiling vents and the onset of waterflow through sprinklers are deployed at specified distances below the ceiling and at specified radial distances from the plume–ceiling impingement point. These links are submerged within the relatively high-temperature, high-velocity ceiling jet flow. Because the velocity and temperature of the ceiling jet vary with location and time, the heat transfer to and time of fusing of any particular link design also vary.

The fusing of a ceiling vent link leads to the opening of all vents “ganged” to that link. Once a ceiling vent is open, smoke flows out of the curtained space. Again, as when smoke flows below the curtains, growth of the upper-layer thickness is retarded.

The fusing of a sprinkler link initiates the flow of water through the sprinkler. All of the described phenomena, up to the time that waterflow through a sprinkler is initiated, are simulated by LAVENT. Results cannot be used after water begins to flow through a sprinkler.

### **C.3 The Default Simulation.**

The use of LAVENT is discussed and is illustrated in the following paragraphs where exercises in reviewing and modifying the LAVENT default-simulation input file are provided. To appreciate the process more fully, a brief description of the default simulation is presented at the outset.

Note that, as explained in Section C.4, Getting Started, the user can choose to run LAVENT using either English or metric units. The default simulation uses U.S. customary units. The example in Annex D uses metric units.

The default scenario involves an 84 ft × 84 ft curtained compartment (7056 ft<sup>2</sup> in area) with the ceiling located 30 ft above the floor. A curtain board 15 ft in depth completely surrounds and defines the compartment, which is one of several such compartments in a larger building space. The ceiling is constructed of a relatively thin sheet-steel lower surface that is well insulated from above. [See *Figure C.3(a)*.]

The curtained compartment has four, uniformly spaced 48-ft<sup>2</sup> ceiling vents with a total area of 192 ft<sup>2</sup>, or 2.7 percent of the compartment area. Opening of the ceiling vents is actuated by quick-response fusible links with RTIs of 50 (ft<sup>2</sup> sec)<sup>1/2</sup> and fuse temperatures of 165°F. The links are located at the centers of the vents and 0.3 ft below the ceiling surface.

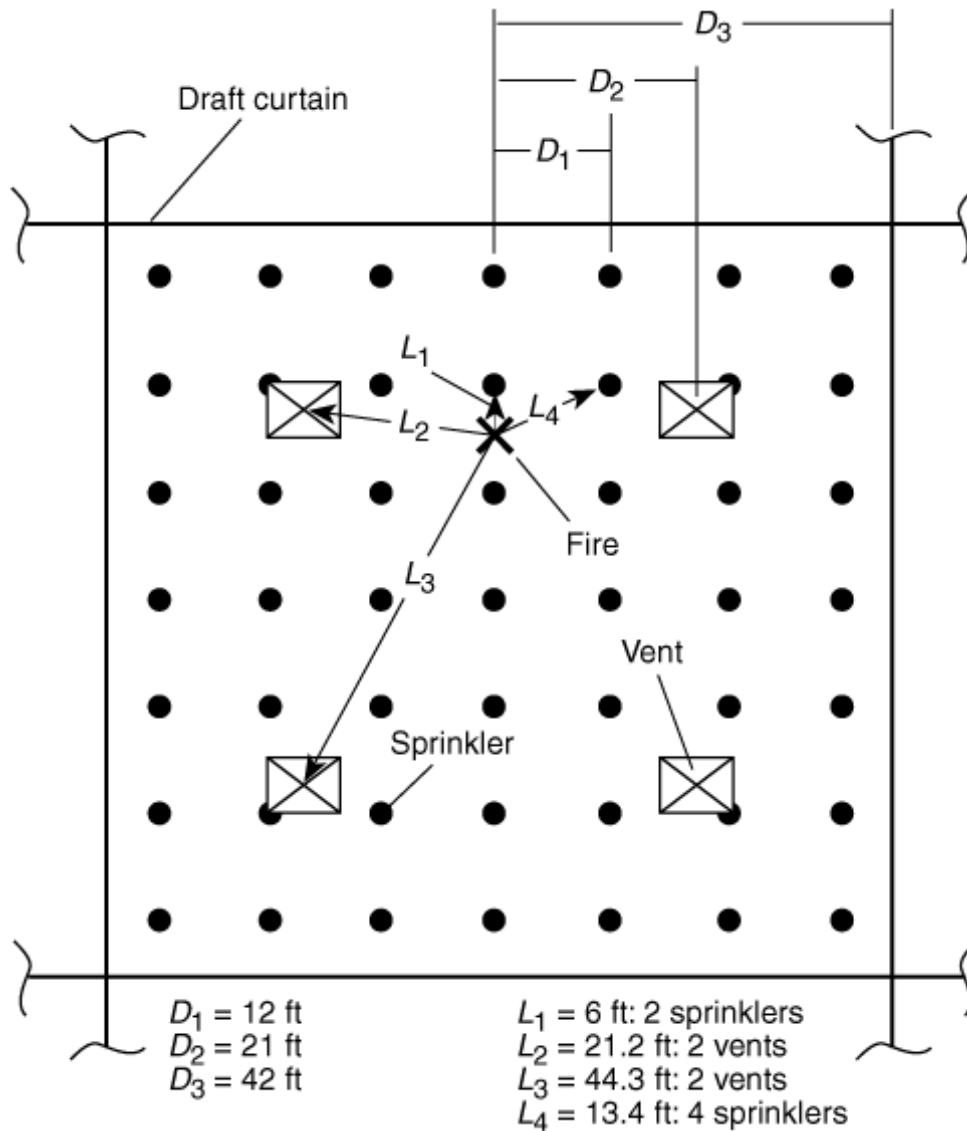


**FIGURE C.3(a) Vent and Sprinkler Spacing and Fire Location for the Default Simulation.**

Fusible-link-actuated sprinklers are deployed on a square grid with 12-ft spacing between sprinklers. The links have RTIs of  $400 \text{ (ft}^2 \text{ s)}^{1/2}$  and fuse temperatures of  $165^\circ\text{F}$ . The sprinklers and links are mounted 1 ft below the ceiling surface.

The simulation fire involves four abutting 5-ft high stacks of  $5 \text{ ft} \times 5 \text{ ft}$  wood pallets. The combined grouping of pallets makes up a combustible array  $10 \text{ ft} \times 10 \text{ ft}$  ( $100 \text{ ft}^2$  in area) on the floor and 5 ft in height. It is assumed that other combustibles in the curtained compartment are far enough away from this array that they cannot be ignited in the time interval to be simulated.

The total energy release rate of the simulation fire,  $\dot{Q}$ , assumed to grow from ignition, at time  $t = 0$ , in proportion to  $t^2$ . According to the guidance in Table F.1(a), in the growth

phase of the fire,  $\dot{Q}$  is taken specifically as follows:

$$\dot{Q} = 1000 \left( \frac{t}{130 \text{ sec}} \right)^2 \text{ Btu/sec}$$

The fire grows according to the preceding estimate until the combustibles are fully involved. It is then assumed that  $\dot{Q}$  levels off to a relatively constant value. Following the guidance of Table 4.1 of [1] and Table 8.2.6, it is estimated that, at the fully developed stage of the fire, the total energy release rate for the 5-ft high stack of wood pallets will be  $330 \text{ Btu/s} \cdot \text{ft}^2$ , or  $33,000 \text{ Btu/sec}$  for the entire  $100\text{-ft}^2$  array. The preceding equation leads to the result that the fully developed stage of the fire will be initiated at  $t_{fd} = 747$  seconds.

A plot of the fire growth according to the preceding description is shown in Figure C.3(b). In the actual calculation, the fire's instantaneous energy release rate is estimated by interpolating linearly between a series of  $N$  input data points at times  $t_n$ ,  $n = 1$  to  $N$ , on

the fire-growth curve. These points are defined by user-specified values of  $[t_n, \dot{Q}(t_n)]$ . For times larger than  $t_N$ , the fire's energy release rate is assumed to stay constant at  $\dot{Q}(t_N)$ . The calculation fire-growth curve involves six input data points (i.e.,  $N = 6$ ). These points are plotted in Figure C.3(b).

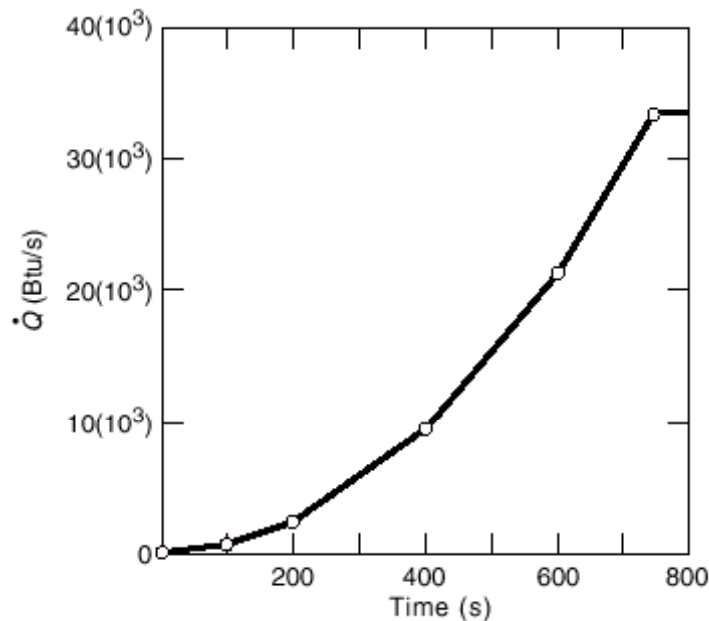


**FIGURE C.3(b) Energy Release Rate Versus Time for the Fire of the Default Simulation.**

The position of the fire's center is identified in Figure C.3(a). In terms of this plan view,

the fire is assumed to be located at the midpoint of a 12-ft line between two sprinkler links, at a distance of 21.2 ft from each of the two closest equidistant vents (a total area of 96 ft<sup>2</sup>) and at a distance of 44.3 ft from the remaining two equidistant vents (a total area of 96 ft<sup>2</sup>). Of the sprinklers and associated links, two are closest and equidistant to the fire-plume axis at radial distances of 6 ft. Figure C.3(a) shows that the second and third closest groups of sprinklers and links are at radial distances of 13.4 ft (four sprinklers and links) and 18 ft (two sprinklers and links). In the default calculation, the opening of each of the four vents occurs, and the flow out of the vents is initiated at the simulated time of fusing of their associated links. Also simulated in the default calculation is the thermal response, including time of fusing, of the pair of sprinkler links closest to the fire.

As a final specification of the fire, it is assumed that the characteristic elevation of the fire remains at a fixed value, 2.5 ft above the floor, at the initial mid-elevation of the array of combustibles. For the purpose of the default calculation, the simulation is carried out to  $t = 400$  seconds, with data output every 30 seconds.

Having described the default simulation, the procedure for getting started and using LAVENT follows.

#### **C.4 Getting Started.**

The executable code, LAVENT.EXE, is found on the floppy disk. Before using it, backup copies should be made. If the user has a hard drive, a separate directory should be created and the executable code should be copied into that directory. The code operates on an IBM PC or compatible computer containing a math coprocessor. It is written in Fortran 77 and needs a minimum of 300 kilobytes of memory.

To execute LAVENT, change to the proper directory or insert a floppy disk containing a copy of the executable code and enter LAVENT <ret>. In this case, <ret> refers to the ENTER or RETURN key. The first prompt provides an option for English or metric units:

1 FOR ENGLISH UNITS

2 FOR METRIC UNITS

The program has a unit conversion function and transforms files that are in one set of units to another set. The code executes in SI units; therefore, conversion is done only on input and output in order to avoid rounding errors.

For the purposes of getting started, choose Option 1, ENGLISH UNITS. Enter 1 <ret>. The following menu will be displayed on the screen:

1 READ AND RUN A DATA FILE

2 READ AND MODIFY A DATA FILE

3 MODIFY THE DEFAULT CASE TO CREATE A NEW FILE

4 RUN THE DEFAULT CASE

If Option 1 or 2 is chosen, the program will ask for the name of the data file to be used. If the chosen file resides on the hard disk, this question should be answered by typing the path of the file name, for example, C:\subdirectory\filename. If the file is on a floppy disk, type

A:filename or B:filename, depending on whether the A or B drive is being used. It is recommended that all data files use a common extender such as “.dat” to facilitate identification of these files.

A first-time user should select Option 4, RUN THE DEFAULT CASE, by entering 4 <ret>. This selection will ensure that the code has been transferred intact. The default-case output is provided in Figure C.4 and is discussed in Section C.8. As a point of information, the times needed to carry out the default simulation on IBM PC-compatible 486/33 MHZ and Pentium/90 MHZ computers were 40 seconds and 8 seconds, respectively.

Now restart the code and, at this point, choose Option 3, MODIFY THE DEFAULT CASE, to review and modify the default input data. Enter 3 <ret>.

CEILING HEIGHT = 30.0 FT  
 ROOM LENGTH = 84.0 FT  
 ROOM WIDTH = 84.0 FT  
 CURTAIN LENGTH = 336.0 FT  
 CURTAIN HEIGHT = 15.0 FT  
 MATERIAL = INSULATED DECK (SOLID POLYSTYRENE)  
 CEILING CONDUCTIVITY = .240E-04 BTU/FT F S  
 CEILING DENSITY = .655E+02 LB/FT3  
 CEILING HEAT CAPACITY = .277E+00 BTU/LB F  
 CEILING THICKNESS = .500E+00 FT  
 FIRE HEIGHT = 2.5 FT  
 FIRE POWER/AREA = 0.3300E+03 BTU/S FT2

LINK NO = 1 RADIUS = 6.0 FT DIST CEILING = 1.00 FT  
 RTI= 400.00 SQRT FUSION TEMPERATURE FOR LINK = 165.00 K  
 LINK NO = 2 RADIUS = 21.2 FT DIST CEILING = 0.30 FT  
 RTI= 50.00 SQRT FUSION TEMPERATURE FOR LINK = 165.00 K  
 LINK NO = 3 RADIUS = 44.3 FT DIST CEILING = 0.30 FT  
 RTI= 50.00 SQRT FUSION TEMPERATURE FOR LINK = 165.00 K

VENT = 1 VENT AREA = 96.0 FT2 LINK CONTROLLING VENT = 2  
 VENT = 2 VENT AREA = 96.0 FT2 LINK CONTROLLING VENT = 3

TIME (S)= 0.000 LYR TEMP (F)= 80.0 LYR HT (FT)= 30.00 LYR MASS (LB)= 0.000E+0  
 FIRE OUTPUT (BTU/S)= 0.0000E+00 VENT AREA (FT2)= 0.00  
 LINK = 1 LINK TEMP (F)= 80.00 JET VELOCITY (FT/S)= 0.000 JET TEMP (F) = 80  
 LINK = 2 LINK TEMP (F)= 80.00 JET VELOCITY (FT/S)= 0.000 JET TEMP (F) = 80  
 LINK = 3 LINK TEMP (F)= 80.00 JET VELOCITY (FT/S)= 0.000 JET TEMP (F) = 80  
 R (FT)= 0.00 TSL (F)= 80.0 QB (BTU/FT2 S)= 0.000E+00 QT (BTU/FT2 S)= 0.000E+00  
 R (FT)= 12.41 TSL (F)= 80.0 QB (BTU/FT2 S)= 0.000E+00 QT (BTU/FT2 S)= 0.000E+00  
 R (FT)= 24.82 TSL (F)= 80.0 QB (BTU/FT2 S)= 0.000E+00 QT (BTU/FT2 S)= 0.000E+00  
 R (FT)= 37.23 TSL (F)= 80.0 QB (BTU/FT2 S)= 0.000E+00 QT (BTU/FT2 S)= 0.000E+00  
 R (FT)= 49.64 TSL (F)= 80.0 QB (BTU/FT2 S)= 0.000E+00 QT (BTU/FT2 S)= 0.000E+00  
 R (FT)= 62.05 TSL (F)= 80.0 QB (BTU/FT2 S)= 0.000E+00 QT (BTU/FT2 S)= 0.000E+00

TIME (S)= 30.000 LYR TEMP (F)= 89.6 LYR HT (FT)= 28.90 LYR MASS (LB)= 0.562E+0  
 FIRE OUTPUT (BTU/S)= 0.1776E+03 VENT AREA (FT2)= 0.00  
 LINK = 1 LINK TEMP (F)= 80.78 JET VELOCITY (FT/S)= 1.866 JET TEMP (F) = 94  
 LINK = 2 LINK TEMP (F)= 85.37 JET VELOCITY (FT/S)= 2.077 JET TEMP (F) = 95  
 LINK = 3 LINK TEMP (F)= 81.83 JET VELOCITY (FT/S)= 0.873 JET TEMP (F) = 87  
 R (FT)= 0.00 TSL (F)= 84.5 QB (BTU/FT2 S)= 0.312E-01 QT (BTU/FT2 S)= 0.847E-18  
 R (FT)= 12.41 TSL (F)= 81.7 QB (BTU/FT2 S)= 0.122E-01 QT (BTU/FT2 S)= 0.847E-18  
 R (FT)= 24.82 TSL (F)= 80.8 QB (BTU/FT2 S)= 0.570E-02 QT (BTU/FT2 S)= 0.847E-18  
 R (FT)= 37.23 TSL (F)= 80.4 QB (BTU/FT2 S)= 0.325E-02 QT (BTU/FT2 S)= 0.847E-18  
 R (FT)= 49.64 TSL (F)= 80.3 QB (BTU/FT2 S)= 0.212E-02 QT (BTU/FT2 S)= 0.847E-18  
 R (FT)= 62.05 TSL (F)= 80.2 QB (BTU/FT2 S)= 0.152E-02 QT (BTU/FT2 S)= 0.847E-18

TIME (S)= 60.000 LYR TEMP (F)= 96.5 LYR HT (FT)= 27.34 LYR MASS (LB)= 0.134E+0

**FIGURE C.4 Printout of the Default-Case Output.**

R (FT)= 0.00 TSL (F)= 102.4 QB (BTU/FT2 S)= 0.687E-01 QT (BTU/FT2 S)= 0.847E-18  
R (FT)= 12.41 TSL (F)= 89.7 QB (BTU/FT2 S)= 0.317E-01 QT (BTU/FT2 S)= 0.847E-18  
R (FT)= 24.82 TSL (F)= 84.7 QB (BTU/FT2 S)= 0.156E-01 QT (BTU/FT2 S)= 0.847E-18  
R (FT)= 37.23 TSL (F)= 82.7 QB (BTU/FT2 S)= 0.908E-02 QT (BTU/FT2 S)= 0.847E-18  
R (FT)= 49.64 TSL (F)= 81.8 QB (BTU/FT2 S)= 0.598E-02 QT (BTU/FT2 S)= 0.847E-18  
R (FT)= 62.05 TSL (F)= 81.1 QB (BTU/FT2 S)= 0.987E-03 QT (BTU/FT2 S)= 0.847E-18

TIME (S)= 120.000 Lyr TEMP (F)= 111.5 Lyr HT (FT)= 23.85 Lyr MASS (LB)= 0.301E+0  
FIRE OUTPUT (BTU/S)= 0.9470E+03 VENT AREA (FT2)= 0.00

LINK = 1 LINK TEMP (F)= 90.30 JET VELOCITY (FT/S)= 3.614 JET TEMP (F) = 129  
LINK = 2 LINK TEMP (F)= 118.43 JET VELOCITY (FT/S)= 3.966 JET TEMP (F) = 132  
LINK = 3 LINK TEMP (F)= 96.66 JET VELOCITY (FT/S)= 1.667 JET TEMP (F) = 106  
R (FT)= 0.00 TSL (F)= 115.6 QB (BTU/FT2 S)= 0.113E+00 QT (BTU/FT2 S)= 0.847E-18  
R (FT)= 12.41 TSL (F)= 96.2 QB (BTU/FT2 S)= 0.543E-01 QT (BTU/FT2 S)= 0.847E-18  
R (FT)= 24.82 TSL (F)= 87.9 QB (BTU/FT2 S)= 0.266E-01 QT (BTU/FT2 S)= 0.847E-18  
R (FT)= 37.23 TSL (F)= 84.6 QB (BTU/FT2 S)= 0.154E-01 QT (BTU/FT2 S)= 0.847E-18  
R (FT)= 49.64 TSL (F)= 83.0 QB (BTU/FT2 S)= 0.101E-01 QT (BTU/FT2 S)= 0.847E-18  
R (FT)= 62.05 TSL (F)= 82.0 QB (BTU/FT2 S)= 0.728E-02 QT (BTU/FT2 S)= 0.847E-18

TIME (S)= 150.000 Lyr TEMP (F)= 124.4 Lyr HT (FT)= 21.85 Lyr MASS (LB)= 0.390E+0  
FIRE OUTPUT (BTU/S)= 0.1479E+04 VENT AREA (FT2)= 0.00

LINK = 1 LINK TEMP (F)= 97.16 JET VELOCITY (FT/S)= 4.364 JET TEMP (F) = 149  
LINK = 2 LINK TEMP (F)= 137.37 JET VELOCITY (FT/S)= 4.754 JET TEMP (F) = 153  
LINK = 3 LINK TEMP (F)= 105.49 JET VELOCITY (FT/S)= 1.998 JET TEMP (F) = 117  
R (FT)= 0.00 TSL (F)= 136.5 QB (BTU/FT2 S)= 0.158E+00 QT (BTU/FT2 S)= 0.847E-18  
R (FT)= 12.41 TSL (F)= 107.0 QB (BTU/FT2 S)= 0.810E-01 QT (BTU/FT2 S)= 0.847E-18  
R (FT)= 24.82 TSL (F)= 93.3 QB (BTU/FT2 S)= 0.405E-01 QT (BTU/FT2 S)= 0.847E-18  
R (FT)= 37.23 TSL (F)= 87.7 QB (BTU/FT2 S)= 0.236E-01 QT (BTU/FT2 S)= 0.847E-18  
R (FT)= 49.64 TSL (F)= 85.1 QB (BTU/FT2 S)= 0.155E-01 QT (BTU/FT2 S)= 0.847E-18  
R (FT)= 62.05 TSL (F)= 83.5 QB (BTU/FT2 S)= 0.112E-01 QT (BTU/FT2 S)= 0.847E-18

TIME (S)= 180.000 Lyr TEMP (F)= 140.2 Lyr HT (FT)= 19.77 Lyr MASS (LB)= 0.477E+0  
FIRE OUTPUT (BTU/S)= 0.2012E+04 VENT AREA (FT2)= 0.00

LINK = 1 LINK TEMP (F)= 106.66 JET VELOCITY (FT/S)= 5.008 JET TEMP (F) = 171  
LINK = 2 LINK TEMP (F)= 159.68 JET VELOCITY (FT/S)= 5.414 JET TEMP (F) = 176  
LINK = 3 LINK TEMP (F)= 116.69 JET VELOCITY (FT/S)= 2.275 JET TEMP (F) = 130  
R (FT)= 0.00 TSL (F)= 160.3 QB (BTU/FT2 S)= 0.195E+00 QT (BTU/FT2 S)= 0.847E-18  
R (FT)= 12.41 TSL (F)= 120.4 QB (BTU/FT2 S)= 0.106E+00 QT (BTU/FT2 S)= 0.847E-18  
R (FT)= 24.82 TSL (F)= 100.2 QB (BTU/FT2 S)= 0.545E-01 QT (BTU/FT2 S)= 0.847E-18  
R (FT)= 37.23 TSL (F)= 91.8 QB (BTU/FT2 S)= 0.322E-01 QT (BTU/FT2 S)= 0.847E-18  
R (FT)= 49.64 TSL (F)= 87.8 QB (BTU/FT2 S)= 0.213E-01 QT (BTU/FT2 S)= 0.847E-18  
R (FT)= 62.05 TSL (F)= 85.3 QB (BTU/FT2 S)= 0.332E-02 QT (BTU/FT2 S)= 0.847E-18

**FIGURE C.4** *Continued*

R (FT)= 0.00 TSL (F)= 218.6 QB (BTU/FT2 S)= 0.299E+00 QT (BTU/FT2 S)= 0.847E-18  
R (FT)= 12.41 TSL (F)= 156.6 QB (BTU/FT2 S)= 0.180E+00 QT (BTU/FT2 S)= 0.847E-18  
R (FT)= 24.82 TSL (F)= 119.9 QB (BTU/FT2 S)= 0.971E-01 QT (BTU/FT2 S)= 0.847E-18  
R (FT)= 37.23 TSL (F)= 103.7 QB (BTU/FT2 S)= 0.582E-01 QT (BTU/FT2 S)= 0.847E-18  
R (FT)= 49.64 TSL (F)= 95.7 QB (BTU/FT2 S)= 0.389E-01 QT (BTU/FT2 S)= 0.847E-18  
R (FT)= 62.05 TSL (F)= 90.3 QB (BTU/FT2 S)= 0.288E-01 QT (BTU/FT2 S)= 0.847E-18

TIME (S)= 270.000 LYR TEMP (F)= 217.5 LYR HT (FT)= 20.17 LYR MASS (LB)= 0.407E+0  
FIRE OUTPUT (BTU/S)= 0.4852E+04 VENT AREA (FT2)= 192.00

LINK = 1 LINK TEMP (F)= 155.49 JET VELOCITY (FT/S)= 6.854 JET TEMP (F) = 271  
LINK = 2 LINK TEMP (F)= 253.19 JET VELOCITY (FT/S)= 7.244 JET TEMP (F) = 277  
LINK = 3 LINK TEMP (F)= 167.24 JET VELOCITY (FT/S)= 3.043 JET TEMP (F) = 188

TIME LINK 2 OPENS EQUALS 186.7478 (S)

TIME LINK 3 OPENS EQUALS 266.9820 (S)

R (FT)= 0.00 TSL (F)= 254.4 QB (BTU/FT2 S)= 0.339E+00 QT (BTU/FT2 S)= 0.847E-18  
R (FT)= 12.41 TSL (F)= 181.1 QB (BTU/FT2 S)= 0.217E+00 QT (BTU/FT2 S)= 0.847E-18  
R (FT)= 24.82 TSL (F)= 133.9 QB (BTU/FT2 S)= 0.121E+00 QT (BTU/FT2 S)= 0.847E-18  
R (FT)= 37.23 TSL (F)= 112.2 QB (BTU/FT2 S)= 0.735E-01 QT (BTU/FT2 S)= 0.847E-18  
R (FT)= 49.64 TSL (F)= 101.5 QB (BTU/FT2 S)= 0.494E-01 QT (BTU/FT2 S)= 0.847E-18  
R (FT)= 62.05 TSL (F)= 93.7 QB (BTU/FT2 S)= 0.371E-01 QT (BTU/FT2 S)= 0.847E-18

TIME (S)= 300.000 LYR TEMP (F)= 253.4 LYR HT (FT)= 22.84 LYR MASS (LB)= 0.281E+0  
FIRE OUTPUT (BTU/S)= 0.5918E+04 VENT AREA (FT2)= 192.00

LINK = 1 LINK TEMP (F)= 179.59 JET VELOCITY (FT/S)= 6.901 JET TEMP (F) = 308  
LINK = 2 LINK TEMP (F)= 289.67 JET VELOCITY (FT/S)= 7.195 JET TEMP (F) = 311  
LINK = 3 LINK TEMP (F)= 189.77 JET VELOCITY (FT/S)= 3.023 JET TEMP (F) = 211

TIME LINK 1 OPENS EQUALS 282.8710 (S)

TIME LINK 2 OPENS EQUALS 186.7478 (S)

TIME LINK 3 OPENS EQUALS 266.9820 (S)

R (FT)= 0.00 TSL (F)= 287.1 QB (BTU/FT2 S)= 0.352E+00 QT (BTU/FT2 S)= 0.847E-18  
R (FT)= 12.41 TSL (F)= 205.5 QB (BTU/FT2 S)= 0.238E+00 QT (BTU/FT2 S)= 0.847E-18  
R (FT)= 24.82 TSL (F)= 148.7 QB (BTU/FT2 S)= 0.138E+00 QT (BTU/FT2 S)= 0.847E-18  
R (FT)= 37.23 TSL (F)= 121.5 QB (BTU/FT2 S)= 0.851E-01 QT (BTU/FT2 S)= 0.847E-18  
R (FT)= 49.64 TSL (F)= 107.8 QB (BTU/FT2 S)= 0.574E-01 QT (BTU/FT2 S)= 0.847E-18  
R (FT)= 62.05 TSL (F)= 98.8 QB (BTU/FT2 S)= 0.428E-01 QT (BTU/FT2 S)= 0.847E-18

TIME (S)= 330.000 LYR TEMP (F)= 284.4 LYR HT (FT)= 24.25 LYR MASS (LB)= 0.216E+0  
FIRE OUTPUT (BTU/S)= 0.6983E+04 VENT AREA (FT2)= 192.00

LINK = 1 LINK TEMP (F)= 206.05 JET VELOCITY (FT/S)= 7.109 JET TEMP (F) = 342  
LINK = 2 LINK TEMP (F)= 322.58 JET VELOCITY (FT/S)= 7.227 JET TEMP (F) = 341  
LINK = 3 LINK TEMP (F)= 211.77 JET VELOCITY (FT/S)= 3.036 JET TEMP (F) = 231

TIME LINK 1 OPENS EQUALS 282.8710 (S)

TIME LINK 2 OPENS EQUALS 186.7478 (S)

TIME LINK 3 OPENS EQUALS 266.9820 (S)

R (FT)= 0.00 TSL (F)= 316.3 QB (BTU/FT2 S)= 0.366E+00 QT (BTU/FT2 S)= 0.847E-18  
R (FT)= 12.41 TSL (F)= 229.1 QB (BTU/FT2 S)= 0.257E+00 QT (BTU/FT2 S)= 0.847E-18  
R (FT)= 24.82 TSL (F)= 163.7 QB (BTU/FT2 S)= 0.153E+00 QT (BTU/FT2 S)= 0.847E-18

**FIGURE C.4** *Continued*

```
R (FT)= 37.23 TSL (F)= 140.5 QB (BTU/FT2 S)= 0.105E+00 QT (BTU/FT2 S)= 0.847E-18
R (FT)= 49.64 TSL (F)= 120.8 QB (BTU/FT2 S)= 0.709E-01 QT (BTU/FT2 S)= 0.847E-18
R (FT)= 62.05 TSL (F)= 107.5 QB (BTU/FT2 S)= 0.530E-01 QT (BTU/FT2 S)= 0.847E-18

TIME (S)= 390.000 LYR TEMP (F)= 327.0 LYR HT (FT)= 24.81 LYR MASS (LB)= 0.185E+00
FIRE OUTPUT (BTU/S)= 0.9113E+04 VENT AREA (FT2)= 192.00
LINK = 1 LINK TEMP (F)= 262.32 JET VELOCITY (FT/S)= 8.168 JET TEMP (F) = 397
LINK = 2 LINK TEMP (F)= 376.92 JET VELOCITY (FT/S)= 7.811 JET TEMP (F) = 392
LINK = 3 LINK TEMP (F)= 249.19 JET VELOCITY (FT/S)= 3.281 JET TEMP (F) = 264
TIME LINK 1 OPENS EQUALS 282.8710 (S)
TIME LINK 2 OPENS EQUALS 186.7478 (S)
TIME LINK 3 OPENS EQUALS 266.9820 (S)
R (FT)= 0.00 TSL (F)= 372.0 QB (BTU/FT2 S)= 0.398E+00 QT (BTU/FT2 S)= 0.847E-18
R (FT)= 12.41 TSL (F)= 275.6 QB (BTU/FT2 S)= 0.294E+00 QT (BTU/FT2 S)= 0.847E-18
R (FT)= 24.82 TSL (F)= 194.1 QB (BTU/FT2 S)= 0.181E+00 QT (BTU/FT2 S)= 0.847E-18
R (FT)= 37.23 TSL (F)= 150.3 QB (BTU/FT2 S)= 0.114E+00 QT (BTU/FT2 S)= 0.847E-18
R (FT)= 49.64 TSL (F)= 127.5 QB (BTU/FT2 S)= 0.773E-01 QT (BTU/FT2 S)= 0.847E-18
R (FT)= 62.05 TSL (F)= 113.2 QB (BTU/FT2 S)= 0.574E-01 QT (BTU/FT2 S)= 0.847E-18

TIME (S)= 400.000 LYR TEMP (F)= 333.5 LYR HT (FT)= 24.77 LYR MASS (LB)= 0.185E+00
FIRE OUTPUT (BTU/S)= 0.9468E+04 VENT AREA (FT2)= 192.00
LINK = 1 LINK TEMP (F)= 271.98 JET VELOCITY (FT/S)= 8.387 JET TEMP (F) = 406
LINK = 2 LINK TEMP (F)= 385.32 JET VELOCITY (FT/S)= 7.936 JET TEMP (F) = 400
LINK = 3 LINK TEMP (F)= 254.85 JET VELOCITY (FT/S)= 3.333 JET TEMP (F) = 270
TIME LINK 1 OPENS EQUALS 282.8710 (S)
TIME LINK 2 OPENS EQUALS 186.7478 (S)
TIME LINK 3 OPENS EQUALS 266.9820 (S)
R (FT)= 0.00 TSL (F)= 381.3 QB (BTU/FT2 S)= 0.403E+00 QT (BTU/FT2 S)= 0.847E-18
R (FT)= 12.41 TSL (F)= 283.5 QB (BTU/FT2 S)= 0.300E+00 QT (BTU/FT2 S)= 0.847E-18
R (FT)= 24.82 TSL (F)= 199.2 QB (BTU/FT2 S)= 0.186E+00 QT (BTU/FT2 S)= 0.847E-18
R (FT)= 37.23 TSL (F)= 153.6 QB (BTU/FT2 S)= 0.117E+00 QT (BTU/FT2 S)= 0.847E-18
R (FT)= 49.64 TSL (F)= 129.7 QB (BTU/FT2 S)= 0.794E-01 QT (BTU/FT2 S)= 0.847E-18
R (FT)= 62.05 TSL (F)= 115.0 QB (BTU/FT2 S)= 0.589E-01 QT (BTU/FT2 S)= 0.847E-18
```

**FIGURE C.4** *Continued*

## **C.5 The Base Menu.**

**C.5.1 Modifying the Default Case — General.** When Option 3, MODIFY THE DEFAULT CASE, is chosen, the following menu is displayed:

- 1 ROOM PROPERTIES
- 2 PHYSICAL PROPERTIES

3 OUTPUT PARAMETERS

4 FUSIBLE LINK PROPERTIES

5 FIRE PROPERTIES

6 SOLVER PARAMETERS

0 NO CHANGES

This menu will be referred to as the *base menu*.

Entering the appropriate option number of the base menu and then <ret> will always transfer the user to the indicated item on the menu. Entering a zero will transfer the user to the file status portion of the input section discussed in Section C.6.

The next subsections discuss data entry under Options 1 through 6 of the base menu.

Now choose Option 1, ROOM PROPERTIES, of the base menu to review and modify the default room-property input data. Enter 1 <ret>.

**C.5.2 Room Properties.** When Option 1, ROOM PROPERTIES, of the base menu is chosen, the following room properties menu is displayed:

```
1      30.000 CEILI
      00      NG
           HEIG
           HT
           (FT)
2      84.000 ROO
      00      M
           LENG
           TH
           (FT)
3      84.000 ROO
      00      M
           WIDT
           H (FT)
4      2      NUM
           BER
           OF
           VENT
           S,
           ETC.
5      336.00 CURT
      000     AIN
           LENG
           TH
           (FT)
6      15.000 HEIG
      00      HT
           TO
           BOTT
           OM
           OF
           CURT
           AIN
```

0 (FT)  
TO  
CHAN  
GE  
NOTH  
ING

All input values are expressed in either S.I. or U.S. customary units, and the units are prompted on the input menus.

Note that the default number of vents is 2, not 4, because the symmetry of the default scenario, as indicated in Figure C.3(a), leads to “ganged” operation of each of two pairs of the four vents involved.

To change an input value in the preceding room properties menu — for example, to change the ceiling height from 30 ft to 20 ft — the user would enter 1 <ret> and 20. <ret>. The screen would show revisions using the new value of 20 ft for the ceiling height. This value or other values on this screen can be changed by repeating the process.

***WARNING:** The user is warned that it is critical to end each entry number with a decimal point when a noninteger number is indicated (i.e., when the screen display shows a decimal point for that entry). The user is warned further that the code will attempt to run with any specified input file and that it will not distinguish between realistic and unrealistic input values.*

Option 6, HEIGHT TO BOTTOM OF CURTAIN, of the room properties menu is used to define the height above the floor of the bottom of the curtain. As can be seen, in the default data, this is 15 ft. Where this height is chosen to be identical to the ceiling height, the user should always define the very special idealized simulation associated with an extensive, unconfined ceiling fire scenario (i.e., by whatever means, it is assumed that the flow of the ceiling jet is extracted from the compartment at the extremities of the ceiling). Under such a simulation, an upper layer never develops in the compartment. The lower-ceiling surface and fusible links are submerged in and respond to an unconfined ceiling jet environment, which is unaffected by layer growth. This idealized fire scenario, involving the unconfined ceiling, is used, for example, in [1] to simulate ceiling response and in [2] and [3] to simulate sprinkler response.

The choice of some options on a menu, such as Option 4, NUMBER OF VENTS, ETC., of the room properties menu, leads to a subsequent display/requirement of additional associated input data. Menu options that necessitate multiple entries are indicated by the use of “ETC.” In the case of Option 4, NUMBER OF VENTS, ETC., three values are involved for each vent or group of vents actuated by a fusible link. As indicated under Option 4, NUMBER OF VENTS, ETC., the default data describe a scenario with two vents or groups of vents.

Now choose Option 4, NUMBER OF VENTS, ETC., to review and modify the default input data associated with these two vents or groups of vents. Enter 4 <ret>. The following is displayed on the screen:

VENT NO. = 1 FUSIBLE LINK = 2 VENT AREA = 96.00000 FT2

VENT NO. = 2 FUSIBLE LINK = 3 VENT AREA = 96.00000 FT2

ENTER 6 TO REMOVE A VENT

ENTER VENT NO., LINK NO., AND VENT AREA (FT<sup>2</sup>) TO ADD OR MODIFY A VENT

MAXIMUM NO. OF VENTS IS 5

ENTER 0 TO RETURN TO THE MENU

This display indicates that the two simulated vents or groups of vents are numbered 1 (VENT NO. = 1) and 2 (VENT NO. = 2), that they are actuated by fusible links numbered 2 (FUSIBLE LINK = 2) and 3 (FUSIBLE LINK = 3), respectively, and that each of the two vents or groups of vents has a total area of 96 ft<sup>2</sup> (VENT AREA = 96.00000 FT<sup>2</sup>).

In the default fire scenario, it would be of interest to study the effect of “ganging” the operation of all four vents (total area of 192 ft<sup>2</sup>) to fusing of the closest vent link. To do so, it would be necessary to first remove vent number 2, as identified in the preceding menu, and then to modify the area of vent number 1.

To remove vent number 2, enter 6 <ret>. The following is now displayed on the screen:

ENTER NUMBER OF VENT TO BE ELIMINATED

ENTER 0 TO RETURN TO MENU

Now enter 2 <ret>. This completes removal of vent 2, with the following revision displayed on the screen:

VENT NO. = 1 FUSIBLE LINK = 2 VENT AREA = 96.00000 FT<sup>2</sup>

ENTER 6 TO REMOVE A VENT

ENTER VENT NO., LINK NO., AND VENT AREA (FT<sup>2</sup>) TO ADD OR MODIFY A VENT

MAXIMUM NO. OF VENTS IS 5

ENTER 0 TO RETURN TO THE MENU

Now modify the characteristics of vent number 1. To do so, enter 1 <ret>, 2 <ret>, 192. <ret>. The screen will now display the following:

VENT NO. = 1 FUSIBLE LINK = 2 VENT AREA = 192.00000 FT<sup>2</sup>

ENTER 6 TO REMOVE A VENT

ENTER VENT NO., LINK NO., AND VENT AREA (FT<sup>2</sup>) TO ADD OR MODIFY A VENT

MAXIMUM NO. OF VENTS IS 5

ENTER 0 TO RETURN TO THE MENU

To add or reimplement vent number 2, actuated by link number 3 and of area 96 ft<sup>2</sup>, enter 2 <ret>, 3 <ret>, 96. <ret>. Now return to the original default scenario by bringing the area of vent number 1 back to its original 96 ft<sup>2</sup> value; enter 1 <ret>, 2 <ret>, and 96. <ret>.

The user can now continue to modify or add additional ceiling vents or return to the room properties menu by entering 0 <ret>. If the user tries to associate a vent with a link not yet entered in the program, the code will warn the user, give the maximum number of links available in the present data set, and request a new link value. If the user deletes a link that is assigned to a vent, the code will assign the link with the next smallest number to that vent. The best method for assigning vents to links is to first use Option 4, FUSIBLE LINK PROPERTIES, of the base menu (to be discussed in C.5.5) to assign the link parameters and then to use Option 1, ROOM PROPERTIES, followed by the option NUMBER OF VENTS, ETC. to assign vent properties.

Now return to the room properties menu by entering 0 <ret>, then to the base menu by entering 0 <ret> again.

With the base menu back on the screen, choose Option 2, PHYSICAL PROPERTIES, to review and/or modify the default room property input data. Enter 2 <ret>.

**C.5.3 Physical Properties.** When Option 2, PHYSICAL PROPERTIES, of the base menu is chosen, the following physical properties menu is displayed:

MATERIAL = INSULATED DECK (SOLID POLYSTYRENE)

HEAT CONDUCTIVITY = 2.400E-05 (BTU/S LB F)

HEAT CAPACITY = 2.770E-01 (BTU/LB F)

DENSITY = 6.550E+01 (LB/FT3)

```
1      80.000  AMBI
      00      ENT
           TEMP
           ERAT
           URE
           (F)
2      0.5000  MATE
      0       RIAL
           THIC
           KNES
           S (FT)
3      MATE  INSU
      RIAL  LATE
      =     D
           DECK
           (SOLI
           D
           POLY
           STYR
           ENE)
0      CHAN
      GE
      NOTH
      ING
```

The values in Options 1 and 2 are modified by entering the option number and then the new value.

Now choose Option 3 by coding 3 <ret>. The following menu is displayed:

- 1 CONCRETE
- 2 BARE METAL DECK
- 3 INSULATED DECK (SOLID POLYSTYRENE)
- 4 WOOD
- 5 OTHER

By choosing one of Options 1 through 4 of this menu, the user specifies the material properties of the ceiling according to the table of standard material properties in [4]. When the option number of one of these materials is chosen, the material name, thermal conductivity, heat capacity, and density are displayed on the screen as part of an updated physical properties menu.

Now choose Option 5, OTHER, by entering 5 <ret>. The following screen is displayed:

ENTER MATERIAL NAME  
THERMAL CONDUCTIVITY (BTU/S FT F)  
HEAT CAPACITY (BTU/LB F)  
DENSITY (LB/FT3)

The four indicated inputs are required. After they are entered, the screen returns to an updated physical properties menu.

Now return to the default material, INSULATED DECK (SOLID POLYSTYRENE). To do so, enter any arbitrary material name with any three property values (enter MATERIAL <ret>, 1. <ret>, 1. <ret>, 1. <ret>); then choose Option 3, MATERIAL, from the menu displayed (enter 3 <ret>); and, from the final menu displayed, choose Option 3, INSULATED DECK (SOLID POLYSTYRENE) by entering 3 <ret>.

Now return to the base menu. Enter 0 <ret>. Choose Option 3, OUTPUT PARAMETERS, of the base menu to review or modify the default output-parameter data. Enter 3 <ret>.

**C.5.4 Output Parameters.** When Option 3, OUTPUT PARAMETERS, of the base menu is chosen, the following output-parameters menu is displayed:

```
1      400.00 FINA
      0000    L
           TIME
           (S)
2      30.000 OUTP
      000    UT
           INTE
           RVAL
           (S)
0      CHAN
      GE
      NOTH
      ING
```

FINAL TIME represents the ending time of the calculation. OUTPUT INTERVAL controls the time interval between successive outputs of the calculation results. All times are in seconds. For example, assume that it is desired to run a fire scenario for 500 seconds with an output of results each 10 seconds. First choose Option 1 with a value of 500 (enter 1 <ret>, 500. <ret>), then Option 2 with a value of 10 (enter 2 <ret>, 10. <ret>). The following revised output-parameters menu is displayed:

```

1      500.00 FINA
      0000    L
           TIME
           (S)
2      10.000 OUTP
      000    UT
           INTE
           RVAL
           (S)
0      CHAN
      GE
      NOTH
      ING

```

Return to the original default output parameters menu by entering 1 <ret>, 400. <ret>, followed by 2 <ret>, 30. <ret>.

Now return to the base menu from the output parameters menu by entering 0 <ret>.

With the base menu back on the screen, choose Option 4, FUSIBLE LINK PROPERTIES, to review or modify the default fusible link properties data. Enter 4 <ret>.

**C.5.5 Fusible Link Properties.** When Option 4, FUSIBLE LINK PROPERTIES, of the base menu is chosen, the following fusible link properties menu is displayed:

TO ADD OR CHANGE A LINK, ENTER LINK NO., RADIUS (FT), DISTANCE BELOW CEILING (FT), RTI (SQRT[FT S]), AND FUSE TEMPERATURE (F).

MAXIMUM NUMBER OF LINKS EQUALS 10.

ENTER 11 TO REMOVE A LINK.

ENTER 0 TO RETURN TO THE MENU.

LINK #	RADI US (FT)	DIST ANCE (FT) BELOW CEILING	RTI SQRT (FT S)	FUSE TEM P (F)
1	6.000	1.000	400.00 0	165.00 0
2	21.200	0.300	50.000	165.00 0
3	44.300	0.300	50.000	165.00 0

Each fusible link must be assigned a link number (e.g., LINK # = 1), radial position from the plume–ceiling impingement point (e.g., RADIUS = 6.00 FT), ceiling-to-link separation distance (e.g., DISTANCE BELOW CEILING = 1.00 FT), response time index (e.g., RTI = 400.00 SQRT[FT S]), and fuse temperature (e.g., FUSE TEMPERATURE = 165.00 F).

Suppose that in the default fire scenario it was desired to simulate the thermal response of the group of (four) sprinkler links second closest to the fire. According to the description of C.3 and Figure C.3(a), this would be done by adding a fourth link, link number 4, at a radial distance of 13.4 ft, 1 ft below the ceiling, with an RTI of 400 (ft/sec)<sup>1/2</sup> and a fusion temperature of 165°F. To do this, enter 4 <ret>, 13.4 <ret>, 1. <ret>, 400. <ret>, 165. <ret>. Then the following screen is displayed:

TO ADD OR CHANGE A LINK, ENTER LINK NO., RADIUS (FT), DISTANCE BELOW CEILING (FT), RTI (SQRT[FT S]), AND FUSE TEMPERATURE (F).

MAXIMUM NUMBER OF LINKS EQUALS 10.

ENTER 11 TO REMOVE A LINK.

ENTER 0 TO RETURN TO THE MENU.

LINK #	RADI US (FT)	DIST ANCE (FT) BELOW CEILING	RTI SQRT (FT S)	FUSE TEM P (F)
1	6.000	1.000	400.00	165.00
			0	0
2	13.400	1.000	400.00	165.00
			0	0
3	21.200	0.300	50.000	165.00
				0
4	44.300	0.300	50.000	165.00
				0

Note that the new link, which was entered as link number 4, was sorted automatically into the list of the original three links and that all four links were renumbered according to radial distance from the fire. The original link-vent assignments are preserved in this operation. Hence, the user need not return to Option 4, NUMBER OF VENTS, ETC., unless it is desired to reassigned link-vent combinations.

*A maximum of 10 link responses can be simulated in any one simulation.*

Now remove link number 2 to return to the original default array of links. To do so, enter 11 <ret>. The following screen is displayed:

ENTER THE NUMBER OF THE LINK TO BE REMOVED

Enter 2 <ret> to remove link 2.

Now return to the base menu from the fusible link properties menu by entering 0 <ret>.

With the base menu back on the screen, choose Option 5, FIRE PROPERTIES, to review

or modify the default fire properties data. Enter 5 <ret>.

**C.5.6 Fire Properties.** When Option 5, FIRE PROPERTIES, from the base menu is chosen, the following fire properties menu is displayed:

```
1      2.5    FIRE
          HEIG
          HT
          (FT)
2      330.0  FIRE
          POWE
          R/AR
          EA
          (BTU/
          S
          FT2),
          ETC.
3
          FIRE
          OUTP
          UT AS
          A
          FUNC
          TION
          OF
          TIME
0
          CHAN
          GE
          NOTH
          ING
```

The value associated with Option 1 is the height of the base of the fire above the floor. Change this to 3 ft, for example, by entering 1 <ret> and 3. <ret>. Then return to the default data by entering 1 <ret> and 2.5 <ret>.

The value associated with Option 2 is the fire energy release rate per fire area. It is also possible to consider simulations where the fire area is fixed by specifying a fixed fire diameter. The fire energy release rate per fire area can be changed, or the fixed fire area type of specification can be made by choosing Option 2 by entering 2 <ret>. This leads to a display of the following menu:

```
1          WOOD PALLETS, STACK, 5 FT HIGH          330 (BTU/S FT2)
2          CARTONS, COMPARTMENTED, STACKED 15      200 (BTU/S FT2)
          FT HIGH
3          PE BOTTLES IN COMPARTMENTED              540 (BTU/S FT2)
          CARTONS 15 FT HIGH
4          PS JARS IN COMPARTMENTED CARTONS 15      1300 (BTU/S FT2)
          FT HIGH
5          GASOLINE                                  200 (BTU/S FT2)
6          INPUT YOUR OWN VALUE IN (BTU/S FT2)
7          SPECIFY A CONSTANT DIAMETER FIRE IN
          FT
0          CHANGE NOTHING
```

Options 1 through 5 of the preceding menu are for variable area fires. The Option 1 to 5 constants displayed on the right are the fire energy release rate per unit fire area. They are

taken from Table 4.1 of [1]. If one of these options is chosen, an appropriately updated fire properties menu is then displayed on the screen. Option 0 would lead to the return of the original fire properties menu.

Option 6 allows any other fire energy release rate per unit fire area of the user's choice. Option 7 allows the user to specify the diameter of a constant area fire instead of an energy release rate per unit area fire. Choice of Option 6 or 7 must be followed by entry of the appropriate value. Then an appropriately updated fire properties menu appears on the screen.

To try Option 7, SPECIFY A CONSTANT DIAMETER FIRE IN FEET, enter 7 <ret>. The following screen is displayed:

ENTER YOUR VALUE FOR FIRE DIAMETER IN FT

Assume the fire diameter is fixed at 5 ft. Enter 5. <ret>. Then the following screen is displayed:

```
1      2.5000  FIRE
        0      HEIG
           HT
           (FT)
2      5.0000  FIRE
        0      DIAM
           ETER
           (FT),
           ETC.
3      FIRE
        OUTP
        UT AS
        A
        FUNC
        TION
        OF
        TIME
0      CHAN
        GE
        NOTH
        ING
```

Now return to the original default fire properties menu by entering 2 <ret>. The previous menu will be displayed. In this, choose Option 1, WOOD PALLETS, STACK, 5 ft high, by entering 1 <ret>.

Option 3, FIRE OUTPUT AS A FUNCTION OF TIME, of the fire properties menu allows the user to prescribe the fire as a function of time. The prescription involves (1) linear interpolation between adjacent pairs of user-specified points with coordinates (time in seconds, fire energy release rate in BTU/sec) and (2) continuation of the fire to an arbitrarily large time at the fire energy release rate of the last data point.

Now choose Option 3 by entering 3 <ret>. The following screen associated with the default fire output data is displayed:

```
1      TIME(  POWE
        s) =   R(BT
```

```

0.0000 U/S) =
0      0.0000
      0E+0
2      TIME( POWE
      s) = R(BT
100.00 U/S) =
00     0.5920
      0E+03
3      TIME( POWE
      s) = R(BT
200.00 U/S) =
00     0.2367
      0E+04
4      TIME( POWE
      s) = R(BT
400.00 U/S) =
00     0.9468
      0E+04
5      TIME( POWE
      s) = R(BT
600.00 U/S) =
00     0.2130
      2E+05
6      TIME( POWE
      s) = R(BT
747.00 U/S) =
00     0.3300
      0E+05

```

ENTER DATA POINT NO., TIME (S), AND POWER (BTU/S)

ENTER 11 TO REMOVE A POINT

ENTER 0 TO RETURN TO MENU

As discussed in Section C.3, with use of the six preceding data points, the default simulation will estimate the fire's energy release rate according to the plot of Figure C.3(b).

Additional data points can be added to the fire growth simulation by entering the new data point number, <ret>, the time in seconds, <ret>, the energy release rate in BTU/sec, and <ret>.

The maximum number of data points permitted is 10. The points can be entered in any order. A sorting routine will order the points by time. One point must correspond to zero time.

As an example of adding an additional data point to the preceding six, assume that a closer match to the “*t*-squared” default fire growth curve was desired between 200 seconds and 400 seconds. From Section C.3 it can be verified that the fire energy release rate will be 5325 BTU/sec at  $t = 300$ . To add this point to the data, thereby forcing the fire growth curve to pass exactly through the “*t*-squared” curve at 300 seconds, enter 7 <ret>, 300. <ret>, and 5325. <ret>. The following revised screen will be displayed:

```

1      TIME( POWE
      s) = R(BT

```

```

0.0000 U/S) =
0.0000
0E+00
2 TIME( POWE
s) = R(BT
100.00 U/S) =
00 =0.592
00E+0
3
3 TIME( POWE
s) = R(BT
200.00 U/S) =
00 0.2367
0E+04
4 TIME( POWE
s) = R(BT
300.00 U/S) =
00 0.5325
0E+04
5 TIME( POWE
s) = R(BT
400.00 U/S) =
00 =0.946
80E+0
4
6 TIME( POWE
s) = R(BT
600.00 U/S) =
00 0.2130
2E+05
7 TIME( POWE
s) = R(BT
747.00 U/S) =
00 0.3300
0E+05

```

ENTER DATA PT. NO., TIME (S), AND POWER (BTU/S)

ENTER 11 TO REMOVE A POINT

ENTER 0 TO RETURN TO MENU

Note that the revised point, which was entered as point number 7, has been resorted into the original array of data points and that all points have been renumbered appropriately.

Now remove the point just added (which is now point number 4). First enter 11 <ret>. Then the following screen is displayed:

ENTER THE NUMBER OF THE DATA POINT TO BE REMOVED

Now enter 4 <ret>. This brings the fire growth simulation data back to the original default set of values.

Now return to the fire properties menu. Enter 0 <ret>. Then return to the base menu by entering again 0 <ret>.

With the base menu back on the screen, it is assumed that the inputting of all data required to define the desired fire simulation is complete. Now choose Option 0, NO CHANGES, to proceed to the file status menu. Enter 0 <ret>.

**C.5.7 Solver Parameters.** Users of the code will generally have no need to refer to this section (i.e., especially when learning to use the LAVENT code, a user should now skip to Section C.6), since they are rarely, if ever, expected to run into a situation where the code is not able to obtain a solution for a particular application or is taking an inordinate amount of time to produce the solution. However, if this does happen, there are a number of variations of the default solver parameter inputs that can resolve the problem.

Start the input part of the program to get to the base menu. Then choose Option 6, SOLVER PARAMETERS, by entering 6 <ret>. The following input options menu will be displayed:

```
1      0.6500 GAUS
      E+00 S-
           SEIDE
           L
           RELA
           XATI
           ON
2      0.1000 DIFF
      E-04 EQ
           SOLV
           ER
           TOLE
           RANC
           E
3      0.1000 GAUS
      E-04 S-
           SEIDE
           L
           TOLE
           RANC
           E
4      2.0000 FLUX
      00 UPDA
           TE
           INTE
           RVAL
           (S)
5      6      NUM
           BER
           OF
           CEILI
           NG
           GRID
           POIN
           TS,
           MIN=
           2,
           MAX
           =50
6      0.1000 SMAL
```

```

E-07  LEST
      MEA
      NING
      FUL
      VALU
      E
7      CHAN
      GE
      NOTH
      ING

```

The solvers used in this code consist of a differential equation solver DDRIVE2, used to solve the set of differential equations associated with the layer and the fusible links, and a Gauss–Seidel/tridiagonal solver using the Crank–Nicolson formalism to solve the set of partial differential equations associated with the heat conduction calculation for the ceiling. Because two different solvers are being used in the code, there is potential for the solvers to become incompatible with each other, particularly if the upper layer has nearly reached a steady-state temperature but the ceiling is still increasing its temperature. When this occurs, the differential equation solver will try to take time steps that are too large for the Gauss–Seidel solver to handle, and a growing oscillation in the ceiling temperature variable might occur. By reducing the FLUX UPDATE INTERVAL, the growing oscillation can be suppressed. The smaller the FLUX UPDATE INTERVAL, the slower the code will run.

The GAUSS–SEIDEL RELAXATION coefficient can be changed to produce a faster running code or to handle a case that will not run with a different coefficient. Typical values of this coefficient should range between 0.2 and 1.0.

The DIFF EQ SOLVER TOLERANCE and the GAUSS–SEIDEL TOLERANCE can also be changed. Decreasing or increasing these values can provide a faster running code for a given case, and by decreasing the value of the tolerances, the accuracy of the calculations can be increased. If the tolerance values are made too small, the code will either run very slowly or not run at all. Suggested tolerances would be in the range of 0.00001 to 0.000001.

Consistent with the model assumptions, accuracy in the radial ceiling temperature distribution around the plume–ceiling impingement point is dependent on the NUMBER OF CEILING GRID POINTS. Relatively greater or lesser accuracy is achieved by using relatively more or fewer grid points. This leads, in turn, to a relatively slower or faster computer run.

### **C.6 File Status—Running the Code.**

When Option 0, NO CHANGES, of the base menu is chosen, the following file status menu is displayed:

```

1      SAVE
      THE
      FILE
      AND
      RUN
      THE
      CODE
2      SAVE

```

```

THE
FILE
BUT
DON'
T
RUN
THE
CODE
3 DON'
T
SAVE
THE
FILE
BUT
RUN
THE
CODE
4 ABOR
T THE
CALC
ULAT
ION

```

If one of the save options is selected, the user will be asked to supply a file name to designate the file where the newly generated input data are to be saved. The program will automatically create the new file. File names may be as long as 8 characters and should have a common extender such as .DAT (for example MYFILE.DAT). The maximum length that can be used for the total length of input or output files is 25 characters. For example, C:\SUBDIRECT\FILENAME.DAT would allow a file named FILENAME.DAT to be read from the subdirectory SUBDIRECT on the C drive. To read a file from a floppy disk in the A drive, use A:FILENAME.DAT. If Option 4 is chosen, the program will end without any file being saved.

A request for an output file name can appear on the screen. File names can be as long as 8 characters and should have an extender such as “.OUT” so that the output files can easily be recognized. To output a file to a floppy disk in the A drive, name the file A:FILENAME.OUT. To output a file to a subdirectory other than the one that is resident to the program, use C:\SUBDIRECT\FILENAME.OUT for the subdirectory SUBDIRECT.

Once the output file has been designated, the program will begin to execute. The statement PROGRAM RUNNING will appear on the screen. Each time the program writes to the output file, a statement such as T = 3.0000E01 S will appear on the screen to provide the user with the present output time.

### **C.7 The Output Variables and the Output Options.**

The program generates two separate output files. An example of the first output file is appended at the end of this document. This file is named by the user and consists of a listing of the input data plus all the relevant output variables in a format where the output units are specified and the meanings of all but three of the output variables are clearly specified. These latter variables are *TSL*, *QB*, and *QT*, the temperature of the ceiling inside the enclosure, the net heat transfer flux to the bottom surface of the ceiling, and the net heat

transfer flux to the top surface of the ceiling, respectively. The variables are output as a function of radius with  $R = 0$  being the center of the fire plume projected on the ceiling. Other abbreviations include LAYER TEMP, LAYER HT, LAYER MASS, JET VELOCITY, and JET TEMP — the upper-layer (layer adjacent to the ceiling) temperature, height of the upper-layer interface above the floor, mass of gas in the layer, ceiling jet velocity, and ceiling jet temperature at the position of each fusible link, respectively. The VENT AREA is the total area of roof vents open at the time of output.

The second output file, GRAPH.OUT, is used by the graphics program GRAPH. GRAPH is a Fortran program that makes use of a graphics software package to produce graphical output of selected output variables[5, 6]. To use the graphics program, the file GRAPH.OUT must be in the same directory as the program GRAPH. GRAPH is a menu-driven program that provides the user with the ability to plot two sets of variables on the PC screen. An option exists that permits the user to print the plots from the screen to a printer. If using an attached EPSON-compatible printer, enter <ret> to produce a plot using the printer. To generate a PostScript file for use on a laser printer, enter <ret> and provide a file name when the file name prompt appears in the upper left hand corner of the graph. To exit to screen mode from the graphics mode, enter <ret>. The file GRAPH.OUT will be destroyed each time the code LAVENT is run. If the user wishes to save the graphics file, it must be copied using the DOS copy command into another file with a different file name.

To demonstrate the use of GRAPH, start the program by entering graph <ret>. GRAPH will read in the graphics output file GRAPH.OUT, and the following screen will be displayed:

```
ENTER 0 TO PLOT POINTS, ENTER 1 TO PLOT AND CONNECT POINTS
```

The graphics presented in Figure C.7(a) through Figure C.7(e) were done with GRAPH using option 0. Enter 0 <ret> and the following graphics menu is displayed:

```
ENTER THE X AND Y VARIABLES FOR THE DESIRED TWO GRAPHS
```

```
1     TIME
2     LAYE
      R
      TEMP
      ERAT
      URE
3     LAYE
      R
      HEIG
      HT
4     LAYE
      R
      MASS
5     FIRE
      OUTP
      UT
6     CEILI
      NG
      VENT
      AREA
7     PLUM
      E
      FLOW
```

```
8     LINK
      TEMP
      ERAT
      URE
9     JET
      VELO
      CITY
      AT
      LINK
10    JET
      TEMP
      ERAT
      URE
      AT
      LINK
```

Two plots can be studied on a single screen. For example, from the default simulation, assume that displays of the plots of Figure C.7(a) and Figure C.7(b), LAYER HEIGHT vs. TIME and LAYER TEMPERATURE vs. TIME, respectively, are desired. Then enter 1 <ret>, 3 <ret>, 1 <ret>, and 2 <ret>. The program will respond with the following prompt:

ENTER THE TITLES FOR THE TWO GRAPHS, 16 CHARACTERS MAX.

The user might choose titles that would identify particular cases such as LY HT RUN 100 <ret> and LY TEMP RUN 100 <ret>. If a title longer than 16 characters is chosen, it will be truncated to 16 characters. After the titles have been entered, the program will respond with the following prompt:

ENTER 1 FOR DEFAULT SCALING, 2 FOR USER SCALING.

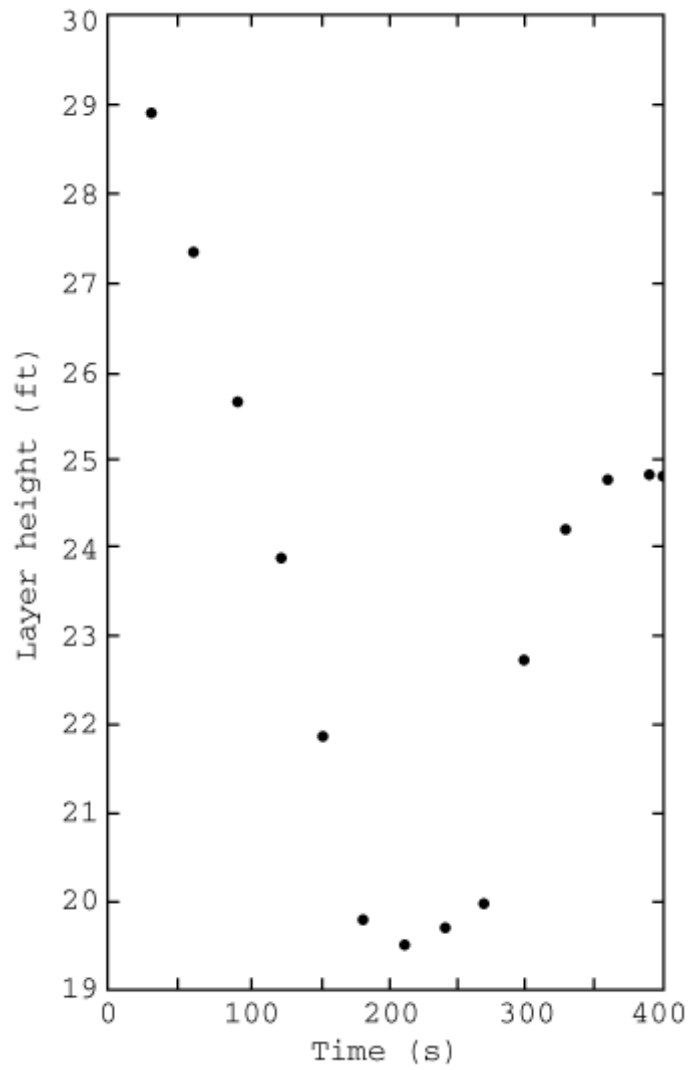


**FIGURE C.7(a) Plot of the Height of the Smoke Layer Interface vs. Time for the Default Simulation.**

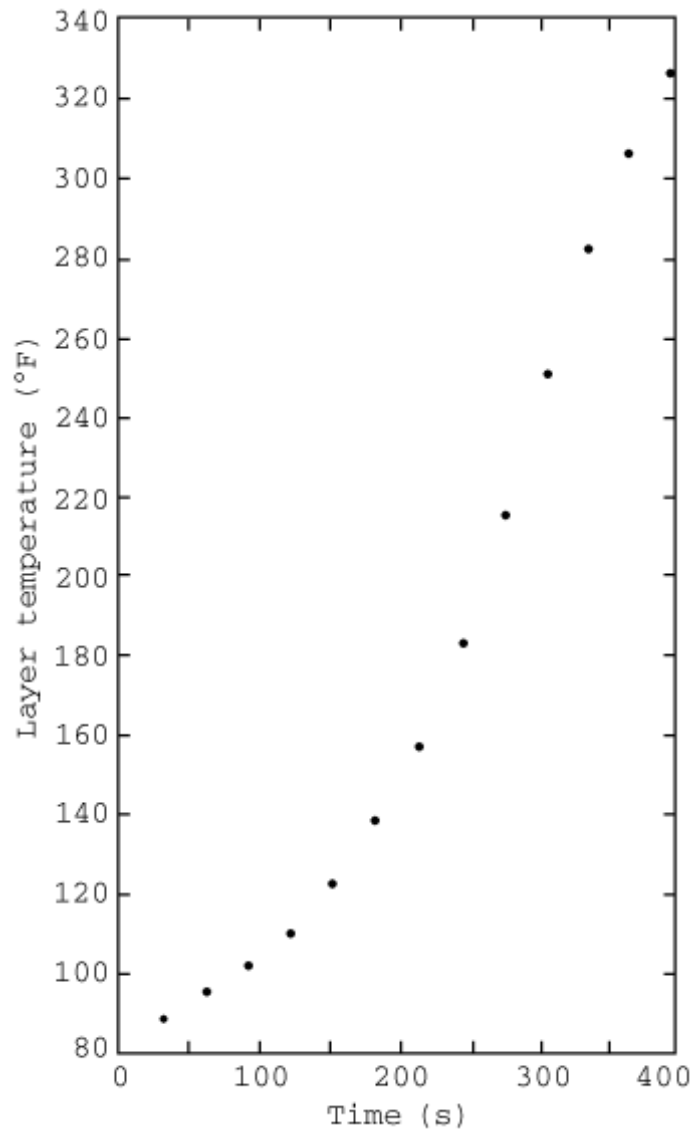


**FIGURE C.7(b) Plot of the Temperature of the Smoke Layer vs. Time for the Default Simulation.**

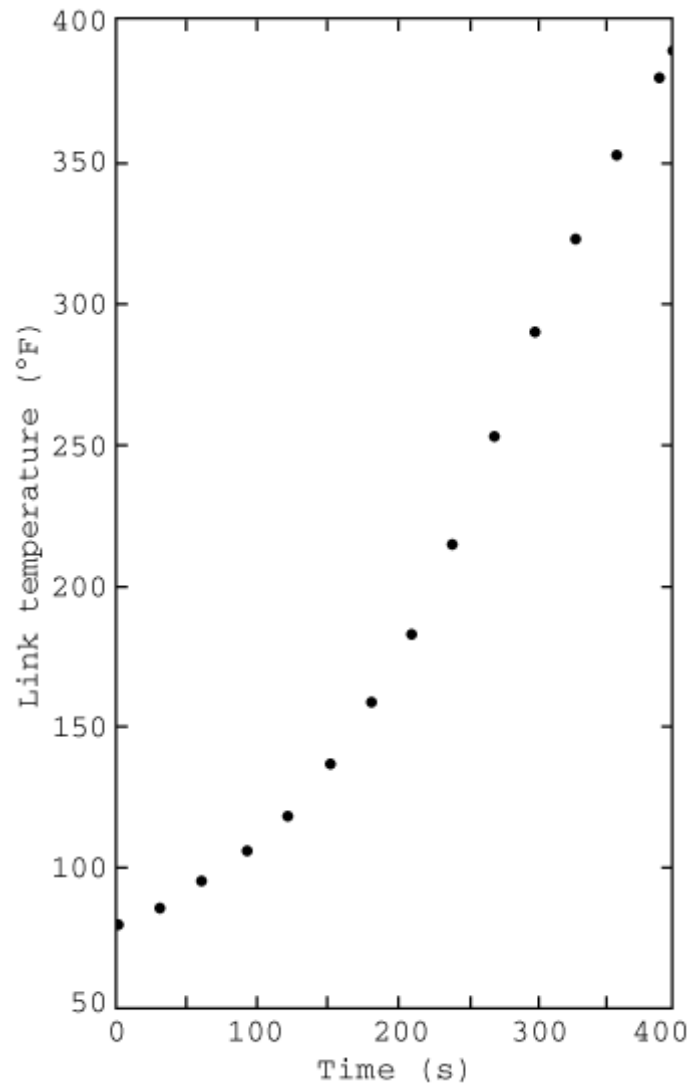


**FIGURE C.7(c) Plot of the Closest ( $R = 21.2$  ft) Vent-Link Temperature vs. Time for the Default Simulation.**

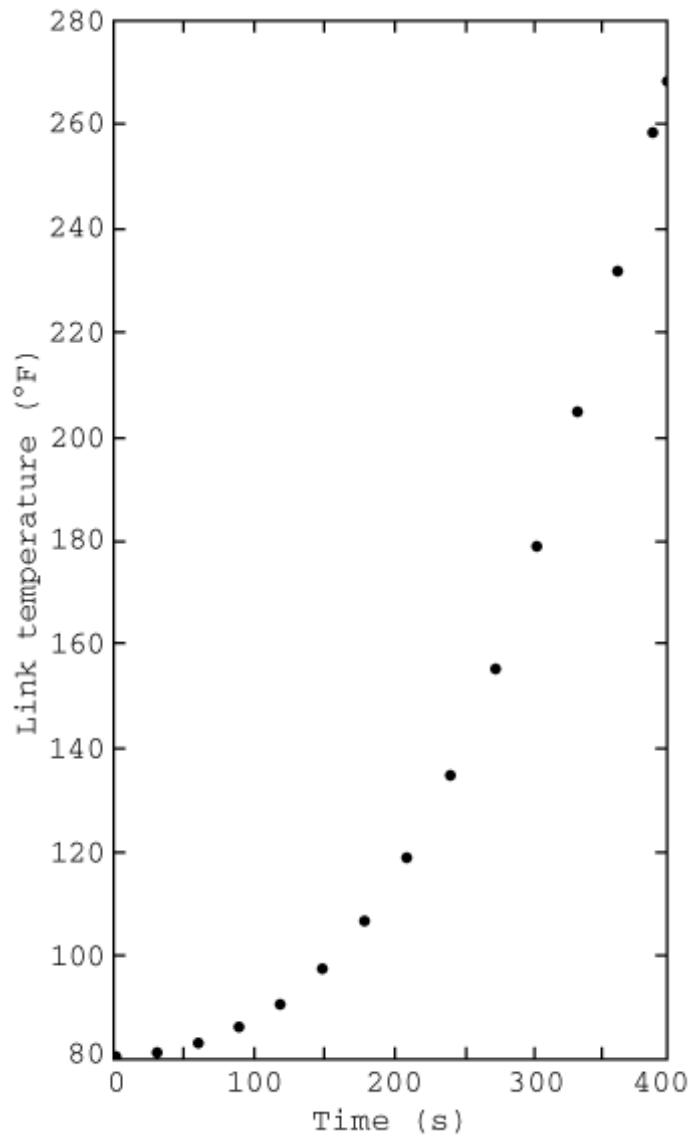


**FIGURE C.7(d) Plot of the Far ( $R = 44.3$  ft) Pair of Vent-Link Temperatures vs. Time for the Default Simulation.**

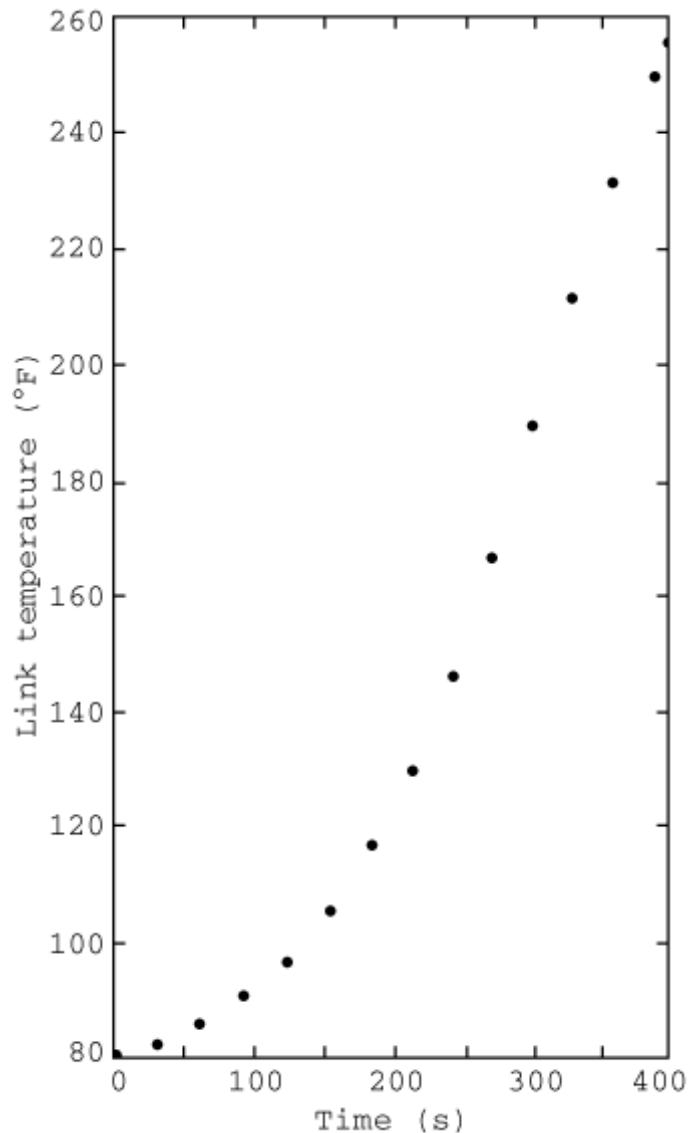


**FIGURE C.7(e) Plot of the Closest ( $R = 6$  ft) Sprinkler-Link Temperatures vs. Time for the Default Simulation.**

If the user chooses option 1, the desired plots will appear on the screen with an internal scaling for the  $x$ - and  $y$ -axis of each graph. If the user chooses option 2, the program will respond with the following prompt:

ENTER THE MINIMUM AND MAXIMUM VALUES FOR THE X AND Y AXIS OF EACH GRAPH.

ENTER 0 FOR THE MINIMUM AND MAXIMUM VALUES OF EACH AXIS WHERE DEFAULT SCALING IS DESIRED. FOR EXAMPLE, VALUES SHOULD BE ENTERED AS 0.,100.,0.,200.,10.,50.,20.,100. <ret> FOR X1(0-100), Y1(0-200), X2(10-50), Y2(20-100).

Use of this option allows a number of different cases to be compared using similar values for the  $x$ - and  $y$ -axis of each graph. All eight numbers must be entered and separated with commas before entering <ret>. Once the entry is made, the plots will appear on the screen.

Note that this option permits a mixture of default scaling and user-specified scaling.

Once a pair of plots are displayed on the screen, the user would have the choice of entering <ret> to obtain a hard-copy plot of the graphs or of entering <ret> to exit the graphics mode.

To plot a second pair of graphs, the user would exit the graphics mode by entering <ret> and then repeat the preceding process by entering graph <ret>, and so forth.

If the user selects plots that involve variables defined by Option 8, 9, or 10, then, following the entry 8 <ret>, 9 <ret>, or 10 <ret>, the following prompt for identifying the desired link number (in the default simulation with three simulated links) will be displayed immediately:

```
ENTER LINK NUMBER, MAXIMUM NUMBER = 3
```

The user would then enter the desired link number followed by <ret> and continue entering the remaining input data that define the desired plots.

As an example of generating link-related plots, consider displaying the pair of plots LINK TEMPERATURE vs. TIME and JET VELOCITY AT LINK vs. TIME for link number 3 in the default simulation. First enter 1 <ret> (for TIME on the  $x$ -axis) and 8 <ret> (for LINK TEMPERATURE on the  $y$ -axis). At this point, “ENTER LINK NUMBER . . .” would be displayed on the screen. Continue by entering 3 <ret> (for link number 3). This would complete the data entry for the first of the two plots. For the second plot, enter 1 <ret> (for TIME on the  $x$ -axis) and 9 <ret> (for LINK TEMPERATURE on the  $y$ -axis). At this point, “ENTER LINK NUMBER . . .” would be displayed a second time. Then conclude data input for the pair of plots by entering 3 <ret> (for link number 3). At this point the desired pair of plots would be displayed on the screen.

### **C.8 An Example Simulation — The Default Case.**

This section presents and reviews briefly the simulation of the default case.

The tabular output of the default simulation is presented in Figure C.4. Plots of the layer-interface height and of the layer temperature as functions of time are plotted in Figure C.7(a) and Figure C.7(b), respectively. Plots of the thermal response of the two pairs of vent links and the pair of sprinkler links closest to the fire are presented in Figure C.7(c) through Figure C.7(e), respectively.

From Figure C.4 and Figure C.7(c) through Figure C.7(e), it is seen that the sequence of link fusing (at 165°F) is predicted to be the near pair of vents at 187 seconds, the far pair of vents at 267 seconds, and the pair of closest sprinklers at 283 seconds. Although the sprinkler links are closer to the fire than any of the vent links, and although all links have the same fuse temperatures, the simulation predicts that the sprinkler links fuse after all of the vent links. There are two reasons for this. First, the RTIs of the sprinkler links are larger than those of the vent links and, therefore, slower to respond thermally. Second, the two sprinkler links simulated are far enough from the ceiling as to be below the peak temperature of the ceiling jet, which is relatively thin at the 6-ft radial position (see the lower sketch of Figure C.2).

The effect on layer growth of fusing of the two pairs of vent links and opening of their corresponding vents at 187 seconds and 267 seconds can be noted in Figure C.7(a). Note that the opening of the first pair of vents effectively stops the rate-of-increase of layer thickness and the opening of the second pair of vents leads to a relatively rapid rate-of-decrease in the layer thickness. All of this is of course occurring at times when the energy release rate of the fire is growing rapidly.

As can be seen in Figure C.7(a), up until the 400 seconds of simulation time, the smoke is still contained in the original curtained compartment and has not “spilled over” to adjacent spaces. From this figure it appears that with no venting, the layer would have dropped below the bottom of the curtain boards prior to fusing of the first sprinkler links. This could be confirmed with a second simulation run of LAVENT, where all vent action was removed from the default data.

### **C.9 References for Annex C.**

1. L.Y. Cooper and D.W. Stroup, “Thermal Response of Unconfined Ceilings Above Growing Fires and the Importance of Convective Heat Transfer,” *Journal of Heat Transfer* 109:172–178, 1987.
2. D.D. Evans, “Calculating Sprinkler Activation Time in Compartments,” *Fire Safety Journal* 9:147–155, 1985.
3. D.W. Stroup, and D.D. Evans, “Use of Computer Fire Models for Analyzing Thermal Detector Spacing,” *Fire Safety Journal* 14:33–45, 1988.
4. D. Gross, “Data Sources for Parameters Used in Predictive Modeling of Fire Growth and Smoke Spread,” NBSIR 85– 3223, National Bureau of Standards (presently National Institute of Standards and Technology), Gaithersburg MD, September 1985.
5. D. Kahaner, C. Moher, and S. Nash, *Numerical Methods and Software*, New York: Prentice Hall, 1989.
6. D. Kahaner, National Institute of Standards and Technology, private communication.

## **Annex D Sample Problem Using Engineering Equations (Hand Calculations) and LAVENT**

*This annex is not a part of the requirements of this NFPA document but is included for informational purposes only.*

### **D.1 Abstract.**

The following example problem illustrates the use of the information, engineering equations, hand calculations, and computer model described in this document. The impact of a fire on a nonsprinklered retail storage building and its occupants is assessed. The effects of an anticipated fire on the subject building are predicted, and the impact of smoke and heat vents is illustrated.

Design goals and objectives were developed, and a high-challenge fire, likely to occur in the subject building, was identified. The fire impact was assessed using three different

methods:

- (1) Hand calculations assuming a quasi-steady fire
- (2) Hand calculations assuming a continuous growth ( $t$ -squared) fire
- (3) The computer model LAVENT

Hand calculations are useful for generating quick estimates of the impact of vents on fire effects. However, hand calculations are not able to assess time-varying events. A number of simplifying assumptions have been used to facilitate problem solving via algebraic equations. Hand-calculated results are considered valid, but they produce slightly different estimates of fire effects such as upper-layer temperature. A computer model such as LAVENT generally provides a more complete analysis of the fire-produced effects and, in some instances, is preferable over hand calculations.

## **D.2 Introduction.**

The following example problem illustrates the use of engineering equations and a computer model to assess the impact of a fire in a nonsprinklered retail storage building. The problem illustrates the impact of vents and predicts the effect of the anticipated fire on the building.

**D.2.1 Goal.** Develop a vent design for the subject building that will maintain a tenable environment for a period of time at least equal to the time required to evacuate the building and equal to the time required to maintain the hot upper layer a minimum of 3 m above floor level until the local fire department enters the building.

**D.2.2 Objective.** Determine the vent area required to maintain the smoke layer at least 3 m above floor level for 300 seconds following detection of the fire by an automatic detection system. Also, limit the heat flux at floor level to a maximum of  $2.5 \text{ kW/m}^2$ , the threshold irradiance that causes severe pain to exposed skin [1], during the time required for evacuation of the building occupants.

**D.2.3 Building Details.** The building is 73 m wide, 73 m long, and 9.1 m high. It is not subdivided, nor is it provided with a sprinkler system. The roof is an insulated deck (solid polystyrene). A complete fire alarm system is to be installed using heat detectors spaced 15.2 m on center and 6.1 m from walls. Detectors will have an activation temperature of  $74^\circ\text{C}$  and an RTI of  $55 (\text{m} \cdot \text{s})^{1/2}$  and are to be located 0.3 m below the roof. Sixteen vents are proposed, spaced 18.3 m on center. Vents will be located 9.05 m from walls. The vents will be activated by fusible links with an activation temperature of  $74^\circ\text{C}$  and an RTI of  $28 (\text{m} \cdot \text{s})^{1/2}$  and are to be located 0.3 m below the roof. Inlet air openings will be equal to 1.5 the total vent area. (*See Figure D.2.3.*)

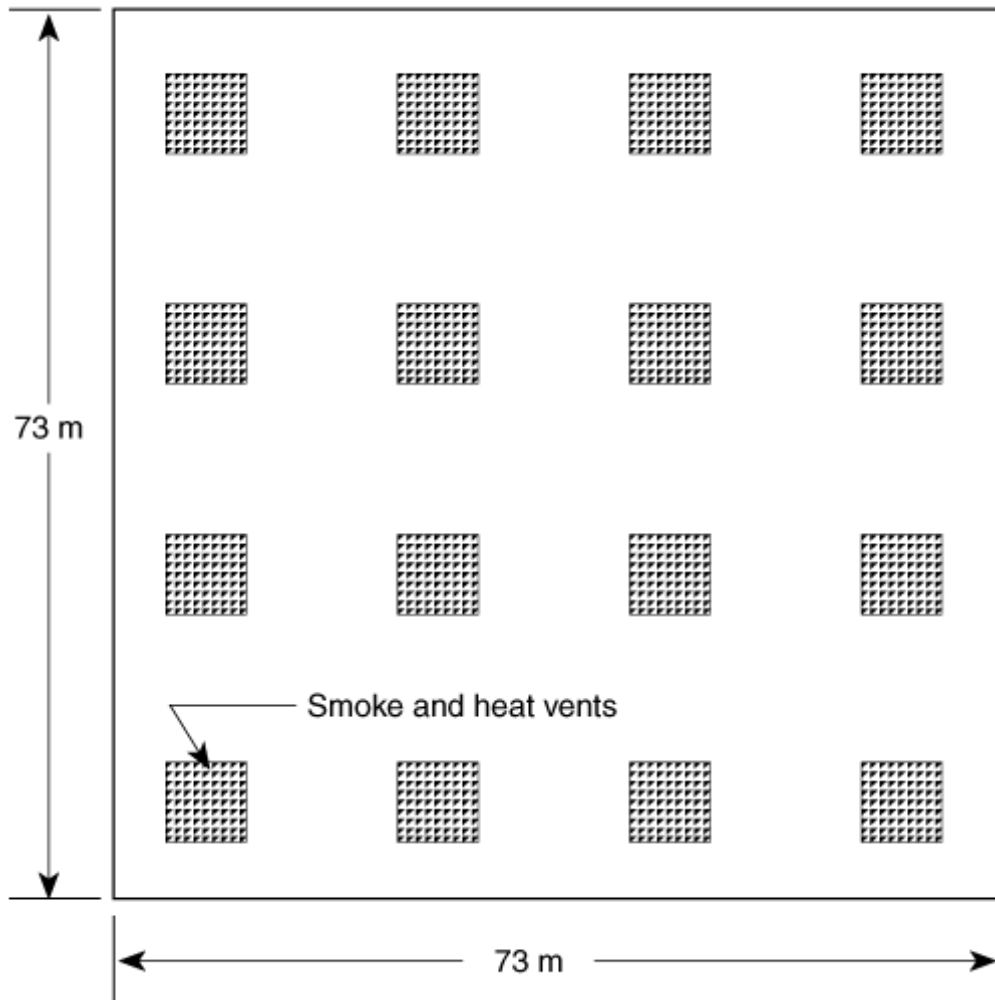


**FIGURE D.2.3 Vent Plan View.**

**D.2.4 Occupancy Details.** The building is to be occupied for retail storage. This analysis deals with a fire in rack storage of sofas in the center of the building. The sofas are to be stored in two racks, each 9.75 m long and 1.2 m wide and separated from each other by 2.4 m. Each rack will have four tiers of storage, four sofas per tier, and a total storage height of 7.6 m. Distance to combustibles surrounding the racks will be sufficient to prevent fire spread to those combustibles during the time period covered by this analysis. The sofas are identified as specimen F32 contained within Table E.5.3(d). Data for the same sofas are contained within a database of Hazard I [2], where the sofas are identified as specimen UPS001. Each sofa will contain 51.5 kg of combustible mass and be wrapped in polyethylene.

**D.2.5 Ignition.** An ignition is assumed to occur in a sofa on the first tier of one of the racks. Ignition of a sofa on the first tier is a probable worst-case scenario and, as a practical matter, is a location where ignition could be expected. Also, placing the fire near floor level results in near-maximum smoke production (entrainment).

### **D.3 Fire Growth.**

First, an estimate of the anticipated fire growth must be developed. A  $t$ -squared fire will be

assumed (see 8.3.1 and A.8.3.1). In a  $t$ -squared fire,

$$Q = \alpha_g t^2$$

where:

$Q$  = total heat release rate (kW)

$\alpha_g$  = fire growth coefficient

$t$  = time (seconds)

The data base within Hazard I [2] contains data from furniture calorimeter tests of sofas. A sofa (UPS001) was tested and demonstrated a growth time ( $t_g$ ) to 1 MW of approximately 200 seconds. The fire in the sofa in this example is assumed to have a growth time of 150 seconds to 1 MW as a reasonable, conservative approximation of the anticipated fire in the sofas stored in the example building. If a more precise estimate of the burning characteristics of an individual sofa is necessary, the exact sofa to be stored in the building could be tested in a calorimeter. A fire growth time of 150 seconds results in an  $\alpha_g$  for the individual sofa of 0.044 kW/s<sup>2</sup> (see Equation 8.3). That is,

$$\alpha_g = \frac{1000}{t_g^2} = \frac{1000}{150^2} = 0.044 \text{ kW/s}^2$$

Accordingly, fire growth in the first sofa ignited can be approximated by a fast ( $\alpha_g = 0.044 \text{ kW/sec}^2$ )  $t$ -squared fire. Further, according to 8.3.1,  $\alpha_g$  is directly proportional to the storage height. Therefore, the fire growth constant ( $\alpha_g$ ) for sofas stacked four high is 4 times 0.044 kW/s<sup>2</sup>, or  $\alpha_g$  equals 0.18 kW/s<sup>2</sup>, and initial fire growth is approximated as

$$Q = \alpha_g t^2$$

where  $\alpha_g = 0.18 \text{ kW/s}^2$

Fire growth in the first rack of sofas results in radiant heat transfer to a second rack of sofas separated from the first rack by 2.4 m. It must be determined when the second rack of sofas ignite. The fire size, when ignition of the second rack of sofas occurs, is determined using Equation 8.1 with its terms rearranged:

$$Q = \frac{W}{0.042^2}$$

where:

$W$  = aisle width (m)

$Q$  = fire output (kW)

Next, the time of ignition of the second rack is computed:

$$t = \left( \frac{Q}{\alpha_g} \right)^{1/2} = \left( \frac{3250}{0.18} \right)^{1/2} = 134 \text{ s}$$

Where  $Q = \alpha_g t^2$

When the second rack of sofas is ignited at 134 seconds, the fire growth coefficient,  $\alpha_g$ , for the two racks burning together is assumed to double the value for the first rack burning alone ( $\alpha_g = 0.36 \text{ kW/s}^2$ ). At that time, the fire appears to have originated at effective ignition time,  $t_{0g}$ . For  $t > 134$  seconds,

$$Q = 0.36(t - t_{0g})^2 \text{ kW}$$

Determine  $t_{0g}$  as follows:

$$3250 = 0.36(134 - t_{0g})^2$$

where  $t_{0g} = 39$  seconds. Then, for  $t > 134$  seconds,

$$Q = 0.36(t - 39)^2$$

The maximum fire size is now estimated. Sofa UPS001 from the Hazard I database [2] [specimen F32 in Table E.5.3(d)] has a peak burning rate of 3120 kW. Maximum fire size,  $Q_{max}$ , is based on the assumption that all 32 sofas are burning at their individual peak rates, 3120 kW:

$$Q_{max} = 32(3120) \cong 100 \text{ MW}$$

The time,  $t_{max}$ , to reach 100 MW must be determined using

$$Q_{max} = 0.36(t - 39)^2$$

When  $Q = 100,000 \text{ kW}$ ,

$$100,000 = 0.36(t_{max} - 39)^2$$

$$t_{max} = \frac{(100,000)^{1/2}}{0.36} + 39 = 566 \text{ s}$$

An estimate of fire duration,  $t_{end}$ , is now made using data from the Hazard I [2] database for sofa UPS001,

where:

individual sofa combustible mass = 51.5 kg

sofa effective heat of combustion = 18,900 kJ/kg

maximum fire size = 100,000 kW

The mass consumed from  $t = 0$  to  $t = 134$  seconds is determined from the total heat release as follows:

$$\int_0^{134} Q dt = \frac{0.18}{3} t^3 \Big|_0^{134} = \frac{0.18}{3} (134)^3 = 144,366 \text{ kJ}$$

Since  $Q = \dot{m}h_c$  (see Equation E.1), mass loss,  $\Delta m$ , for  $t = 134$  seconds, is determined as follows:

$$\Delta m = \frac{144,366 \text{ kJ}}{18,900 \text{ kJ/kg}} = 7.6 \text{ kg} \quad \text{or} \quad \cong 8 \text{ kg}$$

The mass consumed from  $t = 134$  seconds to  $t_{max}$ , the time the maximum fire size is reached, is similarly determined from the total heat release rate after 134 seconds, as follows:

$$\int_{134}^{t_{max}} Q dt = \int_{134}^{566} 0.36(t - 39)^2 dt = \int_{134-39}^{566-39} 0.36\beta^2 d\beta = \frac{0.36}{3} (t)^3 \Big|_{95}^{527}$$

Total heat release from  $t = 134$  to  $t = 566$  is then =  $0.12[(527)^3 - (95)^3] = 17,460,697$  kJ, and the mass lost,  $\Delta m$ , is  $\Delta m = 17,460,697 \text{ kJ}/18,900 \text{ kJ/kg} = 923.8 \cong 924$  kg.

Approximately  $(924 + 8) \text{ kg} = 932$  kg is consumed during the 566-second time interval required to reach  $Q_{max}$ . The total combustible mass is  $51.5 \text{ kg} \times 32 = 1648$  kg. Therefore, around  $(1648 - 932) \text{ kg} = 716$  kg is available to burn at  $Q = Q_{max} = 100$  MW, after  $t = 566$  seconds, from which the fire duration can be calculated as follows:

$$Q_{max} (t_{end} - 566) = 100,000 (t_{end} - 566) = 716(18,900)$$

$$t_{end} = 566 + \frac{716(18,900)}{100,000} = 701.3 \text{ seconds} \cong 700 \text{ s}$$

The combustible mass of the sofas alone is able to support the anticipated fire for

approximately 700 seconds. In reality, the fire in the sofas would reach a maximum of 100 MW at 550–600 seconds and burn briefly at the 100-MW peak until the combustible mass available began to be consumed, at which time the fire's rate of heat release would begin to decline. Using a  $t_{end}$  of 700 seconds is conservative.

In summary, the analysis to this point leads to the following estimate for the anticipated fire:

$$Q = 0.18t^2 \quad \text{for } 0 < t \leq 134 \text{ s}$$

$$Q = 0.36(t - 39)^2 \quad \text{for } 134 < t \leq 566 \text{ s}$$

$$Q = 100,000 \text{ kW} \quad \text{for } t > 566 \text{ s}$$

(See Figure D.3.)

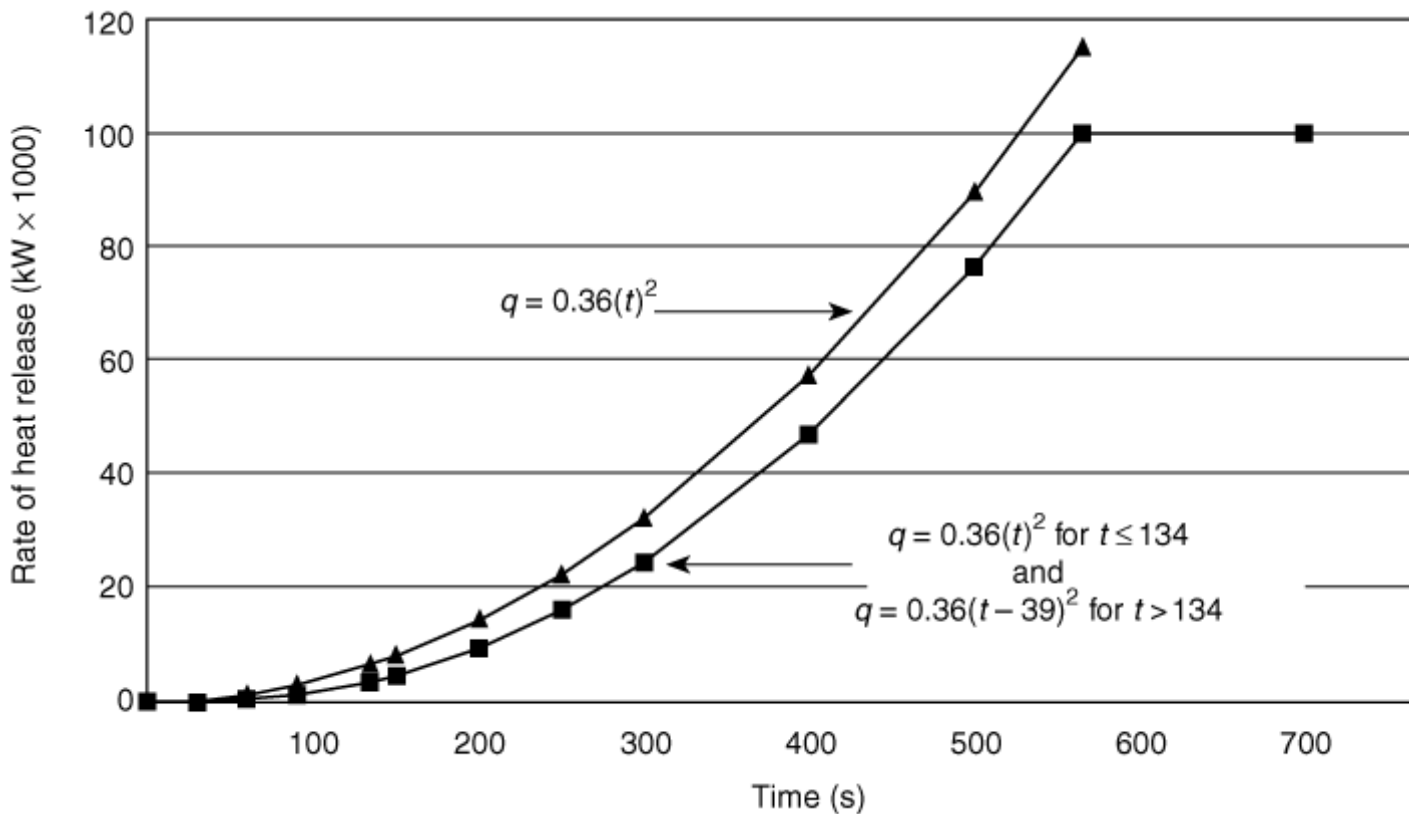


**FIGURE D.3 Fire Output.**

#### D.4 Fire Detection.

The time of fire detection is now calculated given the fire and building as described. The time of detection will be estimated based on the actual composite fire already described. Detection time can be calculated using Equation 9.7. DETACT-QS (see A.9.2.5.4.4.2) is a readily available computational tool that performs this calculation.

A complete fire alarm system is to be installed using heat detectors that are spaced 15.2 m

on center (6.1 m from walls), have an activation temperature of 74°C, and have an RTI of 55 (m<sup>2</sup> s)<sup>1/2</sup>. Assuming the anticipated fire is as described, the maximum distance from a detector to the fire axis is the diagonal  $[2(15.2/2)^2]^{1/2} = 10.7$  m, the ambient temperature is 21°C, and the fire is 0.5 m above floor level, DETACT-QS predicts the activation of a heat detector at 230 seconds. In the event quicker detection is judged to be necessary, smoke detector activation can be predicted by DETACT-QS using the guidance provided in A.9.2.5.4.4.1. Detection time for smoke detectors is based on the gas temperature rise at the detector site. Smoke detector activation can be approximated using DETACT-QS, assuming the smoke detector will respond like a heat detector, which has a small RTI [e.g., 1(m<sup>2</sup> s)<sup>1/2</sup>] and a certain activation temperature above ambient (*see A.9.2.5.4.4.1*). Tests involving burning of the sofa upholstery with the actual detector to be installed have determined that 10°C above ambient is a representative activation condition. Assuming smoke detectors are spaced 9.1 m on center (located a maximum of 6.5 m from the axis of the fire), smoke detector activation is predicted by DETACT-QS at 48 seconds.

Using DETACT-QS, vent operation is predicted using fusible links having an activation temperature of 74°C and an RTI of 28 (m<sup>2</sup> s)<sup>1/2</sup>. Assuming the anticipated fire is located in the center of the building, the ambient temperature is 21°C, and assuming the fire is 0.5 m above floor level, activation of the first vents (equidistant from the fire) separated  $[2(18.3/2)^2]^{1/2} = 12.9$  m from the fire is predicted by DETACT-QS at 228 seconds. The next set of vents (equidistant from the fire at 28.9 m) are predicted to open at 317 seconds. Similarly, the third set of four vents, 38.8 m from the fire axis, open at 356 seconds. All 16 vents are open at 356 seconds. Alternatively, if fusible links having the same RTI as the heat detectors  $[55 (m^2 s)^{1/2}]$  are used, all vents are predicted to be open at 384 seconds.

## D.5 Vent Design.

Of main concern in this example is the temperature of the smoke layer, which governs the heat flux radiated to the floor. Assuming an emissivity of 1 and a configuration factor of 1, the radiant heat flux at the floor is calculated as follows:

$$\text{Flux}_f = k\epsilon\phi T^4$$

where:

$T$  = temperature of the layer (K)

$k$  = Stefan–Boltzmann constant =  $5.67 \times 10^{-11}$  kW/m<sup>2</sup> K<sup>4</sup>

$\epsilon$  = emissivity = 1

$\phi$  = configuration factor = 1

$$\text{Flux}_f = (5.67 \times 10^{-11}) T^4 \text{ kW/m}^2$$

For a flux limit of 2.5 kW/m<sup>2</sup>, as stated in the objective, the temperature of the smoke layer is calculated as 458 K, or 164 K above the ambient temperature of 294 K.

## D.6 Steady Fire — Smoke Layer Temperature.

First, conditions following attainment of the maximum heat release rate of 100 MW can be examined (i.e., at times greater than 566 seconds) assuming a smoke layer at the lowest acceptable height, 3 m above the floor. (The heat detector installation contemplated was calculated to provide alarm at 230 seconds; 300 seconds following detection places the time of interest at 530 seconds, close to the attainment of the maximum heat release rate.)

The effective diameter of the fire is required for the calculations. This diameter can be determined with the aid of Equation 8.5, setting  $Q = 100,000$  kW and selecting an appropriate value for the heat release rate per unit floor area  $Q''$ . The two racks facing each other across the 2.4-m wide aisle are 9.75 m long and 1.2 m wide (see Figure D.6). The heat release rate per unit area is taken as the fully involved heat release rate, 100,000 kW, divided by the combined area of the two racks plus the aisle, or  $(9.75)(1.2)(2.2) + (9.75)(2.4) = 46.8$  m<sup>2</sup>. Accordingly, the heat release rate per unit area is

$$Q'' = \frac{100,000}{46.8} = 2136 \text{ kW/m}^2$$

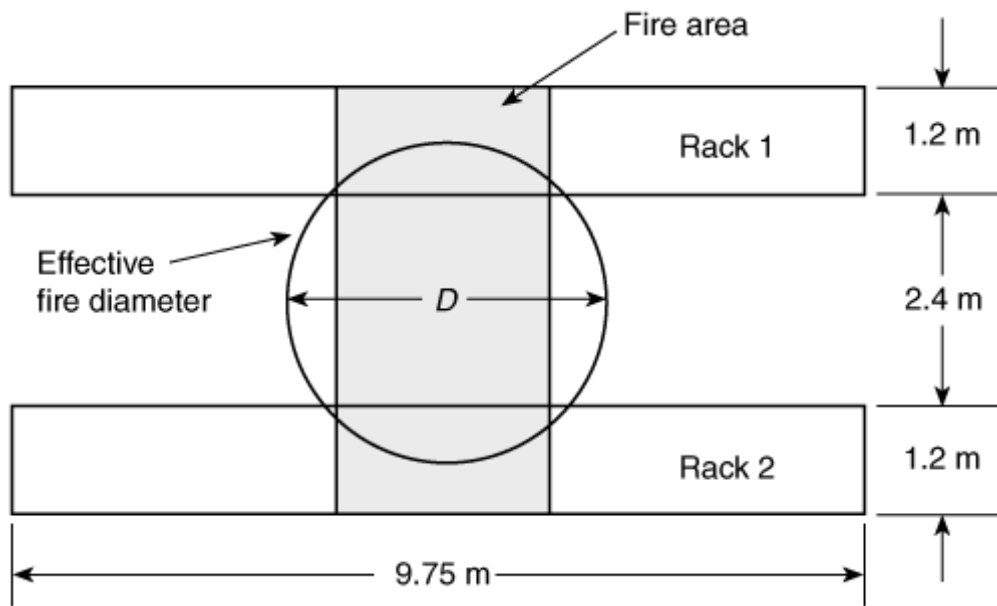


**FIGURE D.6 Effective Fire Diameter.**

This value can be assumed to be representative of most of the fire history, except for the initial stage. The effective diameter of the fire at 100,000 kW is then, using Equation 8.5,

$$D = \left[ \frac{4(100,000)}{\pi(2136)} \right]^{1/2} = 7.72 \text{ m}$$

Equation 9.6 is used to estimate the smoke layer temperature rise. The mass flow rate in the plume as it enters the smoke layer,  $\dot{m}_p$ , is calculated from Equation 9.3 or 9.4, depending on whether the flame height is smaller or larger than the height of the smoke layer above

the base of the fire,  $3 - 0.5 = 2.5$  m. The flame height is calculated from Equation 9.1:

$$L = [-1.02(7.72)] + [0.235(100,000)^{2/5}] = 15.6 \text{ m}$$

which is greater than the height of the smoke layer. (It is even greater than the ceiling height so that the flames will impinge on the ceiling and flow radially outward.) Therefore, the mass flow rate in the plume as it enters the smoke layer is calculated from Equation 9.4 as follows (assuming  $Q_c = 0.7 Q$ ):

$$\dot{m}_p = 0.0056(0.7 \times 100,000) \frac{2.5}{15.6} = 62.8 \text{ kg/s}$$

Now the temperature rise in the smoke layer can be estimated using Equation 9.6, with  $C_p = 1.00 \text{ kJ/kg} \cdot \text{K}$  and the value of  $r = 0.5$  recommended in 6.1.3.4:

$$\Delta T = \frac{0.5(70,000)}{1.00(62.8)} = 557 \text{ K}$$

This value is considerably above 164 K; therefore, the floor radiant heat flux can be expected to be much higher than the limit  $2.5 \text{ kW/m}^2$ . Using the equation for radiant heat flux to the floor presented previously, the value  $29.7 \text{ kW/m}^2$  is calculated for a smoke layer temperature of  $557 + 294 = 851 \text{ K}$ .

Not only is the smoke layer temperature,  $557 + 21 = 578^\circ\text{C}$ , so high that it produces unacceptable levels of radiant flux at the floor, but it is also close to the level,  $600^\circ\text{C}$ , where fire can flash over all the combustibles under the smoke layer. Furthermore, it exceeds the value,  $540^\circ\text{C}$ , where unprotected steel begins losing strength. Directly over the fire the temperatures might locally reach  $1135^\circ\text{C}$  (from Equation 9.6, with  $r = 1$ ), far in excess of the threshold for steel damage.

### D.7 Sizing of Vents.

This building arrangement will not meet design objectives. However, it might be instructive to investigate the venting requirements in order to illustrate general procedures that might be used to develop alternative designs.

All 16 vents are predicted to be open prior to 566 seconds — the time of interest.

The aerodynamic vent area,  $A_{va}$ , is determined with the aid of Equation 9.5:

$$\dot{m}_v = (2\rho_o^2 g)^{1/2} \left( \frac{T_o \Delta T}{T^2} \right)^{1/2} A_{va} d^{1/2}$$

At equilibrium, the mass flow through the vents is equal to the smoke production rate,

$\dot{m}_p$ . Substituting  $\dot{m}_p = 62.6 \text{ kg/s}$  for  $\dot{m}_v$  in Equation 9.5, together with

$$\rho_o = 1.2 \text{ kg/m}^3$$

$$g = 9.81 \text{ m/s}^2$$

$$T_o = 294 \text{ K}$$

$$\Delta T = 559 \text{ K}$$

$$T = 294 + 559 = 853 \text{ K}$$

$$d = 9.1 - 3 = 6.1 \text{ m}$$

the equation can be solved for the aerodynamic vent area. The result is

$$A_{va} = 10.04 \text{ m}^2$$

The vents are assumed to have a discharge coefficient of 0.61; therefore, the corresponding actual vent area is (see A.9.2.4.2)

$$A_v = \frac{10.04}{0.61} = 16.46 \text{ m}^2 \text{ (geometric vent area)} \cong 16.5 \text{ m}^2$$

The building design contemplates that inlet air openings will be 1.5 times the vent area. Equation F.2 is used to calculate a correction,  $M$ , for the limited inlet air openings.

$$M = \left[ 1 + \left( \frac{A_v}{A_r^2} \right) \left( \frac{T_o}{T} \right) \right]^{1/2}$$

$$M = \left[ 1 + \left( \frac{1}{1.5^2} \right) \left( \frac{294}{853} \right) \right]^{1/2} = 1.07$$

The corrected actual vent area is

$$(1.07)(16.5) = 17.66 \text{ m}^2$$

Distributed among the 16 vent locations, the actual area per vent is

$$\frac{17.66}{16} = 1.10 \text{ m}^2$$

The nearest commercial vent size equal to or larger than this unit vent area would be selected.

The following equation is used to check for  $Q_{feasible}$ :

$$Q_{feasible} = 23,200(H - d)^{5/2}$$

$$Q_{feasible} = 229,265 \text{ kW} \cong 230 \text{ MW}$$

where:

$$H = 9.1 - 0.5 = 8.6 \text{ m}$$

$$d = 6.1 \text{ m}$$

This value is higher than the projected heat release rate, 100 MW, and by itself is not of direct concern.

### D.8 Increased Height of Smoke Interface.

Inspection of Equation 9.4 indicates that the larger the height of the smoke interface above the base of the fire, the larger the value of mass entrained in the plume,  $\dot{m}_p$ , and Equation 9.6 indicates that the temperature rise in the smoke layer will be reduced. The calculations just completed for a smoke layer height of 3 m above the floor can be repeated for other smoke layer heights in search of acceptable alternative designs. The two additional smoke layer heights of 6 m and 7.3 m have been investigated, the latter near the maximum associated with the minimum recommended curtain depth for the 9.1-m high building (see Section 7.3). The final results of these additional calculations indicate values of temperature rise in the smoke layer of 253 K for the 6-m high level and 205 K for the 7.3-m high level. Although these values for smoke layer temperature rise are still a little high compared to the target of 164 K, they represent a major improvement. Furthermore, the temperatures are low enough so as not to represent a flashover hazard or endanger structural steel.

The calculations for the three smoke layer heights at the maximum heat release rate are summarized in Table D.8, entered as cases 1–3. In the table,  $H_c$  represents the height of the ceiling above the floor,  $H_c - d$  is the height of the smoke interface above the floor, and  $H - d$  is the height of the smoke interface above the base of the fire. In cases 1–3, the radiant heat flux at floor level, flux  $_{fl}$ , is seen to decrease to 5.1 kW/m<sup>2</sup> and 3.5 kW/m<sup>2</sup> as the smoke interface is raised but still remains above 2.5 kW/m<sup>2</sup>. The total required vent area (corrected  $A_v$ ) increases sharply as the smoke layer interface is raised. For the largest interface height, the total vent area of 89.2 m<sup>2</sup> corresponds to an area per vent of 89.2/16 = 5.57 m<sup>2</sup>, which is still smaller than the maximum vent area discussed in 5.4.1 [(i.e.,  $2d^2 = 2(1.8)^2 = 6.48 \text{ m}^2$ ).

**Table D.8 Results of Calculations for Vent Design**

Case	Time (s)	$Q$ (MW)	$D$ (m)	$L$ (m)	$H_c - d$ (m)	$H - d$ (m)	$d$ (m)	$\Delta T$ (K)
1	$\geq 566$	100	7.7	15.6	3.0	2.5	6.1	557
2	$\geq 566$	100	7.7	15.6	6.0	5.5	3.1	253

3	$\geq 566$	100	7.7	15.6	7.3	6.8	1.8	205
4	530	86.8	7.2	14.9	3.0	2.5	6.1	531
5	530	86.8	7.2	14.9	6.0	5.5	3.1	241
6	530	86.8	7.2	14.9	7.3	6.8	1.8	195
7	348	34.4	4.5	10.7	3.0	2.5	6.1	383
8	348	34.4	4.5	10.7	6.0	5.5	3.1	174
9	348	34.4	4.5	10.7	7.3	6.8	1.8	141

### D.9 Growing Fire.

Cases 4–6 in Table D.8 correspond to the growing fire with detection at 230 seconds using heat detectors. The state of the fire is represented at a time 300 seconds following detection with heat detectors (i.e., at  $230 + 300 = 530$  seconds). It is assumed that all 16 vents are operated together at the alarm of the first heat detector; alternatively, the vents are actuated individually with fusible links of the same RTI and activation temperature as the heat detectors, for which it might be confirmed with DETACT-QS that all vents open prior to 530 seconds. The calculations are parallel to cases 1–3, except that the fire is slightly smaller, as determined from the following:

$$Q = 0.36(t - 39)^2 = 0.36(530 - 39)^2 = 86,800 \text{ kW}$$

In cases 4–6, the smoke layer temperatures ( $\Delta T$ ) and radiant fluxes to the floor are only slightly reduced from the corresponding steady fire situations, cases 1–3. Also, there is little change in the required vent areas.

Cases 7–9 in Table D.8 correspond to the growing fire, with detection at 48 seconds using smoke detectors. Again, the state of the fire is represented at a time 300 seconds from detection (i.e., at 348 seconds). It is assumed that the 16 vents are operated together at the alarm of the first smoke detector. The calculations are executed at a state of fire development as follows:

$$Q = 0.36(t - 39)^2 = 0.36(348 - 39)^2 = 34,400 \text{ kW}$$

It is seen that case 9 meets the design objective of heat fluxes to the floor that are calculated as being lower than  $2.5 \text{ kW/m}^2$ , and case 8 nearly does so. The required vent areas are  $28.3 \text{ m}^2$  and  $47.8 \text{ m}^2$  for cases 8 and 9, respectively, corresponding to unit vent areas (16 vents) of  $1.8 \text{ m}^2$  and  $3.0 \text{ m}^2$ , both of which are well below their respective maxima,  $2 d^2$ , based on 5.4.1.

It will be noted that the case 8 solution using “hand calculations” provides an approximation close to the LAVENT predictions, which are summarized next.

### D.10 LAVENT Analysis.

The case 8 vent design in Table D.8 will now be analyzed using the computer program LAVENT [3]. LAVENT is able to assess the time-varying events associated with the

predicted fire. The fire has been previously determined as follows:

$$Q = 0.18t^2 \text{ for } 0 < t \leq 134 \text{ s}$$

$$Q = 0.36(t - 39)^2 \text{ for } 134 < t \leq 566 \text{ s}$$

$$Q = 100,000 \text{ kW for } t > 566 \text{ s}$$

The values for this fire will be used as input for LAVENT. The fire is assumed to start in the center of the building.

A complete smoke detection system is to be installed with detectors spaced 9.1 m on center. Detectors are located a maximum of 6.5 m from the fire axis (i.e., one-half the diagonal distance between detectors). As noted in A.9.2.5.4.4.1, detectors have an activation temperature of 31°C (10°C above ambient) and are located 0.1 m below the ceiling.

The vent design will use sixteen 1.76-m<sup>2</sup> vents located 18.3 m on center. All vents automatically open on activation of the first smoke detector.

LAVENT predicts that the upper-layer temperature will be 377°C and that the upper “hot” layer will be 4.6 m above floor level at 600 seconds. A 3 m clear layer is maintained throughout the 600-second time interval. However, heat flux at floor level is projected to be approximately 10 kW/m<sup>2</sup> at 600 seconds, and the design objective of limiting heat flux to 2.5 kW/m<sup>2</sup> at floor level is exceeded. At 342 seconds, the time of detection plus 300 seconds, however, the design objectives are met. At 360 seconds, LAVENT predicts the upper-layer temperature as 444 K (171°C), with the layer being 7.3 m above the floor. The predicted 150 K temperature rise is limited to less than the target value of 164 K, and heat flux at floor level is predicted to be 2.2 kW/m<sup>2</sup>. Therefore, the design objectives are satisfied for a time interval greater than the time of detection plus 300 seconds.

Inlet air is 1.5 times the vent area. To maintain the vent flow predicted by LAVENT, inlet air net free area should be maintained at a minimum of twice the open vent area. Although the net free inlet air area is less than required, the inlet area is sufficiently large that LAVENT predictions can be assumed to be reasonably valid. However, consideration should be given to increasing the vent area to account for the restrictions in inlet air.

See Figure D.10(a) through Figure D.10(h), and Figure D.10(i) for a computer printout of the LAVENT output.

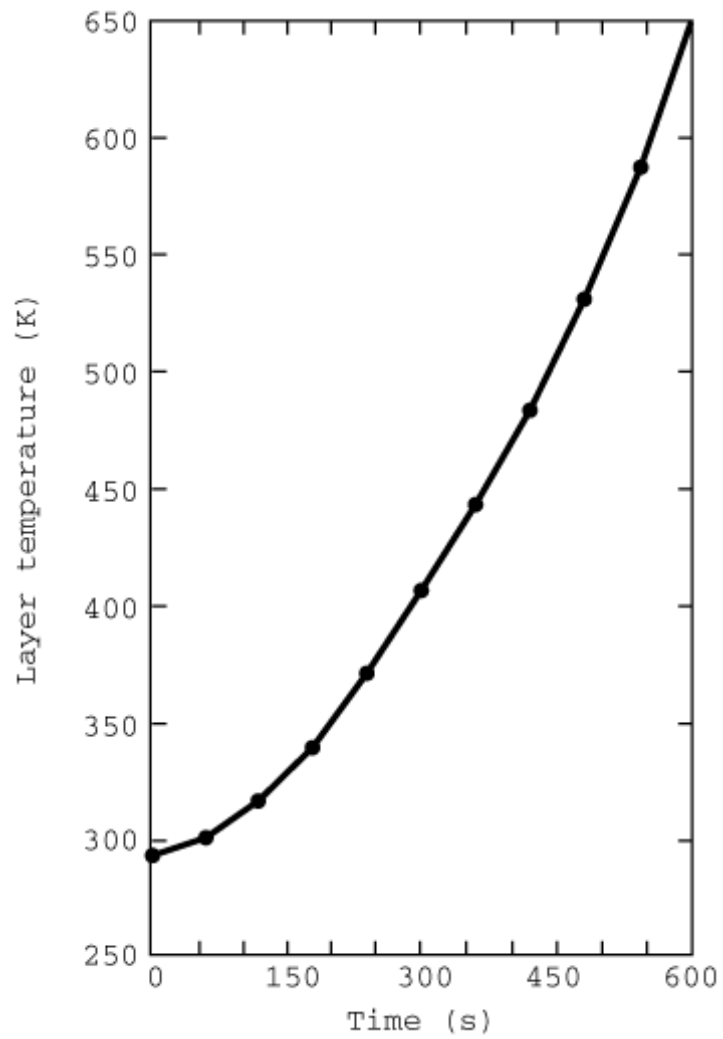


**FIGURE D.10(a) Temperature.**

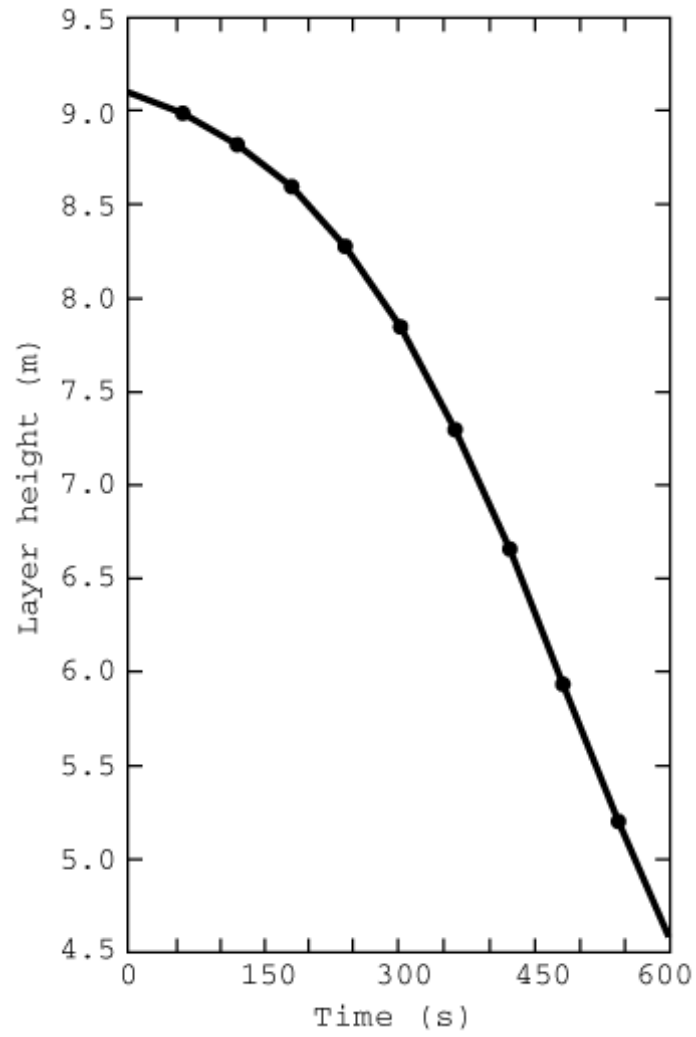


**FIGURE D.10(b) Layer Height.**

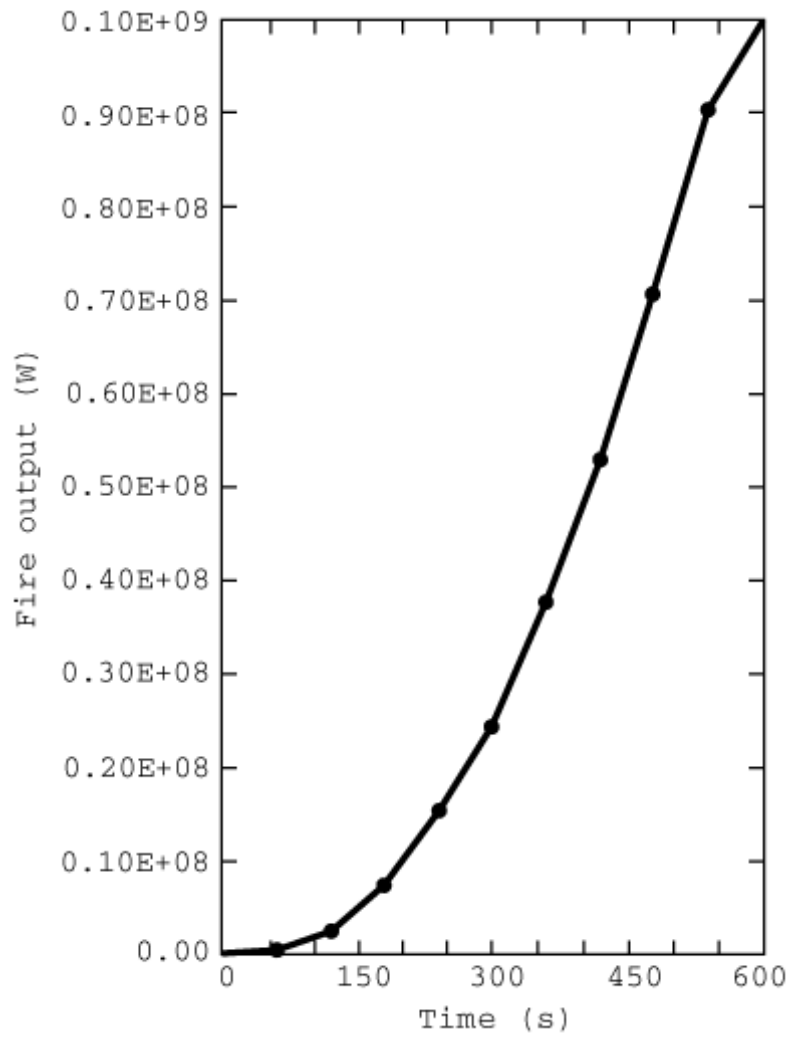


**FIGURE D.10(c) Fire Output.**

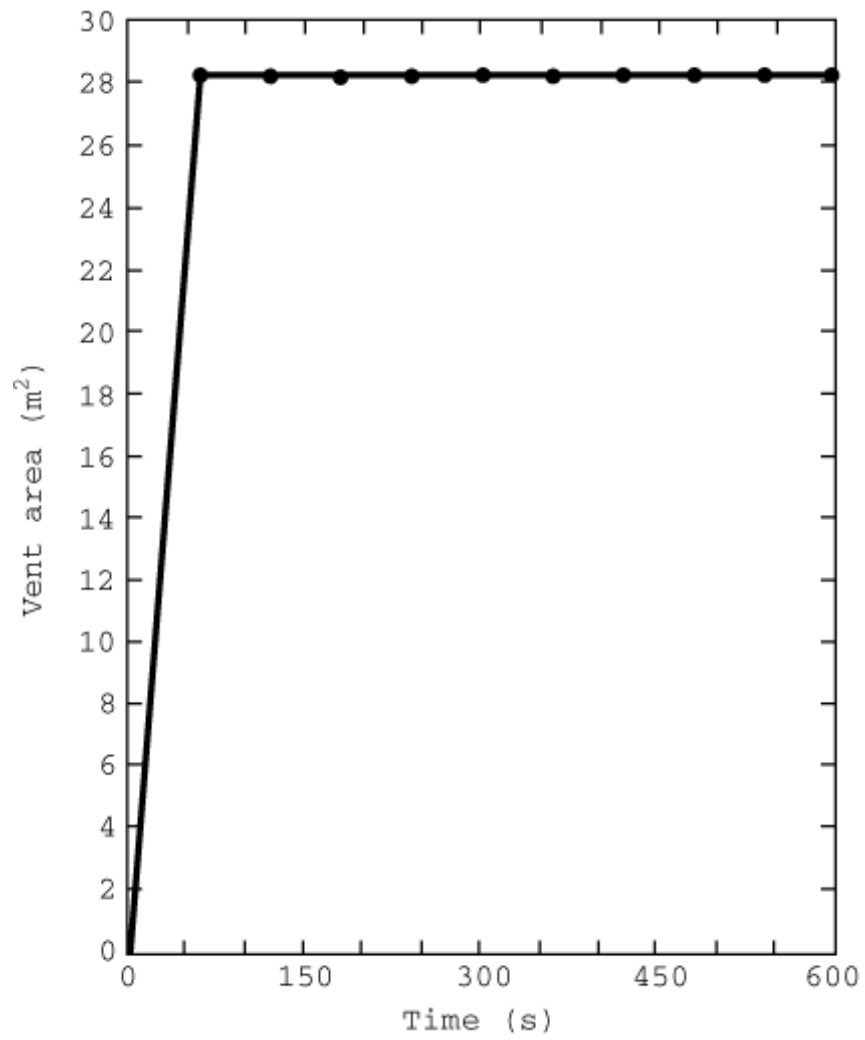


**FIGURE D.10(d) Vent Area.**

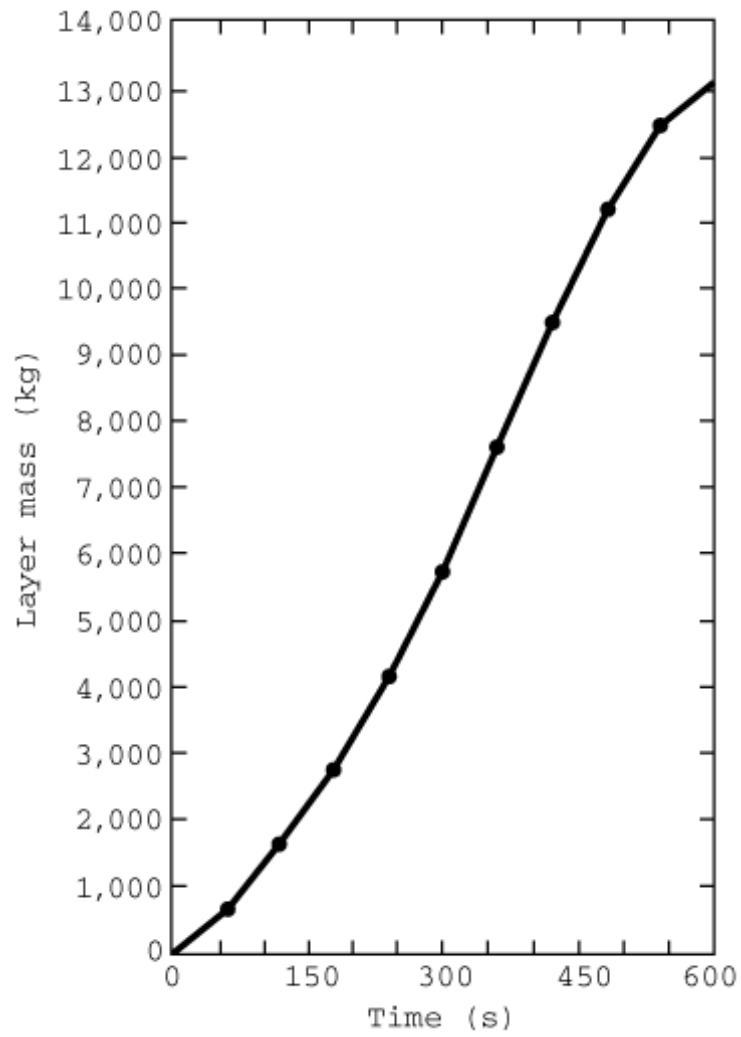


**FIGURE D.10(e) Layer Mass.**

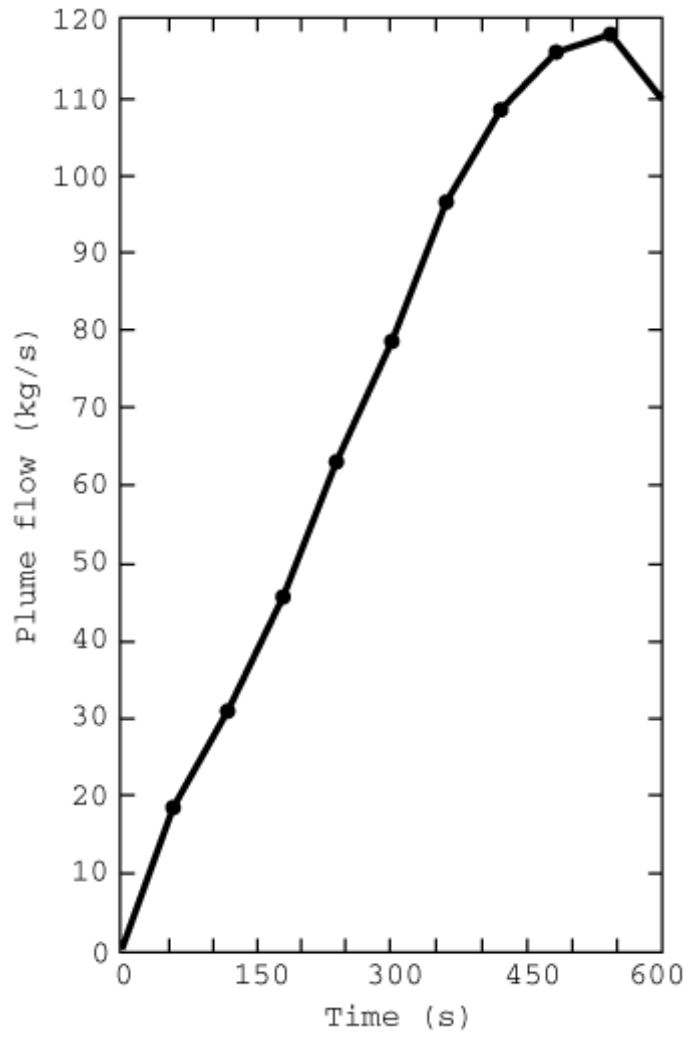


**FIGURE D.10(f) Plume Flow.**

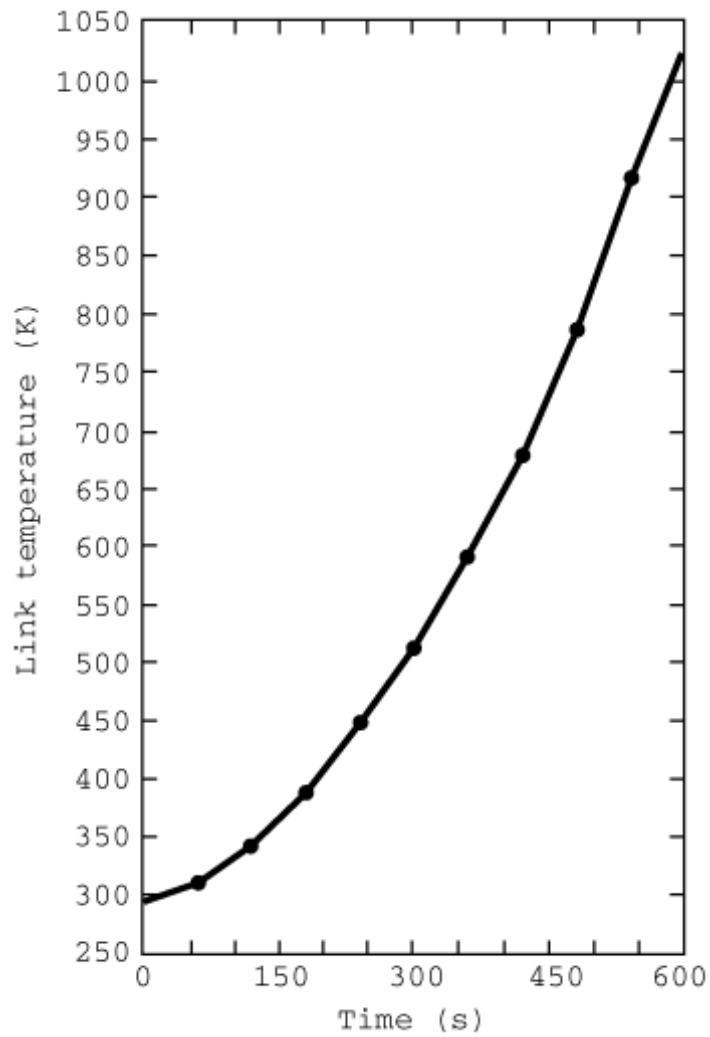


**FIGURE D.10(g) Detector Temperature.**

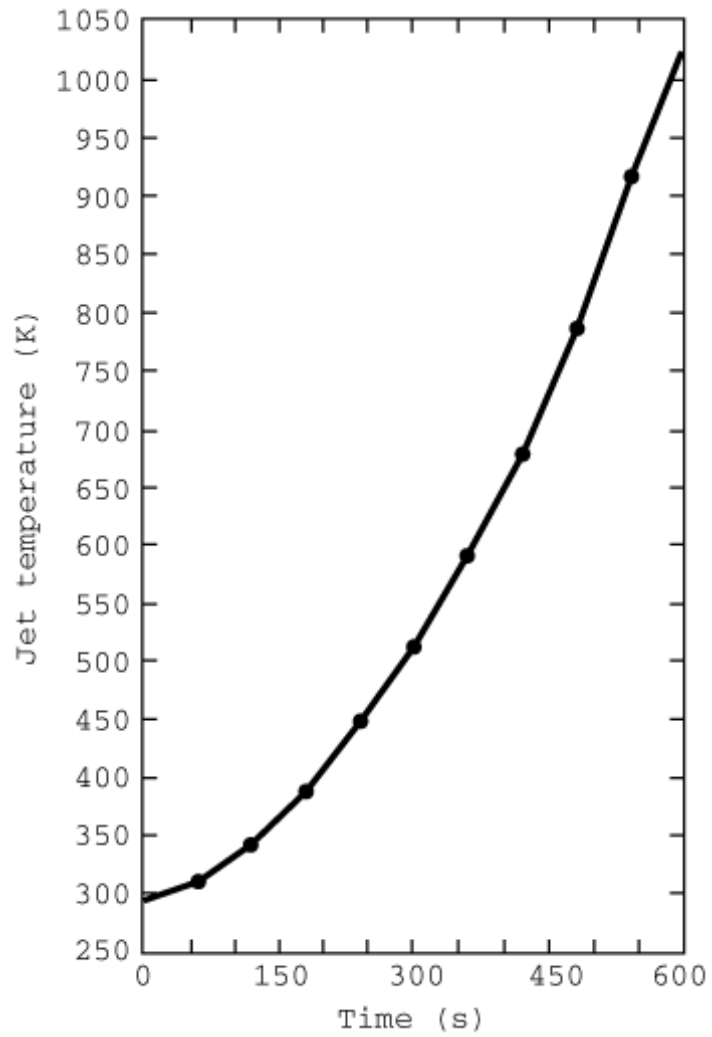


**FIGURE D.10(h) Jet Temperature.**

CEILING HEIGHT = 9.1 M  
ROOM LENGTH = 73.0 M  
ROOM WIDTH = 73.0 M  
CURTAIN LENGTH = 292.0 M  
CURTAIN HEIGHT = 0.0 M  
MATERIAL = INSULATED DECK (SOLID POLYSTYRENE)  
CEILING CONDUCTIVITY = .149E+00 W/M K  
CEILING DENSITY = .116E+04 KG/M3  
CEILING HEAT CAPACITY = .105E+04 J/M K  
CEILING THICKNESS = .152E+00 M  
FIRE HEIGHT = 0.5 M  
FIRE POWER/AREA = 0.2136E+07 W/M2

LINK NO = 1 RADIUS = 6.5 M DIST CEILING = 0.1 M  
RTI = 1.00 SQRT(MS) FUSION TEMPERATURE FOR LINK = 304.00 VENT = 1  
VENT AREA = 28.2 M2 LINK CONTROLLING VENT = 1

TIME (S)= 0.0000 LVR TEMP (K)= 294.0 LVR HT (M) = 9.10  
LVR MASS (KG)=0.000E+00 FIRE OUTPUT (W) = 0.0000E+00 VENT AREA (M2) = 0.00  
LINK = 1 LINK TEMP (K) = 294.00 JET VELOCITY (M/S) = 0.000 JET TEMP (K) = 294.0  
R (M) = 0.00 TSL (K) = 294.0 QB (W/M2) = 0.000E+00 QT (W/M2) = 0.000E+00  
R (M) = 1.74 TSL (K) = 294.0 QB (W/M2) = 0.000E+00 QT (W/M2) = 0.000E+00  
R (M) = 3.48 TSL (K) = 294.0 QB (W/M2) = 0.000E+00 QT (W/M2) = 0.000E+00  
R (M) = 5.22 TSL (K) = 294.0 QB (W/M2) = 0.000E+00 QT (W/M2) = 0.000E+00  
R (M) = 6.95 TSL (K) = 294.0 QB (W/M2) = 0.000E+00 QT (W/M2) = 0.000E+00  
R (M) = 8.69 TSL (K) = 294.0 QB (W/M2) = 0.000E+00 QT (W/M2) = 0.000E+00  
R (M) = 10.43 TSL (K) = 294.0 QB (W/M2) = 0.000E+00 QT (W/M2) = 0.000E+00  
R (M) = 12.17 TSL (K) = 294.0 QB (W/M2) = 0.000E+00 QT (W/M2) = 0.000E+00  
R (M) = 13.91 TSL (K) = 294.0 QB (W/M2) = 0.000E+00 QT (W/M2) = 0.000E+00  
R (M) = 15.65 TSL (K) = 294.0 QB (W/M2) = 0.000E+00 QT (W/M2) = 0.000E+00  
R (M) = 17.39 TSL (K) = 294.0 QB (W/M2) = 0.000E+00 QT (W/M2) = 0.000E+00  
R (M) = 19.12 TSL (K) = 294.0 QB (W/M2) = 0.000E+00 QT (W/M2) = 0.000E+00  
R (M) = 20.86 TSL (K) = 294.0 QB (W/M2) = 0.000E+00 QT (W/M2) = 0.000E+00  
R (M) = 22.60 TSL (K) = 294.0 QB (W/M2) = 0.000E+00 QT (W/M2) = 0.000E+00  
R (M) = 24.34 TSL (K) = 294.0 QB (W/M2) = 0.000E+00 QT (W/M2) = 0.000E+00  
R (M) = 26.08 TSL (K) = 294.0 QB (W/M2) = 0.000E+00 QT (W/M2) = 0.000E+00  
R (M) = 27.82 TSL (K) = 294.0 QB (W/M2) = 0.000E+00 QT (W/M2) = 0.000E+00  
R (M) = 29.56 TSL (K) = 294.0 QB (W/M2) = 0.000E+00 QT (W/M2) = 0.000E+00  
R (M) = 31.29 TSL (K) = 294.0 QB (W/M2) = 0.000E+00 QT (W/M2) = 0.000E+00  
R (M) = 33.03 TSL (K) = 294.0 QB (W/M2) = 0.000E+00 QT (W/M2) = 0.000E+00  
R (M) = 34.77 TSL (K) = 294.0 QB (W/M2) = 0.000E+00 QT (W/M2) = 0.000E+00  
R (M) = 36.51 TSL (K) = 294.0 QB (W/M2) = 0.000E+00 QT (W/M2) = 0.000E+00  
R (M) = 38.25 TSL (K) = 294.0 QB (W/M2) = 0.000E+00 QT (W/M2) = 0.000E+00  
R (M) = 39.99 TSL (K) = 294.0 QB (W/M2) = 0.000E+00 QT (W/M2) = 0.000E+00  
R (M) = 41.73 TSL (K) = 294.0 QB (W/M2) = 0.000E+00 QT (W/M2) = 0.000E+00  
R (M) = 43.46 TSL (K) = 294.0 QB (W/M2) = 0.000E+00 QT (W/M2) = 0.000E+00  
R (M) = 45.20 TSL (K) = 294.0 QB (W/M2) = 0.000E+00 QT (W/M2) = 0.000E+00  
R (M) = 46.94 TSL (K) = 294.0 QB (W/M2) = 0.000E+00 QT (W/M2) = 0.000E+00

**FIGURE D.10(i) LAVENT Analysis Output.**

R (M) = 15.65 TSL (K) = 294.6 QB (W/M2) = 0.619E+02 QT (W/M2) = 0.000E+00  
R (M) = 17.39 TSL (K) = 294.5 QB (W/M2) = 0.522E+02 QT (W/M2) = 0.000E+00  
R (M) = 19.12 TSL (K) = 294.4 QB (W/M2) = 0.448E+02 QT (W/M2) = 0.000E+00  
R (M) = 20.86 TSL (K) = 294.3 QB (W/M2) = 0.389E+02 QT (W/M2) = 0.000E+00  
R (M) = 22.60 TSL (K) = 294.3 QB (W/M2) = 0.343E+02 QT (W/M2) = 0.000E+00  
R (M) = 24.34 TSL (K) = 294.3 QB (W/M2) = 0.305E+02 QT (W/M2) = 0.000E+00  
R (M) = 26.08 TSL (K) = 294.2 QB (W/M2) = 0.274E+02 QT (W/M2) = 0.000E+00  
R (M) = 27.82 TSL (K) = 294.2 QB (W/M2) = 0.248E+02 QT (W/M2) = 0.000E+00  
R (M) = 29.56 TSL (K) = 294.2 QB (W/M2) = 0.226E+02 QT (W/M2) = 0.000E+00  
R (M) = 31.29 TSL (K) = 294.2 QB (W/M2) = 0.207E+02 QT (W/M2) = 0.000E+00  
R (M) = 33.03 TSL (K) = 294.2 QB (W/M2) = 0.191E+02 QT (W/M2) = 0.000E+00  
R (M) = 34.77 TSL (K) = 294.2 QB (W/M2) = 0.177E+02 QT (W/M2) = 0.000E+00  
R (M) = 36.51 TSL (K) = 294.1 QB (W/M2) = 0.165E+02 QT (W/M2) = 0.000E+00  
R (M) = 38.25 TSL (K) = 294.1 QB (W/M2) = 0.154E+02 QT (W/M2) = 0.000E+00  
R (M) = 39.99 TSL (K) = 294.1 QB (W/M2) = 0.144E+02 QT (W/M2) = 0.000E+00  
R (M) = 41.73 TSL (K) = 294.1 QB (W/M2) = 0.136E+02 QT (W/M2) = 0.000E+00  
R (M) = 43.46 TSL (K) = 294.1 QB (W/M2) = 0.128E+02 QT (W/M2) = 0.000E+00  
R (M) = 45.20 TSL (K) = 294.1 QB (W/M2) = 0.121E+02 QT (W/M2) = 0.000E+00  
R (M) = 46.94 TSL (K) = 294.1 QB (W/M2) = 0.115E+02 QT (W/M2) = 0.000E+00  
R (M) = 48.68 TSL (K) = 294.0 QB (W/M2) = 0.122E+01 QT (W/M2) = 0.000E+00  
R (M) = 50.42 TSL (K) = 294.0 QB (W/M2) = 0.110E+01 QT (W/M2) = 0.000E+00

TIME (S)= 120.0000 LYR TEMP (K)= 317.2 LYR HT (M) = 8.83

LYR MASS (KG)=0.162E+04 FIRE OUTPUT (W) = 0.2743E+07 VENT AREA (M2) = 28.20

LINK = 1 LINK TEMP (K) = 339.83 JET VELOCITY (M/S) = 1.761

JET TEMP (K) = 340.2 TIME LINK 1 OPENS EQUALS 41.7098 (S)

R (M) = 0.00 TSL (K) = 332.0 QB (W/M2) = 0.242E+04 QT (W/M2) = 0.000E+00  
R (M) = 1.74 TSL (K) = 322.4 QB (W/M2) = 0.188E+04 QT (W/M2) = 0.000E+00  
R (M) = 3.48 TSL (K) = 314.9 QB (W/M2) = 0.142E+04 QT (W/M2) = 0.000E+00  
R (M) = 5.22 TSL (K) = 308.8 QB (W/M2) = 0.102E+04 QT (W/M2) = 0.000E+00  
R (M) = 6.95 TSL (K) = 304.7 QB (W/M2) = 0.753E+03 QT (W/M2) = 0.000E+00  
R (M) = 8.69 TSL (K) = 302.1 QB (W/M2) = 0.569E+03 QT (W/M2) = 0.000E+00  
R (M) = 10.43 TSL (K) = 300.2 QB (W/M2) = 0.441E+03 QT (W/M2) = 0.000E+00  
R (M) = 12.17 TSL (K) = 298.9 QB (W/M2) = 0.350E+03 QT (W/M2) = 0.000E+00  
R (M) = 13.91 TSL (K) = 298.0 QB (W/M2) = 0.285E+03 QT (W/M2) = 0.000E+00  
R (M) = 15.65 TSL (K) = 297.3 QB (W/M2) = 0.236E+03 QT (W/M2) = 0.000E+00  
R (M) = 17.39 TSL (K) = 296.8 QB (W/M2) = 0.199E+03 QT (W/M2) = 0.000E+00  
R (M) = 19.12 TSL (K) = 296.4 QB (W/M2) = 0.171E+03 QT (W/M2) = 0.000E+00  
R (M) = 20.86 TSL (K) = 296.1 QB (W/M2) = 0.149E+03 QT (W/M2) = 0.000E+00  
R (M) = 22.60 TSL (K) = 295.8 QB (W/M2) = 0.131E+03 QT (W/M2) = 0.000E+00  
R (M) = 24.34 TSL (K) = 295.6 QB (W/M2) = 0.117E+03 QT (W/M2) = 0.000E+00  
R (M) = 26.08 TSL (K) = 295.5 QB (W/M2) = 0.105E+03 QT (W/M2) = 0.000E+00  
R (M) = 27.82 TSL (K) = 295.3 QB (W/M2) = 0.951E+02 QT (W/M2) = 0.000E+00  
R (M) = 29.56 TSL (K) = 295.2 QB (W/M2) = 0.867E+02 QT (W/M2) = 0.000E+00  
R (M) = 31.29 TSL (K) = 295.1 QB (W/M2) = 0.795E+02 QT (W/M2) = 0.000E+00  
R (M) = 33.03 TSL (K) = 295.0 QB (W/M2) = 0.734E+02 QT (W/M2) = 0.000E+00  
R (M) = 34.77 TSL (K) = 294.9 QB (W/M2) = 0.680E+02 QT (W/M2) = 0.000E+00  
R (M) = 36.51 TSL (K) = 294.9 QB (W/M2) = 0.632E+02 QT (W/M2) = 0.000E+00

**FIGURE D.10(i) *Continued***

R (M) = 5.22 TSL (K) = 334.5 QB (W/M2) = 0.244E+04 QT (W/M2) = 0.000E+00  
R (M) = 6.95 TSL (K) = 324.0 QB (W/M2) = 0.183E+04 QT (W/M2) = 0.000E+00  
R (M) = 8.69 TSL (K) = 316.7 QB (W/M2) = 0.140E+04 QT (W/M2) = 0.000E+00  
R (M) = 10.43 TSL (K) = 311.6 QB (W/M2) = 0.109E+04 QT (W/M2) = 0.000E+00  
R (M) = 12.17 TSL (K) = 308.0 QB (W/M2) = 0.864E+03 QT (W/M2) = 0.000E+00  
R (M) = 13.91 TSL (K) = 305.3 QB (W/M2) = 0.702E+03 QT (W/M2) = 0.000E+00  
R (M) = 15.65 TSL (K) = 303.4 QB (W/M2) = 0.582E+03 QT (W/M2) = 0.000E+00  
R (M) = 17.39 TSL (K) = 301.9 QB (W/M2) = 0.491E+03 QT (W/M2) = 0.000E+00  
R (M) = 19.12 TSL (K) = 300.8 QB (W/M2) = 0.420E+03 QT (W/M2) = 0.000E+00  
R (M) = 20.86 TSL (K) = 299.9 QB (W/M2) = 0.365E+03 QT (W/M2) = 0.000E+00  
R (M) = 22.60 TSL (K) = 299.2 QB (W/M2) = 0.321E+03 QT (W/M2) = 0.000E+00  
R (M) = 24.34 TSL (K) = 298.6 QB (W/M2) = 0.286E+03 QT (W/M2) = 0.000E+00  
R (M) = 26.08 TSL (K) = 298.1 QB (W/M2) = 0.256E+03 QT (W/M2) = 0.000E+00  
R (M) = 27.82 TSL (K) = 297.7 QB (W/M2) = 0.232E+03 QT (W/M2) = 0.000E+00  
R (M) = 29.56 TSL (K) = 297.4 QB (W/M2) = 0.211E+03 QT (W/M2) = 0.000E+00  
R (M) = 31.29 TSL (K) = 297.1 QB (W/M2) = 0.193E+03 QT (W/M2) = 0.000E+00  
R (M) = 33.03 TSL (K) = 296.9 QB (W/M2) = 0.178E+03 QT (W/M2) = 0.000E+00  
R (M) = 34.77 TSL (K) = 296.7 QB (W/M2) = 0.165E+03 QT (W/M2) = 0.000E+00  
R (M) = 36.51 TSL (K) = 296.5 QB (W/M2) = 0.154E+03 QT (W/M2) = 0.000E+00  
R (M) = 38.25 TSL (K) = 296.3 QB (W/M2) = 0.143E+03 QT (W/M2) = 0.000E+00  
R (M) = 39.99 TSL (K) = 296.2 QB (W/M2) = 0.134E+03 QT (W/M2) = 0.000E+00  
R (M) = 41.73 TSL (K) = 296.0 QB (W/M2) = 0.126E+03 QT (W/M2) = 0.000E+00  
R (M) = 43.46 TSL (K) = 295.9 QB (W/M2) = 0.119E+03 QT (W/M2) = 0.000E+00  
R (M) = 45.20 TSL (K) = 295.8 QB (W/M2) = 0.113E+03 QT (W/M2) = 0.000E+00  
R (M) = 46.94 TSL (K) = 295.7 QB (W/M2) = 0.107E+03 QT (W/M2) = 0.000E+00  
R (M) = 48.68 TSL (K) = 294.2 QB (W/M2) = 0.136E+02 QT (W/M2) = 0.000E+00  
R (M) = 50.42 TSL (K) = 294.2 QB (W/M2) = 0.123E+02 QT (W/M2) = 0.000E+00

TIME (S)= 240.0000 LVR TEMP (K)= 371.5 LVR HT (M) = 8.28  
LVR MASS (KG)=0.414E+04 FIRE OUTPUT (W) = 0.1541E+08 VENT AREA (M2) = 28.20  
LINK = 1 LINK TEMP (K) = 447.57 JET VELOCITY (M/S) = 3.186  
JET TEMP (K) = 448.2 TIME LINK 1 OPENS EQUALS 41.7098 (S)

R (M) = 0.00 TSL (K) = 469.7 QB (W/M2) = 0.816E+04 QT (W/M2) = 0.000E+00  
R (M) = 1.74 TSL (K) = 439.3 QB (W/M2) = 0.700E+04 QT (W/M2) = 0.000E+00  
R (M) = 3.48 TSL (K) = 408.8 QB (W/M2) = 0.570E+04 QT (W/M2) = 0.000E+00  
R (M) = 5.22 TSL (K) = 380.2 QB (W/M2) = 0.439E+04 QT (W/M2) = 0.000E+00  
R (M) = 6.95 TSL (K) = 359.0 QB (W/M2) = 0.335E+04 QT (W/M2) = 0.000E+00  
R (M) = 8.69 TSL (K) = 343.8 QB (W/M2) = 0.259E+04 QT (W/M2) = 0.000E+00  
R (M) = 10.43 TSL (K) = 332.8 QB (W/M2) = 0.203E+04 QT (W/M2) = 0.000E+00  
R (M) = 12.17 TSL (K) = 324.9 QB (W/M2) = 0.162E+04 QT (W/M2) = 0.000E+00  
R (M) = 13.91 TSL (K) = 319.1 QB (W/M2) = 0.132E+04 QT (W/M2) = 0.000E+00  
R (M) = 15.65 TSL (K) = 314.8 QB (W/M2) = 0.109E+04 QT (W/M2) = 0.000E+00  
R (M) = 17.39 TSL (K) = 311.6 QB (W/M2) = 0.922E+03 QT (W/M2) = 0.000E+00  
R (M) = 19.12 TSL (K) = 309.1 QB (W/M2) = 0.790E+03 QT (W/M2) = 0.000E+00  
R (M) = 20.86 TSL (K) = 307.1 QB (W/M2) = 0.687E+03 QT (W/M2) = 0.000E+00  
R (M) = 22.60 TSL (K) = 305.5 QB (W/M2) = 0.604E+03 QT (W/M2) = 0.000E+00  
R (M) = 24.34 TSL (K) = 304.2 QB (W/M2) = 0.536E+03 QT (W/M2) = 0.000E+00  
R (M) = 26.08 TSL (K) = 303.2 QB (W/M2) = 0.481E+03 QT (W/M2) = 0.000E+00

**FIGURE D.10(i) *Continued***

TIME (S)= 300.0000 LVR TEMP (K)= 406.7 LVR HT (M) = 7.86  
 LVR MASS (KG)=0.575E+04 FIRE OUTPUT (W) = 0.2452E+08 VENT AREA (M2) = 28.20  
 LINK = 1 LINK TEMP (K) = 511.85 JET VELOCITY (M/S) = 3.699  
 JET TEMP (K) = 512.4 TIME LINK 1 OPENS EQUALS 41.7098 (S)

R (M) =	0.00	TSL (K) =	561.4	QB (W/M2) =	0.962E+04	QT (W/M2) =	-0.297E-11
R (M) =	1.74	TSL (K) =	523.2	QB (W/M2) =	0.859E+04	QT (W/M2) =	-0.297E-11
R (M) =	3.48	TSL (K) =	481.7	QB (W/M2) =	0.731E+04	QT (W/M2) =	-0.297E-11
R (M) =	5.22	TSL (K) =	439.7	QB (W/M2) =	0.588E+04	QT (W/M2) =	-0.297E-11
R (M) =	6.95	TSL (K) =	406.1	QB (W/M2) =	0.464E+04	QT (W/M2) =	-0.297E-11
R (M) =	8.69	TSL (K) =	381.0	QB (W/M2) =	0.365E+04	QT (W/M2) =	-0.297E-11
R (M) =	10.43	TSL (K) =	362.4	QB (W/M2) =	0.289E+04	QT (W/M2) =	-0.297E-11
R (M) =	12.17	TSL (K) =	348.8	QB (W/M2) =	0.234E+04	QT (W/M2) =	-0.297E-11
R (M) =	13.91	TSL (K) =	338.7	QB (W/M2) =	0.191E+04	QT (W/M2) =	-0.297E-11
R (M) =	15.65	TSL (K) =	331.1	QB (W/M2) =	0.159E+04	QT (W/M2) =	-0.297E-11
R (M) =	17.39	TSL (K) =	325.4	QB (W/M2) =	0.135E+04	QT (W/M2) =	-0.297E-11
R (M) =	19.12	TSL (K) =	320.9	QB (W/M2) =	0.116E+04	QT (W/M2) =	-0.297E-11
R (M) =	20.86	TSL (K) =	317.4	QB (W/M2) =	0.101E+04	QT (W/M2) =	-0.297E-11
R (M) =	22.60	TSL (K) =	314.6	QB (W/M2) =	0.887E+03	QT (W/M2) =	-0.297E-11
R (M) =	24.34	TSL (K) =	312.3	QB (W/M2) =	0.789E+03	QT (W/M2) =	-0.297E-11
R (M) =	26.08	TSL (K) =	310.4	QB (W/M2) =	0.708E+03	QT (W/M2) =	-0.297E-11
R (M) =	27.82	TSL (K) =	308.8	QB (W/M2) =	0.640E+03	QT (W/M2) =	-0.297E-11
R (M) =	29.56	TSL (K) =	307.5	QB (W/M2) =	0.583E+03	QT (W/M2) =	-0.297E-11
R (M) =	31.29	TSL (K) =	306.4	QB (W/M2) =	0.535E+03	QT (W/M2) =	-0.297E-11
R (M) =	33.03	TSL (K) =	305.4	QB (W/M2) =	0.493E+03	QT (W/M2) =	-0.297E-11
R (M) =	34.77	TSL (K) =	304.6	QB (W/M2) =	0.456E+03	QT (W/M2) =	-0.297E-11
R (M) =	36.51	TSL (K) =	303.8	QB (W/M2) =	0.425E+03	QT (W/M2) =	-0.297E-11
R (M) =	38.25	TSL (K) =	303.2	QB (W/M2) =	0.397E+03	QT (W/M2) =	-0.297E-11
R (M) =	39.99	TSL (K) =	302.6	QB (W/M2) =	0.372E+03	QT (W/M2) =	-0.297E-11
R (M) =	41.73	TSL (K) =	302.1	QB (W/M2) =	0.350E+03	QT (W/M2) =	-0.297E-11
R (M) =	43.46	TSL (K) =	301.6	QB (W/M2) =	0.330E+03	QT (W/M2) =	-0.297E-11
R (M) =	45.20	TSL (K) =	301.2	QB (W/M2) =	0.312E+03	QT (W/M2) =	-0.297E-11
R (M) =	46.94	TSL (K) =	300.8	QB (W/M2) =	0.296E+03	QT (W/M2) =	-0.297E-11
R (M) =	48.68	TSL (K) =	299.8	QB (W/M2) =	0.286E+03	QT (W/M2) =	-0.297E-11
R (M) =	50.42	TSL (K) =	294.9	QB (W/M2) =	0.390E+02	QT (W/M2) =	-0.297E-11

TIME (S)= 360.0000 LVR TEMP (K)= 443.6 LVR HT (M) = 7.31  
 LVR MASS (KG)=0.760E+04 FIRE OUTPUT (W) = 0.3795E+08 VENT AREA (M2) = 28.20  
 LINK = 1 LINK TEMP (K) = 590.31 JET VELOCITY (M/S) = 4.317  
 JET TEMP (K) = 590.9 TIME LINK 1 OPENS EQUALS 41.7098 (S)

R (M) =	0.00	TSL (K) =	658.1	QB (W/M2) =	0.117E+05	QT (W/M2) =	-0.297E-11
R (M) =	1.74	TSL (K) =	614.7	QB (W/M2) =	0.107E+05	QT (W/M2) =	-0.297E-11
R (M) =	3.48	TSL (K) =	564.3	QB (W/M2) =	0.939E+04	QT (W/M2) =	-0.297E-11
R (M) =	5.22	TSL (K) =	510.0	QB (W/M2) =	0.780E+04	QT (W/M2) =	-0.297E-11
R (M) =	6.95	TSL (K) =	463.8	QB (W/M2) =	0.631E+04	QT (W/M2) =	-0.297E-11
R (M) =	8.69	TSL (K) =	427.5	QB (W/M2) =	0.505E+04	QT (W/M2) =	-0.297E-11
R (M) =	10.43	TSL (K) =	399.9	QB (W/M2) =	0.405E+04	QT (W/M2) =	-0.297E-11
R (M) =	12.17	TSL (K) =	379.3	QB (W/M2) =	0.329E+04	QT (W/M2) =	-0.297E-11
R (M) =	13.91	TSL (K) =	362.9	QB (W/M2) =	0.271E+04	QT (W/M2) =	-0.297E-11
R (M) =	15.65	TSL (K) =	352.9	QB (W/M2) =	0.229E+04	QT (W/M2) =	-0.297E-11
R (M) =	17.39	TSL (K) =	344.9	QB (W/M2) =	0.197E+04	QT (W/M2) =	-0.297E-11
R (M) =	19.12	TSL (K) =	338.9	QB (W/M2) =	0.171E+04	QT (W/M2) =	-0.297E-11
R (M) =	20.86	TSL (K) =	334.9	QB (W/M2) =	0.151E+04	QT (W/M2) =	-0.297E-11
R (M) =	22.60	TSL (K) =	332.9	QB (W/M2) =	0.135E+04	QT (W/M2) =	-0.297E-11
R (M) =	24.34	TSL (K) =	331.9	QB (W/M2) =	0.123E+04	QT (W/M2) =	-0.297E-11
R (M) =	26.08	TSL (K) =	331.9	QB (W/M2) =	0.114E+04	QT (W/M2) =	-0.297E-11
R (M) =	27.82	TSL (K) =	331.9	QB (W/M2) =	0.107E+04	QT (W/M2) =	-0.297E-11
R (M) =	29.56	TSL (K) =	331.9	QB (W/M2) =	0.101E+04	QT (W/M2) =	-0.297E-11
R (M) =	31.29	TSL (K) =	331.9	QB (W/M2) =	0.959E+03	QT (W/M2) =	-0.297E-11
R (M) =	33.03	TSL (K) =	331.9	QB (W/M2) =	0.919E+03	QT (W/M2) =	-0.297E-11
R (M) =	34.77	TSL (K) =	331.9	QB (W/M2) =	0.889E+03	QT (W/M2) =	-0.297E-11
R (M) =	36.51	TSL (K) =	331.9	QB (W/M2) =	0.869E+03	QT (W/M2) =	-0.297E-11
R (M) =	38.25	TSL (K) =	331.9	QB (W/M2) =	0.859E+03	QT (W/M2) =	-0.297E-11
R (M) =	39.99	TSL (K) =	331.9	QB (W/M2) =	0.859E+03	QT (W/M2) =	-0.297E-11
R (M) =	41.73	TSL (K) =	331.9	QB (W/M2) =	0.859E+03	QT (W/M2) =	-0.297E-11
R (M) =	43.46	TSL (K) =	331.9	QB (W/M2) =	0.859E+03	QT (W/M2) =	-0.297E-11
R (M) =	45.20	TSL (K) =	331.9	QB (W/M2) =	0.859E+03	QT (W/M2) =	-0.297E-11
R (M) =	46.94	TSL (K) =	331.9	QB (W/M2) =	0.859E+03	QT (W/M2) =	-0.297E-11
R (M) =	48.68	TSL (K) =	331.9	QB (W/M2) =	0.859E+03	QT (W/M2) =	-0.297E-11
R (M) =	50.42	TSL (K) =	331.9	QB (W/M2) =	0.859E+03	QT (W/M2) =	-0.297E-11

**FIGURE D.10(i) *Continued***

R (M) = 43.46 TSL (K) = 306.0 QB (W/M2) = 0.467E+03 QT (W/M2) = -0.297E-11  
R (M) = 45.20 TSL (K) = 305.3 QB (W/M2) = 0.442E+03 QT (W/M2) = -0.297E-11  
R (M) = 46.94 TSL (K) = 304.7 QB (W/M2) = 0.419E+03 QT (W/M2) = -0.297E-11  
R (M) = 48.68 TSL (K) = 303.7 QB (W/M2) = 0.402E+03 QT (W/M2) = -0.297E-11  
R (M) = 50.42 TSL (K) = 295.4 QB (W/M2) = 0.597E+02 QT (W/M2) = -0.297E-11

TIME (S)= 420.0000 LYR TEMP (K)= 483.7 LYR HT (M) = 6.66  
LYR MASS (KG)=0.949E+04 FIRE OUTPUT (W) = 0.5283E+08 VENT AREA (M2) = 28.20  
LINK = 1 LINK TEMP (K) = 677.18 JET VELOCITY (M/S) = 4.879  
JET TEMP (K) = 677.9 TIME LINK 1 OPENS EQUALS 41.7098 (S)

R (M) = 0.00 TSL (K) = 747.8 QB (W/M2) = 0.129E+05 QT (W/M2) = -0.297E-11  
R (M) = 1.74 TSL (K) = 701.8 QB (W/M2) = 0.120E+05 QT (W/M2) = -0.297E-11  
R (M) = 3.48 TSL (K) = 646.0 QB (W/M2) = 0.108E+05 QT (W/M2) = -0.297E-11  
R (M) = 5.22 TSL (K) = 583.0 QB (W/M2) = 0.920E+04 QT (W/M2) = -0.297E-11  
R (M) = 6.95 TSL (K) = 526.3 QB (W/M2) = 0.764E+04 QT (W/M2) = -0.297E-11  
R (M) = 8.69 TSL (K) = 479.6 QB (W/M2) = 0.625E+04 QT (W/M2) = -0.297E-11  
R (M) = 10.43 TSL (K) = 443.0 QB (W/M2) = 0.510E+04 QT (W/M2) = -0.297E-11  
R (M) = 12.17 TSL (K) = 414.9 QB (W/M2) = 0.419E+04 QT (W/M2) = -0.297E-11  
R (M) = 13.91 TSL (K) = 393.6 QB (W/M2) = 0.347E+04 QT (W/M2) = -0.297E-11  
R (M) = 15.65 TSL (K) = 377.2 QB (W/M2) = 0.292E+04 QT (W/M2) = -0.297E-11  
R (M) = 17.39 TSL (K) = 364.6 QB (W/M2) = 0.249E+04 QT (W/M2) = -0.297E-11  
R (M) = 19.12 TSL (K) = 354.7 QB (W/M2) = 0.214E+04 QT (W/M2) = -0.297E-11  
R (M) = 20.86 TSL (K) = 346.8 QB (W/M2) = 0.187E+04 QT (W/M2) = -0.297E-11  
R (M) = 22.60 TSL (K) = 340.5 QB (W/M2) = 0.165E+04 QT (W/M2) = -0.297E-11  
R (M) = 24.34 TSL (K) = 335.4 QB (W/M2) = 0.147E+04 QT (W/M2) = -0.297E-11  
R (M) = 26.08 TSL (K) = 331.1 QB (W/M2) = 0.132E+04 QT (W/M2) = -0.297E-11  
R (M) = 27.82 TSL (K) = 327.6 QB (W/M2) = 0.119E+04 QT (W/M2) = -0.297E-11  
R (M) = 29.56 TSL (K) = 324.6 QB (W/M2) = 0.108E+04 QT (W/M2) = -0.297E-11  
R (M) = 31.29 TSL (K) = 322.0 QB (W/M2) = 0.994E+03 QT (W/M2) = -0.297E-11  
R (M) = 33.03 TSL (K) = 319.8 QB (W/M2) = 0.916E+03 QT (W/M2) = -0.297E-11  
R (M) = 34.77 TSL (K) = 317.9 QB (W/M2) = 0.849E+03 QT (W/M2) = -0.297E-11  
R (M) = 36.51 TSL (K) = 316.2 QB (W/M2) = 0.790E+03 QT (W/M2) = -0.297E-11  
R (M) = 38.25 TSL (K) = 314.8 QB (W/M2) = 0.737E+03 QT (W/M2) = -0.297E-11  
R (M) = 39.99 TSL (K) = 313.5 QB (W/M2) = 0.691E+03 QT (W/M2) = -0.297E-11  
R (M) = 41.73 TSL (K) = 312.3 QB (W/M2) = 0.650E+03 QT (W/M2) = -0.297E-11  
R (M) = 43.46 TSL (K) = 311.3 QB (W/M2) = 0.613E+03 QT (W/M2) = -0.297E-11  
R (M) = 45.20 TSL (K) = 310.3 QB (W/M2) = 0.580E+03 QT (W/M2) = -0.297E-11  
R (M) = 46.94 TSL (K) = 309.5 QB (W/M2) = 0.549E+03 QT (W/M2) = -0.297E-11  
R (M) = 48.68 TSL (K) = 308.3 QB (W/M2) = 0.525E+03 QT (W/M2) = -0.297E-11  
R (M) = 50.42 TSL (K) = 296.2 QB (W/M2) = 0.820E+02 QT (W/M2) = -0.297E-11

TIME (S)= 480.0000 LYR TEMP (K)= 530.8 LYR HT (M) = 5.94  
LYR MASS (KG)=0.112E+05 FIRE OUTPUT (W) = 0.7059E+08 VENT AREA (M2) = 28.20  
LINK = 1 LINK TEMP (K) = 784.41 JET VELOCITY (M/S) = 5.462  
JET TEMP (K) = 785.2 TIME LINK 1 OPENS EQUALS 41.7098 (S)

R (M) = 0.00 TSL (K) = 837.6 QB (W/M2) = 0.137E+05 QT (W/M2) = -0.297E-11  
R (M) = 1.74 TSL (K) = 789.0 QB (W/M2) = 0.128E+05 QT (W/M2) = -0.297E-11  
R (M) = 3.48 TSL (K) = 732.0 QB (W/M2) = 0.117E+05 QT (W/M2) = -0.297E-11

**FIGURE D.10(i) *Continued***

R (M) = 33.03 TSL (K) = 329.6 QB (W/M2) = 0.117E+04 QT (W/M2) = -0.297E-11  
R (M) = 34.77 TSL (K) = 327.0 QB (W/M2) = 0.109E+04 QT (W/M2) = -0.297E-11  
R (M) = 36.51 TSL (K) = 324.7 QB (W/M2) = 0.101E+04 QT (W/M2) = -0.297E-11  
R (M) = 38.25 TSL (K) = 322.7 QB (W/M2) = 0.944E+03 QT (W/M2) = -0.297E-11  
R (M) = 39.99 TSL (K) = 320.9 QB (W/M2) = 0.886E+03 QT (W/M2) = -0.297E-11  
R (M) = 41.73 TSL (K) = 319.3 QB (W/M2) = 0.833E+03 QT (W/M2) = -0.297E-11  
R (M) = 43.46 TSL (K) = 317.8 QB (W/M2) = 0.786E+03 QT (W/M2) = -0.297E-11  
R (M) = 45.20 TSL (K) = 316.5 QB (W/M2) = 0.743E+03 QT (W/M2) = -0.297E-11  
R (M) = 46.94 TSL (K) = 315.4 QB (W/M2) = 0.705E+03 QT (W/M2) = -0.297E-11  
R (M) = 48.68 TSL (K) = 313.9 QB (W/M2) = 0.673E+03 QT (W/M2) = -0.297E-11  
R (M) = 50.42 TSL (K) = 297.1 QB (W/M2) = 0.108E+03 QT (W/M2) = -0.297E-11

TIME (S) = 540.0000 LYR TEMP (K) = 586.5 LYR HT (M) = 5.20  
LYR MASS (KG) = 0.125E+05 FIRE OUTPUT (W) = 0.9073E+08 VENT AREA (M2) = 28.20  
LINK = 1 LINK TEMP (K) = 915.64 JET VELOCITY (M/S) = 6.041  
JET TEMP (K) = 916.6 TIME LINK 1 OPENS EQUALS 41.7098 (S)

R (M) = 0.00 TSL (K) = 921.9 QB (W/M2) = 0.146E+05 QT (W/M2) = -0.297E-11  
R (M) = 1.74 TSL (K) = 870.2 QB (W/M2) = 0.137E+05 QT (W/M2) = -0.297E-11  
R (M) = 3.48 TSL (K) = 806.7 QB (W/M2) = 0.126E+05 QT (W/M2) = -0.297E-11  
R (M) = 5.22 TSL (K) = 731.6 QB (W/M2) = 0.112E+05 QT (W/M2) = -0.297E-11  
R (M) = 6.95 TSL (K) = 660.0 QB (W/M2) = 0.972E+04 QT (W/M2) = -0.297E-11  
R (M) = 8.69 TSL (K) = 597.0 QB (W/M2) = 0.834E+04 QT (W/M2) = -0.297E-11  
R (M) = 10.43 TSL (K) = 544.2 QB (W/M2) = 0.709E+04 QT (W/M2) = -0.297E-11  
R (M) = 12.17 TSL (K) = 501.5 QB (W/M2) = 0.601E+04 QT (W/M2) = -0.297E-11  
R (M) = 13.91 TSL (K) = 467.5 QB (W/M2) = 0.511E+04 QT (W/M2) = -0.297E-11  
R (M) = 15.65 TSL (K) = 440.7 QB (W/M2) = 0.437E+04 QT (W/M2) = -0.297E-11  
R (M) = 17.39 TSL (K) = 419.5 QB (W/M2) = 0.377E+04 QT (W/M2) = -0.297E-11  
R (M) = 19.12 TSL (K) = 402.6 QB (W/M2) = 0.329E+04 QT (W/M2) = -0.297E-11  
R (M) = 20.86 TSL (K) = 389.0 QB (W/M2) = 0.290E+04 QT (W/M2) = -0.297E-11  
R (M) = 22.60 TSL (K) = 378.0 QB (W/M2) = 0.257E+04 QT (W/M2) = -0.297E-11  
R (M) = 24.34 TSL (K) = 368.9 QB (W/M2) = 0.230E+04 QT (W/M2) = -0.297E-11  
R (M) = 26.08 TSL (K) = 361.4 QB (W/M2) = 0.207E+04 QT (W/M2) = -0.297E-11  
R (M) = 27.82 TSL (K) = 355.0 QB (W/M2) = 0.188E+04 QT (W/M2) = -0.297E-11  
R (M) = 29.56 TSL (K) = 349.7 QB (W/M2) = 0.172E+04 QT (W/M2) = -0.297E-11  
R (M) = 31.29 TSL (K) = 345.1 QB (W/M2) = 0.158E+04 QT (W/M2) = -0.297E-11  
R (M) = 33.03 TSL (K) = 341.1 QB (W/M2) = 0.146E+04 QT (W/M2) = -0.297E-11  
R (M) = 34.77 TSL (K) = 337.7 QB (W/M2) = 0.136E+04 QT (W/M2) = -0.297E-11  
R (M) = 36.51 TSL (K) = 334.7 QB (W/M2) = 0.126E+04 QT (W/M2) = -0.297E-11  
R (M) = 38.25 TSL (K) = 332.0 QB (W/M2) = 0.118E+04 QT (W/M2) = -0.297E-11  
R (M) = 39.99 TSL (K) = 329.6 QB (W/M2) = 0.111E+04 QT (W/M2) = -0.297E-11  
R (M) = 41.73 TSL (K) = 327.5 QB (W/M2) = 0.104E+04 QT (W/M2) = -0.297E-11  
R (M) = 43.46 TSL (K) = 325.6 QB (W/M2) = 0.986E+03 QT (W/M2) = -0.297E-11  
R (M) = 45.20 TSL (K) = 323.9 QB (W/M2) = 0.933E+03 QT (W/M2) = -0.297E-11  
R (M) = 46.94 TSL (K) = 322.4 QB (W/M2) = 0.885E+03 QT (W/M2) = -0.297E-11  
R (M) = 48.68 TSL (K) = 320.7 QB (W/M2) = 0.844E+03 QT (W/M2) = -0.297E-11  
R (M) = 50.42 TSL (K) = 298.2 QB (W/M2) = 0.138E+03 QT (W/M2) = -0.297E-11

TIME (S) = 600.0000 LYR TEMP (K) = 649.9 LYR HT (M) = 4.57

**FIGURE D.10(i) Continued**

R (M) =	22.60	TSL (K) =	398.6	QB (W/M2) =	0.272E+04	QT (W/M2) =	-0.297E-11
R (M) =	24.34	TSL (K) =	387.6	QB (W/M2) =	0.245E+04	QT (W/M2) =	-0.297E-11
R (M) =	26.08	TSL (K) =	378.4	QB (W/M2) =	0.223E+04	QT (W/M2) =	-0.297E-11
R (M) =	27.82	TSL (K) =	370.6	QB (W/M2) =	0.203E+04	QT (W/M2) =	-0.297E-11
R (M) =	29.56	TSL (K) =	364.0	QB (W/M2) =	0.187E+04	QT (W/M2) =	-0.297E-11
R (M) =	31.29	TSL (K) =	358.4	QB (W/M2) =	0.172E+04	QT (W/M2) =	-0.297E-11
R (M) =	33.03	TSL (K) =	353.5	QB (W/M2) =	0.160E+04	QT (W/M2) =	-0.297E-11
R (M) =	34.77	TSL (K) =	349.2	QB (W/M2) =	0.149E+04	QT (W/M2) =	-0.297E-11
R (M) =	36.51	TSL (K) =	345.4	QB (W/M2) =	0.139E+04	QT (W/M2) =	-0.297E-11
R (M) =	38.25	TSL (K) =	342.1	QB (W/M2) =	0.130E+04	QT (W/M2) =	-0.297E-11
R (M) =	39.99	TSL (K) =	339.2	QB (W/M2) =	0.123E+04	QT (W/M2) =	-0.297E-11
R (M) =	41.73	TSL (K) =	336.5	QB (W/M2) =	0.116E+04	QT (W/M2) =	-0.297E-11
R (M) =	43.46	TSL (K) =	334.1	QB (W/M2) =	0.109E+04	QT (W/M2) =	-0.297E-11
R (M) =	45.20	TSL (K) =	332.0	QB (W/M2) =	0.104E+04	QT (W/M2) =	-0.297E-11
R (M) =	46.94	TSL (K) =	330.1	QB (W/M2) =	0.986E+03	QT (W/M2) =	-0.297E-11
R (M) =	48.68	TSL (K) =	328.0	QB (W/M2) =	0.941E+03	QT (W/M2) =	-0.297E-11
R (M) =	50.42	TSL (K) =	299.4	QB (W/M2) =	0.147E+03	QT (W/M2) =	-0.297E-11

**FIGURE D.10(i) Continued**

#### **D.11 References for Annex D.**

- (1) David A. Purser, "Toxicity Assessment of Combustion Products," Section 2/Chapter 8, in *The SFPE Handbook of Fire Protection Engineering*, 2nd edition, Society of Fire Protection Engineers and National Fire Protection Association, 1995.
- (2) Robert D. Peacock et al., *Software User's Guide for the Hazard I Fire Hazard Assessment Method, Version 1.1*, NIST Handbook 146, Volume I, United States Department of Commerce, National Institute of Standards and Technology, 1991.
- (3) Leonard Y. Cooper and William D. Davis, *Estimating the Environment and the Response of Sprinkler Links in Compartment Fires with Draft Curtains and Fusible Link-Actuated Ceiling Vents — Part II: User Guide for the Computer Code Lavent*, NISTIR 89-4122, United States Department of Commerce, National Institute of Standards and Technology, July 1989.

## **Annex E Predicting the Rate of Heat Release of Fires**

*This annex is not a part of the requirements of this NFPA document but is included for informational purposes only.*

### **E.1 Introduction.**

Annex E presents techniques for estimating the heat release rate of various fuel arrays

likely to be present in buildings where smoke and heat venting is a potential fire safety provision. This annex primarily addresses the estimation of fuel concentrations found in storage and manufacturing locations. NFPA 92B, *Guide for Smoke Management Systems in Malls, Atria, and Large Areas*, addresses the types of fuel arrays more common to the types of building situations covered by that guide.

This standard is applicable to situations in which the hot layer does not enhance the burning rate. The methods provided in this annex for estimating the rate of heat release, therefore, are based on “free burning” conditions in which no ceiling or hot gas layer effects are involved. It is assumed, therefore, that the burning rate is relatively unaffected by the hot layer.

## **E.2 Sources of Data.**

The following sources of data appear in their approximate order of priority, given equal quality of data acquisition:

- (1) Actual tests of the array involved
- (2) Actual tests of similar arrays
- (3) Algorithms derived from tests of arrays having similar fuels and dimensional characteristics
- (4) Calculations based on tested properties and materials and expected flame flux
- (5) Mathematical models of fire spread and development

## **E.3 Actual Tests of the Array Involved.**

Where an actual calorific test of the specific array under consideration has been conducted and the data are in a form that can be expressed as rate of heat release, the data can be used as input for the methods in this standard. Because actual test data seldom produce the steady state assumed for a limited-growth fire or the square-of-time growth assumed for a continuous-growth fire, engineering judgment is usually needed to derive the actual input necessary if either of these approaches is used. If LAVENT or another computer model capable of responding to a rate of heat release versus time curve is used, the data can be used directly. Currently there is a listing of limited information from tests of specific arrays. Some test data can be found in technical reports. Alternatively, individual tests can be conducted.

Many fire tests do not include a direct measurement of rate of heat release. In some cases, that measure can be derived, based on measurement of mass loss rate using the following equation:

$$(E.1) \quad Q = m(h_c)$$

where:

$Q$  = total heat release rate (kW)

$m$  = mass loss rate (kg/s)

$h_c$  = heat of combustion (kJ/kg)

In other cases, a direct measurement can be derived based on measurement of flame height above the base of the fire as follows:

$$(E.2) \quad Q = 37(L + 1.02D)^{5/2}$$

where:

$Q$  = total heat release rate (kW)

$L$  = mean flame height above the base of the fire (m)

$D$  = base diameter of the fire (m)

#### E.4 Actual Tests of Arrays Similar to That Involved.

Where an actual calorific test of the specific array under consideration cannot be found, it might be possible to find data on one or more tests that are similar to the fuel of concern in important matters such as type of fuel, arrangement, or ignition scenario. The more the actual tests are similar to the fuel of concern, the higher is the confidence that can be placed in the derived rate of heat release. Added engineering judgment, however, might be needed to adjust the test data to that approximating the fuel of concern. If the rate of heat release has not been measured directly, it can be estimated using the methods provided in Section E.3.

#### E.5 Algorithms Derived from Tests of Arrays Having Similar Fuels and Dimensional Characteristics.

**E.5.1 Pool Fires.** In many cases, the rate of heat release of a tested array has been divided by a common dimension, such as occupied floor area, to derive a normalized rate of heat release per unit area. The rate of heat release of pool fires is the best documented and accepted algorithm in this class.

An equation for the mass release rate from a pool fire is as follows [Babrauskas 1995]:

$$(E.3) \quad \dot{m}'' = \dot{m}_{\infty}'' (1 - e^{-(k_e \beta) D})$$

The variables  $\dot{m}_{\infty}''$  and  $(k_e \beta) D$  for Equation E.3 are as shown in Table E.5.1.

**Table E.5.1 Data for Large Pool Burning Rate Estimates**

Material	Density (kg/m <sup>3</sup> )	$h_c$ (MJ/kg)	$\dot{m}_{\infty}''$
Cryogenics <sup>a</sup>			
Liquid H <sub>2</sub>	70	120.0	0.017
LNG (mostly CH <sub>4</sub> )	415	50.0	0.078
LPG (mostly C <sub>3</sub> H <sub>8</sub> )	585	46.0	0.099
Alcohols			
Methanol (CH <sub>3</sub> OH)	796	20.0	0.017

Ethanol (C <sub>2</sub> H <sub>5</sub> OH)	794	26.8	0.015
Simple organic fuels			
Butane (C <sub>4</sub> H <sub>10</sub> )	573	45.7	0.078
Benzene (C <sub>6</sub> H <sub>6</sub> )	874	40.1	0.085
Hexane (C <sub>6</sub> H <sub>14</sub> )	650	44.7	0.074
Heptane (C <sub>7</sub> H <sub>16</sub> )	675	44.6	0.101
Xylene (C <sub>8</sub> H <sub>10</sub> )	870	40.8	0.090
Acetone (C <sub>3</sub> H <sub>6</sub> O)	791	25.8	0.041
Dioxane (C <sub>4</sub> H <sub>8</sub> O <sub>2</sub> )	1035	26.2	0.018 <sup>b</sup>
Diethyl ether (C <sub>4</sub> H <sub>10</sub> O)	714	34.2	0.085
Petroleum products			
Benzine	740	44.7	0.048
Gasoline	740	43.7	0.055
Kerosene	820	43.2	0.039
JP-4	760	43.5	0.051
JP-5	810	43.0	0.054
Transformer oil, hydrocarbon	760	46.4	0.039 <sup>b</sup>
Fuel oil, heavy	940–1000	39.7	0.035
Crude oil	830–880	42.5–42.7	0.022–0.045
Solids			
Polymethylmethacrylate (C <sub>5</sub> H <sub>8</sub> O <sub>2</sub> ) <sub>n</sub>	1184	24.9	0.020
⇒ Polypropylene (C <sub>3</sub> H <sub>6</sub> ) <sub>n</sub>	905	43.2	0.018
Polystyrene (C <sub>8</sub> H <sub>8</sub> ) <sub>n</sub>	1050	39.7	0.034

<sup>a</sup> For pools on dry land, not over water.

<sup>b</sup> Estimate is uncertain, since only two data points are available.

<sup>c</sup> Value is independent of the diameter in a turbulent regimen.

The mass rates derived from Equation E.3 are converted to rates of heat release using Equation E.1 and the heat of combustion,  $h_c$ , from Table E.5.1. The rate of heat release per unit area times the area of the pool yields heat release data for the anticipated fire.

**E.5.2 Other Normalized Data.** Other data based on burning rate per unit area in tests have been developed. Table E.5.2(a) and Table E.5.2(b) list these data.

**Table  
E.5.2(a)  
Unit Heat  
Release  
Rates for  
Fuels  
Burning in  
the Open**

Com modit y	Heat Releas e Rate (kW)
-------------------	----------------------------------

Wood  
 or  
 PMM  
 A\*  
 (vertical)  
 0.61 100/m  
 m of  
 height width  
 1.83 240/m  
 m of  
 height width  
 2.44 620/m  
 m of  
 height width  
 3.66 1000/  
 m m of  
 height width

Wood  
 or  
 PMM  
 A  
 Top 720/m  
 of <sup>2</sup> of  
 horizontal surface  
 surface

Solid  
 polystyrene  
 (vertical)  
 0.61 220/m  
 m of  
 height width  
 1.83 450/m  
 m of  
 height width  
 2.44 1400/  
 m m of  
 height width  
 3.66 2400/  
 m m of  
 height width  
 Solid 1400/  
 polystyrene m<sup>2</sup> of  
 (horizontal) surface

Solid  
 polypropylene  
 (vertical)

0.61	220/m
m	of
height	width
1.83	350/m
m	of
height	width
2.44	970/m
m	of
height	width
3.66	1600/
m	m of
height	width
Solid	800/m
polypr	<sup>2</sup> of
opylen	surfac
e	e
(horiz	
ontal)	

---

\*  
 PMMA  
 =  
 polymet  
 hyl  
 methacr  
 ylate  
 (Plexigl  
 as,  
 Lucite,  
 acrylic).

**Table  
 E.5.2(b)  
 Unit Heat  
 Release  
 Rate for  
 Commoditie  
 s**

---

<b>Com    modit    y</b>	<b>Heat    Releas    e Rate    (kW    per m  <sup>2</sup> of    floor    area)*</b>
----------------------------------	---

---

Wood 1,420  
pallets,  
stacked  
0.46  
m high  
(6%–  
12%  
moisture)

Wood 4,000  
pallets,  
stacked  
1.52  
m high  
(6%–  
12%  
moisture)

Wood 6,800  
pallets,  
stacked  
3.05  
m high  
(6%–  
12%  
moisture)

Wood 10,200  
pallets,  
stacked  
4.88  
m high  
(6%–  
12%  
moisture)

Mail 400  
bags,  
filled,  
stored  
1.52 m  
high

Carton 1,700  
s,  
compartmented,  
stacked  
4.5  
m high

PE	8,500
letter	
trays,	
filled,	
stacke	
d 1.5	
m high	
on cart	
PE	2,000
trash	
barrels	
in	
carton	
s,	
stacke	
d 4.5	
m high	
PE	1,400
fibergl	
ass	
showe	
r stalls	
in	
carton	
s,	
stacke	
d 4.6	
m high	
FRP	6,200
bottles	
packed	
in	
carton	
s,	
stacke	
d 4.6	
m high	
PE	2,000
bottles	
in	
carton	
s,	
stacke	
d 4.5	
m high	
PU	1,900
insulat	
ion	
board,	
rigid	
foam,	
stacke	
d 4.6	
m high	

FRP 14,200  
jars  
packed  
in  
carton  
s,  
stacke  
d 4.6  
m high  
PS 5,400  
tubs  
nested  
in  
carton  
s,  
stacke  
d 4.2  
m high  
PS toy 2,000  
parts  
in  
carton  
s,  
stacke  
d 4.5  
m high  
PS 3,300  
insulat  
ion  
board,  
rigid  
foam,  
stacke  
d 4.2  
m high  
FRP 3,400  
bottles  
packed  
in  
carton  
s,  
stacke  
d 4.6  
m high  
FRP 4,400  
tubs  
packed  
in  
carton  
s,  
stacke  
d 4.6  
m high

PP and PE  
film in  
rolls,  
stacked  
4.1 m high  
Methyl  
alcohol  
Gasoline  
Kerosene  
Fuel oil, no. 2

6,200
600
2,500
1,700
1,700

---

Note:  
PE =  
polyethy  
lene; PP  
=  
polypro  
pylene;  
PS =  
polystyr  
ene; PU  
=  
polyuret  
hane;  
FRP =  
fiberglas  
s-  
reinforc  
ed  
polyeste  
r.  
\* Heat  
release  
rate per  
unit  
floor  
area of  
fully  
involved  
combust  
ibles,  
based on  
negligibl  
e  
radiative  
feedbac  
k from  
the  
surround  
ings and  
100  
percent  
combust  
ion  
efficienc  
y.

**E.5.3 Other Useful Data.** Examples of other data that are not normalized but that might be useful in developing the rate of heat release curve are included in Table E.5.3(a) through Table E.5.3(d).

---

**Table E.5.3(a) Characteristics of Ignition Sources**

Fuel	Typical Heat Output (W)	Burn Time <sup>a</sup> (s)	Maximum Flame Height (mm)
Cigarette 1.1 g (not puffed, laid on solid surface)			—
Bone dry	5	1,200	
Conditioned to 50% relative humidity	5	1,200	—
Methenamine pill, 0.15 g	45	90	—
Match, wooden (laid on solid surface)	80	20–30	30
Wood cribs, BS 5852 Part 2			
No. 4 crib, 8.5 g	1,000	190	
No. 5 crib, 17 g	1,900	200	
No. 6 crib, 60 g	2,600	190	
No. 7 crib, 126 g	6,400	350	
Crumpled brown lunch bag, 6 g	1,200	80	
Crumpled wax paper, 4.5 g (tight)	1,800	25	
Crumpled wax paper, 4.5 g (loose)	5,300	20	
Folded double-sheet newspaper, 22 g (bottom ignition)	4,000	100	
Crumpled double-sheet newspaper, 22 g (top ignition)	7,400	40	
Crumpled double-sheet newspaper, 22 g (bottom ignition)	17,000	20	
Polyethylene wastebasket, 285 g, filled with 12 milk cartons (390 g)	50,000	200 <sup>b</sup>	550
Plastic trash bags, filled with cellulosic trash (1.2–14 kg) <sup>e</sup>	120,000 to 50,000	200 <sup>b</sup>	200

<sup>a</sup> Time duration of significant flaming.

<sup>b</sup> Total burn time in excess of 1800 seconds.

<sup>c</sup> As measured on simulation burner.

<sup>d</sup> Measured from 25 mm away.

<sup>e</sup> Results vary greatly with packing density.

**Table E.5.3(b) Characteristics of Typical Furnishings as Ignition Sources**

Fuel	Total Mass (kg)	Total Heat Content (MJ)	Maximum Rate of Heat Release (kW)
Wastepaper basket	0.73–1.04	0.7–7.3	4–18
Curtains, velvet/cotton	1.9	24	160–240
Curtains, acrylic/cotton	1.4	15–16	130–150

TV set	27–33	145–150	120–290
Chair mockup	1.36	21–22	63–66
Sofa mockup	2.8	42	130
Arm chair	26	18	160
Christmas tree, dry	6.5–7.4	11–41	500–650

\*Measured at approximately 2 m from the burning object.

**Table  
E.5.3(c)  
Maximum  
Heat  
Release  
Rates from  
Fire  
Detection  
Institute  
Analysis**

<b>Fuel</b>	<b>Approximate Value (kW)</b>
Medium wastebasket with milk cartons	100
Large barrel with milk cartons	140
Upholstered chair with polyurethane foam	350
Latex foam mattress (heat at room door)	1200

Furnis 4000–  
hed 8000  
living  
room  
(heat  
at  
open  
door)

**Table E.5.3(d) Mass Loss and Heat Release Rates of Chairs**

Specimen	Mass (kg)	Mass Combustible (kg)	Style	Frame	Padding	Fabric	Im
C12	17.9	17.0	Traditional easy chair	Wood	Cotton	Nylon	
F22	31.9		Traditional easy chair	Wood	Cotton (FR)	Cotton	
F23	31.2		Traditional easy chair	Wood	Cotton (FR)	Olefin	
F27	29.0		Traditional easy chair	Wood	Mixed	Cotton	
F28	29.2		Traditional easy chair	Wood	Mixed	Cotton	
CO2	13.1	12.2	Traditional easy chair	Wood	Cotton, PU	Olefin	
CO3	13.6	12.7	Traditional easy chair	Wood	Cotton, PU	Cotton	
CO1	12.6	11.7	Traditional easy chair	Wood	Cotton, PU	Cotton	
CO4	12.2	11.3	Traditional easy chair	Wood	PU	Nylon	
C16	19.1	18.2	Traditional easy chair	Wood	PU	Nylon	N
F25	27.8		Traditional easy chair	Wood	PU	Olefin	
T66	23.0		Traditional easy chair	Wood	PU, polyester	Cotton	
F21	28.3		Traditional easy chair	Wood	PU (FR)	Olefin	
F24	28.3		Traditional easy chair	Wood	PU (FR)	Cotton	
C13	19.1	18.2	Traditional easy chair	Wood	PU	Nylon	N
C14	21.8	20.9	Traditional easy chair	Wood	PU	Olefin	N
C15	21.8	20.9	Traditional easy chair	Wood	PU	Olefin	N
T49	15.7		Easy chair	Wood	PU	Cotton	
F26	19.2		Thinner easy chair	Wood	PU (FR)	Olefin	
F33	39.2		Traditional loveseat	Wood	Mixed	Cotton	
F31	40.0		Traditional loveseat	Wood	PU (FR)	Olefin	

F32	51.5		Traditional sofa	Wood	PU (FR)	Olefin
T57	54.6		Loveseat	Wood	PU, cotton	PVC
T56	11.2		Office chair	Wood	Latex	PVC
CO9/T64	16.6	16.2	Foam block chair	Wood (part)	PU, polyester	PU
CO7/T48	11.4	11.2	Modern easy chair	PS foam	PU	PU
C10	12.1	8.6	Pedestal chair	Rigid PU foam	PU	PU
C11	14.3	14.3	Foam block chair		PU	Nylon
F29	14.0		Traditional easy chair	PP foam	PU	Olefin
F30	25.2		Traditional easy chair	Rigid PU foam	PU	Olefin
CO8	16.3	15.4	Pedestal swivel chair	Molded PE	PU	PVC
CO5	7.3	7.3	Bean bag chair		Polystyrene	PVC
CO6	20.4	20.4	Frameless foam back chair		PU	Acrylic
T50	16.5		Waiting room chair	Metal	Cotton	PVC
T53	15.5	1.9	Waiting room chair	Metal	PU	PVC
T54	27.3	5.8	Metal frame loveseat	Metal	PU	PVC
T75/F20	7.5(4)	2.6	Stacking chairs (4)	Metal	PU	PVC

<sup>a</sup> Estimated from mass loss records and assumed  $Wh_c$ .

<sup>b</sup> Estimated from doorway gas concentrations.

## E.6 Calculated Fire Description Based on Tested Properties.

**E.6.1 Background.** It is possible to make general estimates of the rate of heat release of burning materials based on the fire properties of that material. The fire properties involved are determined by small-scale tests. The most important of these tests are the calorimeter tests involving both oxygen depletion calorimetry and the application of external heat flux to the sample while determining time to ignition, rate of mass release, and rate of heat release for the specific applied flux. Most prominent of the current test apparatus are the cone calorimeter (ASTM E 1354, *Standard Test Method for Heat and Visible Smoke Release Rates for Materials and Products Using an Oxygen Consumption Calorimeter*) and the Factory Mutual Fire Propagation Apparatus [ASTM E 2058, *Standard Test Methods for Measurement of Synthetic Polymer Material Flammability Using a Fire Propagation Apparatus (FPA)*].

In addition to the directly measured properties, it is possible to derive ignition temperature, critical ignition flux, effective thermal inertia ( $kPc$ ), heat of combustion, and heat of gasification based on results from these calorimeters. Properties not derivable from these calorimeters and essential to determining flame spread in directions not concurrent with the flow of the flame can be obtained from the LIFT (lateral ignition and flame travel) apparatus (ASTM E 1321, *Standard Test Method for Determining Material Ignition and Flame Spread Properties*).

This section presents a concept of the use of fire property test data as the basis of an analytical evaluation of the rate of heat release involved in the use of a tested material. The approach outlined in this section is based on that presented by Nelson and Forssell [1994].

**E.6.2 Discussion of Measured Properties.** Table E.6.2(a) lists the type of fire properties obtainable from the cone calorimeter ( NFPA 287, *Standard Test Methods for Measurement of Flammability of Materials in Cleanrooms Using a Fire Propagation Apparatus*), the Factory Mutual Fire Propagation Apparatus (ASTM E 2058), and similar instruments.

**Table E.6.2(a) Relation of Calorimeter-Measured Properties to Fire Analysis**

Property	Ignition	Flame Spread	Fire Size (energy)
Rate of heat release <sup>1</sup>		X	X
Mass loss <sup>1</sup>			X
Time to ignition <sup>1</sup>	X	X	
Effective thermal properties <sup>2</sup>	X	X	
Heat of combustion <sup>2</sup>		X	X
Heat of gasification <sup>2</sup>			X
Critical ignition flux <sup>2</sup>	X	X	
Ignition temperature <sup>2</sup>	X	X	

---

<sup>1</sup> Property is a function of the externally applied incident flux.

<sup>2</sup> Derived properties from calorimeter measurements.

In Table E.6.2(a), the rate of heat release, mass loss, and time to ignition are functions of the externally applied incident radiant heat flux imposed on the tested sample. The purpose of the externally applied flux is to simulate the fire environment surrounding a burning item.

In general, it can be estimated that a free-burning fuel package (i.e., one that burns in the open and is not affected by energy feedback from a hot gas layer of a heat source other than its own flame) is impacted by a flux in the range of 25 kW/m<sup>2</sup> to 50 kW/m<sup>2</sup>. If the fire is in a space and conditions are approaching flashover, the flux can increase to the range of 50 kW/m<sup>2</sup> to 75 kW/m<sup>2</sup>. In a fully developed, postflashover fire, a range of 75 kW/m<sup>2</sup> to greater than 100 kW/m<sup>2</sup> can be expected. The following is a discussion of the individual properties measured or derived and the usual form used to report the property.

*Rate of Heat Release.* The rate of heat release is determined by oxygen depletion calorimetry. Each test is run at a user-specific incident flux, either for a predetermined period of time or until the sample is consumed. The complete results are presented in the form of a plot of heat release rate versus time, with the level of applied flux noted. In some cases, the rate of heat release for several tests of the same material at different levels of applied flux is plotted on a single curve for comparison. Figure E.6.2 is an example of such a plotting.

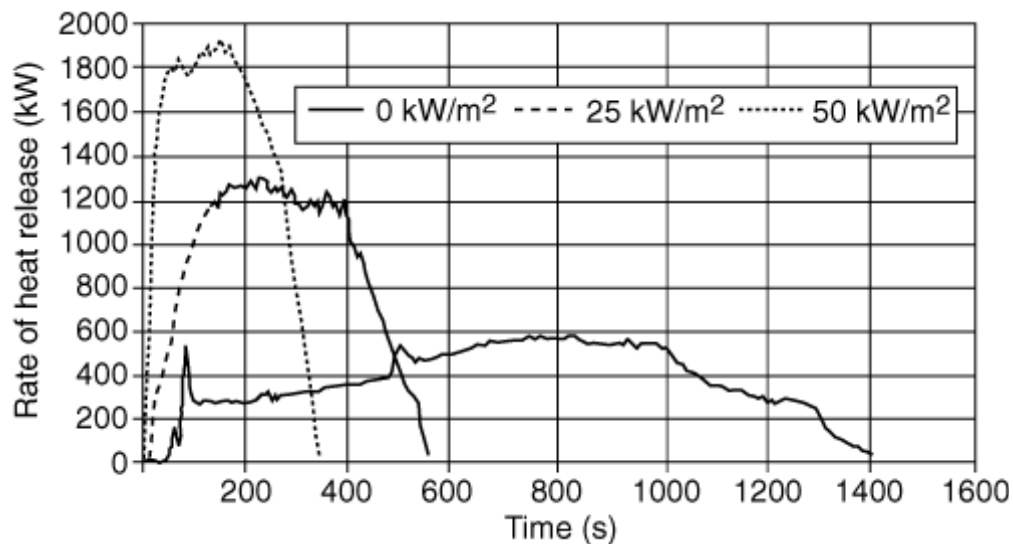


**FIGURE E.6.2 Typical Graphic Output of Cone Calorimeter Test.**

Often only the peak rate of heat release at a specific flux is reported. Table E.6.2(b) is an example.

**Table E.6.2(b) Average  
Maximum Heat Release Rates**

---

<b>(kW/m<sup>2</sup>)</b>				
<b>Material</b>	<b>Orientation</b>	<b>25</b>	<b>50</b>	<b>75</b>
		<b>kW/m<sup>2</sup></b>	<b>kW/m<sup>2</sup></b>	<b>kW/m<sup>2</sup></b>
		<b>Exposing Flux</b>	<b>Exposing Flux</b>	<b>Exposing Flux</b>
PMM A	Horizontal	650	900	1300
	Vertical	560	720	1300
Pine	Horizontal	140	240	265
	Vertical	130	170	240
Sample A	Horizontal	125	200	250
	Vertical	90	130	220
Sample B	Horizontal	140	175	240
	Vertical	60	200	330
Sample C	Horizontal	—	215	250
	Vertical	—	165	170
Sample D	Horizontal	70	145	145
	Vertical	—	125	125

*Mass Loss Rate.* Mass loss rate is determined by a load cell. The method of reporting is identical to that for rate of heat release. In the typical situation in which the material has a consistent heat of combustion, the curves for mass loss rate and rate of heat release are similar in shape.

*Time to Ignition.* Time to ignition is reported for each individual test and applied flux level conducted.

*Effective Thermal Inertia ( $k\rho c$ ).* Effective thermal inertia is a measurement of the heat rise response of the tested material to the heat flux imposed on the sample. It is derived at the time of ignition and is based on the ratio of the actual incident flux to the critical ignition flux and the time to ignition. A series of tests at different levels of applied flux is necessary to derive the effective thermal inertia. Effective thermal inertia derived in this manner can differ from, and be preferable to, handbook data for the values of  $k$ ,  $\rho$ , and  $c$  that are derived without a fire.

*Heat of Combustion.* Heat of combustion is derived by dividing the measured rate of heat release by the measured mass loss rate. It is normally reported as a single value, unless the sample is a composite material and the rates of heat release and mass loss vary significantly with time and exposure.

*Heat of Gasification.* Heat of gasification is the flux needed to pyrolyze a unit mass of fuel. It is derived as a heat balance and is usually reported as a single value in terms of the amount of energy per unit mass of material released (e.g., kJ/g).

*Critical Ignition Flux.* Critical ignition flux is the minimum level of incident flux on the sample needed to ignite the sample, given an unlimited time of application. At incident flux levels less than the critical ignition flux, ignition does not take place.

*Ignition Temperature.* Ignition temperature of a sample is the surface temperature at which flame occurs. This sample material value is independent of the incident flux and is derivable from the calorimeter tests, the LIFT apparatus test, and other tests. It is derived from the time to ignite in a given test, the applied flux in that test, and the effective thermal inertia of the sample. It is reported at a single temperature. If the test includes a pilot flame or spark, the reported temperature is for piloted ignition; if there is no pilot present, the temperature is for auto-ignition. Most available data are for piloted ignition.

**E.6.3 Ignition.** Equations for time to ignition,  $t_{ig}$ , are given for both thermally thin and thermally thick materials, defined as follows. For materials of intermediate depth, estimates for  $t_{ig}$  necessitate considerations beyond the scope of this presentation [Drysdale 1985, Carslaw and Jaeger 1959].

*Thermally Thin Materials.* Relative to ignition from a constant incident heat flux,  $\dot{q}''_i$ , at the exposed surface and with relatively small heat transfer losses at the unexposed surface, a thermally thin material is one whose temperature is relatively uniform throughout its entire thickness,  $l$ , at  $t = t_{ig}$ . For example, at  $t = t_{ig}$ :

$$(E.4) \quad T_{exposed} - T_{unexposed} = T_{ig} - T_{unexposed} < 0.1(T_{ig} - T_o)$$

Equation E.4 can be used to show that a material is thermally thin [Carslaw and Jaeger 1959] where:

$$(E.5) \quad l < 0.6 (t_{ig} \alpha)^{1/2}$$

For example, for sheets of maple or oak wood (where the thermal diffusivity  $\alpha = 1.28 \times 10^{-7} \text{ m}^2/\text{s}$  [DiNenno et al. 1995]), if  $t_{ig} = 35 \text{ s}$  is measured in a piloted ignition test, then, according to Equation E.5, if the sample thickness is less than approximately 0.0013 m, the unexposed surface of the sample can be expected to be relatively close to  $T_{ig}$  at the time of ignition, and the sample is considered to be thermally thin.

The time to ignition of a thermally thin material subjected to incident flux above a critical incident flux is

$$(E.6) \quad t_{ig} = \rho c l \frac{(T_{ig} - T_o)}{\dot{q}''_i}$$

*Thermally Thick Materials.* Relative to the type of ignition test described for thermally thin

materials, a sample of a material of a thickness,  $l$ , is considered to be thermally thick if the increase in temperature of the unexposed surface is relatively small compared to that of the exposed surface at  $t = t_{ig}$ . For example, at  $t = t_{ig}$ ,

$$(E.7) \quad T_{unexposed} - T_o < 0.1(T_{exposed} - T_o) = 0.1(T_{ig} - T_o)$$

Equation E.7 can be used to show that a material is thermally thick [Carslaw and Jaeger 1959] where:

$$(E.8) \quad l > 2(t_{ig} \alpha)^{1/2}$$

For example, according to Equation E.8, in the case of an ignition test on a sheet of maple or oak wood, if  $t_{ig} = 35$  s is measured in a piloted ignition test and if the sample thickness is greater than approximately 0.0042 m, the unexposed surface of the sample can be expected to be relatively close to  $T_o$  at the time of ignition, and the sample is considered to be thermally thick.

Time to ignition of a thermally thick material subjected to incident flux above a critical incident flux is

$$(E.9) \quad t_{ig} = \frac{\pi}{4} k \rho c \left( \frac{T_{ig} - T_o}{\dot{q}_i''} \right)^2$$

It should be noted that a particular material is not intrinsically thermally thin or thick (i.e., the characteristic of being thermally thin or thick is not a material characteristic or property) but rather depends on the thickness of the particular sample (i.e., a particular material can be implemented in either a thermally thick or a thermally thin configuration).

*Propagation between Separate Fuel Packages.* Where the concern is for propagation between individual, separated fuel packages, incident flux can be calculated using traditional radiation heat transfer procedures [Tien et al. 1995].

The rate of radiation heat transfer from a flaming fuel package of total energy release rate,  $Q$ , to a facing surface element of an exposed fuel package can be estimated from the following equation:

$$(E.10) \quad \dot{q}_i'' = \frac{X_r}{4\pi r^2}$$

**E.6.4 Estimating Rate of Heat Release.** As discussed in E.6.2, tests have demonstrated that the energy feedback from a burning fuel package ranges from approximately 25 kW/m<sup>2</sup> to 50 kW/m<sup>2</sup>. For a reasonably conservative analysis, it is recommended that test data developed with an incident flux of 50 kW/m<sup>2</sup> be used. For a first-order approximation, it should be assumed that all of the surfaces that can be simultaneously involved in burning are releasing energy at a rate equal to that determined by testing the material in a fire properties calorimeter with an incident flux of 50 kW/m<sup>2</sup> for a free-burning material and

75 kW/m<sup>2</sup> to 100 kW/m<sup>2</sup> for postflashover conditions.

In making this estimate, it is necessary to assume that all surfaces that can “see” an exposing flame (or superheated gas, in the postflashover condition) are burning and releasing energy and mass at the tested rate. If sufficient air is present, the rate of heat release estimate is then calculated as the product of the exposed area and the rate of heat release per unit area as determined in the test calorimeter. Where test data are taken at the incident flux of the exposing flame, the tested rate of heat release should be used. Where the test data are for a different incident flux, the burning rate should be estimated using the heat of gasification as expressed in Equation E.11 to calculate the mass burning rate per unit area.

$$\dot{m}'' = \frac{\dot{q}_i''}{h_g}$$

(E.11)

The resulting mass loss rate is then multiplied by the derived effective heat of combustion and the burning area exposed to the incident flux to produce the estimated rate of heat release:

$$Q = \dot{m}'' h_c A$$

(E.12)

**E.6.5 Flame Spread.** If it is desired to predict the growth of fire as it propagates over combustible surfaces, it is necessary to estimate flame spread. The computation of flame spread rates is an emerging technology still in an embryonic stage. Predictions should be considered as order of magnitude estimates.

Flame spread is the movement of the flame front across the surface of a material that is burning (or exposed to an ignition flame) but whose exposed surface is not yet fully involved. Physically, flame spread can be treated as a succession of ignitions resulting from the heat energy produced by the burning portion of a material, its flame, and any other incident heat energy imposed on the unburned surface. Other sources of incident energy include another burning object, high-temperature gases that can accumulate in the upper portion of an enclosed space, and the radiant heat sources used in a test apparatus such as the cone calorimeter or the LIFT mechanism.

For analysis purposes, flame spread can be divided into the following two categories:

- (1) Concurrent, or wind-aided, flame spread, which moves in the same direction as the flame
- (2) Lateral, or opposed, flame spread, which moves in any other direction

Concurrent flame spread is assisted by the incident heat flux from the flame to unignited portions of the burning material. Lateral flame spread is not so assisted and tends to be much slower in progression unless an external source of heat flux is present. Concurrent flame spread for thermally thick materials can be expressed as follows:

$$V = \frac{(\dot{q}_i'')^2 L_f}{k\rho c (T_{ig} - T_s)^2}$$

(E.13)

The values for  $k\rho c$  and ignition temperature are calculated from the cone calorimeter as discussed. For this equation, the flame length,  $L_f$  is measured from the leading edge of the burning region, and  $T_s$  is the initial temperature of the solid material.

**E.6.6 Classification of Fires for Engineering Equations.** The engineering equations in Chapter 8 are appropriate for steady fires, limited growth fires, and  $t$ -squared forms of continuous growth fires.

## Annex F Design Information

*This annex is not a part of the requirements of this NFPA document but is included for informational purposes only.*

### F.1

Growth times for combustible arrays have been obtained [see Table F.1(a)]. These are specified for certain storage heights.

**Table F.1(a)**  
**Continuous-  
Growth  
Fires**

Fuel	Growth h Time* (s)
Wood pallets, stacked 0.46 m high (6%–12% moisture)	160–320
Wood pallets, stacked 1.52 m high (6%–12% moisture)	90–190

Wood 80–  
pallets, 120  
stacke  
d 3.05  
m  
high(6  
%–  
12%  
moistu  
re)  
Wood 75–  
pallets, 120  
stacke  
d 4.88  
m  
high(6  
%–  
12%  
moistu  
re)  
Mail 190  
bags,  
filled,  
stored  
1.52 m  
high  
Carton 60  
s,  
compa  
rtment  
ed,  
stacke  
d 4.57  
m high  
Paper, 17–28  
vertica  
l rolls,  
stacke  
d 6.10  
m high  
Cotton 22–43  
(also  
PE,  
PE/cot  
acrylic  
/nylon/  
PE),  
garme  
nts in  
3.66 m  
high  
rack

“Ordinary combustibles” rack storage, 4.57 m–9.14 m high  
Paper products, densely packed in cartons, rack storage, 6.10 m high  
PE letter trays, filled, stacked 1.52 m high on cartons  
PE trash barrels in cartons, stacked 4.57 m high  
FRP shower stalls in cartons, stacked 4.57 m high

PE	85
bottles packed in compa rtment ed carton s, stacke d 4.57 m high	
PE	75
bottles in carton s, stacke d 4.57 m high	
PE	150
pallets, stacke d 0.91 m high	
PE	32-57
pallets, stacke d 1.83 m- 2.44 m high	
PU	120
mattre ss, single, horizo ntal	
PU	8
insulat ion board, rigid foam, stacke d 4.57 m high	

PS jars 55

packed  
in

compa  
rtment

ed

carton

s,

stacke

d 4.57

m high

PS 110

tubs

nested

in

carton

s,

stacke

d 4.27

m high

PS toy 120

parts

in

carton

s,

stacke

d 4.57

m high

PS 7

insulat

ion

board,

rigid

foam,

stacke

d 4.27

m high

PVC 9

bottles

packed

in

compa

rtment

ed

carton

s,

stacke

d 4.57

m high

PP 10

tubs

packed

in

compa

rtment

ed

carton

s,

stacke

d 4.57

m high

PP and 40

PE

film in

rolls,

stacke

d 4.27

m high

Distill 25-40

ed

spirits

in

barrels

,

stacke

d 6.10

m high

---

Note:  
FRP =  
fiberglass-  
reinforced  
polyester  
PE =  
polyethylene  
PP =  
polypropylene  
PS =  
polystyrene  
PU =  
polyurethane  
PVC =  
polyvinyl  
chloride  
\*  
Growth  
times of  
developing  
fires  
in  
various  
combustibles,  
assuming  
100  
percent  
combustion  
efficiency.

Actual tests [Yu and Stavrianidis 1991] have demonstrated that it is reasonable to assume that the instantaneous heat release rate per unit height of the storage array is insensitive to the storage height. Such behavior corresponds to the growth time,  $t_g$ , being inversely proportional to the square root of the storage height. Alternatively, it corresponds to the fire growth coefficient,  $\alpha_g$ , being directly proportional to the storage height. For example, if the storage height is  $\frac{1}{3}$  the tested height, the growth time is  $[1/(\frac{1}{3})]^{1/2} = 1.73$  times the growth time from the test. If the storage height is three times the tested height, the growth time is  $(\frac{1}{3})^{1/2} = 0.58$  times the growth time from the test. For fuel configurations that have not been tested, the procedures discussed in Annex E might be applicable.

*t-Squared Fires.* Over the past decade, those interested in developing generic descriptions

of the rate of heat release of accidental open flaming fires have used a *t-squared* approximation for this purpose. A *t-squared* fire is one in which the burning rate varies proportionally to the square of time. Frequently, *t-squared* fires are classified by their speed of growth as fast, medium, or slow (and occasionally ultra-fast). Where these classes are used, they are determined by the time needed for the fire to grow to a rate of heat release of 1000 kW. The times for each of these classes are provided in Table F.1(b). For many fires involving storage arrays, the time to reach 1000 kW might be much shorter than the 75 seconds depicted for ultra-fast fires.

**Table F.1(b)**  
**Classifications of *t*-Squared Fires**

Class	Time to Reach 1000 kW(s)
Ultra-fast	75
Fast	150
Medium	300
Slow	600

The general equation is as follows:

$$(F.1) \quad Q = \alpha_g t^2$$

where:

$Q$  = rate of heat release (kW)

$\alpha_g$  = a constant describing the speed of growth (kW/s<sup>2</sup>)

$t$  = time (s)

A *t-squared* fire can be viewed as a fire in which the rate of heat release per unit area is constant over the entire ignited surface, and in which the fire spreads in circular form with a steadily increasing radius. In such cases, the increase in the burning area is the square of the steadily increasing fire radius. Of course, other fires that do not have such a conveniently regular fuel array and consistent burning rate might or might not actually produce a *t-squared* curve. The tacit assumption is that the *t-squared* approximation is close enough for reasonable design decisions.

Figure 8.3.1 demonstrates that most fires have an incubation period during which the fire does not conform to a *t-squared* approximation. In some cases, this incubation period might be a serious detriment to the use of the *t-squared* approximation. In most instances, this is not a serious concern in large spaces covered by this standard. It is expected that the rate of heat release during the incubation period will not usually be sufficient to cause

activation of the smoke detection system. In any case, where such activation occurs, or where human observation results in earlier activation of the smoke-venting system, a fortuitous safeguard will result.

Figure F.1(a) compares rate of heat release curves developed by the aforementioned classes of  $t$ -squared fires and two test fires commonly used for test purposes. The test fires are shown as dashed lines labeled as furniture and 6 ft storage. The dashed curves farther from the fire origin show the actual rates of heat release of the test fires used in the development of the residential sprinkler and a standard 6 ft high array of test cartons containing foam plastic pails that also are frequently used as a standard test fire.

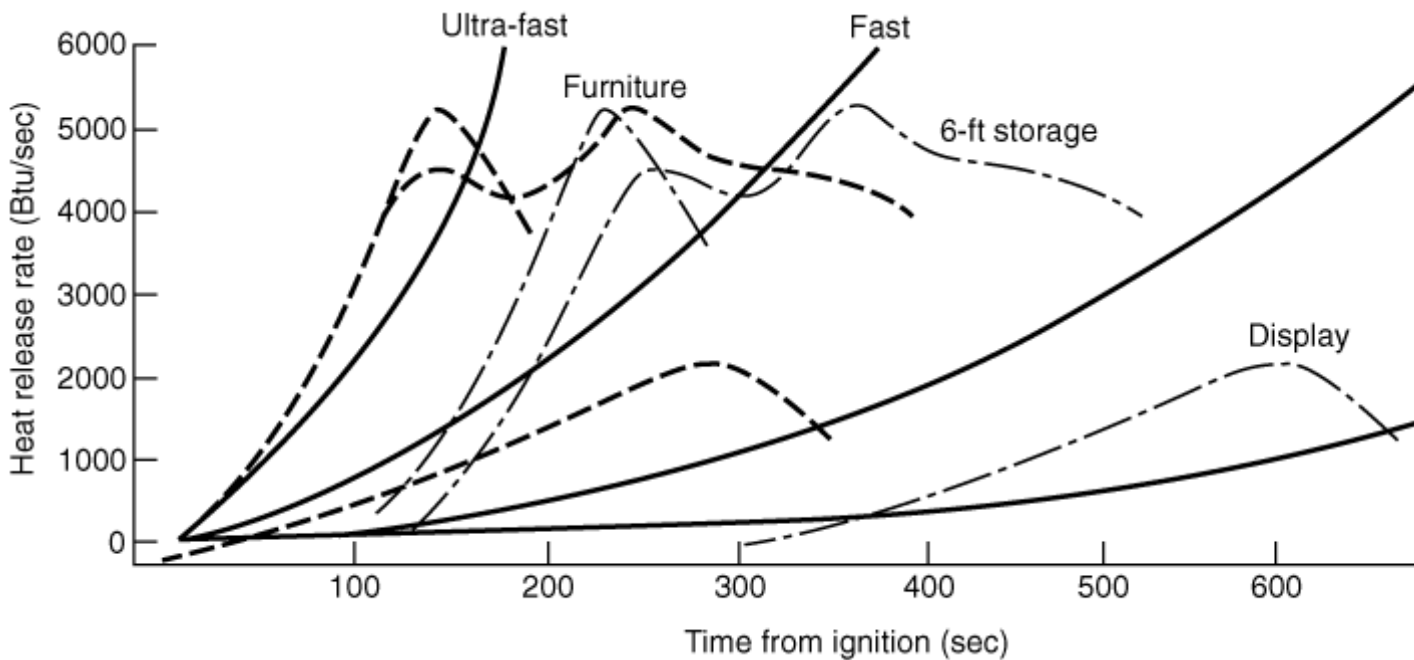


**FIGURE F.1(a) Rates of Energy Release for  $t$ -Squared Fire. (Redrawn from NIST, 1987.)**

The other set of dashed lines in Figure F.1(a) shows these same fire curves relocated to the origin of the graph. This is a more appropriate comparison with the generic curves. It can be seen that the rate of growth in these fires is actually faster than that prescribed for an ultra-fast fire. This is appropriate for a test fire designed to challenge the fire suppression system being tested.

Figure F.1(b) relates the classes of  $t$ -squared fire growth curves to a selection of actual fuel arrays.

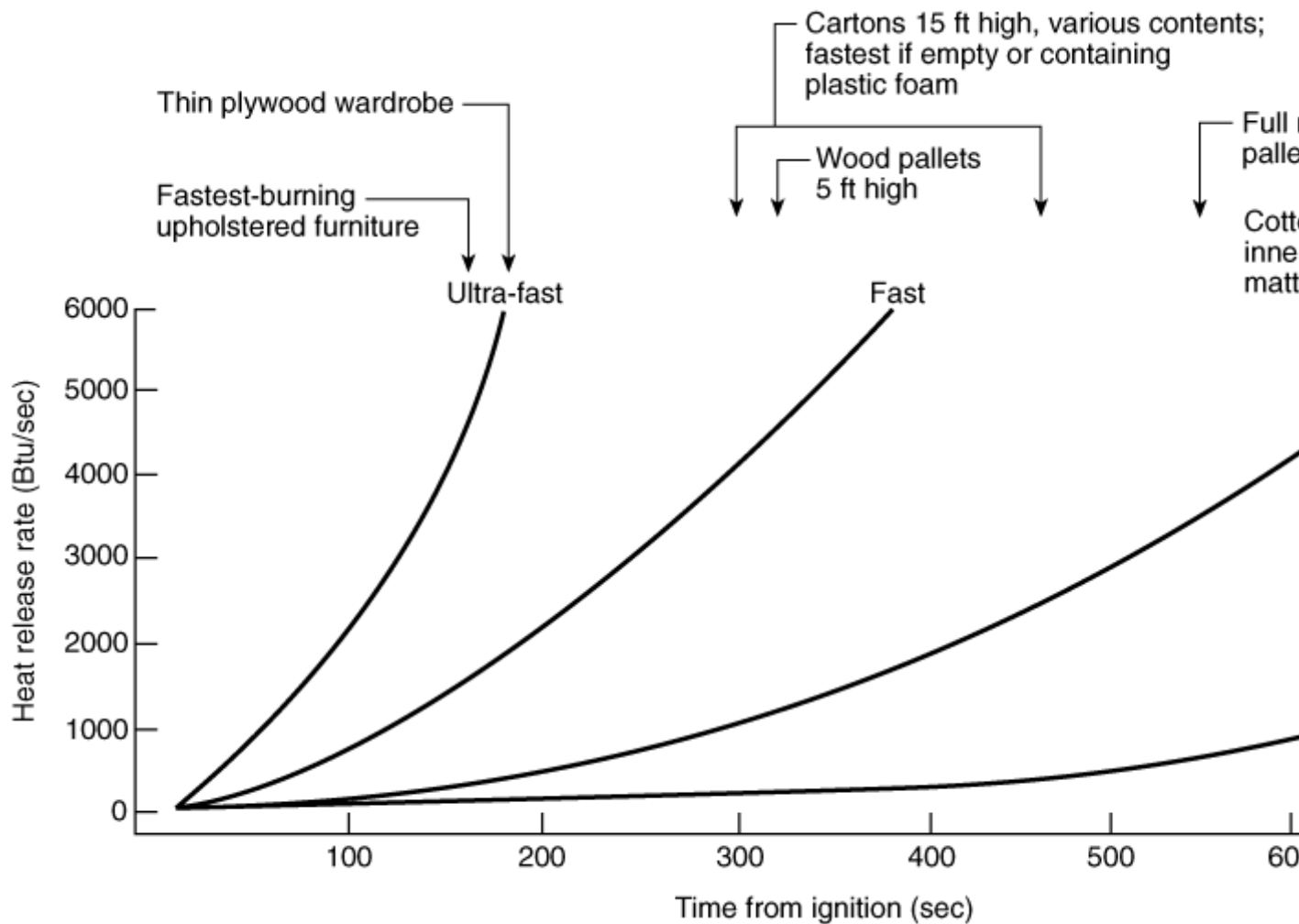


**FIGURE F.1(b) Relation of  $t$ -Squared Fires to Some Fire Tests.**

## F.2

For consistency with Annex B and with referenced documents on the fire model LAVENT, the nomenclature for this section differs from that of the other section in this annex. The definitions for the variables used in this section are provided in Annex B, Section B.7.

A ceiling vent design is successful to the extent that it controls a fire-generated environment developing in a space of fire origin according to any of a variety of possible specified criteria. For example, if the likely growth rate of a fire in a particular burning commodity is known, a vent system with a large enough vent area, designed to provide for timely opening of the vents, can be expected to lead to rates of smoke removal that are so large that fire fighters, arriving at the fire at a specified time subsequent to fire detection, are able to attack the fire successfully and protect commodities in adjacent spaces from being damaged.

To evaluate the success of a particular design, it is necessary to predict the development of the fire environment as a function of any of a number of physical characteristics that define and might have a significant effect on the fire scenario. Examples of such characteristics include the following:

- (1) The floor-to-ceiling height and area of the space and the thermal properties of its ceiling, walls, and floor
- (2) The type of barriers that separate the space of fire origin and adjacent spaces (e.g., full walls with vertical door-like vents or ceiling-mounted draft curtains)
- (3) The material type and arrangement of the burning commodities (e.g., wood pallets in plan-area arrays of 3 m × 3 m and stacked 2 m high)
- (4) The type, location, and method of deployment of devices that detect the fire and actuate the opening of the vents (e.g., fusible links of specified RTI and distributed at a specified spacing distance below the ceiling)
- (5) The size of the open area of the vents themselves

The best way to predict the fire environment and evaluate the likely effectiveness of a vent design is to use a reliable mathematical model that simulates the various relevant physical phenomena that come into play during the fire scenario. Such an analytical tool should be designed to solve well-formulated mathematical problems, based on basic relevant principles of physics and on fundamentally sound, well-established, empirical relationships. Even in the case of a particular class of problem, such as an engineering problem associated with successful vent design, there is a good deal of variation among applicable mathematical models that could be developed to carry out the task. Such models might differ from one another in the number and detail of the individual physical phenomena taken into account. Therefore, the list of physical characteristics that define and could have a significant effect on the fire scenario does not include outside wind conditions, which could have an important influence on the fire-generated environment. A model might or might not include the effect of wind. A model that does include the effect of wind is more difficult to develop and validate and is more complicated to use. Note that the effect of wind is not taken into account in the following discussion of the LAVENT model. However, by using reasonably well accepted mathematical modeling concepts, LAVENT could be developed to the point that it could be used to simulate this effect.

The discussion that follows describes a group of phenomena that represent a physical basis for estimating the fire-generated environment and the response of heat-responsive elements in well-ventilated compartment fires with draft curtains and ceiling vents activated by fusible links, thermoplastic drop-out panels, or other alternative means of activation or smoke detectors. The phenomena include the following:

- (1) Growth of the smoke layer in the curtained area
- (2) The flow dynamics of the buoyant fire plume
- (3) The flow of smoke through open ceiling vents
- (4) The flow of smoke below draft curtains
- (5) Continuation of the fire plume in the upper layer
- (6) Heat transfer to the ceiling surface and the thermal response of the ceiling
- (7) The velocity and temperature distribution of plume-driven, near-ceiling flows

- (8) The response of near-ceiling-deployed heat-responsive elements and smoke detectors

All the phenomena in items (1) through (8) are taken into account in the LAVENT model, which was developed to simulate well-ventilated compartment fires with draft curtains and fusible link-actuated or smoke detector-actuated ceiling vents. Other models that could be developed for a similar purpose typically would also be expected to simulate these basic phenomena.

The space to be considered is defined by ceiling-mounted draft curtains with a fire and with near-ceiling fusible link-actuated ceiling vents and sprinklers. The curtained area should be considered as one of several such spaces in a large building area. Also, by specifying that the curtains be deep enough, they can be thought of as simulating the walls of a single uncurtained area.

This section discusses critical physical phenomena that determine the overall environment in the curtained space up to the time of sprinkler actuation. The objective is to identify and describe the phenomena in a manner that captures the essential features of this generic class of fire scenario and that allows for a complete and general, but concise and relatively simple, mathematical/computer simulation.

The overall building area is assumed to have near-floor inlet air openings that are large enough to maintain the inside environment, below any near-ceiling smoke layers that might form, at outside-ambient conditions. Figure F.2(a) depicts the generic fire scenario considered. It is assumed that a two-layer zone-type model adequately describes the phenomena under investigation. The lower layer is identical to the outside ambient. The upper smoke layer thickness and properties change with time, but the layer is assumed to be uniform in space at any time. Conservation of energy and mass along with the perfect gas law is applied to the upper layer. This leads to equations that necessitate estimates of the net rate of enthalpy flow plus heat transfer and the net rate of mass flow to the upper layer. Qualitative features of the phenomena that contribute to these flows and heat transfer are described briefly.

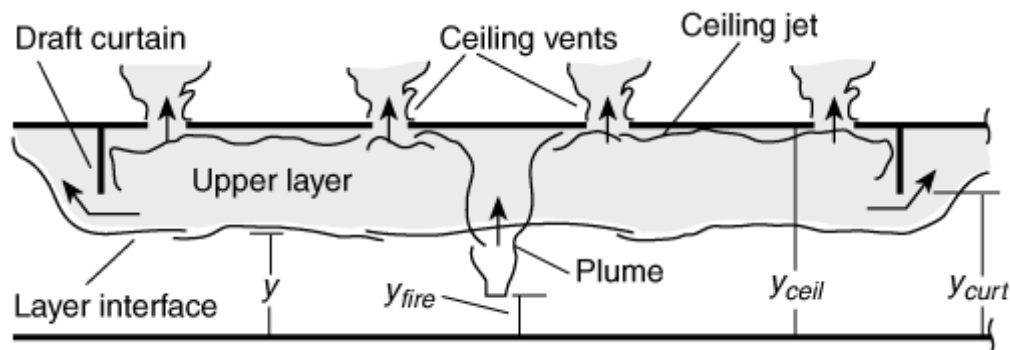


**FIGURE F.2(a) LAVENT Model: Fire in a Building Space with Draft Curtains and Ceiling Vents.**

Flow is driven through ceiling vents by cross-vent hydrostatic pressure differences. The traditional calculation uses orifice-type flow calculations. Bernoulli's equation is applied across a vent, and it is assumed that, away from and on either side of the vent, the environment is relatively quiescent. Figure F.2(b) depicts the known, instantaneous,

hydrostatic pressure distribution in the outside environment and throughout the depth of the curtained space. These pressures are used to calculate the resulting cross-vent pressure difference, then the actual instantaneous mass and enthalpy flow rates through a vent.

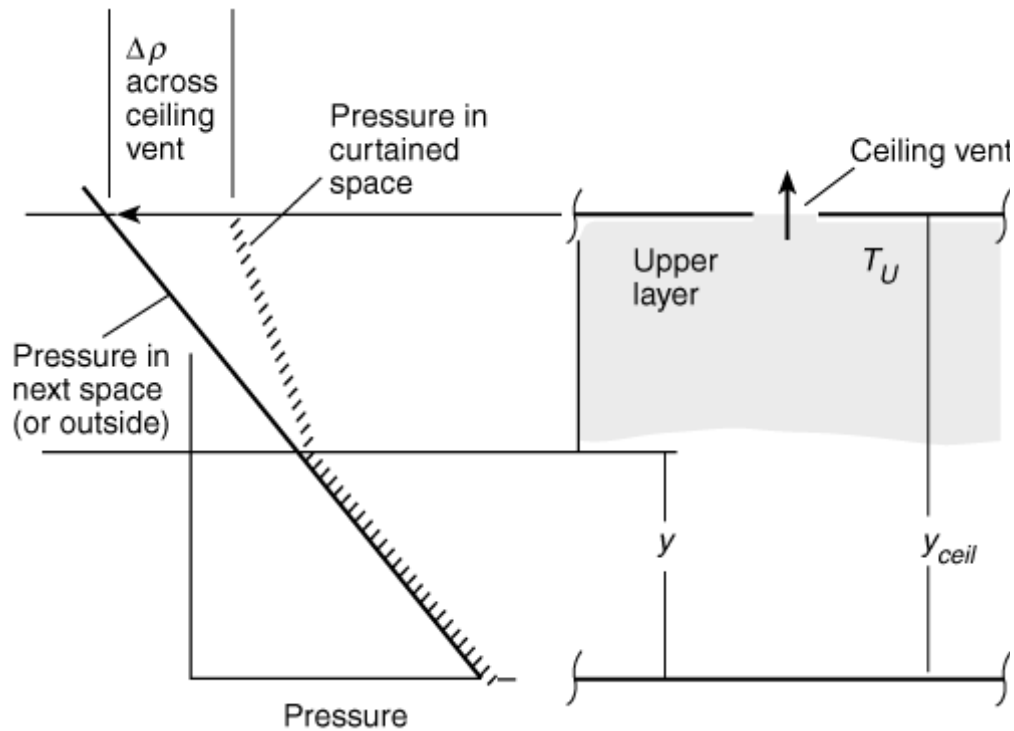


**FIGURE F.2(b) Flow Through a Ceiling Vent.**

If and when the smoke layer boundary face drops below the bottom of the draft curtains, the smoke starts to flow out of the curtained space. As with the ceiling vents, this flow rate is determined by the cross-vent hydrostatic pressure difference. As depicted in Figure F.2(c), however, the pressure difference in this case is not constant across the flow. Nonetheless, even in this configuration, the instantaneous flow rates are easily determined with well-known vertical-vent flow equations used traditionally in zone-type fire models.

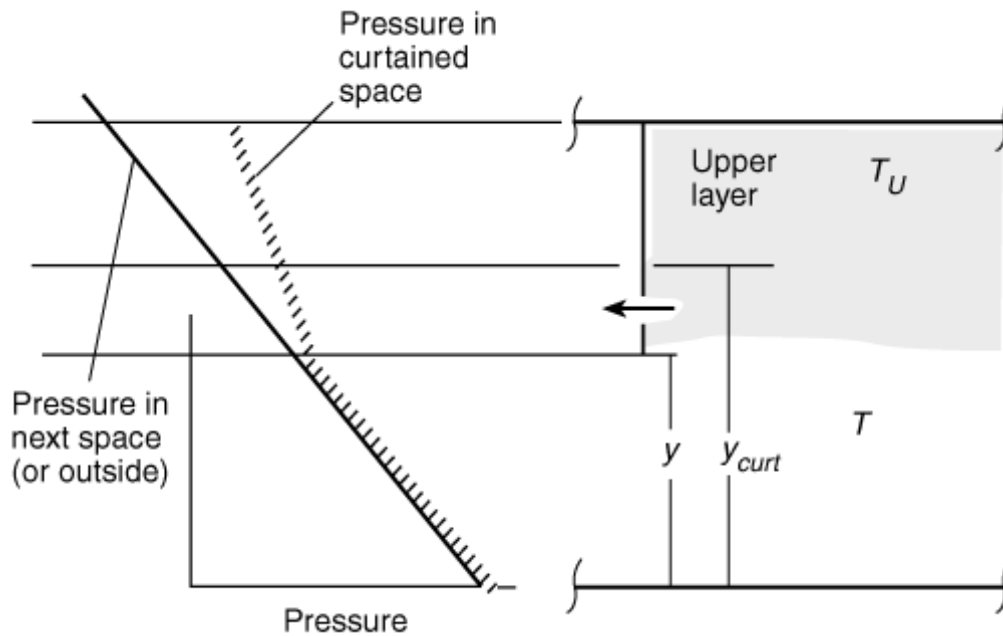


**FIGURE F.2(c) Flow Below a Draft Curtain.**

The major contributors to the upper-layer flow and surface heat transfer are the fire and its plume. These properties are depicted in Figure F.2(d). It is assumed that the rate of energy release of the fire's combustion zone does not vary significantly from known free-burn values that are available and assumed to be specified (see Chapter 8). A known, fixed fraction of this energy is assumed to be radiated isotropically, as in the case of a point source, from the combustion zone. The smoke layer is assumed to be relatively transparent (i.e., all radiation from the fire is incident on the bounding surfaces of the compartment).

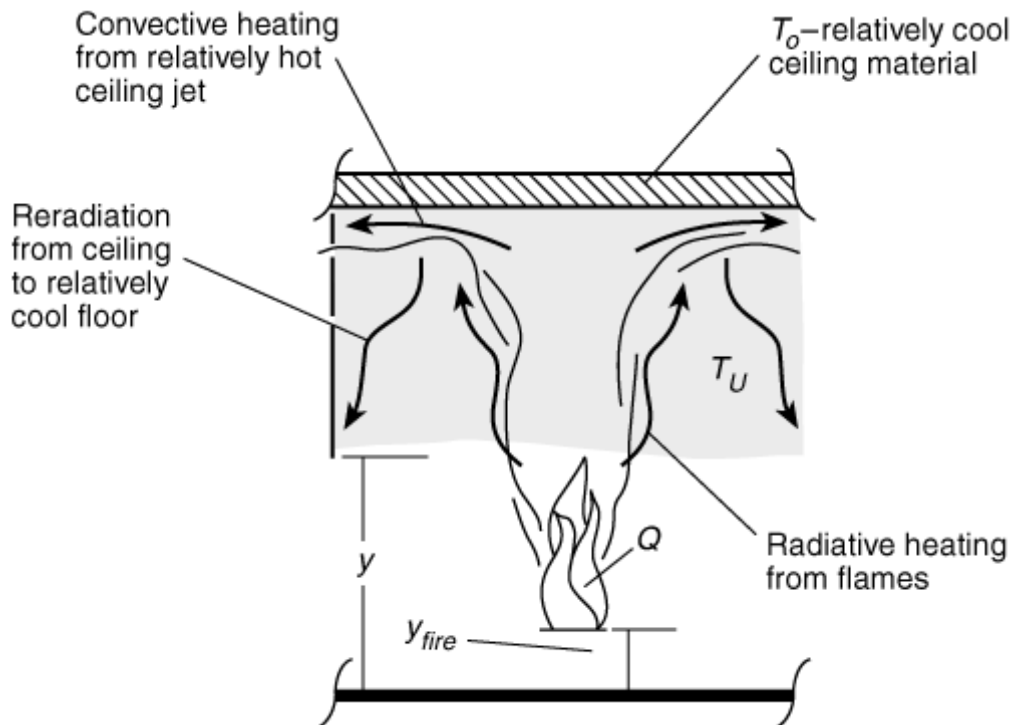


### **FIGURE F.2(d) The Fire, the Fire Plume, and Heat Transfer to the Ceiling.**

A plume model, selected from the several available in the literature, is used to determine the rate of mass and enthalpy flow in the plume at the elevation of the smoke layer boundary. It is assumed that all of this flow penetrates the smoke layer boundary and enters the upper layer. As the plume flow enters the upper layer, the forces of buoyancy that act to drive the plume toward the ceiling are reduced immediately because of the temperature increase of the upper-layer environment over that of the lower ambient. As a result, the continued ascent of the plume gases is less vigorous (i.e., is at a reduced velocity) than it would be in the absence of the layer. Also, as the plume gases continue their ascent, the temperature becomes higher than it would be without the upper layer. Such higher temperatures are a result of the modified plume entrainment, which is now occurring in the relatively high-temperature upper layer rather than in the ambient-temperature lower layer. Methods of predicting the characteristics of the modified upper-plume flow are available.

Having penetrated the smoke layer boundary, the plume continues to rise toward the ceiling of the curtained area. As it impinges on the ceiling surface, the plume flow turns and forms a relatively high-temperature, high-velocity, turbulent-ceiling jet that flows radially outward along the ceiling and transfers heat to the relatively cool ceiling surface. The ceiling jet is cooled by convection, and the ceiling material is heated by conduction. Eventually, the now-cooled ceiling jet reaches the extremities of the curtained space and is deposited into and mixed with the upper layer. The convective heat transfer rate and the ceiling surface temperature on which it depends are both strong functions of the radial distance from the point of plume–ceiling impingement, and both decrease rapidly with increasing radius.

The thermal response of the ceiling is driven by transient heat conduction. For the time period typically considered, radial gradients in ceiling surface conditions are small enough so that the conduction heat transfer is quasi–one dimensional in space. Therefore, the thermal response of the ceiling can be obtained from the solution to a set of one-dimensional conduction problems at a few discrete radial positions. These problems can be solved subject to net convection and radiation heat flux boundary conditions.

Interpolation in the radial direction between the solutions leads to a sufficiently smooth representation of the distributions of ceiling surface temperature and convective heat transfer rate. The latter is integrated over the ceiling surface to obtain the net instantaneous rate of convective heat transfer losses from the ceiling jet.

Convective heating and the thermal response of a near-ceiling heat-responsive element such as a fusible link or thermoplastic drop-out panel are determined from the local ceiling jet velocity and temperature. Velocity and temperature depend on vertical distance below the ceiling and radial distance from the fire plume axis. If and when its fusion (activation) temperature is reached, the device(s) operated by the link or other heat-responsive element is actuated.

For specific radial distances that are relatively near the plume, the ceiling jet is an inertially dominated flow. Its velocity distribution, depicted in Figure F.2(e), can be estimated from the characteristics of the plume, upstream of ceiling impingement. The ceiling jet temperature distribution, depicted in Figure F.2(f) for a relative “hot” or “cool” ceiling surface, is then estimated from the velocity (which is now known), upper-layer

temperature, ceiling-surface temperature, and heat flux distributions.

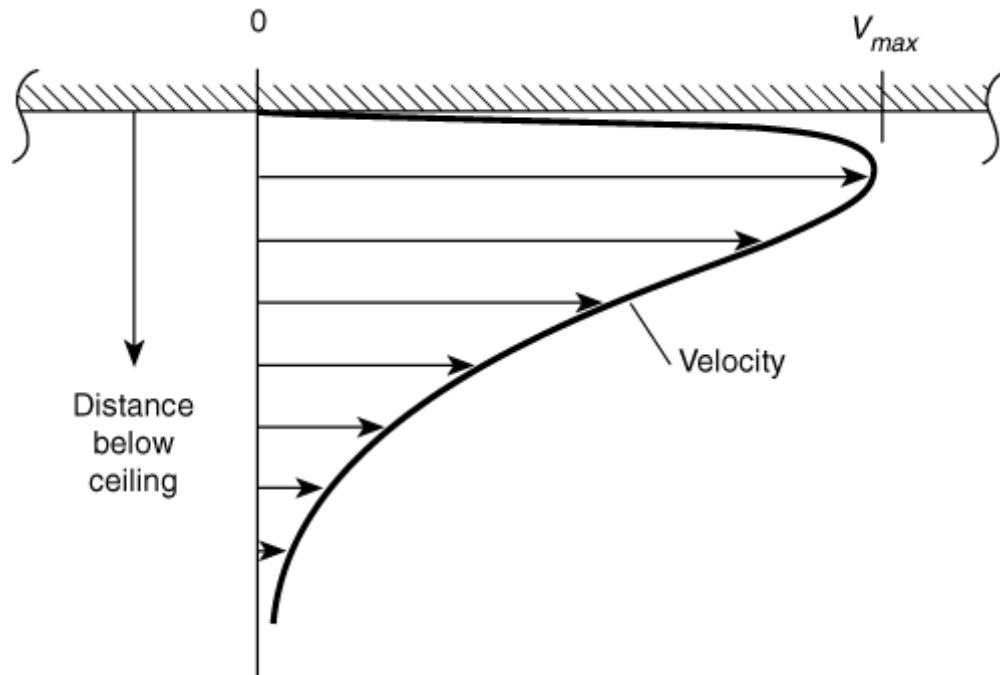


**FIGURE F.2(e) Ceiling Jet Velocity.**

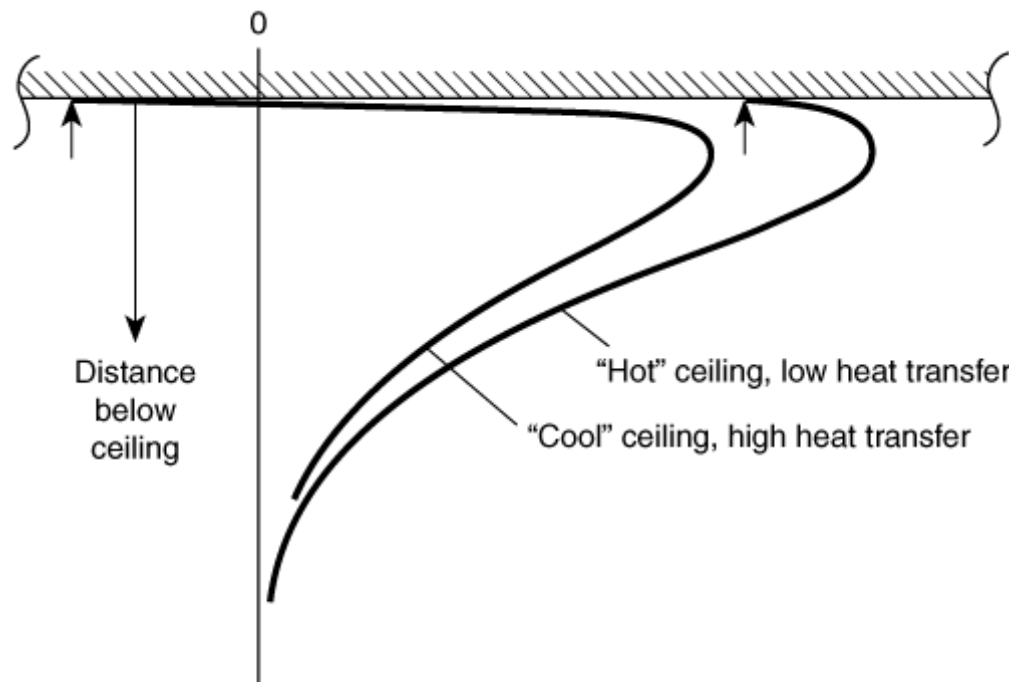


**FIGURE F.2(f) Ceiling Jet Temperature.**

Annex B provides details of all equations of the LAVENT mathematical fire model and its associated computer program, developed to simulate all the phenomena described thus far. LAVENT can be used to simulate and study parametrically a wide range of relevant fire scenarios involving these phenomena.

Included in B.5.5 is a summary of guidelines, assumptions, and limitations to LAVENT. For example, as specified in that subsection, LAVENT assumes that, at all times during a simulated fire, the overall building space containing the curtained area of fire origin is vented to the outside (e.g., through open doorways). It is assumed, furthermore, that the area of the outside vents is large relative to the area of the open ceiling vents in the curtained area.

Therefore, if the total area of the outside vents is  $A_{out}$ , then  $(A_{out}/AV)^2$  is significantly larger than 1 (e.g.,  $A_{out}/AV > 2$ ). If the outside vents are in the bounding walls of the curtained space, not in adjacent spaces, they should be located entirely below the smoke layer boundary. B.5.5 should be referenced for the details of other guidelines, assumptions, and limitations.

If the actual size of the outside vents is not significantly larger than the vent area, consideration should be given to increasing the vent area to account for the restrictions in inlet air using the following multiplier:

$$(F.2) \quad M \left[ 1 + \left( \frac{A_v}{A_{V_{out}}} \right)^2 \frac{T_{amb}}{T_U} \right]^{1/2}$$

where:

$A_V$  = total area of open ceiling in curtained space

$A_{V_{out}}$  = total area of open vents to outside exclusive of  $A_V$

$T_{amb}$  = outside temperature

$T_U$  = upper layer temperature

$M$  = multiplier

Annex C is a user guide for the LAVENT computer code. Annex C includes a comprehensive discussion of the inputs and calculated results of a default simulation involving a fire growing in a large pile of wood pallets ( $t$ -squared growth to a steady 33 MW) in a 9.1-m high curtained warehouse-type space with multiple fusible-link-actuated vents and near-ceiling-deployed fusible sprinkler links. Vents actuated by alternative means such as thermoplastic “drop-out” panels with equivalent performance characteristics can also be modeled using LAVENT. Inputs to LAVENT include the following.

- (1) *Dimensions of the Curtained Area of Fire Origin.* Length, width, and height of the curtained area of fire origin
- (2) *Dimensions of the Draft Curtain.* Floor to bottom of the curtain separation distance and length of the curtain (a portion of the perimeter of the curtained space can include floor-to-ceiling walls)
- (3) *Properties of the Ceiling.* Thickness, density, thermal conductivity, and heat capacity of the ceiling material
- (4) *Characteristics of the Fire.* Elevation of the base of the fire above the floor (see 9.2.3.6); total energy release rate of the fire, at different times during the course of

the simulated fire scenario (the computer code uses linear interpolation to approximate between these times); and the plan area of the fire, or the total energy release rate per unit area of the fire (in cases where the user supplies the latter input, the computer code estimates the changing area of the fire at any moment by using the current total energy release rate)

- (5) *Characteristics of the Ceiling Vent–Actuating Fusible Links or Vent-Actuating Smoke Detectors and of the Corresponding Ceiling Vents.* Horizontal distance from the fire, vertical distance below the ceiling surface, response time index (RTI), and fuse temperature of the ceiling vent–actuating fusible links; also, the clear open area,  $A_V$ , of their associated ceiling vents
- (6) *Characteristics of Fusible Sprinkler Links.* Horizontal distance from the fire, vertical distance below the ceiling surface, RTI, and fuse temperature of fusible sprinkler links

LAVENT is written in Fortran 77. The executable code operates on PC-compatible computers.

LAVENT has had some limited experimental validation in experiments with 3.34 m<sup>2</sup> pool fires in a 37 m × 40 m × 14 m high aircraft hangar [Walton and Notarianni 1993; Notarianni 1992]. The hangar was equipped with near-ceiling–mounted brass disks of known RTI, which were used to simulate sprinkler links or heat detector elements. The experiments did not involve ceiling vents. Experimental validation of the various mathematical submodel equation sets that comprise the generalized LAVENT simulation is also implicit. This is the case, since the mathematical submodels of LAVENT, presented in Annex B, are based on carefully reproduced correlations of data acquired in appropriate experimental studies of the isolated physical phenomena that, taken together, make up the combined effects of a LAVENT-simulated fire scenario. The experimental basis and validation of the LAVENT submodels can be found in the references listed in B.6.

If ceiling vents are actuated by smoke detectors, the guidelines outlined in 9.2.5.4.3 should be followed. LAVENT can be made to simulate this function with a very sensitive fusible link (i.e., a link with a negligibly small RTI) and an appropriate fuse temperature.

As specified in B.4.1, LAVENT always assumes that the flow coefficient,  $C$ , for ceiling vents is 0.68; if the user has reason to believe that a different value,  $C_{user}$ , is more appropriate for a particular vent (such as the value 0.6 suggested in 9.2.4.2), then the input vent area for that vent should be scaled up proportionately (i.e.,  $A_V, \text{input} = A_V C_{user}/0.68$ ).

LAVENT calculates the time that the first sprinkler link fuses and the fire environment that develops in the curtained space prior to that time. Because the model does not simulate the interaction of sprinkler sprays and fire environments, any LAVENT simulation results subsequent to sprinkler waterflow should be ignored.

### F.3

Objectives of the vent system should be defined and considered. Objectives can include the following:

- (1) Provide for fire fighter safety and facilitate post-fire smoke removal by the fire department. The two key issues include activation type (remote or manual removal at roof level by fire fighters), and vent ratio (gross vent area to roof area). Remote activation is a preferred method; however, manual activation at roof level does considerably reduce the time a fire fighter must spend on the roof (versus cutting a hole in the roof) and might be considered acceptable.
- (2) Allow extended egress travel distances.
- (3) Reduce smoke damage to the contents. Design features such as ganging all vents within a sprinkler zone, and automatically activating all of the vents within one zone following sprinkler activation might achieve objectives 2 and 3; however, additional research is needed to validate this concept.

Chapters 4 through 10 represent the state of technology of vent and draft curtain board design in the absence of sprinklers. A broadly accepted equivalent design basis for using sprinklers, vents, and curtain boards together for hazard control (e.g., property protection, life safety, water usage, obscuration) is currently not available. Designers are strongly cautioned that use of venting with automatic sprinklers is an area of ongoing research to determine its benefit and effect in conjunction with automatic suppression.

This annex section provides design considerations for venting systems in sprinkler-protected areas. These design considerations are based on the research that has been conducted.

*Early Research.* For occupancies that present a high challenge to sprinkler systems, concern has been raised that the inclusion of automatic roof venting, draft curtains, or both can be detrimental to the performance of automatic sprinklers. Although there is no universally accepted conclusion from fire experience [Miller 1980], studies on a model scale [Heskestad 1974] suggested the following:

- (1) Venting delays loss of visibility.
- (2) Venting results in increased fuel consumption.
- (3) Depending on the location of the fire relative to the vents, the water demand necessary to achieve control is either increased or decreased over an unvented condition. With the fire directly under the vent, water demand is decreased. With the fire equidistant from the vents, water demand is increased.

A series of tests was conducted to increase the understanding of the role of automatic roof vents simultaneously employed with automatic sprinklers [Waterman 1982]. The data submitted did not provide a consensus on whether sprinkler control was impaired or enhanced by the presence of automatic (roof) vents for the typical spacing and area.

Large-scale fire tests, conducted at the Factory Mutual Research fire test facility without vents, indicated that certain configurations of draft curtains can have a detrimental effect on the performance of a sprinkler system during a high-challenge fire [Troup 1994]. Two tests were conducted, one in which a fire was initiated adjacent to a draft curtain, and one near the junction of two draft curtains. Sprinkler performance in these two tests was considered unsatisfactory because an excessive number of sprinklers operated and damage

significantly increased in comparison to similar tests conducted without draft curtains.

Other large-scale fire tests were conducted [Hinkley et al. 1992] employing liquid fuels, small vent spacings (minimum of 4.7 m), and vents open at ignition. Hinkley reached the following conclusions:

- (1) The prior opening of vents had little effect on the operation of the first sprinkler.
- (2) Venting substantially reduced the total number of sprinkler operations.

In an independent analysis of these tests, Gustafsson [1992] noted that sprinklers near the fire source were often delayed or did not operate at all.

*Recent Research.* The Fire Protection Research Foundation, formerly known as the National Fire Protection Research Foundation, organized large-scale tests to study the interaction of sprinklers, roof vents, and draft curtains [McGrattan et al. 1998], involving heptane spray fires and arrays of cartoned plastic commodity of a standard configuration. The test space was ventilated by a smoke abatement system. The findings were as follows:

- (1) In the heptane spray fires, venting had no significant effect on sprinkler operations, unless a fire was ignited directly under a vent, in which case the number of sprinkler operations decreased.
- (2) When a draft curtain was installed in the heptane spray fires, the number of operating sprinklers increased.
- (3) In five tests with the cartoned plastic commodity, three tests opened 20–23 sprinklers and two tests opened 5–7 sprinklers, attributed to variability in the initial fire growth and not to any of the variables under study.
- (4) One of these tests with ignition near a draft curtain consumed much more fuel than the other tests, attributed to fire spread under the draft curtain.
- (5) Effects of venting through roof vents on smoke obscuration could not be determined because of the dominant effect of the building smoke abatement system.
- (6) In all experiments in this study where, in some cases, vents were open at the start of the fire, and in those instances where the fire was located directly under a vent, sprinklers performed satisfactorily. Satisfactory sprinkler performance is defined by all of the following criteria:
  - (a) Fire did not jump the aisles.
  - (b) The number of spinklers operating did not exceed the design area.
  - (c) Fire did not spread to an end of the fuel array.

While the use of automatic venting and draft curtains in sprinklered buildings is still under review, the designer is encouraged to use the available tools and data referenced in this document for solving problems peculiar to a particular type of hazard control [Miller 1980; Heskestad 1974; Waterman 1982; Troup 1994; Hinkley et al. 1992; Gustafsson 1992; McGrattan et al. 1998].

*Design Considerations.* As a result of the research, the following guidelines are provided for the design of venting systems in those areas of a building protected with an automatic sprinkler system designed and installed in accordance with NFPA 13, *Standard for the Installation of Sprinkler Systems*, for the specific occupancy hazard.

- (1) Draft curtains and open vents of venting systems should not adversely affect sprinklers that are capable of discharging water onto the fire, either in time of operation or in the water discharge pattern.
- (2) Vents that are open prior to sprinkler operations in a region surrounding the ignition point, within a radius of  $1\frac{1}{2}$  sprinkler spacings, can interfere with the opening of sprinklers capable of delivering water to the fire. The vent system design should consider the following:
  - (a) This interference is likely to be a factor if the total vent area is divided among many closely spaced vents, as in the investigation by Hinkley et al. (1992), commented on by Gustafsson (1992).
  - (b) If the vent spacing is several times as large as the sprinkler spacing, model fire tests simulating a  $1.2\text{ m} \times 1.2\text{ m}$  vent in a 7.6-m high building [Heskestad 1995] showed that sprinkler operations were significantly delayed whenever ignition occurred anywhere under the area of an open vent. Otherwise, there was little delay. This delay can be important for systems with early suppression fast response (ESFR) sprinklers.
  - (c) Use of high-temperature, heat-responsive actuation mechanisms, compared to the sprinklers, can mitigate the problem of open vents. For example, for  $74^{\circ}\text{C}$  rated ESFR sprinklers, a minimum  $180^{\circ}\text{C}$  activation temperature should be provided for vents. Another approach would be to provide gang operation of the vents at the moment a conservative number of sprinklers are operating.
  - (d) The vent system design should consider the effects of the venting system on the ceiling jet.
- (3) The location of draft curtains should be determined considering the following:
  - (a) Draft curtains can delay or prevent operation and can interfere with the discharge of sprinklers capable of delivering water to the fire. In practice, sprinklers capable of delivering water to the fire can be considered to be those that are within  $1\frac{1}{2}$  sprinkler spacings of the ignition point.
  - (b) Draft curtains should be located in aisles and should be horizontally separated from combustible contents.
  - (c) The layout of the sprinkler protection and the width of the aisle below the draft curtain should be sufficient to prevent the fire from jumping the aisle space. Accordingly, if a draft curtain is positioned midway between two sprinklers, the nearest possible ignition point should be at least  $\frac{3}{4}$  of one sprinkler spacing away from the draft curtain. In other words, there can be no storage of combustible material within  $\frac{3}{4}$  of one sprinkler spacing of a draft

curtain. Aisles free of combustible storage, centered under draft curtains, should be at least 1 ½ sprinkler spacings wide (e.g., a minimum of 15 ft aisle for 10 ft sprinkler spacing in the direction perpendicular to the draft curtain). For situations where such an aisle width is not practical, the aisle space can be reduced to a minimum of 8 ft, when a line of sprinklers is provided on each side of the draft curtain, 4 in. to 12 in. horizontally from the face of the draft curtain. For existing sprinkler installations, these sprinklers near the draft curtain might need to be staggered horizontally with respect to adjacent line of sprinklers, in order to maintain the minimum separation required by NFPA 13, *Standard for the Installation of Sprinkler Systems*, and to prevent sprinkler skipping.

- (d) Where aisles of sufficient width cannot be maintained, full-height partitions can be used in lieu of draft curtains.
- (4) The design fire's rate of heat release rate–time history should account for the operation of the sprinkler system.
- (5) Determination of the smoke layer temperature should take into account the operation of the sprinkler system.
- (6) The vent flow, smoke movement, and position of the smoke layer boundary should take into account the down-drag effect produced by operation of the sprinkler system.

[Click here to view and/or print an Adobe® Acrobat® version of the index for this document](#)